UNIVERSITY OF BIRMINGHAM

EXTRACTION AND MODIFICATION OF LIGNIN TO SUPPORT ENHANCED UTILISATION USING CRITICAL FLUIDS

By

MUHAMMAD HAZWAN BIN HAMZAH

A thesis submitted to

The University of Birmingham

for the Degree of

Doctor of Philosophy

Supercritical Fluid Technology Research Group

School of Chemical Engineering

College of Engineering and Physical Sciences

The University of Birmingham, United Kingdom

December 2017

ABSTRACT

Lignin is abundant naturally occurring biopolymer currently produced as a by-product from the pulping and paper industry, where the process generates lignin in the form of lignosulphonates. While there are many applications for lignin there are all low value and attempts to add value to lignin are hindered by its complex physico-chemical nature and the presence of sulphur. Adopting the biorefining concept the study evaluates the impact of direct (DE) and sequential extraction (SE) of *Miscanthus x giganteus* using sub-critical water with associated modifiers on the physical and chemical properties of the extracted lignin. Even though higher delignification was achieved by DE (81.5%) than SE (58.0%), the lignin recovered from the SE process showed significantly higher purity (91.5%). Fourier Transform Infrared Spectroscopy (FTIR) analysis also revealed the abundance of free hydroxyl groups (OH) within the lignin derived from SE. Further it was demonstrated that lignin agglomerates, which are widely known to form post extraction, could be de-agglomerated by simply reducing the ethanol concentration from 50% to 1% and therefore intramolecular forces. Although the finding does not offer an adequate explanation regards to the driving forces of lignin aggregates at different ethanol concentration, the esterification reaction to attach C_{12} fatty acids to lignin derived from SE at 50% ethanol concentration (5 mg/mL) demonstrated that the amount of hydroxyl groups available increased the level of fatty acid incorporated onto the lignin macromolecule with 81.2% esterification conversion. A modified lignin produced has the potential to be used as a precursor for added value bio-based materials.

Dedicated to my beloved family…

My parents…

Hamzah Kusno and Fauziah Busin…

My brother and late sister…

Muhammad Haziq Hamzah and Ain Nur Hazwani Hamzah…

&

My wife…

Nur Amalina Abdul Rahim

ACKNOWLEDGMENTS

In the name of Allah, most Gracious, most Compassionate. Thanks to Allah for giving me the courage, patience and confidence in order to complete this work. First and foremost, a very special thanks and appreciation to my supervisory committee, Prof. Mark Simmons, Prof. Philip Cox and Dr. Steve Bowra for giving me the opportunity to work under their supervision and for their valuable time, guidance and immense contribution throughout this work.

I would also like to thank Ministry of Higher Education Malaysia and Universiti Putra Malaysia for the funding and support received for my PhD study at University of Birmingham, United Kingdom.

Many thanks also must go to the wonderful colleagues of Supercritical Fluid Technology Research Group; Dr. Tiejan Lu, Dr. Ricardo Miguel Nunes, Dr. Fabio Antas, Dr. Salis Ibrahim, Dr. Edeh Ifeanyichukwu, Dr. Arielle Muniz De Barros and Dr. Raitis Kalnins.

I also would like to kindly thank all those who helped me including laboratory technician with their valuable support during my work to accomplish this PhD's thesis. Not forgetting respective friends; Haris, Khairul, Ghaddafy, Iqram, Hazmi, Rozzamri, Faiqa, Hafizah, Luqman, Azzam, Dain, and Halim for their kind help and moral supports in doing this work. Last but not least, to my beloved family, thank you for prayers, support, understanding, encouragement, and giving me strength to complete this challenging work.

LIST OF ABBREVIATIONS

Eq	-	Equation
MxG	-	*Miscanthus x giganteus*
SCW	-	Subcritical water
HCW	-	Hot compressed water
AFEX	-	Ammonia fiber expansion
NREL	-	National Renewable Energy Laboratory
FTIR	-	Fourier Transform Infrared Spectroscopy
PCA	-	Principal Component Analysis
SEM	-	Scanning electron microscope
LM	-	Light microscopy
SE	-	Sequential extraction
DE	-	Direct extraction
RPM	-	Revolution per minute
RCF	-	Relative centrifugal forces

TABLE OF CONTENTS

LIST OF TABLES

LIST OF TABLES

LIST OF TABLES

LIST OF FIGURES

CHAPTER 1: INTRODUCTION

1.1 Background

Lignin is the second most abundant natural polymer on earth after cellulose and is found in all terrestrial plants and some aquatic species. The biosphere is estimated to contain 3×10^{11} tonnes of lignin with an annual biosynthetic rate of 2×10^{10} tonnes (Argyropoulos and Menachem, 1997; Hu *et al.*, 2011). Currently, lignin is recovered in large quantities as a by-product from pulping industry (Gan *et al.*, 2014). Lignin is produced by a chemical pulping process which results in a black liquor, leaving cellulose fibres for pulp production. However, the black liquor is predominantly dewatered and burned to supplement the heat requirement of the pulping operation (Mahmood *et al.*, 2016) and only 1 to 2% of the total amount of lignin produced is used in bio-based material applications (Gordobil *et al.*, 2016).

There are two basic pulping processing 1) the sulphite process which uses a mixture of an aqueous sulphur dioxide and a base such as calcium, sodium, magnesium or ammonium bisulphide and 2) the Kraft process which is based on cooking with a sodium hydroxide and sodium sulphide (Hamaguchi *et al.*, 2012; Laurichesse and Avérous, 2014; Tarabanko and Petukhov, 2003). Lignin derived from the Kraft or the sulphite process are recovered from black liquor by acidification. Lignosulphonates contains sulfonic acid groups that makes lignin water soluble. Lignosulphonates exhibit a high molecular weight with a broad distribution of polydispersity index (around 6-8) and are the most utilised lignins with applications including

dispersant, binders and packaging additives (Laurichesse and Avérous, 2014; Lora, 2008; Vishtal and Kraslawski, 2011).

Recently, sulphur-free lignins such as that derived using organosolv process have been explored due to its high purity, high solubility in organic solvents, hydrophobic and a low macromolecular size after fractionation steps (Matsushita, 2015). The organosolv process uses an aqueous organic solvent mixtures with inorganic acid catalysts such as hydrochloric and sulphuric acids to extract lignin (Maurya *et al.*, 2013).

The increasing awareness of the need for renewable and sustainable sources of energy has driven interest in lignocellulosic second-generation bioethanol. Moreover, the possibility of adopting high yielding biomass crops such as *Miscanthus x giganteus* (*MxG*), as a feedstock has attracted interest. Similarly, the concept of biorefining has been voiced as a route whereby cellulose, the substrate for ethanol production can be recovered along with other renewable bio-based chemical building blocks thus potentially improving the overall economic of bioethanol production.

In the context of the preceding, the study was carried out to evaluate the impact of process configuration and solvent on physical chemical properties of lignin extracted from *MxG*. Our group has successfully demonstrated the use of sub-critical water (SCW) modified with ethanol and carbon dioxide (CO_2). Previously our group has referred to the solvent as modified organosolv, where the modification is the replacement of inorganic acids with carbon dioxide which under pressure creates carbonic acid that serve as a catalyst for hydrolysis reaction (Rogalinski *et al*., 2008). The

motivation to replace mineral acids with the CO_2 was to improve the environmental impact as CO_2 is non-toxic, non-flammable and low cost (Abbas *et al*., 2008).

Adopting the biorefinery concept underpinned by SCW as the solvent has the potential to support the generation of, multiple products from hemicellulose and lignin, the two components that in addition to cellulose dominate lignocellulosic biomass. However, the process configuration has the potential to introduce changes to the physical and chemical properties of lignin such as molecular weight, structure and reactivity. Therefore, a major objective of this study was to evaluate the impact of sequential SCW mediated extraction of hemicellulose etc. from *MxG* prior to delignification using SCW with modifiers and to compare the lignin produced with that recovered direct delignification.

Once recovered the major goal has been and remains to develop addition added value applications. In general, lignin in its unmodified state has inherent complex and heterogeneous chemical structure. Despite the fact that it is difficult to use directly unmodified lignin in various bio-based material applications such as cosmetics, pharmaceuticals and polymer composites due to its degree of cross linking inter-unit linkages and steric hindrance effects (Yuan *et al.*, 2010). The unmodified lignin also has a relatively high molecular weight depending on the extraction method and source of lignin. The use of unmodified lignin in polymer materials also is limited by the unmodified lignin's poor blend compatibility (Duval and Lawoko, 2014).

Numerous studies have investigated the incorporation of lignin into a polymeric matrix such as gelatin film (Núñez-Flores *et al.*, 2013), polyurethane (Ignat *et al.*, 2011) and wood adhesives (Mansouri *et al.*, 2007). Currently, the bio-replacement ratios in lignin utilisation for bio-materials are very low in the range of 5 to 30% (Mahmood *et al.*, 2016). Further increasing the bio-replacement ratios resulted in substandard of physico-chemical properties of lignin bio-materials. Lignin exists as a globular supramacromolecular structure which has many interactions such as lignin-lignin and lignin-polysaccharide interactions, and highly reactive, that tend to form large aggregates, thereby affect the biomass deconstruction (Achyuthan *et al.*, 2010).

Currently, efforts to increase the use of lignin in biopolymer applications is related to the degradation or deconstruction of lignin to small monomers by depolymerisation and chemical modification of lignin to increase reactive sites into lignin molecules (Matsushita and Yasuda, 2003; Xu *et al.*, 2014). Moreover, the available reactive hydroxyl groups in lignin demonstrate possibilities for chemical modifications such as esterification prior to lignin valorisation into valuable materials (Duval and Lawoko, 2014). The incorporation of esterified lignin into polyesters, polymeric material is recommended to break up the lignin complexes structure, increase the plasticising ability, therefore the blends of modified lignin with polymer possess good physico-chemical properties (Li and Sarkanen, 2005).

Therefore, the present research explored the lignin aggregates deconstruction at different ethanol concentration of soluble lignin extract by dilution, in which aim to produce lignin with low molecular weight prior to lignin

modification. Lignin with high availability of hydroxyl groups could also improve the bio-contents ratio in the bio-based materials formulation (Mahmood *et al.*, 2016). In summary, the source and extraction method used to recover lignin influences the overall molecular weight, structure and reactivity. Research groups in Europe and the USA are also exploring the potential of Miscanthus sp. for biomass production and ultimately lignocellulosic ethanol production. Therefore, given the current significant volume and evolving interest in Miscanthus sp. in both Europe and the USA, within the emerging biorefining concept, there is a need to evaluate the impact of processing on the potential downstream lignin utilisation.

1.2 Aim and Objectives

The overall aim of this study was to develop an understanding of the impact of the process configuration and the utility of SCW and associated modifiers on the physico-chemical properties of lignin extracted from *MxG*, with the goal of improving the efficacy of esterification of fatty acids on to the lignin macromolecule thereby increasing the opportunity to develop lignin based biomaterials.

This study has the following specific objectives:

i. Develop an understanding of the impact of processing routes on the purity and chemical properties of lignin extracted from *MxG* via SCW (Chapter 4).
ii. Assess and characterise the impact of the size of lignin aggregates on the physico-chemical features of the macromolecule (Chapter 5 and 6).
iii. Assess the impact of dilution on the availability of hydroxyl groups on the overall efficacy of esterification and therefore level of lignin macromolecule modification (Chapter 6).

1.3 Overview of the Thesis

Chapter 1 introduces the subject of the research and the objectives of the thesis. Chapter 2 presents a current literature review on lignocellulosic biomass and research contributions made towards a bio-based economy and integrated biorefinery. In addition, the methods available to extract lignin, currents and emerging applications of lignin as well as lignin depolymerisation and modification are also discussed. Chapter 3 explains the materials of the work and general characterisation techniques for lignin fraction used during the study, followed by Chapters 4, 5 and 6, which present the results and discussion of the study. Chapter 4 gives the results for the assessment of the impact of processing routes (different extraction methods) on the purity and chemical properties of lignin extracted directly from *MxG* using direct SCW extraction and with that obtained from *MxG* which had been subjected to sequential SCW mediated hydrolysis (sequential extraction) of increasing severity. In Chapter 5, the evaluation of organosolv lignin derived aggregates, including both liquid and solid fractions obtained by different ethanol concentrations are presented. Chapter 6 discusses the influence of physico-chemical properties of organosolv lignin aggregates at different lignin concentration on the efficacy of lignin esterification. Finally, Chapter 7 presents the conclusions of the study and recommendations for future work.

CHAPTER 2: LITERATURE REVIEW

2.1 Introduction

The literature review describes the refining of biomass (biorefining) to produce diverse marketable bio-based products and bioenergy. More importantly, the use of lignocellulosic biomass focusing on *Miscanthus x giganteus (MxG)* is explored. The various lignin extraction methods published in the available literature are discussed. Finally, methods of lignin depolymerisation and modification to alter the chemical structure of lignin and to improve lignin reactivity, therefore, the range of biochemicals produced are also discussed.

2.2 Bio-based Economy and Integrated Biorefinery

Energy and material needs play an essential role in the world's future. Currently, about 80% of the world's energy markets rely on crude oil, coal and natural gas which is expected to last for around another 60 and 120 years at the current rate of consumption (Balat and Ayar, 2005; Potumarthi *et al.*, 2014). Global energy requirements, depletion of fossil fuel reserves, high cost of fossil fuels and greenhouse effects caused by fossil fuel usage have caused workers all over the world to seek another alternative and sustainable energy sources (Duku *et al.*, 2011).

First generation biofuels were produced from sugar or starch rich food crops such as sugarcane, corn and wheat. Of major environmental and ethical

concern is that this approach has limited green house gas reduction and competes for land with food production (Sims *et al.*, 2008). In comparison, second generation biofuels derived from agricultural and forest residues, non-food crop feedstocks and lignocellulosic feedstocks have the advantages of lower cost, improved environmental performance and resolve the food versus fuel debate (Havlík *et al.*, 2011; Thompson and Meyer, 2013). Therefore, biomass which has a world production of around 146 billion tonnes a year, and could be source of bioenergy if processed as a biofuel (Balat and Ayar, 2005).

Biomass feedstock can be utilised directly for heat generation as wood fuel or be refined to different products of solid, gaseous or liquid biofuels such as pellets, chips, charcoal, biodiesel, ethanol and biogas (World Bioenergy Association, 2016). These fuels are converted to heat, electricity, transportation or for industrial purposes. The global annual bioenergy potential is estimated at 4500 Exajoules (EJ), which is stored in biomass (World Bioenergy Association, 2016). With world primary energy consumption of 600 EJ/year, this means over eight times is stored in biomass as much as the global energy required (Cigolotti, 2012; Schou *et al.*, 2010). Bioenergy potential of biomass, by 2050, taking into account steady growing population and the world energy demand, could be projected up to 1000 EJ (Moriarty and Honnery, 2012).

An integrated biorefinery is the sustainable processing of biomass into a spectrum of bio-based products such as food, feed, chemical and materials as well as bioenergy including power, heat and biofuels (IEA Bioenergy,

2009). The processes within an integrated biorefinery comprises of various mechanical pretreatments such as extraction, fractionation and separation, thermochemical conversions and enzymatic fermentation. At the end of the biorefining process, a sustainable condition is reached which is economic, environmentally and socially beneficial, as well employs renewable feedstocks (Figure 2.1).

Within the integrated biorefinery concept, an area of research that has gained significant interest is the processing of lignin which, as said, is the second most abundant natural polymer after cellulose and hemicellulose. However, the processing of lignin is not without its problems. Four major issues have been reported (Yuan *et al.*, 2013), namely; difficulties with

- recovery of lignin from the product stream,
- purification of lignin,
- the heterogenous structure of lignin,
- the reactivity of lignin.

This complexity means that development of isolation techniques and chemical modification to produce a selective product is difficult. Nevertheless, lignin could offer a substantial opportunity in enhancing the operation of a lignocellulosic biorefinery for high-value application using various technologies.

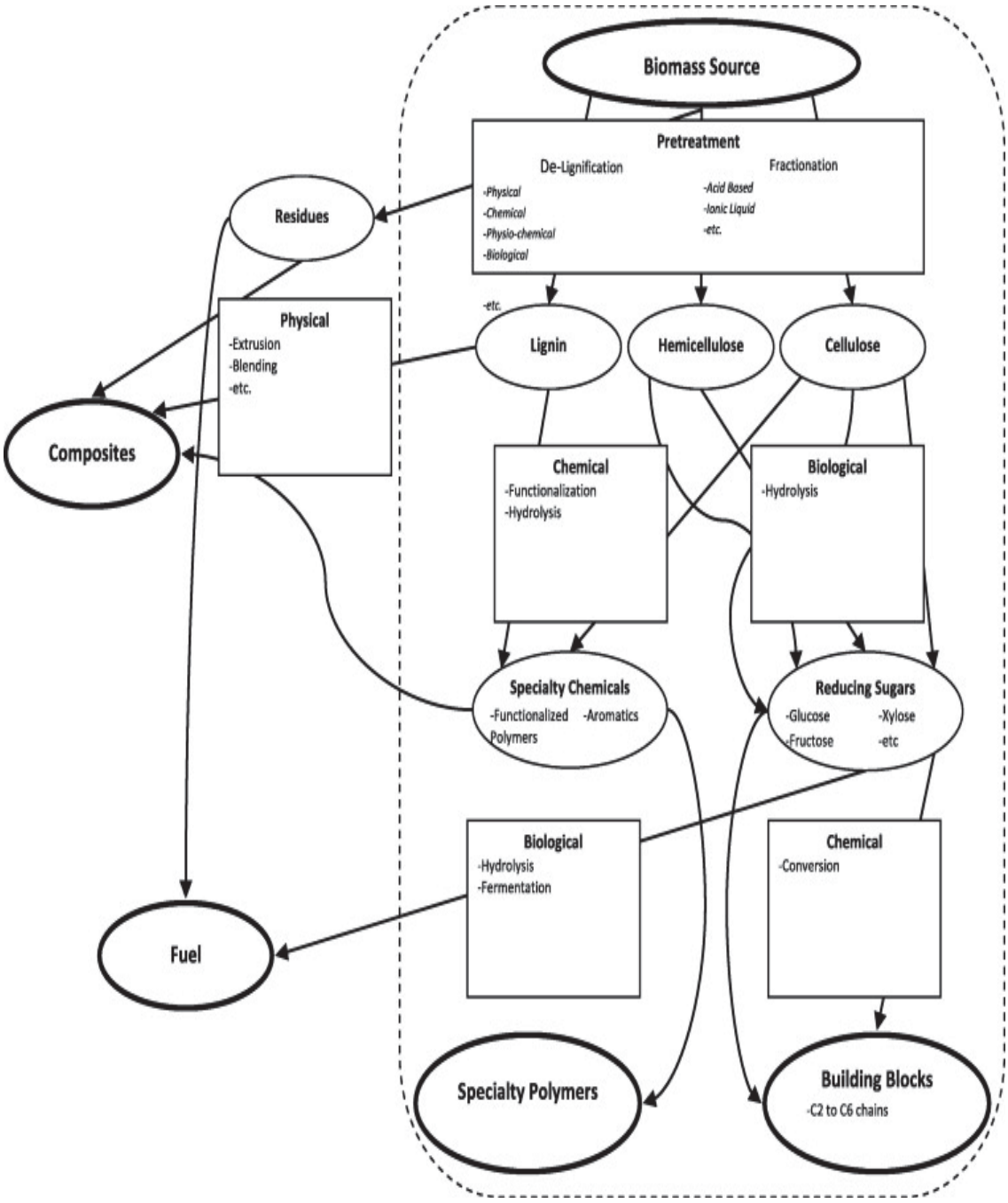

Figure 2.1. Conceptual biorefinery schematic. (Source: Adapted from FitzPatrick *et al.*, 2010).

2.3 Biomass

Biomass can be broadly defined as any biological material derived from living, or recently living organisms. Biomass encompasses numerous raw materials from the biosphere including agricultural crops, timber, marine plants, other conventional agriculture, forestry and fisheries resources, pulp sludge, black liquor and other organic industrial waste, municipal waste such as kitchen garbage, paper waste and sewage sludge (Yokoyama and Matsumura, 2008) as illustrated in Figure 2.2.

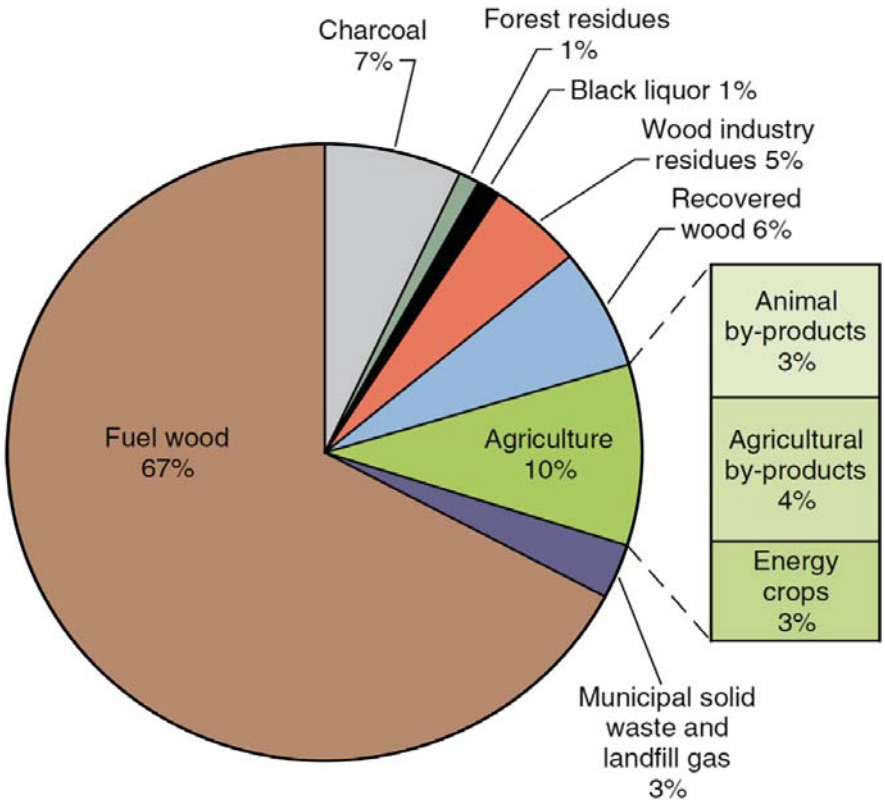

Figure 2.2. The share of biomass sources in the world. (Source: Adapted from *World Energy Balances*, 2009).

The categories and sources of biomass feedstocks are tabulated in Table 2.1.

Table 2.1. Categories and biomass sources. (Source: Adapted and modified from Demirbas, 2009; Slade *et al.*, 2011).

Categories	Biomass Sources
Forest products and residues	Short rotation forestry Wood chips from branches, tips and poor quality stem wood Logging residues Trees, shrubs, sawdust, bark, trimmings
Energy crops	Conventional crops: annual crops (cereals, oil seed rape, sugar beet) Perennial energy crops: short rotation coppice (willow or poplar); plantation tree crops e.g. eucalyptus; energy grasses: miscanthus, switch grass
Agricultural and residues	Straw from cereals, oil seed rape and other crops Animal manures and slurries from cattle, pigs, sheep and poultry Animal bedding such as poultry litter
Marine and residues	Algae, water weed, water hyacinth, reed and rushes
Food waste	Initial production, through processing, handling and distributions to post-consumer food/kitchen waste from hotels, restaurants and individual houses, e.g. peel/skin, shells, husks, cores, pips/stones, fish heads, pulp from juice and oil extraction, etc. Waste material from manufactured foods and drinks including beer, whisky and wine, cheese and other dairy products.
Industrial waste and co-products	Clean and contaminated waste wood Paper/card/board and textile wastes Sewage sludge from waste water treatment works

Biomass production differs by country and by end users. There are a few key factors that influence the potential of biomass production by certain country such as the size of the country and the available of liberated agricultural or marginal lands, the adequacy of its weather, the availability and the cost of the work force (Popp *et al.*, 2014; Walter *et al.*, 2006). Other than

that, the most important factors are the choice of biomass energy crops per unit of land and exploring the difference biomass conversion technologies which could improve the sustainable demand and production besides reduce negative impacts on land use (Bentsen and Felby, 2012; van Dam *et al.*, 2007).

Overall, the biomass supply can be divided into three main sectors, namely; agriculture, forestry and waste sectors. Table 2.2 summarises the overview of global biomass supply sources.

Table 2.2. Global biomass supply sources (Source: Adapted from Kummamuru *et al.*, 2015).

Sector	Fuel sources	Share in primary energy (%)	Primary energy supply (EJ)
Forestry	Fuelwood	67	37.7
	Charcoal*	7	3.94 (13.1)
	Forest residues	1	0.56
	Black liquor	1	0.56
	Wood industry residues	5	2.81
	Recovered wood	6	3.37
Agriculture	Animal by products	3	1.69
	Agricultural by products	4	2.25
	Energy crops	3	1.69
Waste	Municipal solid waste and landfill gas	3	1.69
Total			56.2

*Charcoal is not a primary energy source and is obtained from wood – a conversion factor of 30% from wood to charcoal is used.

Furthermore, the availability of biomass also contributed by the forests which are the dominant terrestrial ecosystem on Earth, totaling over 4 billion

hectares (FAO, 2010; Parikka, 2004). Figure 2.3 shows the global forest cover map. 31% of the forest area is located in Asia, followed by 21% in South America, 17% in Africa, 17% in North and Central America, 9% in Europe, and 5% in Oceania (FAO, 2010). According to Global Forest Resources Assessment (FAO, 2010), the five most forest-rich countries are the Russian Federation, Brazil, Canada, the United States of America and China. As forests are the dominant terrestrial ecosystem of the Earth and account for 80% of Earth's total plant biomass (Kindermann *et al*., 2008), the major part of biomass that consists of cellulose, hemicellulose and lignin is ripe for exploitation for different functions in the future.

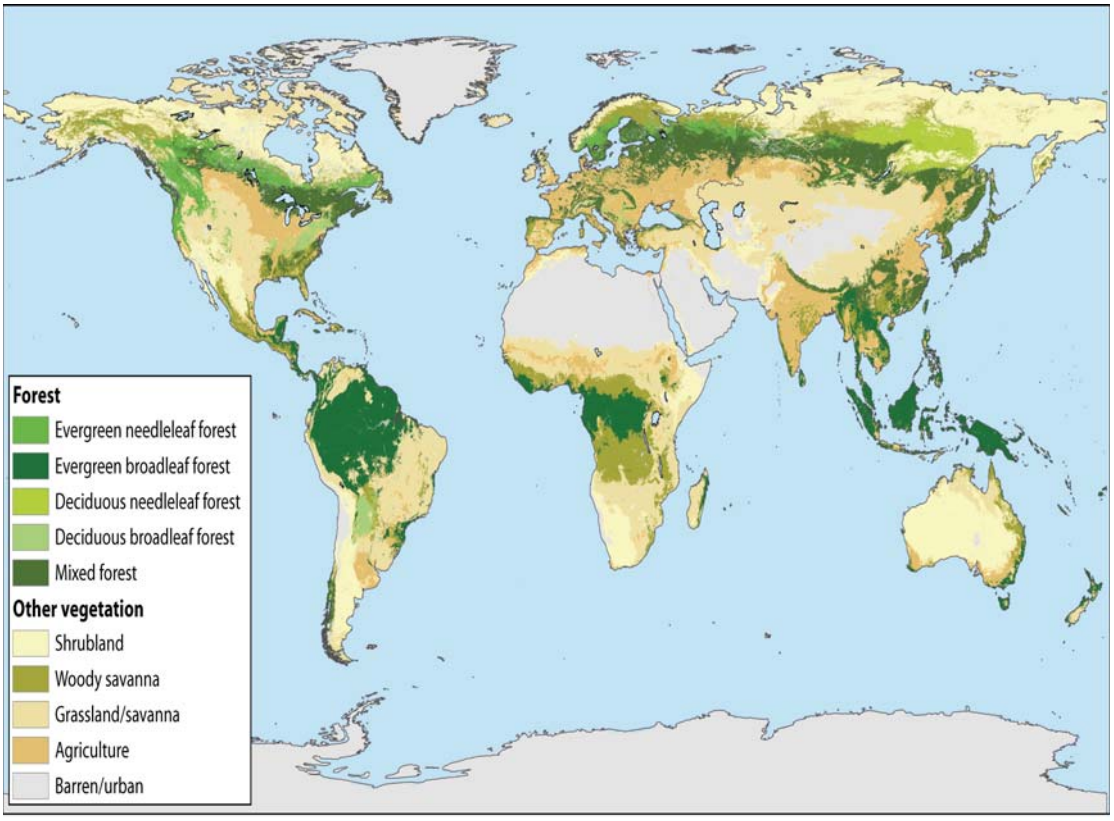

Figure 2.3. Global forest cover map. (Source: Adapted from Pan *et al.*, 2013).

2.4 Lignocellulosic Biomass

In the plant cell wall, lignin is deposited dominantly in secondary cell walls and only smaller amounts are found in primary cell wall. Within the secondary cell walls, the microfibrils formed by cellulose are arranged in a specific pattern and these form 50 to 80% of the cell walls' components (Jain, 2006; Hu and Yue, 2010). As well as cellulose and lignin, hemicellulose is also present in the plant cell wall. Hemicellulose binds and interacts with cellulose microfibrils, and in some cell walls, with lignin which increases their strength (Scheller and Ulvskov, 2010). In general, the lignocellulosic biomass within the cell wall has an intricate structure with typical composition ranges of 35-50% cellulose, 20-35% hemicellulose, 10-15% lignin as well as 15-20% ash and other components (Mood *et al.*, 2013). Figure 2.4 shows the close structural association of cellulose, lignin and hemicellulose.

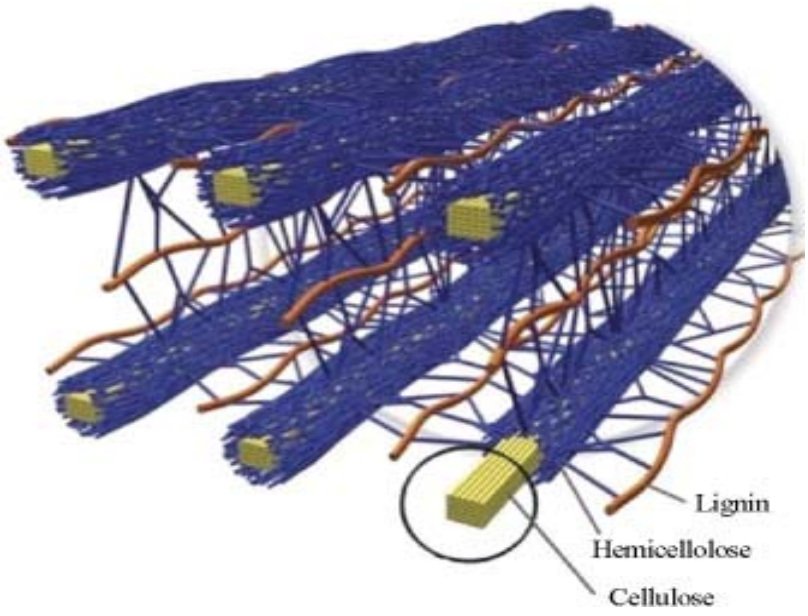

Figure 2.4. Close association of cellulose, hemicellulose and lignin. (Source: Adapted from Doherty *et al.*, 2011).

2.4.1 Cellulose

Cellulose has been considered as the most copious organic compound derived from biomass (Watkins *et al.*, 2015). The systematic study of cellulose was initiated by French agricultural chemist Anselme Payen in 1837 to 1842 (Suhas *et al.*, 2016). Cellulose confers structural support of plants cell walls with fibrous, tough and water insoluble characteristics (Agbor *et al.*, 2011; Suhas *et al.*, 2016). The worldwide production of cellulose has been estimated between 10^{10} to 10^{11} tonnes per year (Samir *et al.*, 2005). Cellulose has been commercialised for various applications including paper, textile, materials and chemical industries (Ummartyotin and Manuspiya, 2015). In bioefineries, cellulose has been converted into glucose for bioethanol production via fermentation or enzymatic hydrolysis process (Sindhu and Pandey, 2016).

Cellulose is comprised of a linear homopolymer chains of β-D-glucopyranose moieties strongly linked via β-1,4 glycosidic bonds with repeating unit of disaccharide cellobiose. The degree of polymerisation of cellulose chains in lignocellulosics of up to 10,000 glucopyranose units has been identified (Khalil *et al.*, 2012) and as high as 15,000 glucopyranose units in native cotton (Agbor *et al.*, 2011). The chemical formula of cellulose is $(C_6H_{10}O_5)_n$ with an average molecular weight of 10,000 (Rubin *et al.*, 2007) and the structure of cellulosic units joined by glycosidic linkages is shown in Figure 2.5. Cellulose chains of 20 to 300 repeating units are incorporated together to form microfibrils that are bound to construct cellulose fibres. (Agbor *et al*., 2011). The degree of crystallinity of cellulose, which determines

the rate of enzymatic hydrolysis in bioethanol production, differs with origin and pre-treatment (Hall *et al.*, 2010).

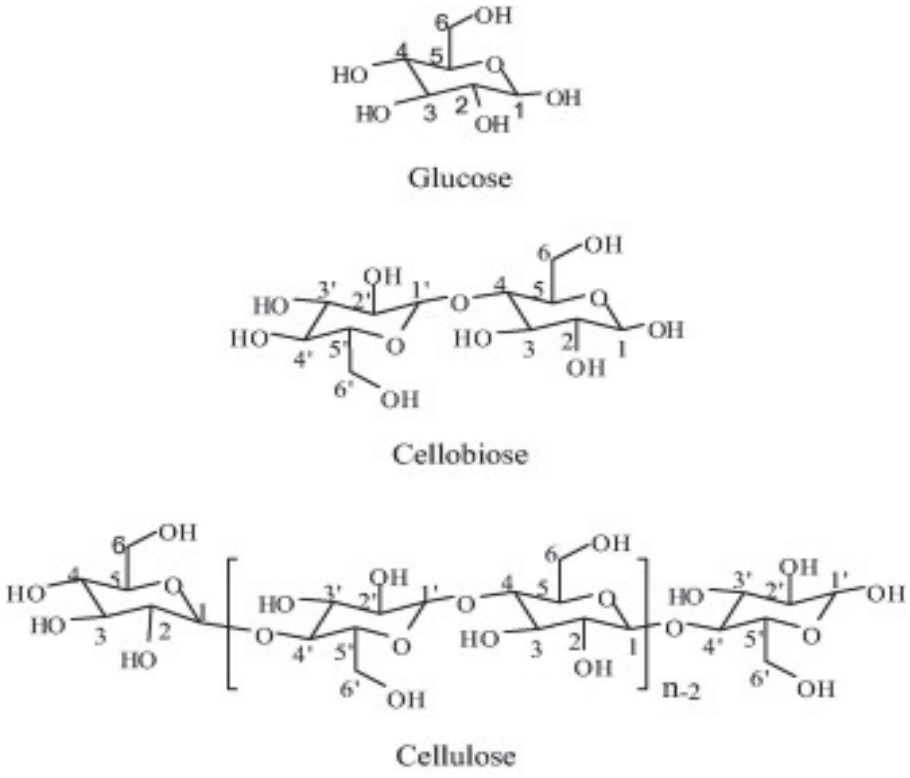

Figure 2.5. Cellulosic units joined by glycosidic linkages. (Source: Adapted from Suhas *et al.*, 2016).

2.4.2 Hemicellulose

In contrast, hemicellulose, $(C_5H_8O_4)_n$, is more amorphous and heterogenous branched biopolymers of various hexoses (glucose, galactose, mannose, and or/rhamnose), pentoses (xylose and arabinose) and acids (glucuronic acid, methyl glucuronic acid, and galacturonic acid) (Zheng *et al.*, 2014). The composition and structure of the hemicellulose varies according to source. For instance, softwood hemicelluloses are comprised mainly of glucomannan, whilst hemicellulose in agricultural biomass such as grasses

and straw contain mainly xylan (Agbor *et al*., 2011). Figure 2.6 shows the main constituents of hemicelluloses.

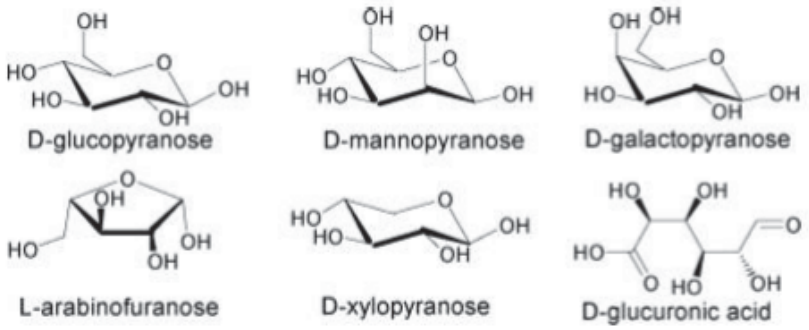

Figure 2.6. Main constituents of hemicellulose. (Source: Adapted from Mohammad, 2008).

Hemicelluloses are easily hydrolysed due to their lower molecular weight compared to cellulose and their branched structure with short lateral chain (Li *et al.*, 2010; Saha, 2003). The degree of polymerisation of hemicelluloses is between 80 to 200 sugar units and average molecular weight of < 30,000 (Anwar *et al.*, 2014; Mohammad, 2008). Substantial amount of hemicelluloses and lignin need to be removed from cellulose fibres, rendering the cellulose more accessible for enzymatic hydrolysis process (Agbor *et al*., 2011). Nevertheless, process conditions including temperature, reaction time, moisture content and pH must be carefully chosen to prevent formation of undesirable products such as fulfural and hydroxymethylfulfural that have been shown to hinder the fermentation process (Agbor *et al.*, 2011; Jönsson and Martín, 2016).

Hemicelluloses provide a renewable material supply for wide variety of industrial applications, for example, xyloglucans from hemicellulose have been used for pharmaceutical applications such as antibiotics and a treatment

for ulcers (Pauly *et al.*, 2013). Hemicellulose sugars, pentose (xylose and arabinose) and hexose (glucose, galactose and mannose) also have been utilised for conversion of lignocellulosic materials to fuel ethanol and other value added fermentation products including 5-hydroxymethylfurfural (HMF), furfural, levulinic acid, and xylitol (Canilha *et al.*, 2003; Saha, 2003). Moreover, hemicelluloses act as wet strength additives in papermaking, viscosity modifiers in food packaging film as well as tablet binders (Peng *et al.*, 2012).

2.4.3 Lignin

Lignin is built up from three different phenyl propane monomers, which form complex macromolecules, which then form an amorphous, three-dimensional polymer. The three phenyl propane monomers, namely *p*-coumaryl, coniferyl and sinapyl alcohol differ in the substitution at the 3 and 5 positions (Mansouri and Salvadó, 2006) as shown in Figure 2.7. Lignin is formed via two types of linkages; condensed linkages (e.g. 5-5 and β-1 linkages) and ether linkages (e.g. α-O-4 and β-O-4 linkages) (Abiven *et al.*, 2011; Zobel and Buijtenen, 1989). Figure 2.8 shows the structure of major bonds in lignin.

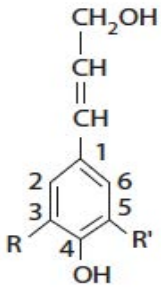

Substituents	Name
R = R' = H	*p*-coumaryl alcohol
R = H, R' = OCH_3	coniferyl alcohol
R = R' = OCH_3	sinapyl alcohol

Figure 2.7. Lignin monomeric building blocks. (Source: Adapted from Lapierre, 2010).

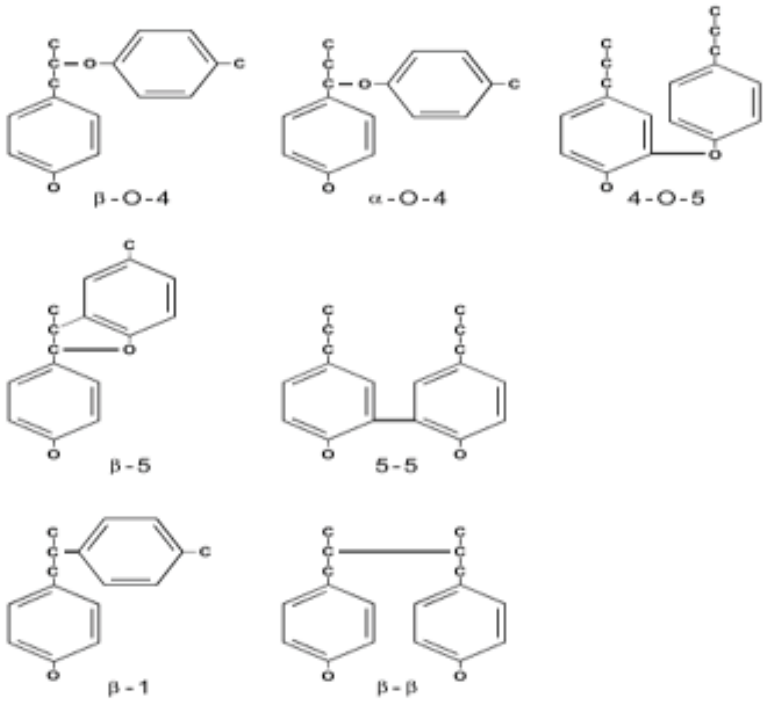

Figure 2.8. Structure of the major bonds in lignin. (Source: Adapted from Kogel-Knobner, 2002).

The starting points for the formation of guaiacyl and syringl structures of lignin are derived from coniferyl and sinapyl alcohol as outlined in Figure 2.9.

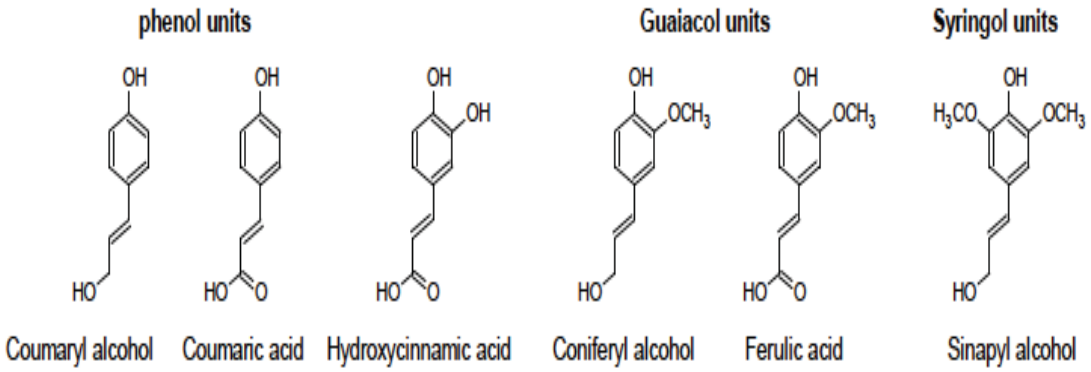

Figure 2.9. Types of phenyl propanoids units found in lignin. (Source: Adapted from Holladay *et al.*, 2007).

Hardwoods or angiosperms are made up of guiacyl and syringl units, while softwoods or gymnosperms contain only guaiacyl units. Besides, grasses contain a variety of acidic guaiacyl units attached as esters and demonstrate more substitution of *p*-coumaryl alcohols such as ferulic, hydroxycinnamic and *p*-coumaric acids (Holladay *et al.*, 2007). Guaiacyl units (G) have one aryl-OCH_3 group, syringyl units (S) have two aryl-OCH_3 groups and *p*-hydroxyphenyl units (H) have no OCH_3 groups.

The composition, molecular weight and even the amount of lignin differ depending on the plant source, the method of extraction as well as among plants of different species (Harkin, 1969; Tejado *et al.*, 2007; Vanholme *et al.*, 2010). Other than in the xylem cells or wood of the trunk, the significant amount of lignin found in the leaves, seeds, pith, bark, roots, fruits and branches within the same plant also varies (Kutscha and Gray, 1970). Lignin composition and overall quantity may also depend on the development state of the cell and tissue, and the effect of environmental stress (Campbell and Sederoff, 1996; Rencoret *et al.*, 2011). The difference in composition with various possibilities of inter-connecting patterns among individual units results in a very complex range of lignin molecules structure (Norgren and Edlund, 2014). A representation of a structural model of lignin demonstrating different inter-connecting patterns is shown in Figure 2.10.

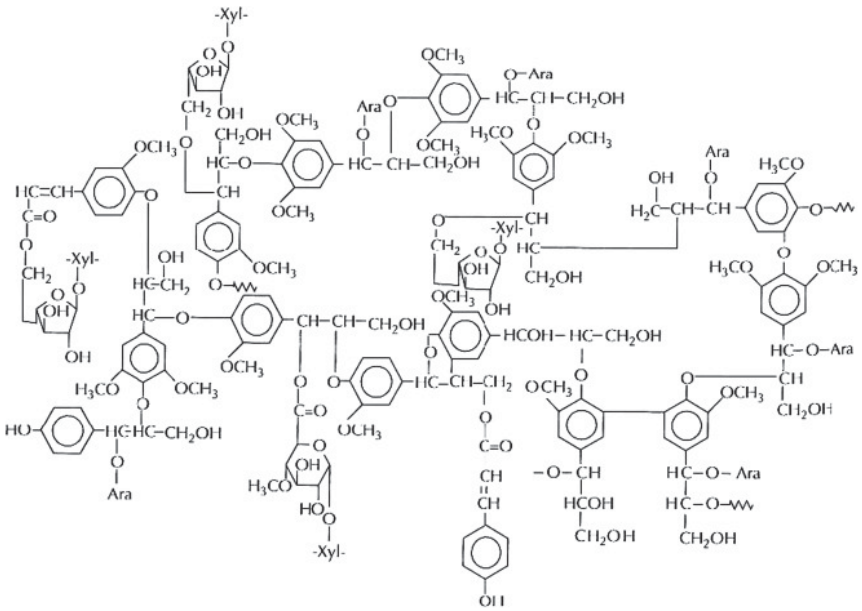

Figure 2.10. A structural model of wheat straw lignin. (Source: Adapted from Ghaffar and Fan, 2014).

Lignin plays various roles in plants, alongside the main natural components of cellulose and hemicellulose. Lignin gives stiffness and structural stability of a plant cell wall by cementing and fixating lignin with other polysaccharides in the plant cell wall (Alberts *et al.*, 1989). The presence of lignin makes the plant fibres more rigid and stiff, providing mechanical support for the stem and branches enabling healthy plant growth (Henriksson, 2009). Besides, lignin also works as glue that binds the individual plant cells and the other carbohydrate polymers in the complex secondary wall (Achyuthan *et al.*, 2010). Lignin makes the cell wall in intercellular regions of xylem by providing the hydrophobic capillary surface needed for nutrient transport (Leisola *et al.*, 2012; Myburg *et al.*, 2013). Moreover, lignin serves an essential function in plant defense. The lignified cell wall serves as a barrier against microorganisms by preventing the

penetration of polysaccharide degrading proteins secreted by microorganisms on the cell wall (Leisola *et al.*, 2012).

2.5 *Miscanthus x giganteus (MxG)*

Biofuel or bioethanol conversion from biomass is recently gaining attention as replacement to petrol. Maize and sugarcane have been used chiefly in the major countries undertaking bioethanol production, USA and Brazil (Hattori and Morita, 2010). The growing concern about food fuel competition and low energy efficiency have driven most countries to shift from sugar or starch-derived bioethanol to cellulosic bioethanol (Sticklen, 2008). Cellulosic bioethanol could be produced from crops residues and dedicated energy crops including switchgrass, willow and Miscanthus. *Miscanthus* sp. has been proven as one of the highest energy biomass potentials according to research done in the USA and Europe in various soils, regions and climate zones over the last 20 year (Kryževičienė, 2011). In the research presented in this thesis, *MxG* was thus the lignocellulosic biomass chosen.

Miscanthus sp. is a perennial rhizomatous grass, native to subtropical and tropical regions of Asia as shown in Figure 2.11. It is a genus comprising of about 25 species. Amongst them, *Miscanthus sinensis, Miscanthus sacchrisflorus* and *MxG*; have the best potential for biomass production (Chung and Kim, 2012; Wahid *et al.*, 2015). From the different species of *Miscanthus* sp., *M. sinensis* and *M. sacchrisflorus* hybridised to form *MxG*. *MxG* is commercially cultivated for biomass production due to its high biomass yield (Chung and Kim, 2012). Globally, *Miscanthus* sp. yields range

from 2 to 44 tonnes/ha dry matter; yields range from 27 to 44 tonnes/ha in Europe and the USA Midwest, and from 10 to 11 tonnes/ha in Canada (Heaton *et al.*, 2008; Pyter *et al.*, 2007; Scurlock, 1999; Xi and Jezowski, 2004).

Figure 2.11. *Miscanthus* sp. energy crop. (Source: Adapted and modified from Falter *et al.*, 2015).

Miscanthus spp. originated in Japan and first cultivated in Europe in the 1930s (Brosse *et al.*, 2012). Seasonal changes and with its bioclimatic location may have affected the relative composition of biomass including *MxG* (Savy and Piccolo, 2014). Other factors that affect the biomass yield and composition of *Miscanthus* sp. are genotypes, soil types, nutrients used as well as crop age (Brosse *et al.*, 2012).

When comparisons are made with other genotypes, *MxG* has a strong range of potential benefits including the possibly unique and exclusive trait for

adaptation to climate and environmental conditions, low levels of nutrient needed, soil carbon storage and ease of harvest and handling (Jørgensen, 2011; Kryževičienė, 2011; Wang *et al.*, 2008; Xi and Jezowski, 2004). *Miscanthus* sp. possesses C4 photosynthesis pathway that shows remarkable potential of higher radiation, water and nitrogen efficiency when compared to C3 plants such as poplar, willow and wheat (Chung and Kim, 2012; Lewandowski *et al.*, 2000). The C4 and C3 plants are differed in the mechanism of carbon fixation by two different types of photosynthesis process (Byrt *et al.*, 2011). In a systematic comparison of C4 and C3 plants based on metabolic network analysis, Wang *et al.* (2012) concluded that the C4 plants increased biomass production, increased the efficiency use of light and facilitate CO_2 concentration than that in C3. In addition, *MxG* also had an efficient rhizome system, which plays a key role as nutrients reserve for the annual shoot growth in the growing season (Lewandowski *et al*., 2000). In summary, the *Miscanthus* spp. are amongst the most-cold tolerant C4-plant and conserve a high CO_2 assimilation at temperatures below 15°C (Jørgensen, 2011; Wang *et al.*, 2008).

2.6 Biomass Pretreatment

Biomass conversion has been focused on the production of desirable chemical products through various technological routes. There are few methods that employ complete biomass degradation including pyrolysis, gasification, liquefaction and the Fischer-Tropsch process (Swain *et al.*, 2011). Current biomass to biofuel processes perform complete biomass

degradation without emphasis on fractionating the main components of the lignocellulosic feedstock; cellulose, hemicellulose and lignin. Nevertheless, the biomass pretreatment has been suggested in the biorefinery concept, so that multiple added-value products can be generated. In general, the conversion of lignocellulosic materials to bioethanol employs two processes, (1) hydrolysis of cellulose in the lignocellulosic materials to fermentable reducing sugars by enzymes, and (2) fermentation of sugars to ethanol by yeasts or bacteria (Manorach *et al.*, 2015; Sun and Cheng, 2002) as illustrated in Figure 2.12.

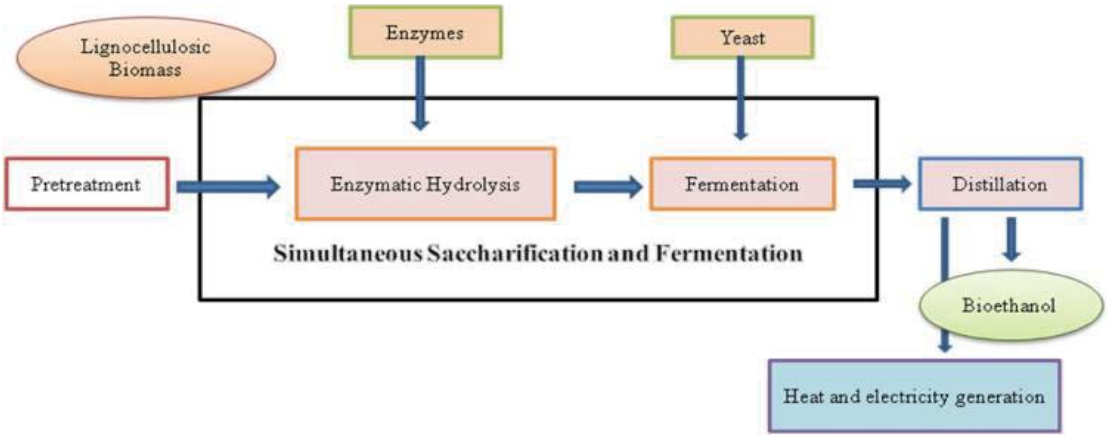

Figure 2.12. Conversion of lignocellulosic biomass to bioethanol. (Source: Adapted from Maurya *et al.*, 2013).

Pretreatment can be performed using combinations of various processes including size reduction followed by biological, chemical and physical treatments. But, after size reduction, lignin and hemicellulose still block the access of cellulase enzymes to the cellulose molecule due the intact cell wall structure or porosity (accessible surface area) of materials (Sun and Cheng, 2002; Tong *et al.*, 2013), thus reducing the efficiency of hydrolysis process. Furthermore, high crystallinity of cellulose make the hydrolysis of

cellulose into glucose for bioethanol production more difficult (Kumar *et al.*, 2009).

The goal of pretreatment focuses on following requirements (1) solubilise hemicellulose and lignin (2) increase the accessible surface area and decrystallise cellulose (3) partial depolymerisation of cellulose and hemicellulose (4) modification of the lignin structure (5) maximise the enzymatic digestibility of the pretreated biomass (6) minimise the loss of sugars and (7) minimise capital and operating costs (Maurya *et al.*, 2013). The schematic of the role of pretreatment on lignocellulosic biomass is shown in Figure 2.13.

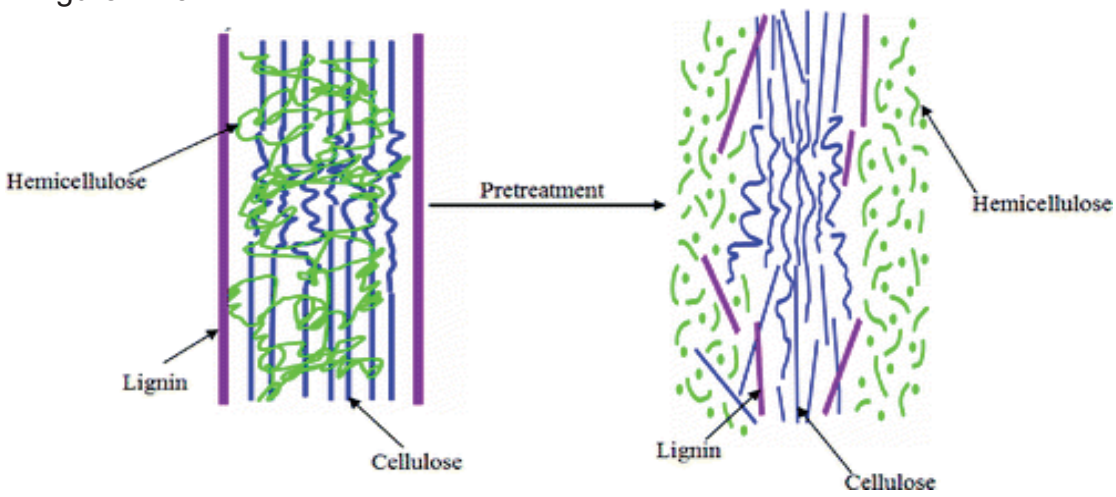

Figure 2.13. Schematic of the role of pretreatment on lignocellulosic biomass. (Source: Adapted from Kumar *et al.*, 2009, Modified from Hsu *et al.*, 1980).

Pretreatment can be divided into four categories: physical methods (e.g. grinding and milling), chemical methods (e.g. using acids, alkali, organic solvents), physicochemical methods (e.g. steam explosion or hydrothermolysis), and biological methods (e.g. using microorganisms and fungi to treat biomass) (Tong *et al.*, 2013). Table 2.3 presents the various

pretreatments which aim to fractionate, solubilise, hydrolyse and separate cellulose, hemicellulose and lignin.

2.7 Lignin Extraction

As already stated, one of the potential alternative energy sources is bioethanol derived from various types of lignocellulosic materials. The effectiveness of bioethanol production in the biorefinery model is to ensure that all components of biomass are fully utilised to produce a wide range of value-added products (Ping *et al.*, 2011). Pretreatment processes enables a clean fractionation of lignocellulosic feedstocks and the recovery of high-quality lignin, resulting in significant interest in order to stimulate development in lignin valorisation (Brosse *et al.*, 2011).

Taking into consideration the range of various promising technologies available to develop a pretreatment process for bioethanol production and lignin recovery, two methods were chosen as they showed a possibility of biomass fractionation which are sub-critical water and the organosolv method.

Table 2.3. Advantages and disadvantages of different pretreatment methods of lignocellulosic biomass. (Source: Adapted and modified from Maurya *et al.*, 2013).

Pretreatment method	Concept	Advantages	Disadvantages
Milling	-The size of feedstock materials is usually 10 to 30 mm after chipping and 0.2 to 2 mm after milling or grinding (Sun and Cheng, 2002). -Mechanical comminution including dry, wet and vibratory ball milling (Mosier *et al.,* 2005).	-Decrease of cellulose crystallinity and degree of polymerisation. -Reduction of particle size to increase speficic area and pore size.	-High power and energy consumption
Steam explosion	-Biomass is promptly heated by a high-pressure saturated steam with or without chemicals for a certain time, then pressure is instantly released and biomass encountered an explosive decompression (Tong *et al.*, 2013)	-Causes lignin transformation and hemicellulose solubilisation. -Lower cost -Higher yield of glucose and hemicellulose in the two-step method.	-Generation of toxic compounds. -Partial hemicellulose degradation
Liquid hot water	-It also known as hot compressed water (HCW), hydrothermal pre-treatment , sub or supercritical water treatment (Roque, 2013). -Water pretreatment at high temperatures that is kept under pressure to maintain it in the liquid state (Maurya *et al.*, 2013).	-Size reduction of the biomass is not needed. -No chemicals are generally required. -No requirement of corrosion-resistant materials.	-High energy and high water requirements. -Very high pressure requirements.
Organosolv	-Use organic solvent or organic solvent mixtures with inorganic acid catalysts,i.e. sulfuric acid and hydrochloric acid and to extract lignin from biomass (Maurya *et al.*, 2013).	-Causes lignin and hemicellulose hydrolysis.	-Solvents need to be drained or recycled. -High cost.

Pretreatment method	Concept	Advantages	Disadvantages
Ammonia fiber expansion (AFEX)	-Biomass is subjected to liquid ammonia at high pressure and temperature for a period of time, and then the pressure is suddenly released (Sun and Cheng, 2002). -Similar concept of steam explosion process.	-Increase accessible surface area. -Less inhibitor formation -Does not require small particle of biomass.	-Not very effective for the biomass with high lignin content. -High cost of large amount of ammonia.
CO_2 explosion	-Similar to steam explosion and AFEX, however, the concept of supercritical CO_2 explosion operated at lower temperature than steam explosion and perhaps a reduce expense than AFEX (Kumar *et al.*, 2009).	-Increase accessible surface area and availability at relatively low cost. -Do not form inhibitory compounds. -Not-flammability. -Easy recovery after extraction and environmental acceptability.	-Very high pressure requirements.
Wet oxidation	-Biomass are treated with water and air/oxygen at temperatures higher than 120°C (Maurya *et al.*, 2013). -Parameters such as temperature, reaction time and oxygen pressure (Palonen *et al.*, 2004)	-High degree of solubisation of hemicellulose and lignin. -Avoid formation of degradation compounds.	-High cost of oxygen and alkaline catalyst.
Ozonolysis	-Biomass treated with ozone as oxidising agent performed at room temperature and pressure in packed beds, fixed beds or stirred semi-batch reactors (Mosier *et al.*, 2005).	-Effectively removes lignin content. -Does not produce toxic residues. -Reaction is carried out at room temperature and pressure.	-High cost of large amount of ozone.

Pretreatment method	Concept	Advantages	Disadvantages
Concentrated acid	Concentrated acids such as H_2SO_4 and HCl have also been used to treat lignocellulosic materials for enzymatic cellulose hydrolysis (Sun and Cheng, 2002)	-High glucose yield. -Ambient temperatures.	-High cost of acid and need to be recovered. -Corrosion-resistant equipment are required. -Concentrated acids are toxic and hazardous.
Diluted acid	-The most conceivable for industrial scale (Tong *et al.*, 2013). -Different types of reactors are developed including percolation, plug flow, batch, shrinking bed, countercurrent reactor and flow-through reactor (Maurya *et al.*, 2013).	-High recovery of sugars at the end of the process. -Low formation of toxic products.	-Concentration of reducing sugars in relatively low. -Generation of degradation products.
Alkali	-The process involving slurrying the lime with water, spraying it onto the biomass, and storing the material in a duration of hours or even weeks (Mosier *et al.*, 2005).	-Decrease in the degree of polymerisation and crystallinity of cellulose. -Disruption of lignin structure	-High cost. -Not used for large-scale plant.
Biological	-Perform via microbial or enzyme treatment to modify the chemical composition of the biomass and improve the sugar release yield by cellulose (Roque, 2013).	-Low energy requirements. -Delignification. -Reduction in degree of polymerisation of cellulose. -Partial hydrolysis of hemicelluloses. -No chemical requirements. -Mild environmental conditions.	-Slow process rate. -Very low treatment rate. -Not very effective for commercial application.

The use of SCW for biomass pretreatment have been gaining attention in the field of green chemistry as the SCW is cheap, non-toxic, non-flammable, non-explosive and has advantages such as the SCW does not require additional catalysts and corrosion-resistant materials for reactors (Rogalinski *et al.*, 2008; Taherzadeh and Karimi, 2008). In addition, the use of SCW and associated modifiers of the modified organosolv pretreatment proposed in this work offers promising path for 'green' methods to support an environmentally process of lignin extraction from lignocellulosic biomass. Since hydrolysis of *MxG* in this work was performed via modified organosolv method using SCW, ethanol and carbon dioxide, there would therefore seem to be a definite need for further explanation of hydrolysis of *MxG* methods, which were discussed in section 2.7.1 and 2.7.2, respectively.

2.7.1 Sub-critical water (SCW)

SCW which is also known as superheated water extraction and pressurised hot water extraction, is an environmentally friendly method whereby water is applied to biomass at pressures up to 218 atm and at temperatures from 100°C to the critical temperature of 374°C to maintain in the liquid state as shown in Figure 2.14 (Yesodharan, 2002; Zakaria and Kamal, 2016).

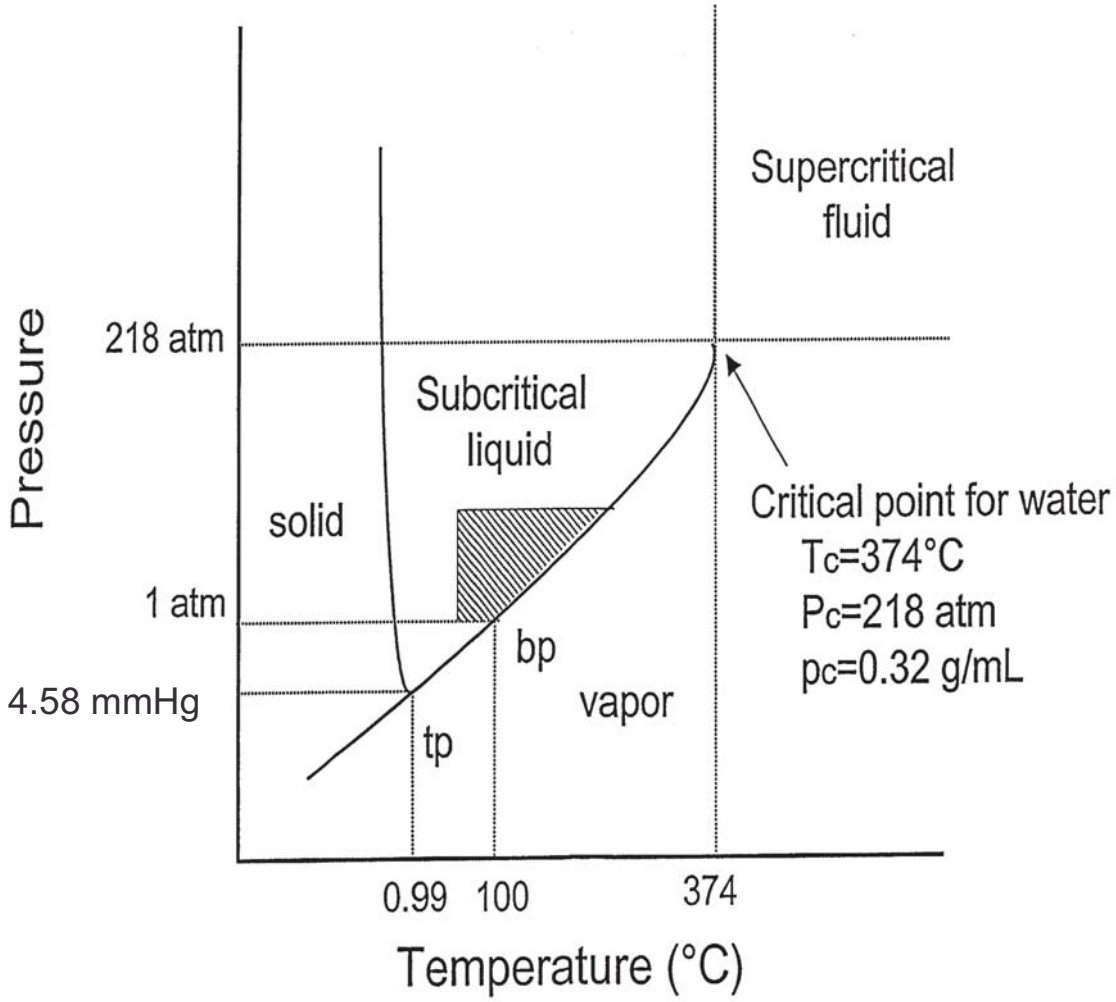

Figure 2.14. Phase diagram of water as a function of temperature and pressure. (Source: Adapted from King and Grabiel, 2007).

The SCW has several unique properties compared to water at ambient conditions especially for its dielectric strength and ionic product that causes dramatic changes in physical properties (Rogalinski *et al.*, 2008). Dramatic rise of temperature in SCW causes a decrease in permittivity, an increase in the diffusion rate and a decrease in the viscosity and surface tension (Asl and Khajenoori, 2013). As a result, more polar target materials with high solubility in water at ambient conditions are extracted most effectively at lower temperatures, while moderately polar and non-polar materials need a less polar medium influenced by elevated temperature (Asl and Khajenoori, 2013;

Smith, 2006). Thus, certain conditions of SCW need to be assessed such as temperature and pressure, so that targeted compounds could be extracted. These interesting properties make SCW an outstanding medium for rapid, homogenous and efficient reactions (Toor *et al.*, 2011). Figure 2.15 illustrated the range of property variations, ionic product (K_W), density and dielectric constant (ε) that occur throughout the SCW depending on the temperature at specific pressure (30 MPa).

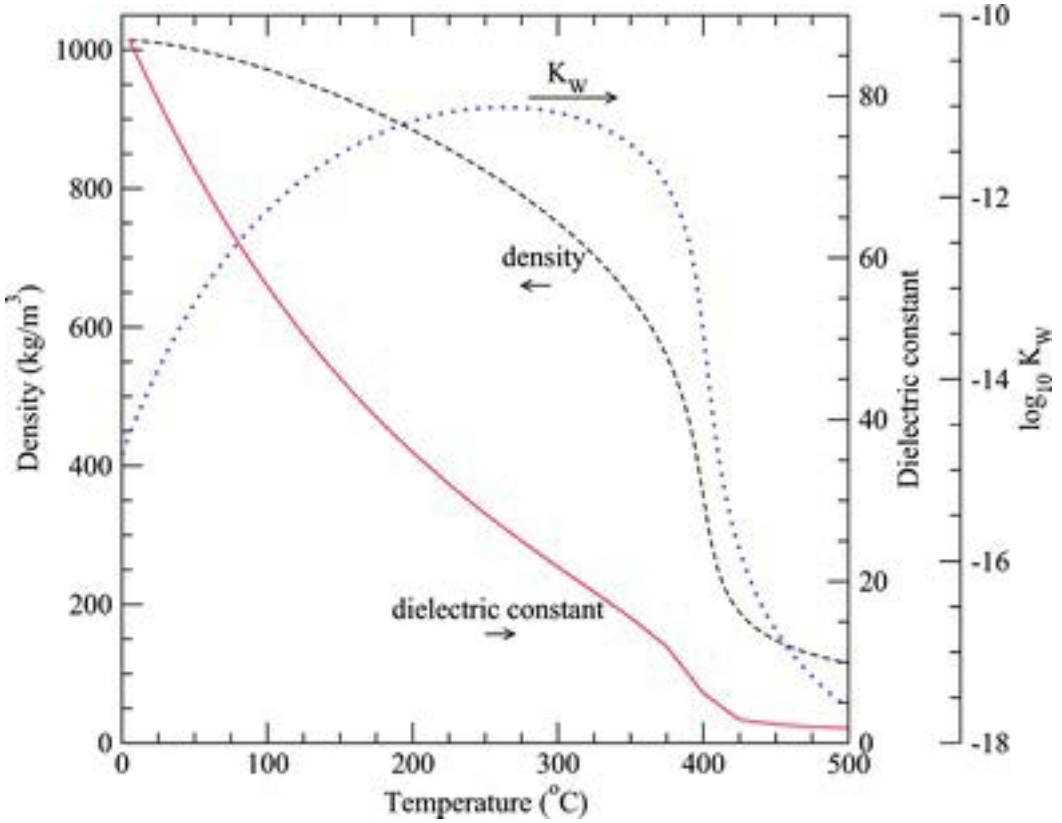

Figure 2.15. Water properties at 30 MPa as a function of temperature. (Source: Adapted from Peterson *et al.*, 2008).

The dielectric constant, ε decreases with the temperature; the resultant H-bond weakening and allows autoionisation of water into acidic hydronium ions (H_3O^+) that act as catalysts in the sub-critical region (Ando *et al*., 2000; Roque, 2013), thus increasing the efficacy of solubilisation in the SCW

process. For example, hydronium ions are generated from acetic acid from acetyl groups and uronic acid that are associated with hemicellulose assist in the liquor acidification by formation of hydrogen ions for extraction reaction (Ruiz *et al.*, 2013). The release of the acids aid to remove oligosaccharides. Nevertheless, hemicelluloses may be further hydrolysed to monomeric sugars and partially degraded to aldehydes (fulfural and 5-hydroxymethyl furfural) that have been found to inhibit the microbial fermentation of bioethanol (Mosier *et al.*, 2005). The dielectric constant, ε and ionic product, K_w decrease drastically at supercritical conditions.

The dielectric constant is the polarity measurement of the solvent as reflected by the hydrogen bonds strength and hydrogen bonding structure. Hydrogen bonds are stronger and the dielectric constant value is higher at lower temperatures leading to an increase of solubility of lignocellulosic targeted components by the process (Carr *et al.*, 2011). The dielectric constant of water is around 80 at room temperature (25°C) and reduces to about 33 at 200°C, which becomes similar to some organic solvents such as methanol and ethanol (Zakaria and Kamal, 2016). Use of SCW instead of organic solvents can be considered as “green” process since SCW is non-flammable and non-toxic (Filly *et al.*, 2016).

Mixing of organic solvents with water could improve the efficiency of SCW extraction. For instance, defatted rice bran treated with combination of ethanol and SCW exhibited an improved antioxidative capacity compared with that obtained using SCW alone (Chiou *et al.*, 2012). The recovery of catechins from tea leaves, grape seeds and phenolic compounds from grape was

enhanced by using a mixture of methanol and SCW (Palma *et al.*, 2002; Piñeiro *et al.*, 2004).

In summary, numerous studies have been conducted to assess the effectiveness of SCW to fractionate cellulose, hemicellulose and lignin over ranges in conditions from different material including sugarcane baggase (Manorach *et al.*, 2015), *MxG* (Hage *et al.*, 2010), oak wood (Cabeza *et al.*, 2016) and grape seed (Yedro *et al.*, 2014). Thus, it was decided within research group that SCW is a preferable and promising method for the utilisation of the main lignocelluosic components in this work.

2.7.2 Organosolv

Organosolv pretreatment was discovered in 1931 by Kleinert and Tayenthal who showed that delignification of wood could be done using a mixture of water and ethanol at elevated temperature and pressure (Sixta, 2006). There are variety of organic solvents have been found to be acceptable for pulp production including methanol, ethanol, acetone, ethylene glycol, triethylene glycol and tetrahydrofurfuryl alcohol (Zhao *et al.*, 2009). The most common organosolv pulping method uses ethanol and methanol, because of low cost, low boiling point, and miscibility with water (Sannigrahi and Ragauskas, 2013; Tong *et al.*, 2013).

Nowadays, the biorefining concept applies the organosolv process that uses organic or aqueous organic solvent mixtures with inorganic acid, which act as catalysts to dissolve lignin and hemicellulose in solvent while cellulose remains as undissolved solids prior to enzymatic hydrolysis (Maurya *et al.*,

2013; Yuan *et al.*, 2013). The organosolv pretreatment is performed at high temperature usually between 185 to 210°C, under atmospheric pressure or high pressure (Zhao *et al.*, 2009), no acid is added to the process since organic acids, i.e. acetic acid and other release acid components from biomass react as catalyst for the breakage of lignin-carbohydrate complex structure (Duff and Murray, 1996). Nonetheless, addition of mineral acid catalysts such as hydrochloric acid, sulphuric acid and phosphoric acid have been shown to improve delignification and accelerate xylan degradation (Sun and Cheng, 2002; Zhao *et al.*, 2009).

In the research presented in this thesis, a modified organosolv method is proposed and is aligned using a mixture of organic solvents, ethanol and water for a delignification process. The mixture of ethanol and water or dual mixture increase the extraction efficiency since one solvent improves analyte solubility whereas the other may improve the analyte desorption (Mustafa and Turner, 2011). The modified organosolv method carried out at higher temperature also improves the mass-transfer kinetics by breaking analyte-matrix interactions especially hydrogen bonding, promotes desorption of analytes from the sample maxtrix, thereby increases the diffusivity and solubility of analytes (Plaza and Turner, 2015). Nevertheless, the modified organosolv method does not use mineral acids owing to the potential environmental issues and neutralisation products after pretreatment.

CO_2 is utilised as a substitute to mineral acids of the organosolv method as CO_2 dissolves in aqueous solution to form carbonic acids which enhance the hydrolysis rate (Sun and Cheng, 2002). CO_2 molecules are

comparable in size to water enabling easy penetration into small and porous pores accessible to water molecules (Abas *et al.*, 2008; Kumar *et al.*, 2009). Consequently, CO_2 disrupts cellulose and hemicellulose structure during explosive release of CO_2 pressure and increases the surface area of substrate available for enzymatic hydrolysis (Zheng *et al.*, 1998).

The application of SCW associated with organosolv treatments have been reported in the literature. Huijgen *et al.* (2012) recovered lignin from wheat straw prior to cellulose enzymatic hydrolysis. They conducted SCW treatment in water acidifed with H_2SO_4 in an autoclave reactor with a regime of temperatures between 160 to 190°C, a reaction time between 30 to 120 minutes to hydrolyse hemicellulose followed by the organosolv method. The organosolv method (ethanol-water mixtures) was carried out using conditions of temperature between 190 to 220°C and a reaction time of 60 minutes. Lignin was recovered depending on various conditions and the effect of solvent concentrations were further discussed in this thesis.

This work is different from the work done by Hage *et al.* (2010). Hage *et al.* (2010) examined the effect of first step pretreatment using SCW with or without 2-Naphtnol pretreatment and followed by organosolv method that utilised sulfuric acid as a catalyst in ethanol-water solution of *MxG.* The first step is to depolymerised hemicelluloses at mild condition. The results demonstrated that an increase in temperature of SCW process from 130 to 150°C affected the lignin structure for the subsequent organosolv delignification at 170°C, whereby the SCW process could enhance the lignin fragmentation and foster re-polymerisation reactions.

Amendola *et al.* (2012) used a two-step process: SCW pretreatment at 180°C for 30 minutes followed by ethanol organosolv at 180°C for 90 minutes for hemicelluloses and lignin recovery from red grape stalks. The results suggest that a milder treatment helped to hydrolyse hemicellulose, whereas the organosolv process did not give a consistent delignification depending on lignin precipitation steps by addition of acetic acid before or after the organosolv pretreatment.

Similarly, Hasegawa *et al.* (2004) proposed a two-step extraction process for thermo-chemical conversion of biomass. In a two-step extraction, hemicellulose was hydrolysed as saccharides via SCW pretreatment at 180°C for an hour and subsequently lignin was recovered as the soluble and cellulose as the residue through water/acetone extraction (50% by volume) at 230°C and an hour extraction time. All of the studies reviewed here support the hypothesis that a combination of SCW with organosolv could be an appropriate method to recover lignin from different materials.

In this work, a three-step process was applied, consisting of SCW pretreatment for first and second step, which to prepare extractives-free fibres and to hydrolyse hemicellulose, respectively; followed by SCW with associated modifiers, for separating lignin from *MxG* cellulose fibres. Compared with work done by Hage *et al.* (2010), instead using mineral acids as a catalyst for organosolv treatment; the third or delignification step in this work utilised CO_2 that form carbonic acid as a catalyst. Even though the utilisation of CO_2 enhances the lignocellulosic bond cleavage, Lü *et al.* (2013) suggested that addition of co-solvent such as water, ethanol and others may

be used to improve the removal of lignin. While Hage *et al.* (2010), Amendola *et al.* (2012) and Hasegawa *et al.* (2004) did not perform any extraction of non-bounded compounds (extractives) step, the first step in this work to remove extractives prior to delignification could increase the purity of lignocellulosic components such as lignin, hemicellulose and cellulose as well as improving the subsequent enzymatic digestibility for bioethanol production (Baptista *et al.*, 2006; Frankó *et al,*, 2017).

2.8 Application of Lignin: Current and Emerging

Lignin has unique and complex chemical structure that allows for use in a broad range of applications. The major sources of lignin are from cooking liquors generated in wood pulping processes (lignosulphonates) and the global production of lignin-based materials and chemicals exceeds 50 million tonnes per annum (Smolarski, 2012). Table 2.4 presents the type of lignin, volume, purity and potential applications.

Table 2.4. Lignin types, volumes, purity and and potential applications. (Source: Adapted from Smolarski, 2012).

Lignin Type	World Annual Production (tonnes)	Lignin Purity	Potential Products
Low-purity lignin	50,000,000	Low	Energy Refinery (carbon cracker)
Lignosulphonates	1,000,000	Low-medium	Refinery (carbon cracker) Cement additives Bitumen
Kraft lignin	60,000	High	Refinery (carbon cracker) Cement additives Biofuel High-grade lignin BTX Activated carbon Phenolic resins Carbon fibres Vanillin Phenol
Organosolv lignin	1000	High	Phenolic resins Activated carbon Phenolic resins Carbon fibres Vanillin Phenol derivatives
High grade lignin	N/A	Very high	Carbon fibres Vanillin Phenol derivatives

Lignosulphonates are also known as lignin sulfonates or sulfite lignins, that result from the sulphite pulping process. In this process, wood is digested at 140-170°C in an aqueous solution of a sulphite or bisulphite salt of either sodium, ammonium, magnesium or calcium (Francisco *et al.*, 2015) . The type of salt and its solubility characteristics determine the pH of the digestion process (Stewart, 2015). For instance, if calcium bisulphite is used as the

pulping agent, the pulping medium will become highly acidic and alkaline for sodium sulphite. The main reaction scheme for lignosulphonate formation during acid sulphite pulping is illustrated in Fig. 2.16.

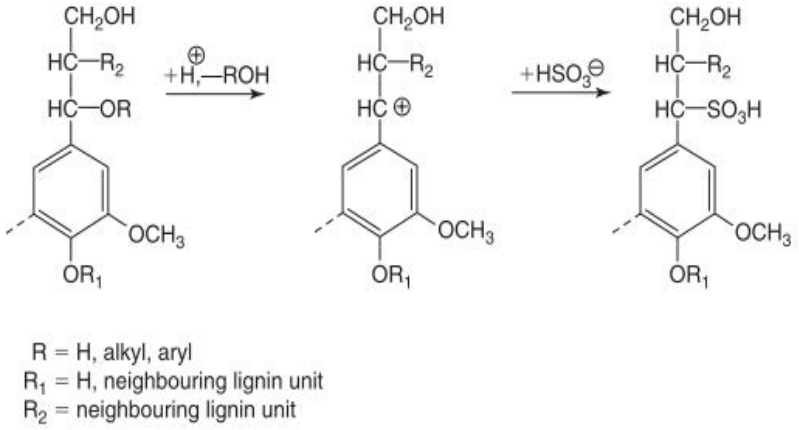

Figure 2.16. Main reaction scheme for lignosulphonate formation during acid sulphite pulping. (Source: Adapted from Lora, 2008).

Lignosulphonate has good water solubility at all values of pH and has been used by industry in a wide variety of applications. Lignosulphonate has been used as a binder or glue in pellets or compressed materials (Tumuluru *et al.*, 2011) and also used to reduce dust particles and stabilise the road surfaces (Edvardsson, 2010). This binding ability makes lignosulfphonate an essential component of materials such as ceramics, animal pellets, coal briquettes and others (Lora, 2008). In addition, lignosulphonate also acts as a dispersant especially in concrete mixes. Lignosulphonate attaches to the particle surface, keeps the particle from being attracted to the other particles and reduces the amount of water needed for cement or concrete mixes (Yang *et al.*, 2008).

Moreover, lignosulphonate works as emulsifier for wax emulsions, pigment and dyes by stabilising emulsions of immiscible liquids such as oil and water (Gupta, 2008). Lignosulphonate also functions as a sequestrant by binding up metal ions, preventing them from reacting with other compounds and becoming insoluble, thus preventing scale deposits in water systems. They are used in several applications such as cleaning compounds, water treatments for boilers and cooling systems (Khanal *et al.*, 2010).

Most recently, many more emerging and sophisticated applications are emerging from lignin. The environmental benefits of the interaction of lignin with others polymers as an alternative to fossil fuel based raw materials has driven the investors or manufacturing producers to seek new value-added products. The ability of lignin to be used as a raw material in a wide range of products is indisputable.

Few studies have been reported about lignin in various applications including coatings for fertilizers (Mulder *et al.*, 2011), food packaging films (Bhat *et al.*, 2013), carbon black (Snowdon *et al.*, 2014), phenol formaldehyde resins (Ciobanu *et al.*, 2004; Thring *et al.*, 1997) and others. Thus, lignin has been incorporated with polymer with various methods including injection, moulding, blending and extrusion technology with different operating conditions to make it more useful as different function and other uses beside to provide as starting materials for huge range of chemicals, building blocks and polymers.

2.9 Chemical Modification

Research into the structure of lignin is very challenging due to its complex and heterogenous structure, its lack of stereoregularity and its different types and molecular weight (Tiainen *et al.*, 1999). The differences in complex structure and physicochemical properties of lignin are influenced by the type and species of woody or non-woody biomass, technical process and the method used to separate lignin from black liquor (Pawar *et al.*, 2016).

Raw lignin has been utilised without chemical modification by incorporating lignin into other polymers to improve the physical and chemical properties of polymer formulations. Raw lignin can be employed in various additives in plastics applications such as in ultraviolet protection, antioxidant, in reinforcement fillers or in flame retardants which can reduce the costs of final products (Kai *et al.*, 2016; Laurichesse and Avérous, 2014; Thakur *et al.*, 2014). However, raw lignin can only be blended in a small amount (~20-30%) within the polymer, i.e. preparation of polyurethane foams, due to its incompatibility with many other polymers (Kai *et al.*, 2016) and further increasing the bio-replacement ratios results in fragile and low strength foams (Mahmood *et al.*, 2016).

Thus, chemical modification of lignin prior to incorporation into the polymer might enhance the versatility of its applications in sustainable biopolymers (Francisco *et al.*, 2015). Chemically, lignin has a variety of functional groups including aliphatic and phenolic hydroxyls, carboxylic, carbonyl and methoxyl groups (Laurichesse and Avérous, 2014; Naseem *et al.*, 2016). Lignin has phenolic hydroxyl groups and aliphatic hydroxyl groups

at C-α and C-γ positions of side chain, and the phenolic hydroxyl groups are the most reactive functional group that particularly influence the material chemical reactivity (Laurichesse and Avérous, 2014) and provide total content of potential active sites for modification process (Gordobil *et al.*, 2016).

The reactivity of lignin could be increased in three main ways (Laurichesse and Avérous, 2014):

- reduction of molecular mass by fragmentation methods;
- modification of structure to create new chemically active sites;
- chemical modification of hydroxyl groups.

2.9.1 Lignin Fragmentation

A lignin depolymerisation approach usually is carried out to fragment and separate lignin structure into aromatic monomers, whereby the depolymerisation method produces low average molecular weight compounds prior to modification process (Ferdosian *et al.*, 2016, 2012). Lignin depolymerisation cleaves not only the lignin monomer linkages including the aryl-ether and C-C bond, but also another functional groups such as methoxy groups that are attached to the lignin aromatic rings (Constant *et al.*, 2016; Li *et al.*,, 2007; Rinaldi *et al.*, 2016; Xu *et al.*, 2014). The thermochemical conversion for lignin depolymerisation have been proposed including pyrolysis, hydrogenolysis and enzymatic depolymerisation (Xu *et al.*, 2014). Table 2.5 shows the summary of lignin depolymerisation method that have been reported in the literature.

Table 2.5. Summary of lignin depolymerisation method.

Depolymerisation	Concept	References
Pyrolysis	- Lignin is heated to around 500℃ without oxygen. - Two different approaches: Slow (conventional) and flash pyrolysis, with reaction time varies between 5 to 30 minutes. - Slow pyrolysis uses slow heating rate than flash pyrolysis - Flash pyrolysis produces 60-75 weight% of liquid crude bio-oil, 15-25 weight% of solid char, and 10-20 weight% of non-condensable gases. - Main compounds in the oil: monomeric/oligomeric phenolic compounds. - Advantages of short reaction times and high efficacy for conversion of lignin to bio-oil (80%).	(Abdelaziz *et al.*, 2016; Laurichesse and Avérous, 2014)
Hydrogenolysis	- Depolymerisation of lignin in the presence of hydrogen at severe conditions of temperature and pressure. - Acid or base catalysts can be used to increase the reaction rate and the product yield with the final product of liquid oil, gases and char. - One of the promising method to produce phenolic products from lignin. - The presence of hydrogen minimises the char formation.	(Abdelaziz *et al.*, 2016; Xu *et al.*, 2012)
Oxidative	- Thermal treatment in the presence of oxygen, oxidative cracking of lignin including breakage of lignin rings, aryl ether bonds and other associates linkages within lignin due to the presence of large number of hydroxyl groups. - Main products: aromatic aldehydes and carboxylic acids - Most use oxidants for the reaction: metal oxides and hydrogen peroxide	(Lange *et al.*, 2013; Pinto and Borges, 2011; Tarabanko and Petukhov, 2003; Xu *et al.*, 2014)
Enzymatic	- Enzymatic deconstruction uses fungi to degrade low molecular weight lignin fractions, common fungus: *Phanerochaete chrysosporium*, *Pycnoporus cinnabarinus* - Example: Lignin-modifying bacterial laccases able to degrade a phenolic model compound into a mixture of different products including vanillin. - Function of fungus: Creates a lignin peroxidase enzyme that deconstruct the lignin molecule in the presence of both nitrogen and carbon sources.	(de Gonzalo *et al.*, 2016; Eggert *et al.*, 1996; Kosa and Ragauskas, 2013; Xu *et al.*, 2014)

Depolymerisation	Concept	References
Ionic liquid	- Consists of ionic organic/inorganic salts that are liquid at low temperatures (<100 ℃) - Has unique properties including low vapour pressures, chemical and thermal stabilities and the ability to dissolve a wide range of compounds. - Involves various ionic liquid cations and anions such as alkylsulfonate, lactates and acetates. E.g. of ionic liquids: 1-*H*-3-Methylimidazolium chloride, 1-ethyl-3-methylimidazolium diethylphosphate - Acts as both acidic catalyst and solvent in the reaction - Drawbacks including costs and investment, environmental hazards, recyclability, etc. - Form various products including phenols, alcohols and sugar.	(Cox *et al.,* 2011; Xu *et al.*, 2014; Yokoo and Miyafuji, 2014)
Sub- or supercritical water	- Hydrolysis reactions of lignin with water in the presence of catalyst via sub- or supercritical water - Sub-critical water pathway occurs between 200 to 374 ℃, and with pressures between 4 and 22 MPa. - Supercritical water occurs above critical point of water at 374 ℃, and with pressures more than 22 MPa. - Supercritical fluid as solvent had good solubility for lignin depolymerisation - Problem with supercritical water: char formation, high cost - Addition of phenol prevent char formation. - Use of H-donating solvents, such as formic acid, and other stabilising compounds, such as alcohols also reduce char formation. - Form products such as cathecol, phenol, syringol and guaiacol.	(Ayusheev and Taran, 2016; Gosselink *et al.*, 2012; Meng *et al.*, 2016; Pandey and Kim, 2011; Peterson *et al.*, 2008; Wang *et al.*, 2013)

2.9.2 Lignin Modification

Isolated lignin produced with high hydroxyl functionality and low molecular weights could make the lignin suitable for the preparation of lignin bio-based materials with higher percentage of bio-replacement ratios (≥50%) prior modification process (Mahmood *et al.*, 2016). Modification of lignin could improve compatibility of polymer lignin as well as to introduce reactive sites. Here, it is suggested that presence of hydroxyl groups on lignin molecule which are reactive and plentiful could act as local centres of high polarity capable of hydrogen bonding depending on the functionalisation of hydroxyl groups (Duval and Lawoko, 2014; Sivasankarapillai and McDonald, 2011).

Modification of these reactive nuclei resulted in beneficial alteration of lignin solubility (Thielemans and Wool, 2005). Furthermore, it could create lignin polyol derivatives to improve solubility of lignin by converting the most reactive hydroxyl groups, phenolic hydroxyl groups into more reactive aliphatic hydroxyl units (Pandey *et al.*, 2015). Increasing the aliphatic chain reduced the polarity of lignin and enhanced its solubility characteristics. There are various reagents that has been used to form stable chemical bonds as substitute for these reactive hydroxyl groups include alkyl or acid chlorides, anhydrides, carboxylic acids, epoxides, isocyanates, lactones, and nitriles (Chen *et al.*, 2014).

There are various methods to functionalise hydroxyl groups such as esterification, etherification, phenolation and urethanisation. For instance, when lignin is modified by esterification, the modification leads the conversion of phenolic hydroxyl groups into more reactive aliphatic hydroxyl groups with

ester substituent by nucleophilic substitution (Cachet *et al.*, 2014; Wang *et al.*, 2017) and thus, reduce the intermolecular interactions of hydrogen bonding, providing a plasticisation phenomena and mobility of the chains (Lisperguer *et al.*, 2009). Figure 2.17 showed the esterification mechanism of kraft lignin modified using acid chlorides that produces kraft lignin with more reactive aliphatic hydroxyl units.

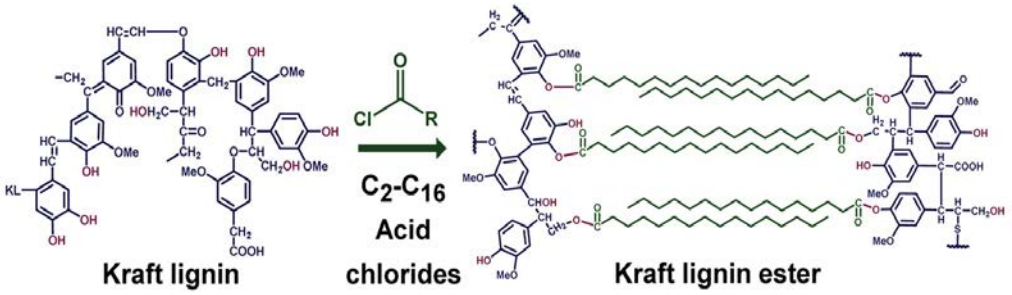

(a)

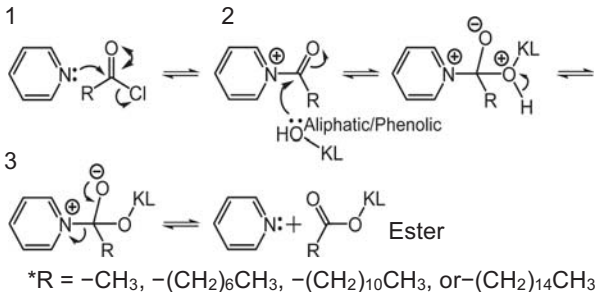

1.Addition of the nucleophile.
2.Elimination of the leaving group, forming the tetrahedral intermediate.
3.Loss of a proton.

(b)

Figure 2.17. (a) Esterification of kraft lignin using acid chlorides (b) Mechanism of pyridine catalysed klason lignin esterification with C_2–C_{16} fatty acid chlorides (Source: Adapted and modified from Koivu *et al.*, 2016).

2.9.2.1 Esterification

Esterification is one of the simplest ways to modify the hydroxyl groups within lignin and depends on the reaction parameters and reactants used

(Laurichesse and Avérous, 2014). There are various esterifying agents including acidic compounds, acid anhydrides and acid chlorides for lignin esterification (Kai *et al.*, 2016). Traditionally, the most common way to make simple esters was by Fischer esterification introduced by the German chemist, Emil Fischer in 1902. The reaction involves an acid base catalysed reaction between a carboxylic acid and an alcohol yielding a specific ester (Juhascik *et al.*, 2012) as shown in Figure 2.18. Esterification has been thus allows for the synthesis of epoxy resins, polyesters and elastomeric materials.

Figure 2.18. Fischer esterification. (Source: Adapted from Cumpstey, 2013).

For instance, a study of esterification modification of soda lignin by acetylation and further blending with low density polyethylene showed an improvement in terms of miscibility of acetylated lignin with non-polar polyethylene and therefore, acetylated lignin has potential to be utilised as an additive in lignin-polyethylene matrices (Buono *et al.*, 2016). The scheme of lignin esterification by acetylation is shown in Figure 2.19. The derivatisation of hydroxyl groups as a platform for chemical modification helps to improve the lignin-polymer interactions and enhancing lignin dispersion into the hydrophobic polymer matrix (Frigerio *et al.*, 2014).

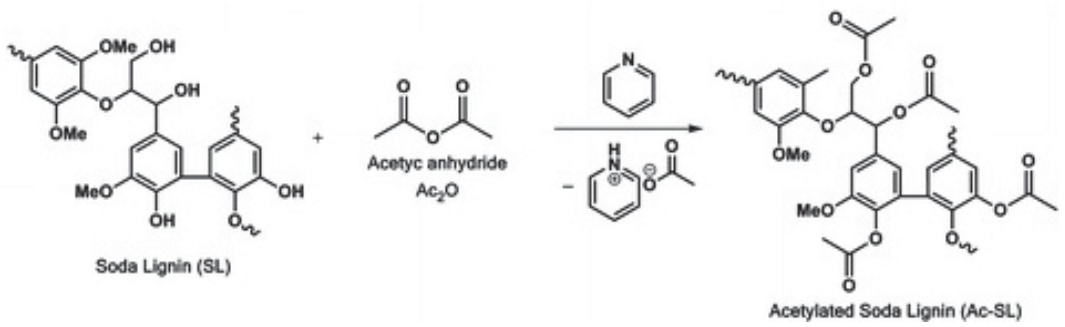

Figure 2.19. Scheme of lignin acetylation. (Source: Adapted from Buono *et al.*, 2016).

2.9.2.2 Etherification

Etherification is another approach to modify lignin with the aim of producing new macropolyols (Sadeghifar *et al.*, 2012; Kai *et al.*, 2016). Hydroxylalkylation and methylation are among the most industrially important methods to focus on etherification of phenolic hydroxyl groups (Figure 2.20). Hydroxyalkylation is usually carried out in aqueous alkali solutions or organic solvents (e.g., toluene) by treating lignin with alkylene oxides such as ethylene oxide, propylene oxide, and butylene oxide (Wang *et al.*, 2016). Other catalysts have been studied to catalyse hydroxylalkylation with hydroxyl groups such as potassium hydroxide, polyphosphazene or polyphosphazenium ion, cesium hydroxide and aluminium tetraphenyl porphine (Laurichesse and Avérous, 2014). Methylation is usually performed in aqueous alkali solutions or organic solvents such as dimethyl sulfoxide or dimethyl formamide by treating lignin with dimethyl carbonate, dimethyl sulfate or methyl iodide (Wang *et al.*, 2016).

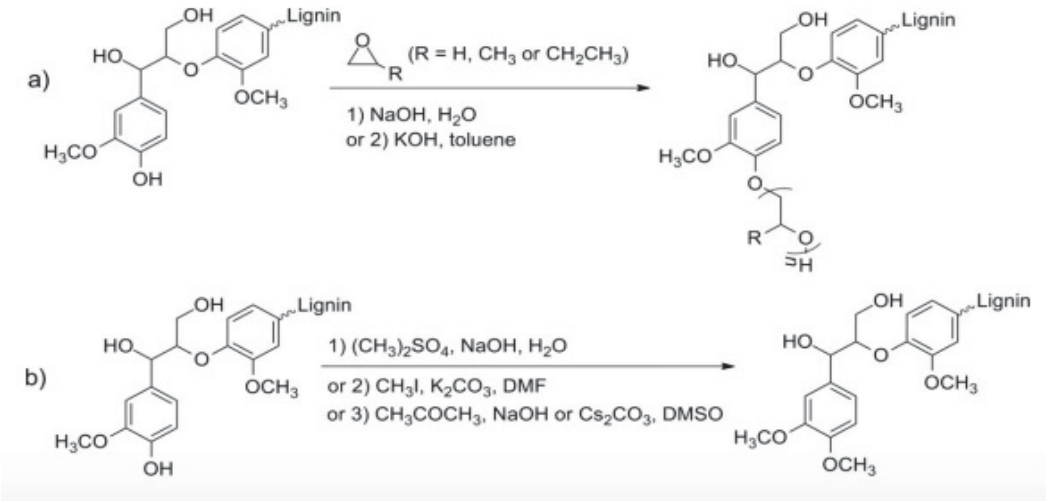

Figure 2.20. a) Hydroxyalkylation and b) methylation of lignin. (Source: Adapted from Wang *et al.*, 2016).

Generally, lignin etherification is associated with polyurethane or polyesters synthesis. In an optimisation study investigating the oxypropylation process, lignin from various sources were modified with propylene oxide and potassium hydroxide as a catalyst (Cateto *et al.*, 2009). Lignin has been used for preparation of polyurethane rigid foams at different conditions including lignin and propylene oxide ratio and catalyst contents. Cateto *et al.* (2009) reported that higher catalyst content or higher lignin/propylene oxide ratio favour hydroxyl activation, formation of short grafts takes place, a lower molecular weight and hydrodynamic volume, in addition to high viscosity with respects to more pronounced homopolymer content (plasticiser role). Moreover, liquid oxypropylated lignin products from modification with alkylene oxides hold great promise in polyurethane foams because of their tensile strength and a great reduction of the glass transition temperatures which depend on the experimental conditions and reactivity of functional groups (Lora and Glasser, 2002).

2.9.2.3 Phenolation

Lignin treated with phenol in the presence of organic solvents, such as ethanol or methanol, prior to resin synthesis is known as phenolation or phenolysis (Effendi *et al.*, 2008). Lignin is thermally treated with phenol in an acidic medium, leading to the condensation of phenol with the lignin aromatic rings and side chains together with cleavage of ether bonds that produces lignin derived monomeric products, thereby decreasing the molecular weight of lignin molecule (Hu *et al.*, 2011).

This chemical modification method is most often used for lignosulphonate. The phenolation could increase the phenolic hydroxyl groups and simplify lignosulphonate structure, thus decreasing the molecular weight of lignosulphonate prior to polymerisation with formaldehyde (Zhao *et al.*, 1994), specifically for synthesis for phenol-formaldehyde resins (Figure 2.21). There has been substantial research focused on utilisation of lignin to substitute petroleum phenol for the past 10 to 15 years in various applications including particleboard production (Çetin and Özmen, 2002; Vallejos *et al.*, 2011), wood adhesive (Mankar *et al.*, 2012; Qiao *et al.*, 2014), coating and moulding materials (Sahoo *et al.*, 2013; Yuan *et al.*, 2010).

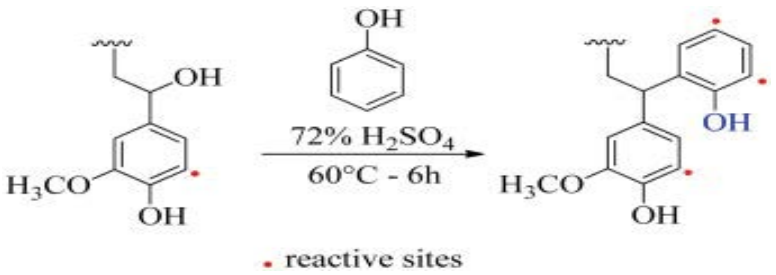

Figure 2.21. Phenolysis reaction and potential reactive sites of phenolised lignin. (Source: Adapted from Laurichesse and Avérous, 2014).

2.9.2.4 Urethanisation

The first urethane was discovered as early as 1849 by Wurtz. Works conducted by Dr. Otto Bayer at IG Farbenindustrie, Germany in 1937 synthesised the first polyurethane using the urethanisation process involving terminal hydroxyl groups in reaction with addition of di-isocyanates or polyisocyanates, forming polyurethane groups in the polymer backbone as shown in Figure 2.22 (Ionescu, 2005; Upton and Kasko, 2015).

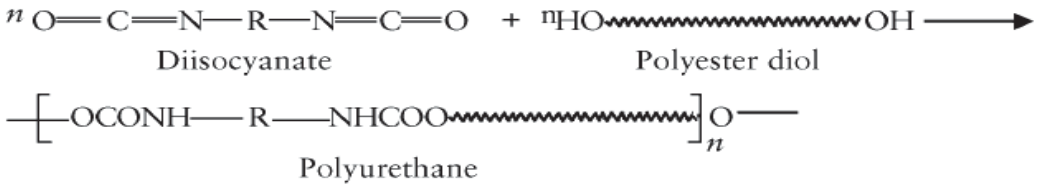

Figure 2.22. Reaction involving hydroxyl groups with isocyanate groups, active RNC=O sites to form a urethane. (Source: Ionescu, 2005).

Lignin is utilised either directly without further chemical modification or after chemical modification with different polyols to produce polyurethane; the latter approach is the most practical method for industrial applications (Laurichesse and Avérous, 2014). A study by Ciobanu *et al.* (2004) of lignin-polyurethane films reported various properties in a series of blends prepared by solvent casting technique obtained in dimethyl formamide solutions from a polyurethane elastomer and different proportions of flax/soda pulping lignin. A major finding was observed in that adding up to 5% lignin contributed to the polyurethane elastomer strength and biodegradability, simultaneously with lower decomposition temperature and elasticity. Hatakeyama *et al.* (2005) studied the mechanical properties of polyurethane-based biocomposites derived from lignin and molasses that could be applied in the field of housing

and construction industry. The mechanical properties of biocomposites developed including the compression strength and modulus of biocomposites were improved in the presence of polyurethane. The biocomposites showed outstanding biocompatible building material characteristics and applicable for practical purposes.

2.10 Summary of Literature Review

As outlined within this chapter, the literature review contains insight into lignocellulosic biomass used within the various pretreatments to fractionate lignocellulosic biomass into its main components; cellulose, hemicellulose and lignin. This chapter also has discussed the established research covering SCW and organosolv methods which has been proposed in this research work. Even though there has been much research and discussion conducted via SCW and organosolv methods, the research within this thesis attempts to focus on comparison of direct and sequential approach for delignification carried out specifically on *MxG* using both SCW and associated modifiers of extraction methods. Lignin produced may result in few reactive sites in particular with respect to lignin modification and further valorisation. What is not covered in the established literature is the aggregation behavior of lignin especially on the structure and morphology of lignin aggregates at different ethanol concentrations. Moreover, this research aims to gain understanding on SCW with associated modifiers, followed via dilution method by prior established modification method which introduces reactive sites and increases the lignin reactivity.

CHAPTER 3: MATERIALS AND METHOD

3.1 Introduction

This chapter describes the general materials and methods used throughout the work for characterisation and quantification analysis.

3.2 Feedstock and Reagents

Miscanthus x giganteus (*MxG*), a lignocellulosic biomass, was grown and harvested in Aberystwyth, Wales, United Kingdom and provided by the Institute of Biological, Environmental and Rural Sciences (IBERS, UK) and Phytatec (UK) Ltd. The biomass was stored dry and in the dark.

Absolute ethanol (Fisher Scientific, UK), nitrogen (compressed oxygen free nitrogen, BOC, UK) and carbon dioxide (vapour withdrawal, BOC, UK) used had ≥ 99.8% purity. 72% sulphuric acid (Fluka-Sigma Aldrich, UK), pyridine (Sigma-Aldrich, UK), dodecanoyl chloride (Sigma-Aldrich, UK), hydrochloric acid (VWR, UK), and HPLC grade water, HiPerSolv CHROMANOR® (VWR Chemicals, France) were used as reagents.

3.3 Klason Lignin Assay

3.3.1 Background

The methods to quantify lignin fall into two categories, (1) gravimetric analysis and (2) non-invasive analysis. The oldest and most frequently used methods for quantifying lignin are gravimetric methods such as Klason lignin and acid detergent treatment (Brunow, 2004).

The non-invasive methods such as ultra-violet spectrophotometry, nuclear magnetic response and infrared spectroscopy are suitable for both quantitative and qualitative characterisation of lignin, and are widely used to determine structure and composition of lignin. However, non-invasive methods require calibration against known standards to be quantitative.

Klason lignin quantification and acid detergent lignin quantification both use concentrated sulphuric acid. However, the acid detergent method is thought to underestimate the amount of lignin due to the addition of the detergent (Fukushima *et al.*, 2015; Jung *et al.*, 1999).

In summary, it is understood there is no one specific method that provides accurate measurement of lignin content. Therefore the Klason lignin method was chosen and used throughout the study to ensure consistency when quantifying total lignin content (Hatfield and Fukushima, 2005) and to compare the results of lignin quantification within research group.

3.3.2 Removal of Extractives

Removal of extractives from biomass such as non-structural sugars, nitrogenous materials and lipids are important to prevent interference with the Klason lignin method for quantifying lignin content. Therefore a two step extraction protocol using water followed by ethanol were performed according to National Renewable Energy Laboratory procedure for quantification and characterisation of extractives in biomass (Sluiter *et al.*, 2008).

3.3.3 Method

The Soxhlet apparatus is shown in Figure 3.1. The Soxhlet apparatus set-up consists of glass Soxhlet extraction tubes, a heating mantle, a glass condenser and a 250 mL volumetric flask. Firstly, the empty cellulose thimble (Whatman®, 25x100 mm, single thickness) was weighed (T1). 10 g of *MxG* was added to the pre-weighed cellulose thimble and the weight recorded (T2). The cellulose thimble was folded on the top edge to avoid the biomass spreading out from the thimble during the extraction process. The biomass was weighed for moisture content determination according to method described in 3.3.5 at the same time as the biomass extractives determination to prevent errors due to changes in humidity.

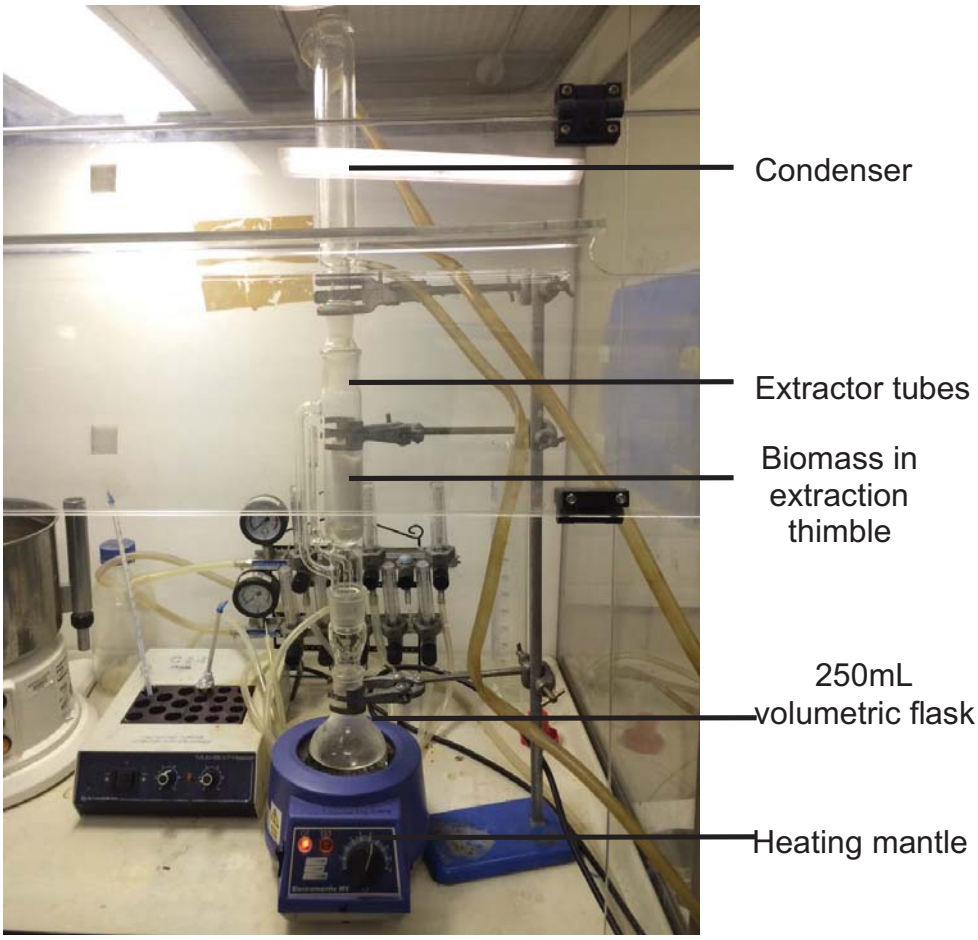

Figure 3.1. Soxhlet apparatus experimental set-up.

The thimble containing the Miscanthus biomass was placed into a Soxhlet apparatus. 200 mL of HPLC grade water added to the receiving flask before it was coupled to the Soxhlet apparatus. The water was refluxed through the biomass for 16 hours, before replacing with 200 mL ethanol. The ethanol was again refluxed for another 16 hours. At the end of ethanol extraction step, the thimble was removed from the Soxhlet apparatus and the residual biomass was filtered through a Pyrex sintered disc funnel porosity 2 using a vacuum filtration unit (VP100 High Savant Vacuum Pump). The biomass was washed three times with 100 mL of fresh ethanol and then dried

at 65°C for 72 hours before weighing (T3). The percentage of total extractives (TE) removed from biomass was calculated using Equation (Eq) 3.1.

$$\mathrm{TE} = \frac{\mathrm{T3}-\mathrm{T1}}{\mathrm{T2}-\mathrm{T1}} \mathrm{x}\ 100\% \quad (3.1)$$

3.3.4 Klason Lignin Quantification

Lignin quantification was conducted using the Klason lignin assay following the National Renewable Energy Laboratory (NREL) procedure for determination of structural carbohydrate and lignin in biomass (Sluiter *et al.*, 2012).

Crucibles (Gooch sintered borosilicate glass, porosity 4, 30 mL, Pyrex, Fisher Scientific, United Kingdom) were labelled and placed in a furnace (Gallen Kamp) at 575°C for four hours to remove any residues before cooling to room temperature in a desiccator and recording the weight of the crucibles.

About 300 ± 10 mg of *MxG* was placed into pre-weighed test tubes (W1), before 4.92 ± 0.01 g of 72% sulphuric acid was added (Fluka Sigma-Aldrich, United Kingdom). The test tubes were placed in a water bath (VWR Model 1211 7072, United Kingdom) set at 30°C and incubated for 60 minutes. Samples were stirred using a Teflon stir rod for every 10 minutes without removing the test tubes from the bath to ensure uniform acid hydrolysis.

After 60 minutes, the mixture was transferred from the test tube into a glass bottle (Fisherbrand, 100 mL) and 84 mL distilled water were added to create 4% acid concentration. To perform the second acid hydrolysis step the

glass bottle was placed in a Gallen Kamp Vacuum Oven for 60 minutes which was set at 120°C. After 60 minutes, the bottles were cooled to room temperature and the samples were transferred to the pre-weighed crucibles and vacuum filtered (VP100 High Savant Vacuum Pump). 50mL of distilled water was used to rinse the glass bottles.

The crucibles were dried in the oven at 105°C (Gallen Kamp Vacuum Oven) for 6 hours before cooling to room temperature in a desiccator. The weight of the crucibles and sample was recorded (W2) before they were placed in the furnace (Gallen Kamp) for 4 hours and the weight of crucibles and ash were recorded (W3) after cooling in a desiccator to room temperature. The percentage of total solid (T_s) for samples were determined using the method described in 3.3.5. The percentage of Klason lignin on a dry-weight basis was then calculated using Eq 3.2.

$$\%\ \text{of Klason lignin} = \frac{\text{W2}-\text{W3}}{\text{W1}\ (\frac{\text{Ts}}{100})}\ \text{x}\ 100\% \tag{3.2}$$

3.3.5 Moisture Content Determination

An empty plastic eppendorf was weighed (A1). *MxG* (approximately 1 g) was placed in the eppendorf and the weight was recorded (A2). The Eppendorf was then dried to constant weight (72 hours) at 65°C and re-weighed (A3). The percentage of moisture content (M_c) and total solids (T_s) obtained by drying at 65°C was obtained using Eq 3.3 and 3.4, respectively.

$$M_c = \frac{(\text{A2}-\text{A1})-(\text{A3}-\text{A1})}{(\text{A2}-\text{A1})}\ \text{x}\ 100\% \tag{3.3}$$

$$T_S = 100\% - M_c \tag{3.4}$$

3.4 Fourier Transform Infrared Spectroscopy (FTIR)

3.4.1 Background

FTIR has been used to describe lignin structure as early as 1984 (Jones, 1984). Most lignin fundamental molecular vibrations fall within the frequency range from 4000 to 400 cm^{-1} (Agarwal and Atalla, 2010). By using FTIR, the lignin functional group compositional analysis including the presence of syringyl and guaiacyl bands could be observed. Also, the size of the peaks in the spectrum is a direct indication of the amount of species present in the sample. Even though the spectra could be analysed for quantitative analysis using modern software algorithms, there is no standard method and interpretation of spectra is very challenging (Dowell and Wang, 2013; Rodriguez-Saona and Allendorf, 2011; Sim *et al.*, 2012).

FTIR works based on the light absorption of molecules in the infra-red region of electromagnetic spectrum whereby the vibrations of the atoms of a molecule relate to a frequency of a specific to part of a sample molecule (Rodriguez-Saona and Allendorf, 2011). The frequency ranges give a characteristic IR absorption of specific functional groups. A background scan of spectra is usually recorded, then automatically subtracted from sample spectra. There are advantages for using FTIR; the advantages are the frequency measurement speed is fast, the method is accurate as well as very sensitive and the instruments are self-calibrating (Nicolet, 2001). Nevertheless, there is also limitation; the overlapping and broad spectra bands during spectra analysis can result in inaccurate quantification of

species present in the sample (Manley, 2014). Thus, it is very challenging to interpret the overlapping peaks.

In summary, FTIR spectra contain a large amount of information including chemical bonds and compositional; thus, chemometric techniques analysis, such as multivariate analysis, are promising methods for further details of spectra analysis (Xu *et al.*, 2013).

3.4.2 Principal Component Analysis (PCA) on FTIR data

PCA is an essential mathematical tool to verify the correlations that exists within multivariable data. Analysis of FTIR spectra datasets by PCA determines the differences between spectra in terms of chemical structure and composition of the samples (Chen *et al.*, 1998; Labbé *et al.*, 2006). PCA transforms a one-dimensional dataset to multi-dimensional dataset that is dependent on the projection of principal components. The principle of PCA is denoted with a matrix of data with N rows (observations) or Y and K columns (variables) or X in a multidimensional variable space as shown in Figure 3.2. Y can be analytical samples and X can be spectral origin or chromatographic origin.

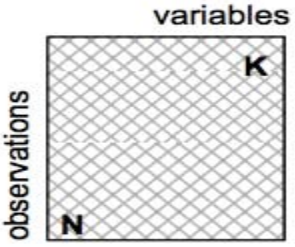

Figure 3.2. Notation used in PCA. (Source: Adapted from Eriksson *et al.*, 2006).

Each observation is represented by a point in the variable space. The whole dataset then constitutes a swarm of points in the variable space. PCA finds a line or planes in K dimensional variable space that approximates the data using the principle of least squares and statistically minimising the variance (Eriksson *et al.*, 2006). Figure 3.3 shows the derivation of a PCA model. The line is the direction of the first principal component (PC1) and points in the direction of the maximum variation.

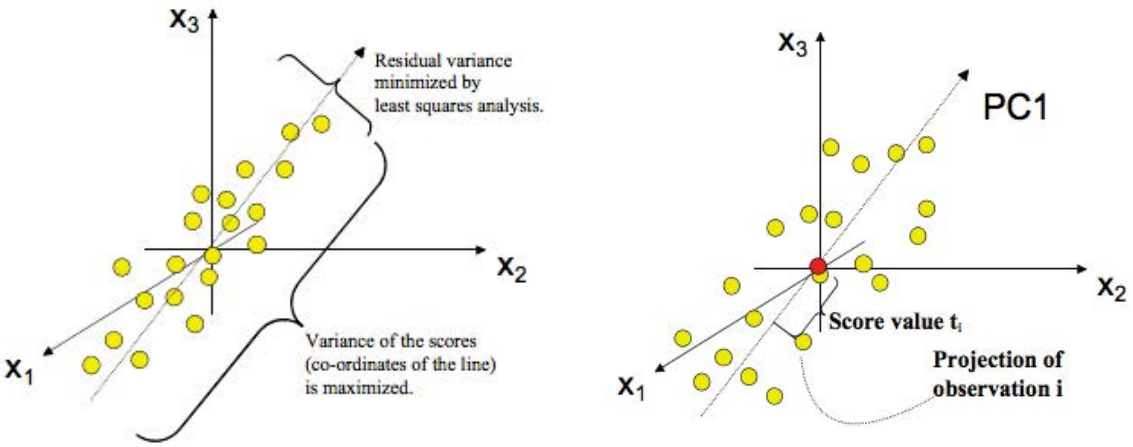

Figure 3.3. Derivation of a PC1 model. (Source: Adapted from Eriksson *et al.*, 2006).

The first principal component may not be enough to explain the data variation. By projecting the samples onto the new coordinate system, there may still unexplained variance. If the projection process is extended orthogonal to the first PC in the remaining part of the space, the second principal component (PC2) is created as shown in Figure 3.4. The process can be continued to find more PCs.

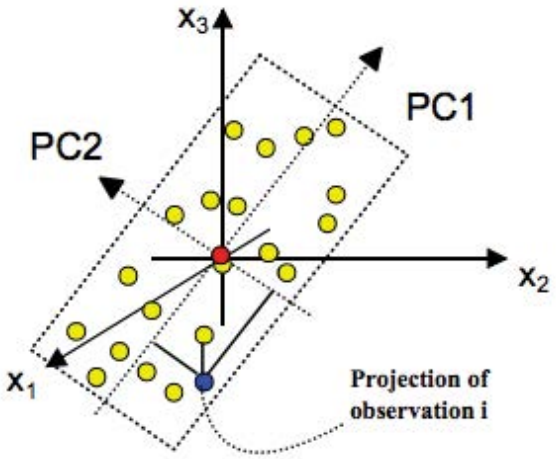

Figure 3.4. Second Principal Component (PC2). (Source: Adapted from Eriksson *et al.*, 2006).

The percentage of explained variance decreases with increasing of principal components, and could describe the variability between spectra (Grootveld, 2012). The explained variance gives the results based on calibrated and validated variance. The calibrated variance measures the model fit whereas the validated variance measures the new variance data or predicting the difference or error associated between projected and measurement data (Esbensen *et al.*, 2002).

A two-dimensional plot of the projected objects by using PC1 and PC2 create a new coordinate system and a map of objects in the principal components plot a so-called a score plot. In the case of spectra analysis, score is described by the degree of correlation for each spectra of each principal component whereas each principal component is associated with loadings that contribute by wavenumbers (Cordella, 2012; Kline *et al.*, 2010).

The score plot reveals the sample patterns, groupings, similarities and differences amongst the distribution of samples. For instance, in the

determination of lignin content in grass, hard and soft woods following analysis of biomass dissolved in ionic liquids, the cluster of grass, hard and soft wood could be observed in Figure 3.5. Thereby, spectra that cluster together on the scores plot reveal any similarity of chemical composition and structure between spectra. Thus, if the spectra from samples showed similar characteristics, these spectra were chosen for analysis.

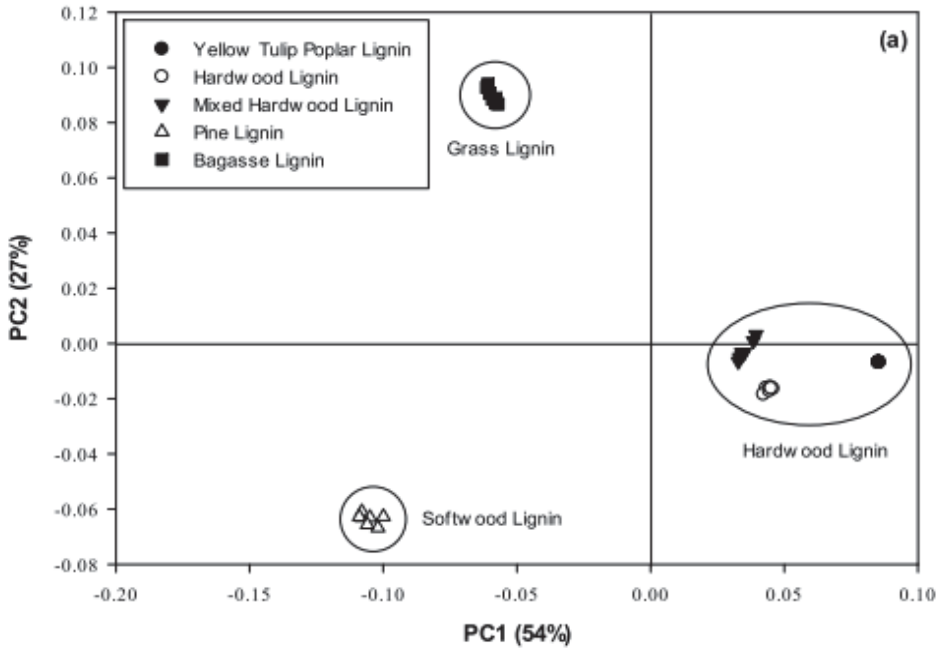

Figure 3.5. Score plot as a function of PC1 and PC2. (Source: Adapted from Kline *et al.*, 2010).

Loading plot is used to find correlation patterns among variables and the more significant variables (Lupoi *et al.*, 2013). For example, in the work to evaluate the influence of formulation and process variables on mechanical properties of oral mucoadhesive films using multivariate analysis, further analysis on data of films without a nonwoven textile were studied (Landová *et al.*, 2014). In the loading plot shown in Figure 3.6, the variables that are close to each other to the left loadings plot (dotted line of circle) and far from the center circle, very close to the 100% explained variance, which means,

therefore, they correlate positively (Cordella, 2012). Here, the analysis of the loadings plot emphasises the PC1 that captures maximum variability in the data.

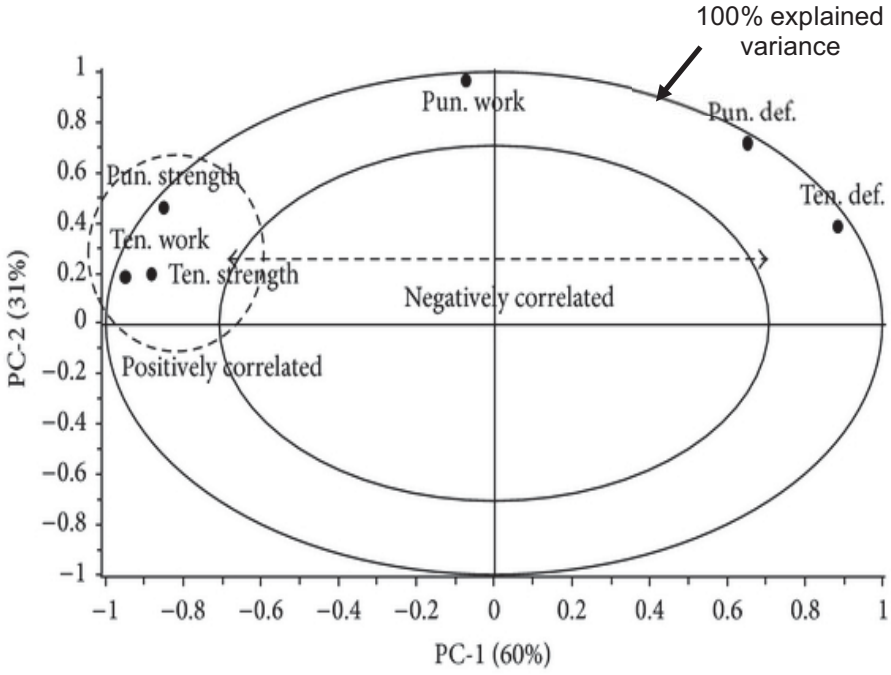

Figure 3.6. Loading plot for PC1 and PC2 for data of films without a nonwoven textile (Source: Adapted and modified from Landová *et al.*, 2014).

In general, the similarities or differences among sample and variables could not be detected easily in terms of the raw data. In practice, there is often a need to slightly modify the shape of the data to better suit an analysis, such modification is called preprocessing or pretreatment. There are various pretreatments including baseline correction, scatter correction, derivatives, normalisation or spectroscopic transformations (Luthria *et al.*, 2013).

Here, the spectra data collected was subjected to two types of pretreatment including smoothing and normalisation prior to PCA analysis. A smoothing function is to reduce noise and improve spectral resolution (Stuart, 2004). Normalisation of FTIR data transforms and maps the data into a

specific range based on a shift of maximum and width peaks that improve efficiency and accuracy of PCA analysis (Dinc *et al.*, 2014).

3.4.3 Method

FTIR analysis was carried out on the samples without any pretreatment. The IR spectra was determined from a FTIR-6300 JASCO Japan Spectrometer over a wavenumber range from 4000 to 600 cm^{-1}. The resolution was 4 cm^{-1} and 32 scans were averaged. Principle Component Analysis (PCA) was performed using the Unscrambler™ Version 10.3 software (CAMO). Two different pre-processing methods (firstly smoothing then normalisation) were performed on each of the three repeated spectrum measurements in the regions of 4000 to 600 cm^{-1}.

3.5 Particle Size Analysis

3.5.1 Background

Isolation of lignin under different conditions resulted a wide diversity of lignin physical properties that affect lignin valorisation towards various applications such as chemicals, fuel components or materials. Measurement of particle size analysis of lignin aggregates in addition to chemical composition could give robust information about behavior of lignin, so that the complexity of lignin could be addressed (Abdelaziz and Hulteberg, 2017). Particle size characterisation is employed in both research and development as well as industrial working in broad range of field for better control and

understanding of product, ingredients and process quality (Lee *et al.*, 1996; Malvern Instruments Ltd, 2012).

Particle size analysis can become a complex and challenging process. There are various classification techniques in particle size analysis including size range, degree of separation, imaging versus non-imaging and weighting: intensity, volume, surface and number (Particle Sciences, 2009). Taken together, among the available methods to determine particle size, the light scattering technique is a favored and a standard technique in the laboratory due to few advantages such as high speed, good reliability and high reproducibility (Ma *et al.*, 2000).

Here, the scattering methods were performed by using two different instruments, Zetasizer Nano ZS and Mastersizer 2000. Both particle size analysis measure using the concept of equivalent spheres. Mastersizer 2000 detects the size range of 0.02 μm to 2000 μm using laser diffraction technique. The laser diffraction technique or static light scattering measures particle size distribution according to light scatter at an angular variation as particles pass through a laser beam. The angular intensity of the scattered light is then analysed to determine the size of particles using Mie theory that requires optical properties such as refractive index and absorption coefficient (Malvern Instruments Ltd, 2000; Nobbmann and Morfesis, 2009). The results of analysis are presented based on a volume-weighted distribution.

Zetasizer Nano ZS measures particles in the range of 0.3 nm to 10 μm using dynamic light scattering with non-invasive back-scattering optics. The measured diameter or particle size is calculated based on the way particle in

suspension undergo Brownian motion within a fluid (Malvern Instruments Ltd, 2000). The dynamic light scattering produces an intensity-weighted distribution. Conversion from intensity-weighted distribution to volume-weighted distribution by the instrument could be done using the provided Mie optical properties.

Particle size analysis also could be achieved using imaging techniques includes photography, holography, microscopy and video. In this work, two types of imaging techniques have been chosen; scanning electron microscopy and light microscopy. The microscopy technique is applied together with ensemble particle sizing method of light scattering, not only to give further insight visualisation of the sample size, but also to verify the ensemble based measurements (Malvern Instruments Ltd, 2012; Vippola *et al.*, 2016). However, the imaging techniques suffer drawbacks of sampling errors and only a few particles being included as well as long analysis time. Also single plane projected images can be difficult to interpret (Kelly *et al.*, 2006).

Finally, although particle size analysis can be measured by various methods, the focus of this work was to understand the aggregation behavior of lignin using methods that could analyse a 3-dimensional particle. The particle size of lignin was measured based on the suspended solids in an ethanol-water solution of various ethanol concentration which depends on the experimental conditions. Use of the methods above in combination also enabled the data to be verified by independent techniques.

3.5.2 Malvern Zetasizer Nano ZS

Lignin particle size analysis was performed according to protocol described with modification (Aleš *et al.*, 2015; Šurina *et al.*, 2015). Lignin particle size was analysed at 23°C. To achieve a good colloidal dispersion, the samples were ultrasound-treated for 10 s at room temperature using 500 W Fisher Scientific™ Model 505 Sonic Dismembrator prior to measurement. The obtained size distribution graphs represented the dependencies of the relative intensity of scattered light on the hydrodynamic diameter of lignin particles. The intensity (%) shows the contribution of a particle size mode to the intensity of scattered light. The measurement of the diameters was carried out in triplicate and the results were reported as averages of the reading.

3.5.3 Malvern Mastersizer 2000

To achieve a good colloidal dispersion, the samples were ultrasound-treated for 10s at room temperature using 500 W Fisher Scientific™ Model 505 Sonic Dismembrator prior to measurement. A refractive index of 1.6 (Donaldson, 1985) and absorption of 0.01 for lignin were used by the instrument to calculate the particle size distributions (Stewart, 2015). The mean particle size was reported in terms of D3,2 values. The D3,2 is the surface area mean diameter and refers to the diameter of a sphere of equivalent volume to surface area of the particles in the sample as Eq 3.8. The measurement of the diameters was carried out in triplicate and the results were reported as averages of the reading.

Surface mean diameter is generally defined in terms of the surface diameter, d_s and volume diameter, d_v.

$$d_s = \sqrt{\frac{A_p}{\pi}} \tag{3.5}$$

$$d_v = \left(\frac{6V_p}{\pi}\right)^{\frac{1}{3}} \tag{3.6}$$

$$\frac{V_p}{A_p} = \frac{\frac{4}{3}\pi(^{d_v}/_2)^3}{4\pi(^{d_s}/_2)^2} = \frac{(^{d_v}/_2)^3}{3(^{d_s}/_2)^2} = \frac{D[3,2]}{6} \tag{3.7}$$

$$\mathrm{D}[3,2] = 6\frac{V_p}{A_p} \tag{3.8}$$

Where D[3,2] is the surface weighted mean, μm and V_p and A_p are the volume and surface area of the particle, respectively.

3.5.4 Scanning Electron Microscopy (SEM)

Images of precipitated lignin and dried supernatant were captured using a Philips XL30 FEG ESEM scanning electron microscope operating at 10 kV with various magnifications. Prior to analysis, samples were coated with platinum for 120 s using Emscope SC500 sputter coater.

3.5.5 Light Microscopy (LM)

0.01 mL of soluble lignin extract at different ethanol concentration were examined under the light microscopy (Olympus BX50, Japan) at 100x magnification equipped with a digital camera (Motic MC35X, China).

3.5.6 ImageJ Analysis

Using images captured by the light microscope, particle size analysis was conducted by ImageJ freeware (1.50v). Prior to particle size analysis, images were calibrated, despeckled to reduce visual noise and converted to gray scale. Image analysis captured a 2-dimensional image of a 3-dimensional particle and the projected area of lignin macromolecules enclosed by the outer contour of a particle from 2-dimensional image was analysed based on assumption that center of mass (similar to centroid but brightness weighted) (Olson, 2011; Willen, 2008)(Eq 3.9).

$$\mathrm{A} = \pi\, r^2 \tag{3.9}$$

Where A is projected area, μm^2; r is the radius of circle.

The circle equivalent diameter which is the the diameter of a circle with the same area as the 2-dimensional image of the particle was calculated using Eq. 3.10 (Olson, 2011).

$$D_{CE} = \sqrt{\frac{4A}{\pi}} \tag{3.10}$$

Where D_{CE} is circle equivalent diameter; A is projected area, μm^2.

The circularity, a dimensional value was determined based on the projected area and perimeter of particle (Eq. 3.11). The circularity value is indicative of the importance of particle shape in the overall particle behaviour and interaction in terms of particle form and roughness, and therefore the reactivity of lignin macromolecules (Liu *et al.*, 2015). Lower circularity value ($C \leq 1$) indicates that the lignin macromolecules are away from a perfectly round and smooth circle (Olson, 2011).

$$C = \sqrt{\frac{4\pi A}{P^2}} \quad (3.11)$$

Where C is circularity; A is projected area, μm^2; P is perimeter.

CHAPTER 4: AN EVALUATION OF IMPACT OF DIRECT AND SEQUENTIAL EXTRACTION PROCESSES ON THE PURITY AND CHEMICAL PROPERTIES OF LIGNIN FROM *MISCANTHUS X GIGANTEUS*

4.1 Introduction

In the biorefinery approach, lignin and carbohydrates which are the biomass recalcitrant components need to be removed, so that the cellulose fibres become more accessible and amenable for bioethanol production via enzymatic and microbial hydrolysis (Pu *et al.*, 2013). In such a context of the biorefinery approach, this work is carried out by sequential processing, thus enabling recovery of multiple naturally occurring biopolymers namely hemicellulose, cellulose and lignin which then become the feedstock for either direct application or subsequent downstream transformation.

In this chapter, sub-critical water (SCW) is applied at pressures up to 50 bar over a temperature range from 120°C to 200°C, depending on the targeted components to recover. Several studies have demonstrated that temperature has a pronounced influence on conversion rate of lignocellulosic biomass in SCW hydrolysis. The extraction temperature used is commonly within the range of 130°C to 240°C, conversion also depends on other factors such as particle size and solid to liquid ratio (Borrega *et al.*, 2011). From another point of view, Yedro *et al.* (2014) proposed that the SCW fractionation can be performed at mild conditions (<100°C) to remove the water-soluble

extractives and hydrolyse hemicelluloses (<180°C), yielding a solid phase enriched in lignin and cellulose.

Here, the SCW extraction with associated modifiers was performed for delignification process. In general, organosolv method utilises a mixture of organic solvents with inorganic acid catalyst (HCl or H_2SO_4) in aqueous form in lignocelluosic pretreatment (Behera *et al.*, 2014). In order to increase the efficiency of SCW hydrolysis of biomass via modified organosolv method, CO_2 has been used as a catalyst in place of inorganic acids to enhance delignification by the formation and dissociation of carbonic acid (Rogalinski *et al.*, 2008). In addition, the utilisation of CO_2 provides a reduction in neutralisation products after pretreatment.

Due to the low polarity of CO_2, a polar co-solvent, ethanol which is of lower toxicity compared with other polar co-solvents is added to enhance the compounds' solubility in SCW (Salleh *et al.*, 2013). The utilisation of 100% ethanol was not preferable for delignification due to the unavailability of nucleophilic agents. The modified organosolv method uses mixture of organic solvents; ethanol and water; ethanol could then be recovered by distillation (Zhao *et al.*, 2009; Roque, 2013). The addition of water as a nucleophilic agent stimulates the cleavage of lignin but decrease the capability of solvent to dissolve lignin in the delignification process (Jahan *et al.*, 2008; Pasquini *et al.*, 2005). A previous study has demonstrated that the optimum delignification was achieved with a 1:1 (v/v) ethanol-water mixture (Roque *et al.*, 2012).

The study attempts to evaluate the impact of processing *MxG* via two different routes towards delignification:

(1) *MxG* was delignified via direct SCW treatment, yielding lignin and hemicellulose enriched soluble fraction;
(2) *MxG* was subjected to a sequential SCW mediated hydrolysis, yielding a lignin enriched soluble fraction.

The specific objective of the work presented in this chapter is to compare the purity and chemical properties of lignin extracted from each of the two different processing routes.

4.2 Material and Methods

4.2.1 Direct and Sequential Lignin Extraction

The steps taken for extracting lignin in this work are outlined in Figure 4.1. The Miscanthus biomass was treated through a three-stage temperature profile sequential extraction (**SE**) in order to differentially separate extractives, hemicellulose, cellulose and lignin. The first step applies SCW at 120°C with an equilibrium time of 30 minutes and 50 bar of nitrogen gas pressure to remove extractives such as starch, protein, glucose, lipids and pectin which could interfere with the isolation and later analytical steps. The second step used a SCW at regime of 180°C, for a reaction time of 30 minutes under 50 bar of nitrogen gas to attempt to hydrolyse hemicelluloses prior to delignification. The final step involves extraction of lignin via a SCW with associated modifiers using a water:ethanol (50:50 v/v) mixture at 200°C, a reaction time of 60 minutes and 50 bar of carbon dioxide gas. For direct

extraction (**DE**), *MxG* was subjected to a single treatment step which is similar to third treatment in SE by the SCW with associated modifiers.

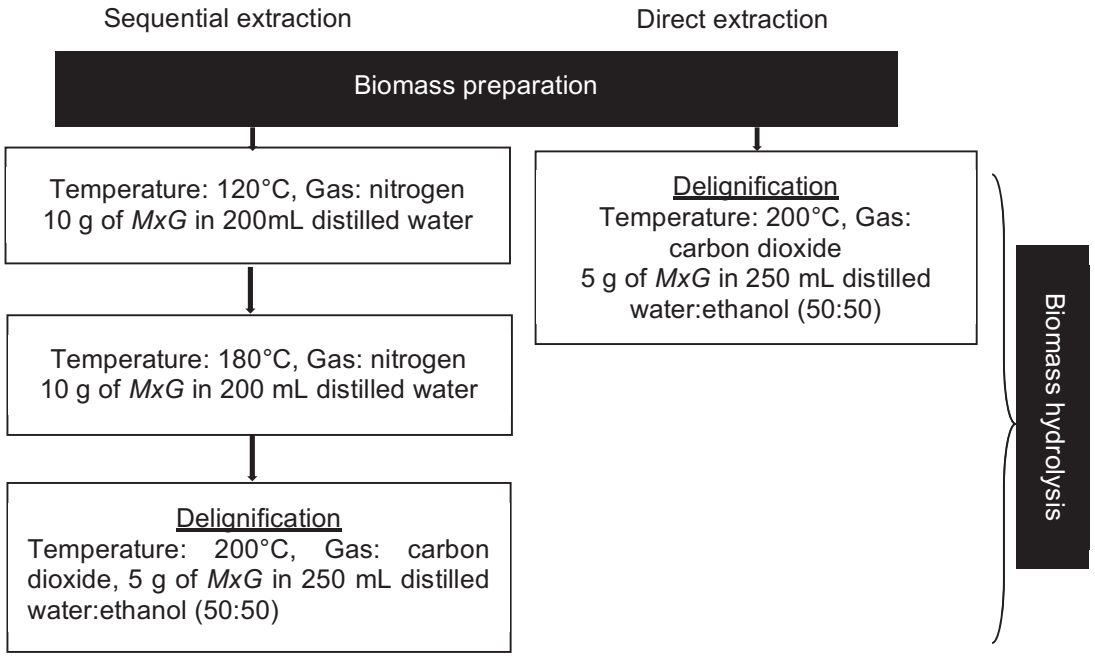

Figure 4.1. Flow chart of SE and DE.

4.2.2 Biomass Preparation

Materials used in this work are described in section 3.2. Prior to hydrolysis, the Miscanthus biomass was mixed in distilled water, then warmed to 50°C to soften the grass. The mixture was then soaked for 20 minutes to rehydrate the grass. The mixture was milled for three minutes in a domestic blender to reduce the particle size of material. The grinding conditions of temperature, soaking time, grinding time and solid:liquid ratio were previously optimised to yield an average particle size of 500 µm (Roque, 2013).

The Miscanthus biomass slurry was placed inside the reactor directly after sample preparation for SE at 120°C. Then, the sequentially processed

biomass for 180°C and 200°C was mixed in distilled water and ethanol-water (50:50) solution, respectively by warming to 50°C with a wetting time of five minutes prior to each hydrolysis step. The Miscanthus biomass preparation conditions for DE were ethanol-water solution (50:50), warming to 50°C and a soaking time 20 minutes prior to delignification. Further experimental conditions for each biomass hydrolysis are outlined in Figure 4.1.

4.2.3 Biomass Hydrolysis

The schematic diagram of the experimental set-up for Miscanthus biomass hydrolysis for DE and SE is presented in Figure 4.2. The Miscanthus biomass slurry was transferred to a 500 mL stirred pressure vessel (Alloy C276 Parr, USA). The reactor was closed and pressurised with desired gas to 50 bar. The set point temperature was increased to the set temperature and it was kept stable during the reaction time by a controller (4386 Parr, USA). After the reaction, the reactor temperature was decreased by operating a cooling system which comprises of a cooling coil inside the pressure vessel where a coolant flows at an initial -7°C. When the temperature fell below 50°C, the reactor was depressurised slowly to atmospheric pressure before the reactor was opened. Finally, the solid fibres and solution were separated using a laboratory sieve (BS410-1 size 45 μm, Endecotts Ltd, England) for SE carried out at 120°C and 180°C. The solid fibres for both DE and SE steps carried out at 200°C were recovered by vacuum filtration through a Pyrex sintered disc of porosity 2, rinsed with mixture of distilled water and ethanol (50:50) and then dried to constant mass at 65°C then set aside for further analysis. The solutions were dried at 65°C in the drying cabinet and weighed

after cooling in a desiccator for calculation of biomass solubilisation. The percentage of biomass solubilisation was calculated using Eq 4.1.

$$\%\ \text{of biomass solubilisation} = \frac{A}{B}\ \text{x}\ 100\% \quad (4.1)$$

Where A is the weight of dried solution, g; B is the initial weight of biomass, g.

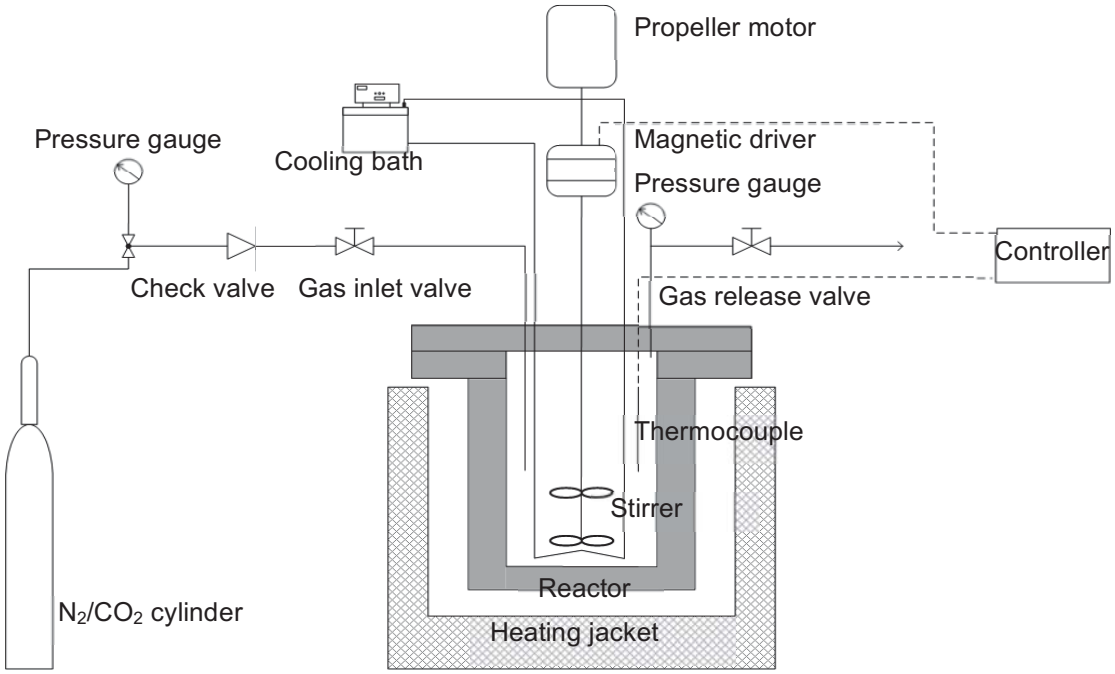

Figure 4.2. Schematic diagram of experimental set-up of Miscanthus biomass hydrolysis for DE and SE.

4.2.4 Lignin Precipitation

The filtrate from vacuum filtration was placed in a freezer at -20°C for 2 hours, after which the ethanol concentration was adjusted to 25% by adding distilled water. Lignin was recovered using a Beckman, model J2-21 centrifuge with a JA-10 rotor at 4°C and at 10,000 revolutions per minute (RPM), 17700 relative centrifugal force (RCF) for 10 minutes. The remaining supernatant was dried at 65°C for further Klason lignin assay and FTIR

analysis. The resulting precipitated lignin was air-dried and stored in 2 mL Eppendorf tubes at room temperature and later analysed by Klason lignin assay and FTIR analysis.

4.2.5 Klason Lignin Quantification

The Miscanthus biomass fibre, precipitated lignin and dried supernatant were analysed for lignin content using the method described in section 3.3.4. The amount of precipitated lignin was compared to the total amount of lignin in initial soluble fraction (precipitated lignin and dried supernatant) giving the percentage of lignin recovery using Eq 4.2.

$$\%\ \text{of lignin recovery} = \frac{\text{A}}{\text{A+B}}\ \text{x}\ 100\% \tag{4.2}$$

Where A is the amount of precipitated lignin, g; B is the amount of lignin derived from dried supernatant, g.

Percentage of delignification was calculated by comparing the lignin in the insoluble fraction to the lignin present in the starting material using Eq 4.3. The starting material for DE was the raw Miscanthus biomass without any pretreatment whereas the starting material for SE was the Miscanthus biomass that had undergone pretreatment of increasing severity prior to delignification.

$$\%\ \text{of delignification} = \frac{\text{A}-\text{B}}{\text{A}}\ \text{x}\ 100\% \tag{4.3}$$

Where A is the amount of lignin in starting biomass prior to delignification, g; B is the amount of lignin in insoluble fraction after delignification, g.

4.2.6 FTIR Analysis

FTIR analysis was carried out on the samples without any special pretreatment using the method described in 3.4.3. Precipitated lignin, dried supernatant, biomass fibre before and after delignification from both DE and SE were analysed.

4.2.7 Statistical Analysis

SPSS software (Version 22) was used for statistical analysis. One way analysis of variance was carried out at $\alpha = 0.05$ to compare the different extraction methods on the impact of process parameters on lignin extraction.

4.3 Results and Discussion

4.3.1 Percentage of Klason Lignin for Starting Material Prior Delignification

The percentage of Klason lignin was calculated for *MxG* fibres in the raw state, and after each step of pretreatment at 120°C and at 180°C for experimental work, as shown in Figure 4.3. Comparison of the raw material to the other fractions showed the amount of Klason lignin substantially increased after the first temperature step from 120°C and 180°C, giving values of 28.1% and 32.5%, respectively.

A difference in percentage of Klason lignin in the starting materials prior to delignification was observed due to composition differences. Thus, the

percentage of Klason lignin in starting materials prior to delignification was higher for SE than DE (32.5% and 27.9%, respectively).

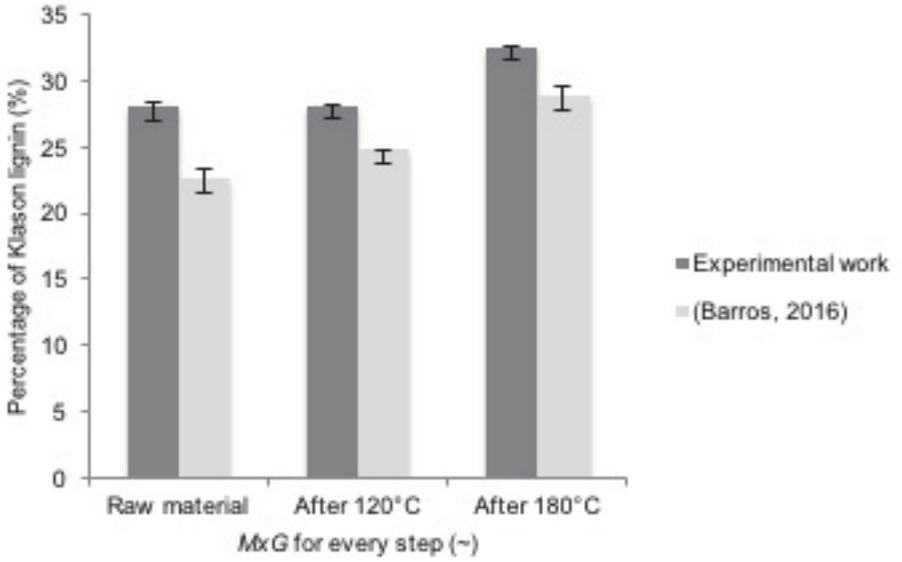

Figure 4.3. Percentage of Klason lignin of experimental work and work done within research group, Barros (2016).

Figure 4.3 also compares the percentage of Klason lignin between experimental work and the work conduced within the research group (Barros, 2016). Both work, the experimental work and work done by Barros (2016) have found that the percentage of Klason lignin in dry weight increased significantly for *MxG* fibres in the raw state, and after each step of pretreatment at 120°C and at 180°C prior to delignification. When comparison is made independently for *MxG* fibres in the raw state and each step of biomass hydrolysis between experimental work and work conducted by Barros (2016), the results obtained by Barros (2016) showed lower percentage of Klason lignin than experimental work. The value differences of lignin content are attributed to different batch of *MxG* fibres used that varies

with the weather condition and harvesting period (Brosse *et al.*, 2012; Savy and Piccolo, 2014).

Overall, the SE process of increasing severity resulted in an increase in the concentration of lignin or more purified lignin after each respective stage prior to delignification due to non-structural components such as pectins, starch, glucose, fructose, lipids and hemicellulose, being removed before the delignification step (200°C). Hemicellulose is definitely solubilised and removed at 180°C, resulting in lignin and cellulose-enriched fibres used for delignification of SE processing routes (Alvira *et al.*, 2010; Pielhop *et al.*, 2015). Compared with DE processing routes, the starting materials contain less purity of lignin since the fibres consist of other components of lignocellulosic biomass including hemicellulose and extractives. Therefore, using *MxG* fibre as a feedstock that is mostly free from extractives and hemicellulose prior to delignification enables pure lignin to be extracted, leaving a cellulose-enriched fibre.

4.3.2 Impact of Process Parameters on Percentage of Biomass Solubilisation

The impact of the different extraction methods was investigated by noting the relative percentage of biomass solubilisation. The results, shown in Figure 4.4, showed that the percentage of solubilisation from SE (45.6%) was higher than for DE (35.6%). The percentage of biomass solubilisation differed significantly between processes ($p<0.05$).

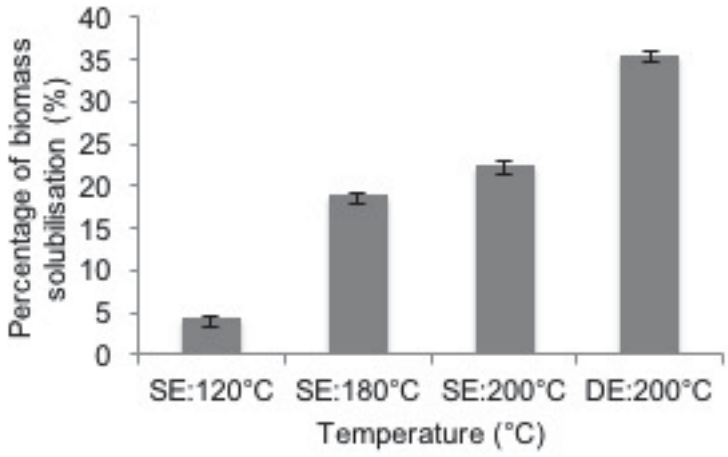

Figure 4.4. Percentage of biomass solubilisation for SE and DE.

The total percentage of solubilisation for SE was calculated by adding the proportion of material post solubilisation after each step of the extraction at 120°C (4.3%), at 180°C (18.9%) and at 200°C (22.4%). The increase in solubilisation with temperature also suggested that more specific lignocellulosic biomass components could be removed or degraded from the liquid fraction at each step of hydrolysis.

Figure 4.4 showed that the percentage of solubilisation increased as the temperature of solution increased. This was due to the unique properties of SCW which is related to polarity of water. Polarity of water is directly dependent upon the temperature (Asl and Khajenoori, 2013; Wu *et al.*, 2015); when the temperature of water increased, the polarity of water decreased, thus promoting dissolution of previously insoluble compounds (Lu and Ralph 2011). In high-temperature water H-bonding weakens, the degree of autoionisation of water increases, thus hydronium ions are generated which act as weak acid or catalysts in SCW processes. These ions break down

intermolecular and intramolecular bonds between cellulose, hemicellulose and lignin in the biomass structure (Lee *et al.*, 2014; Ruiz *et al.*, 2013).

Ligero *et al.* (2011) observed the effects of time and temperature upon the percentage of solubilisation for *MxG*, by direct extraction autohydrolysis. Results ranged from 31 to 37% at 200°C for times from 5 minutes to 60 minutes (Ligero *et al.*, 2011) which is similar to the work for DE presented here. They also agreed that at higher temperatures, more degradation products form in the process liquor with maximum solubilisation at 200°C rather than at around 120°C and 180°C for SE.

Furthermore, the use of CO_2 offers benefits of acid catalysts by creating the carbonic acid that increases the solubilisation of targeted components. Findings in Figure 4.4 revealed the the final step of SE processing routes that utilised CO_2 had higher percentage of solubilisation than the previous two steps. Similarly, the high percentage of solubilisation was also observed for DE. Although carbonic acid is comparatively mild and does not provide the same capability as sulphuric acid; hydrolysis of xylose, sugar monomers in hemicellulose improved compared with pretreatment using SCW alone (Van Walsum, 2001; Van Walsum *et al.*, 2007). The release of CO_2 also promotes the disruption of cellulose structure, reduces the degree of crystallinity and increases the permeability of cellulose for enzymatic hydrolysis process (Morais *et al.*, 2015; Yizhou Zheng *et al.*, 1998).

As can be seen from Figure 4.4, 4.3% solubilisation was observed at 120°C; at this temperature the liquid fraction contains primarily biomass extractives. Comparison was made between the biomass extractives

extracted using the procedure described in section 4.2.1 with the most standard protocol by the National Renewable Energy Laboratory (NREL) in section 3.3.3. Using the NREL method, 7.8% of biomass extractives were obtained, a greater value than due to the method given in section 4.2.1. The proportion of extractives of *MxG* varied significantly depending on the different extraction reagents, methods and parts of *MxG* (i.e. stems and leaves) (Brosse *et al.*, 2012). Therefore, it was considered that the SCW extraction at 120°C was able to extract only 55.1% of biomass extractives.

In summary, the different processing routes performed in the work affected the solubilisation of targeted components. Organosolv delignification process aims to solubilise lignin and hemicellulose into the aqueous phase and leaving the cellulose-rich fibre as solid (Cybulska *et al.*, 2017). If DE delignification was chosen as method to recover lignin and hemicellulose from cellulose fibre, separation of hemicellulose from the aqueous phase that also contains lignin and other extractives become more onerous even though lignin can be recovered from the aqueous phase by centrifugation. Thus, the proposed method of SE with increasing severity could improve the extraction of hemicellulose, lignin and cellulose in a biorefinery concept.

4.3.3 Impact of Process Parameters on Percentage of Delignification and Lignin Recovery

The lignin content in the insoluble fraction was compared to the amount of lignin in the starting material giving the percentage of delignification.

According to Figure 4.5, percentage delignification for SE (58.0%) was significantly lower than DE (81.5%), $p<0.05$.

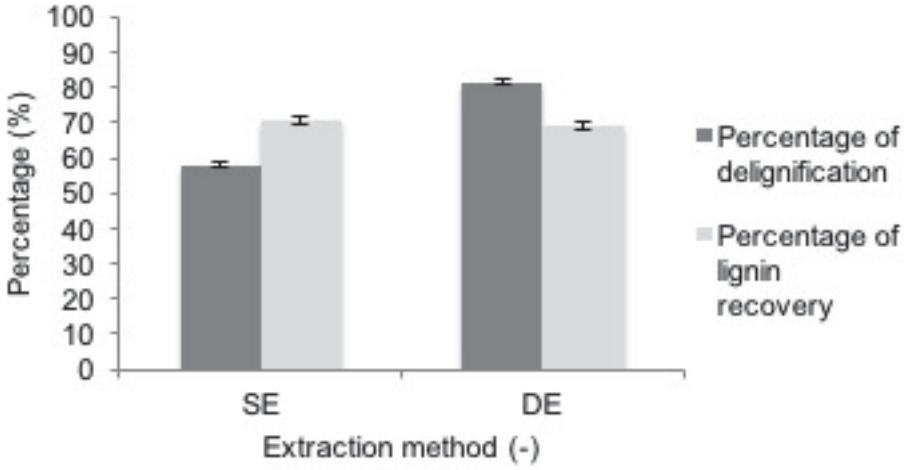

Figure 4.5. Percentage of delignification and lignin recovery for SE and DE.

Table 4.1 shows the mass balance of lignin (in grams) for SE and DE process that would clarify the percentage of delignification and lignin recovery. As can be seen from Table 4.1, the mass of lignin in liquid fraction was almost similar for both DE and SE processing routes even though the delignification was more efficient in DE processing route in terms of percentage. Similarly, a cellulose purification study within research group also reported that the delignification was more efficient in DE route (71.7%) than SE (60.9%), but the mass of lignin extracted during delignification was similar for both DE and SE routes (Barros, 2016).

Table 4.1. Mass balance of lignin for SE and DE.

Extraction method	Initial lignin in starting material (g)	Solid fraction	Liquid fraction
		Residual lignin in cellulose fibres (g)	Extracted lignin (g)
DE	1.32 ± 0.01	0.24 ± 0.02	1.08± 0.01
SE	1.57 ± 0.01	0.66 ± 0.02	0.91 ± 0.02

The first step of SE process is performed at low severity to remove extractives, whilst hemicelluloses are hydrolysed in the second step at higher severity. The autohydrolysis prior to delignification enables solubilisation of hemicellulose and the cleavage of lignin-carbohydrate bonds, however the efficiency of subsequent delignification process could be affected (Hage *et al.*, 2010).

Furthermore, autohydrolysis resulted in maximum extractability of lignin only in a narrow range of reaction severity after severe conditions of long reaction time and high temperature, this thus decreases the lignin reactivity, solubility and overall delignification rate (Bardet *et al.*, 1988; Lora and Wayman, 1978; Timilsena *et al.*, 2013). The lower percentage of delignification for SE also may be caused by the repolymerisation of polysaccharides degradation products such as furfural from hemicellulose formed during the increasing severe pretreatment (Li *et al.*, 2005, 2007).

Besides, the polymerisation of carbohydrate and lignin degradation products form a lignin-like material, termed pseudo-lignin, especially under high severity pretreatment conditions (Hu *et al.*, 2012). The formation of pseudo-lignin can artificially raise the Klason lignin content of pretreated biomass material and alter the calculation for percentage of delignification (Hu *et al.*, 2012; Sannigrahi *et al.*, 2011).

Figure 4.6 shows that the percentage of Klason lignin for cellulose fibre after delignification for pretreated *MxG* via SE was higher than DE values, thus this suggests that more residual lignin remained associated with the cellulose fibres after an attempted delignification. Furthermore, Table 4.1

shows that there is a clear evidence of high residual lignin in grams remained in the cellulose fibres for SE than DE processing routes. High residual lignin with cellulose fibres after delignification process for SE process could be associated with covalent bond between lignin and cellulose that making the lignin strongly adsorbed to available carbohydrate during delignification process (Panda, 2016).

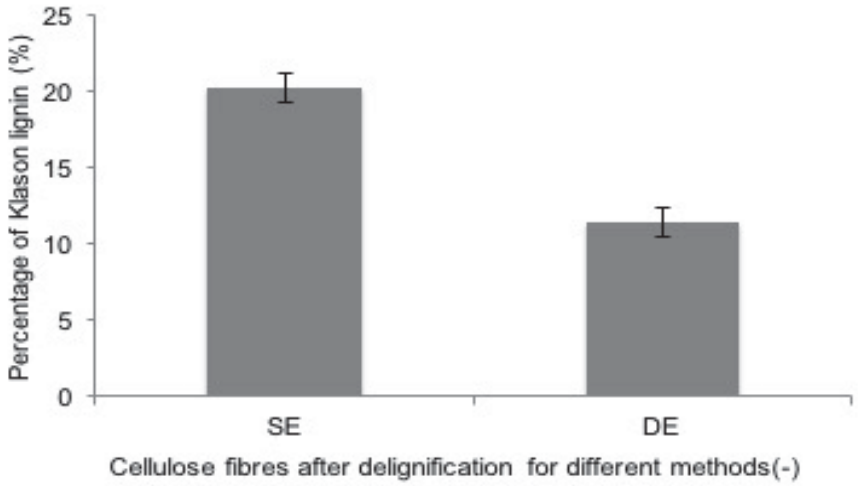

Figure 4.6. Percentage of Klason lignin for cellulose fibres after delignification for SE and DE.

An alternative hypothesis is that lignin encounters extensive condensation or re-polymerisation during delignification during which it becomes intractable and unreactive (Jeffries, 1994; Reid and Paice, 1994). In addition, the lignin condensation reactions could result in an increased molecular weight of lignin which is insoluble in water-ethanol mixtures; thus the recovery of lignin would be decreased as it is trapped within the cellulose fibres (Li *et al.*, 2015; Sannigrahi and Ragauskas, 2013). From the data in Table 4.1, it is apparent that the lignin recovery was almost similar even though the initial lignin in starting material for SE was higher than DE due to

several reasons described above including carbohydrate degradation, formation of pseudo-lignin, condensation reactions and re-precipitation of lignin into the remaining fibres.

The percentage of lignin recovery for SE and DE was 70.3% and 69.3%, which are not significantly different with a 95% confidence level ($p=0.4$). Lignin recovery via centrifugation method resulted in two fractions, namely, precipitates after dilution with water and the lignin remaining in the filtrate (Nitsos *et al.*, 2016). The emergence of colloidal suspensions in the filtrate are very recalcitrant to remove (Yasarla and Ramarao, 2013), thus another promising method has been suggested to improve the efficiency of lignin recovery including dissolved air flotation (Macfarlane *et al.*, 2009). While the effect of different methods did not have a significant impact on percentage of lignin recovery, the difference in purity of lignin was examined.

4.3.4 Impact of Process Parameters on Percentage of Lignin Purity

As stated above, the soluble lignin fraction was fractionated according to its solubility in ethanol under centrifugation, thereby generating two fractions, a precipitated fraction and supernatant fraction. The precipitated lignin and dried supernatant were analysed by Klason lignin assay to reveal the proportion of lignin in each part. Both precipitated lignin and lignin derived from the dried supernatant from SE (91.5% and 23.7%, respectively) exhibited a significantly higher purity of lignin ($p<0.05$) than from DE which gave 88.4% and 14.1%, respectively as presented in Figure 4.7.

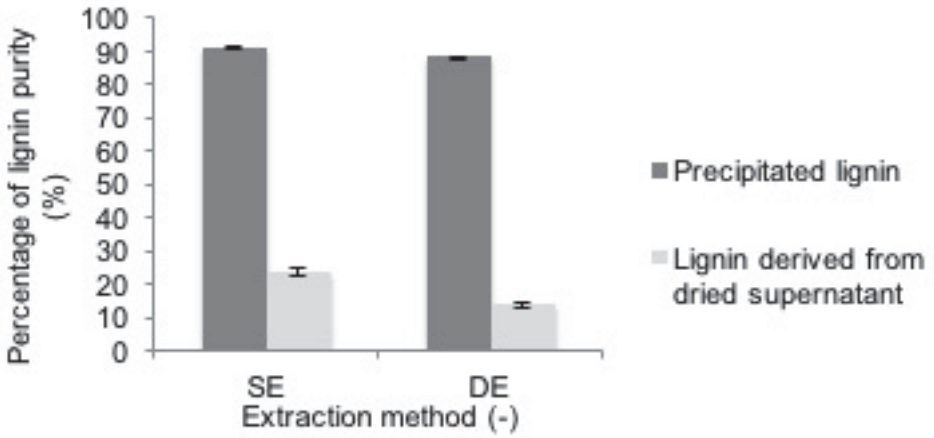

Figure 4.7. Percentage of lignin purity for precipitated lignin and lignin derived from dried supernatant for SE and DE.

Organosolv lignin delivers high purity, low molecular weight, sulfur free products which are soluble in many organic solvents (Espinoza-Acosta *et al.*, 2014; Fernando, 2010; Sannigrahi and Ragauskas, 2013) and several studies have proved the high purity of lignin of various biomass obtained using the organosolv method. For instance, a study of lignin recovery from spent liquors from ethanol-water fractionation of sugar cane bagasse achieved a lignin purity of 94% (Fernando, 2010). Similarly, lignin recovered from wheat straw either using acetic and formic acid based organosolv or an ethanol based organosolv method produced 91% and 95% purity lignin, respectively (Wild *et al.*, 2015). In a study conducted by Roque (2013) within research group, it was shown that the purity of lignin from DE resulted in 86.56%.

High purity of lignin is required for an excellent blending of lignin in polymer composites (Faruk *et al.*, 2015). Hosseinaei *et al.* (2017) stated that impurities such as hemicelluloses, ash and protein-based components impeded fusion and flow during melt-spinning of lignin-based carbon fibres,

thus producing defective surface of lignin-based carbon fibres and reduce the fibres carbon yield.

In this study, lignin derived from dried supernatant of SE exhibited higher purity than DE. Thus, it is possible to examine and optimise the operating conditions of the lignin precipitation process to recover more lignin from the process. Lignin removal relies not only on cleavage of ether bonds in lignin macromolecules but also on the capacity of aqueous ethanol solution to dissolve lignin fragments in the solution (Xu *et al.*, 2007). Few factors including solvent concentration, temperature, pH and turbidity affect lignin precipitation process. For instance, in ethanol pulping of pulp fibres, when ethanol concentration is reduced, lignin precipitation occurs. This is ascribed to ethanol evaporation or dilution of ethanol concentration spent liquor in washing process (Xu *et al.*, 2007). In experimental work carried out on lignin recovery from spent liquors from ethanol-water fractionation of sugarcane bagasse, it was also found that temperature also affected the lignin precipitation process. As the temperature increased, the precipitation and recovered lignin yields decreased (Fernando, 2010).

4.3.5 FTIR Analysis

As the solid fractions (*MxG* fibre as starting material before and after delignification) and liquid fractions (precipitated lignin and dried supernatant) were difficult to compare or differentiate from spectra analysed by PCA (results not shown), this suggested that the solid and liquid fraction should be analysed separately.

4.3.5.1 PCA of Solid Fraction

The explained variance plot was interpreted to select the optimal number of components in the model. The explained variance describes how much variation exists between the experimental data by giving information about the calibrated and validated variance as presented in Figure 4.8.

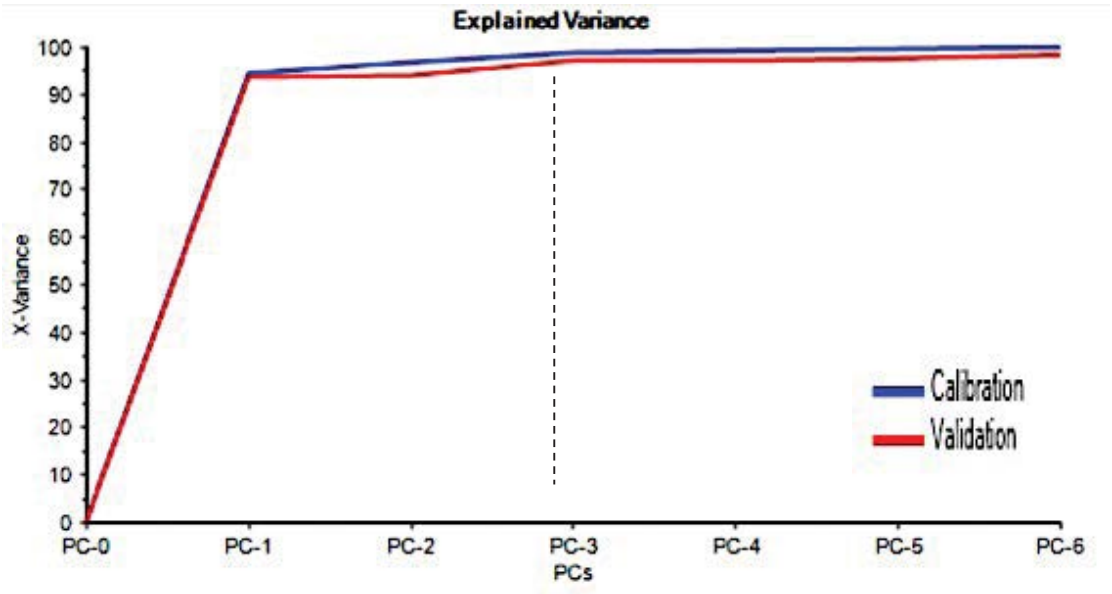

Figure 4.8. PCA explained variation for solid fraction.

Three principal components described 97% of the validated variation data and 99% of the calibrated variation data, thus verifying the optimal number of components in the model (dotted line showed constant variance; Figure 4.8).

The score plot for the dataset as functions of the two principal components, PC3 (accounting for 2% of the variance) versus PC1 (94%), is shown in Figure 4.9. Two distinct clusters are observed. On the left hand side were the spectra for *MxG* fibre as starting material before delignification and

MxG fibre after delignification for *MxG* which had been subjected to sequential sub-critical water mediated hydrolysis (SE). A second cluster on the right hand side, consists of the spectra for *MxG* fibre before and after delignification for DE. Thereby, Figure 4.9 shows the spectra of DE and SE were distinguishable from each other.

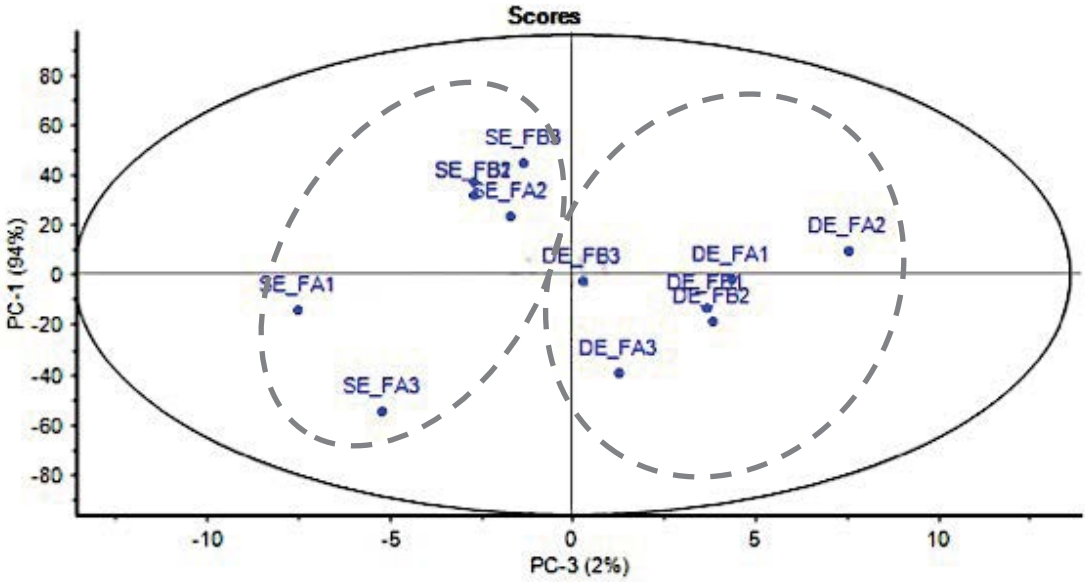

Legend:
SE_FA: Sequential extraction- *MxG* fibre after delignification
SE_FB: Sequential extraction- *MxG* fibre before delignification
DE_FA: Direct extraction- *MxG* fibre after delignification
DE_FB: Direct extraction- *MxG* fibre before delignification
**1,2,3- Repetition of spectra

Figure 4.9. PCA scores plot for solid fraction.

When comparison is made between samples among SE itself, (SE_FB1 and SE_FB2) and (SE_FA1 and SE_FA3) correlations were in the same quadrant. For DE, (DE_FB1 and DE_FB2) and (DE_FA1 and DE_FA3) correlations were in the same quadrant too. The closer the spectra are in the same quadrant; the spectra possess similar chemical composition. Thus, only a spectra was chosen from spectra that have similar chemical composition to be analysed for FTIR analysis.

Based on the correlation loadings plot in Figure 4.10, it is possible to acquire information related the chemical aspects involved in the DE and SE process. All wavenumbers related to lignocellulosic biomass as identified by FTIR (4000 to 600 cm^{-1}) have an extreme position on the top of the correlation loadings plot except for a wavenumber of 780 cm^{-1}.

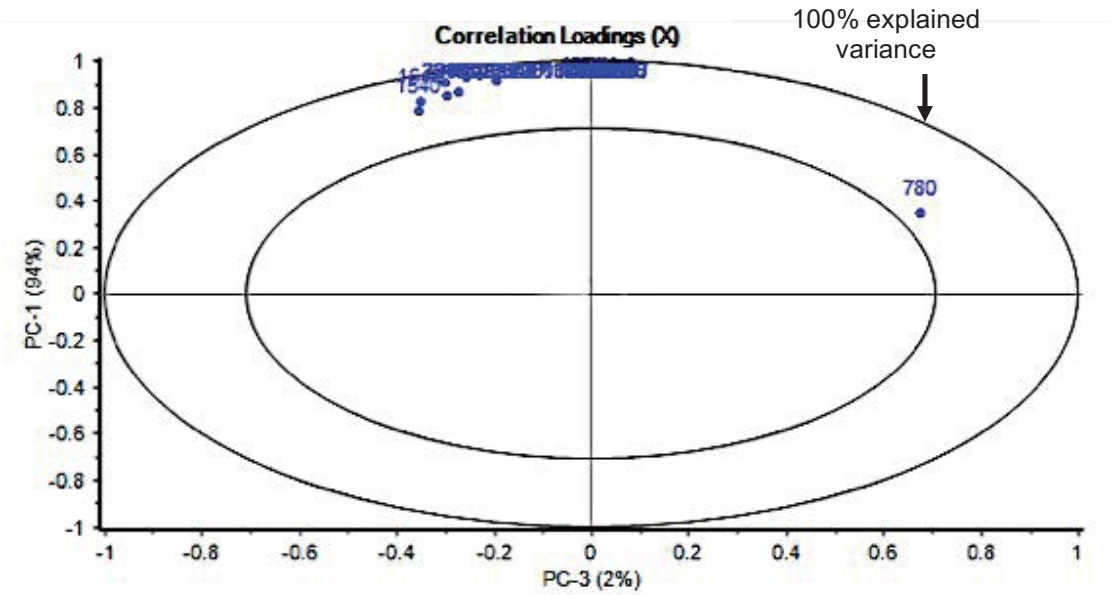

Figure 4.10. PCA correlation loadings plot for solid fraction.

The wavenumbers at the top of the plot are close to each other, and far from the centre of circle, very close to the 100% explained variance circle; they correlate positively. Wavenumber of 780 cm^{-1} which refers to 1,2-disubstitution (ortho) C-H aromatic ring (aryl) groups (Coates, 2000) had influenced the result of PCA score plot. In spite of fact that, even though the loadings plot could not explain clearly what PC1 and PC3 describes, the score plot can differentiate the samples according to different extraction methods and to answer simple questions such as if the spectra represent significant differences.

4.3.5.2 PCA of Liquid Fraction

Figure 4.11 shows the PCA explained variance plot for liquid fractions. Two principal components are optimal and described 97% of the validated variation and 98% of the calibrated variation data. Overall, spectra of samples that were analysed via PCA, whose first two principles components explained 85% and 13% of the spectral variance, respectively.

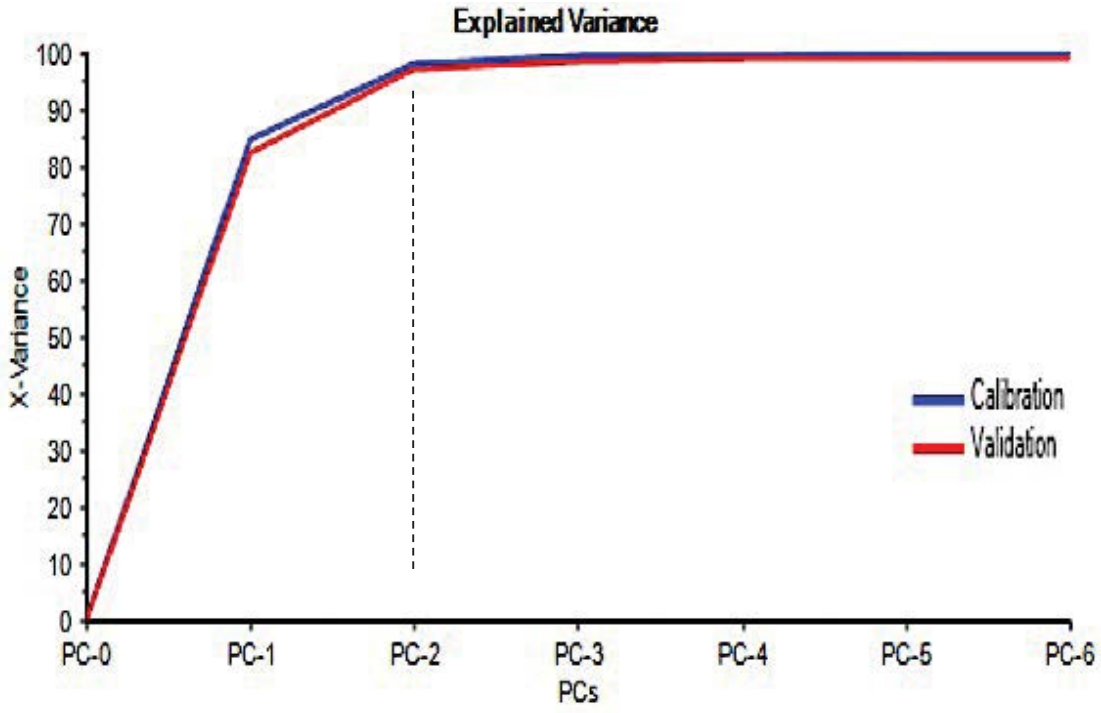

Figure 4.11. PCA explained variation for liquid fraction.

Figure 4.12 shows that there are two definite clusters in the PCA data. On the left hand side were the spectra for lignin and dried supernatant of SE. A second cluster on the right hand side, consists of spectra of lignin and dried supernatant for DE. These findings suggested that in general, the impact of operating parameters upon lignin and supernatant were different between SE and DE. As shown in Table 4.2, scores of respective samples of DE and SE were close within each other in the same quadrant (Figure 4.12), the same

scores illustrated that the spectra possess similar chemical composition.

Table 4.2. Scores table for similar chemical composition.

Spectra category	Spectra of similar chemical composition
SE_L	SE_L2 and SE_L3
SE_S	SE_S1 and SE_S2
DE_L	DE_L1 and DE_L2
DE_S	DE_S1, DE_S2 and DE_S3

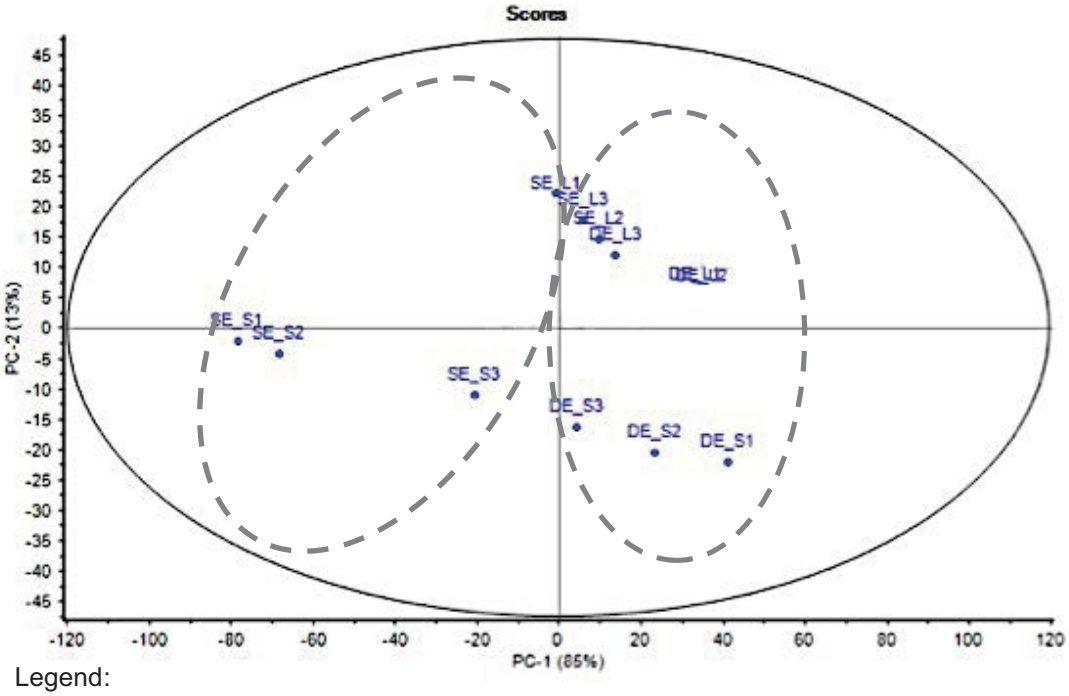

Legend:
SE_L: Sequential extraction- Precipitated lignin
SE_S: Sequential extraction- Dried supernatant
DE_L: Direct extraction- Precipitated lignin
DE_S: Direct extraction- Dried supernatant
**1,2,3-repetition of spectra

Figure 4.12. PCA scores plot for liquid fraction.

PCA correlation loadings are shown in Figure 4.13. Two wavenumbers, 2340 and 780 cm^{-1} are separated from the other wavenumbers corresponding to lignocellulosic biomass of FTIR analysis (4000 to 600 cm^{-1}) which affected the data variability of PCA. The wavenumbers of 2340 and 780 cm^{-1} are negatively correlated negatively as they are near to the centre and far from

the circle at 100% explained variance.

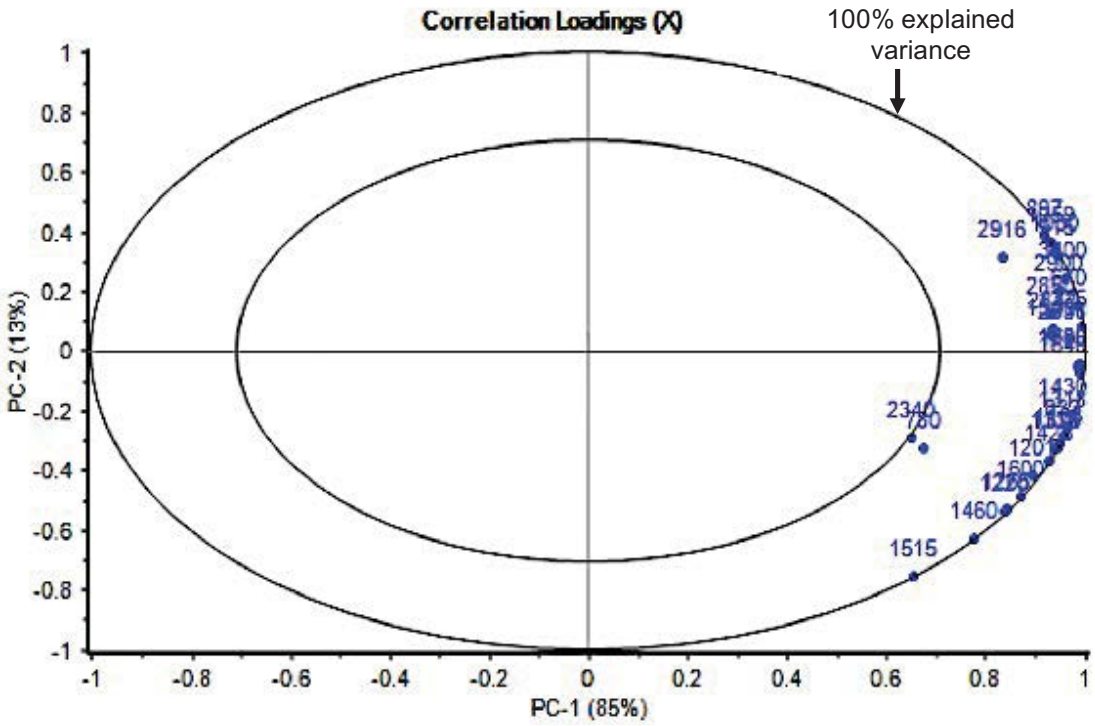

Figure 4.13. PCA correlation loadings plot for liquid fraction.

4.3.5.3 Spectra of Precipitated Lignin

Spectra of precipitated lignin, analysed by FTIR, for both DE and SE are shown in Figure 4.14. In general, spectra of precipitated lignin for SE presents stronger and broader intensity spectra than DE. The typical peaks at wavenumbers of lignin were found: 3400, 1705, 1600, 1650, 1515, 1460, 1425, 1326, 1265, 1220, 1033, 1118, 915 and 833 cm^{-1}. The details of wavenumbers and interpretations are outlined in Table 4.3.

Table 4.3. Wavenumber and interpretations.

Wavenumber (cm^{-1})	Interpretation	Wavenumber (cm^{-1})	Interpretation
3400-3460	Aromatic and aliphatic hydroxyl groups (Alriols *et al.*, 2010; Boeriu *et al.*, 2004) Hydrogen-bonded OH stretching (Alriols *et al.*, 2010; Pandey, 1999)	1705-1720	Weak to medium bands originating from unconjugated carbonyl/carboxyl stretching (Boeriu *et al.*, 2004) Ester carbonyl vibration in acetyl, feryloyl, p-coumaryl, groups in lignin and hemicelluloses (ester bonds between hydroxycinnamic acids and lignin were cleaved during hydrolysis)(Pandey, 1999)
2916, 2938, 2842 and 2850	CH stretching in aromatic methoxyl groups and in methyl and methylene groups of side chains(Szczepkowski *et al.*, 2007)	1640-1650	OH bending with adsorbed water (Boeriu *et al.*, 2004; Pandey, 1999) conjugated carbonyl groups with the aromatic ring (Alriols *et al.*, 2010) Carbonyl moieties (unconjugated C = O in xylans (hemicellulose) (Pandey, 1999)
2900	CH stretching (Alriols et al., 2010; Pandey, 1999)	1540	Aromatic ring stretching in lignin (Radotić *et al.*, 2012)
2340-2360	OH stretch from strong H-bonded-COOH (Davis *et al.*, 1999) CO_2 absorption (Abdel-Ghani *et al.*, 2014; Bakiz *et al.*, 2012)	1460	C-H aliphatic bonds (Boeriu *et al.*, 2004)
1600, 1515 and 1425	Aromatic phenylpropane skeleton vibrations (Boeriu *et al.*, 2004)	1430	C-H deformation (asymmetric) (Alriols *et al.*, 2010; Boeriu *et al.*, 2004)
		1110	Glucose ring stretch (Pandey, 1999)

Wavenumber (cm^{-1})	Interpretation	Wavenumber (cm^{-1})	Interpretation
1326	S ring breathing with C-O stretching (Boeriu *et al.*, 2004) S ring plus G ring condensed and the vibration at $833cm^{-1}$, that arise from the C-H out-of-plane in position 2 and 6 of S units (Alriols *et al.*, 2010; Boeriu *et al.*, 2004)	1030, 1033, 915	G-type aromatic C-H in-plane and out of the plane bending at $1033cm^{-1}$, the former and at $915cm^{-1}$ (Boeriu *et al.*, 2004) C-O primary alcohol, guaicyl C-H (Xiao *et al.*, 2011)
1375	C-H deformation (symmetric) (Alriols *et al.*, 2010; Boeriu *et al.*, 2004)	1059	CO stretching (Boeriu *et al.*, 2004; Pandey, 1999)
1318	CH_2 wagging (Boeriu *et al.*, 2004; Pandey, 1999)	897	Vibration attributed to $\beta(1\rightarrow4)$ linkage (glucosidic bond between two glucose units) formation of $\beta(1\rightarrow4)$ glucopyranose macromolecules (cellulose) and hemicellulose (Abidi *et al.*, 2008; Boeriu *et al.*, 2004) Increases with the increase of amorphous cellulose (Ibrahim *et al.*, 2011)
1265	G ring breathing with C-O stretching (Boeriu *et al.*, 2004)	1118	Syringyl (S)-type aromatic C-H in-plane deformations (Alriols *et al.*, 2010)
1220	Ether bridges (Boeriu *et al.*, 2004) C-C plus C-O plus C=O stretching (Szczepkowski *et al.*, 2007)	833	S-type aromatic C-H out-of-plane deformation (Boeriu *et al.*, 2004)
1201	OH deformation (Boeriu *et al.*, 2004; Pandey, 1999)	780	1,2-Disubstitution (ortho) C-H aromatic ring (aryl) group (Coates, 2000)
1163	COC asymmetric vibration (Boeriu *et al.*, 2004; Pandey, 1999)	670	C-OH-out-of-plane bending mode (Boeriu *et al.*, 2004)

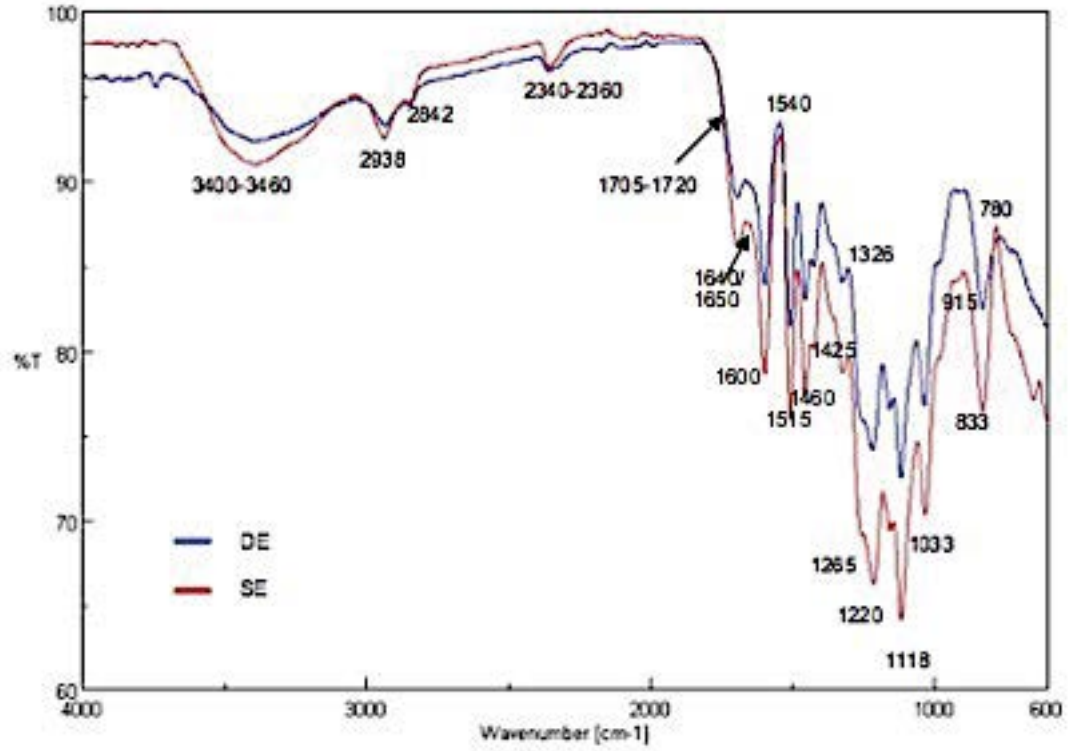

Figure 4.14. FTIR spectra for precipitated lignin of DE and SE.

The major finding of precipitated lignin at different processing routes is the lignin of SE showed a wider intensity band at 3400 cm^{-1} than DE, which indicated the presence of OH stretching vibrations in aromatic and aliphatic OH groups (Alriols *et al.*, 2010; Boeriu *et al.*, 2004). The wider intensity of hydroxyl groups characterisation for lignin of SE was due to the cleavage association of polysaccharides such as starch, hemicellulose and cellulose with lignin during the pretreatment of increasing severity (Cao *et al.*, 2012; Wang et al., 2016). Removal of lignin from polysaccharides is beneficial to recover purified lignin, that exposing more accessible hydroxyl group of lignin derived from SE (Sasaki *et al.*, 2015). The abundance of hydroxyl groups, demonstrating that lignin recovered can be a good alternative to polyols in the

production of lignin polymer composites through lignin depolymerisation and modification at higher bio-replacement ratios (Mahmood *et al.*, 2016).

The wavenumbers of 2938 and 2842 cm^{-1} are attributed to C-H stretching in aromatic methoxyl groups and in methyl and methylene groups of side chains (Boeriu *et al.*, 2004). An asymmetry and broadening of the spectra at 1705 and 1600 cm^{-1} probably resulted from weak absorptions around 1650 cm^{-1} due to protein impurity and water associated with lignin, respectively (Boeriu *et al.*, 2004). The ether bridges at 1220 cm^{-1} are associated with the extraction process; SCW cleaves hemiacetal linkages, thus, liberating acetic acids during biomass treatment, which then facilitates the breakage of ether linkages in biomass (Behera *et al.*, 2014). The generated acetic acids act as a catalyst causing autohydrolysis, the formation and removal of oligosaccharides, and further hydrolyse hemicellulose to monomeric sugars, furfural and hydroxymethylfurfural (Mosier *et al.*, 2005; Xiao *et al.*, 2011). In addition, spectra which wavenumber apportioned to lignin is strongly enhanced (600 cm^{-1} to 1700 cm^{-1}) in SE compared with DE, where these peaks are reduced. This could be due to a relative increase in the purity of lignin in the SE as hemicellulose was removed in the previous step in the pretreatment before the delignification process (Mosier *et al.*, 2005).

4.3.5.4 Spectra of Dried Supernatant

The FTIR spectra of dried supernatant from both extraction methods are presented in Figure 4.15. In comparison to DE and SE, the spectra of dried supernatant of DE had a weaker intensity than for SE. Most of

wavenumbers in the spectra are attributed to lignin, but there are also those which relate to cellulose and hemicellulose characteristics (1705 to 1720, 1650 and 897 cm^{-1}). However, the intensity of the wavenumbers was low compared to the lignin wavenumbers. Strong intensity spectra of dried supernatant for SE revealed that there is might be more lignin in dried supernatant. This finding of strong intensity spectra for SE also supported that the purity of lignin in dried supernatant for SE higher (23.7%) than DE (14.1%).

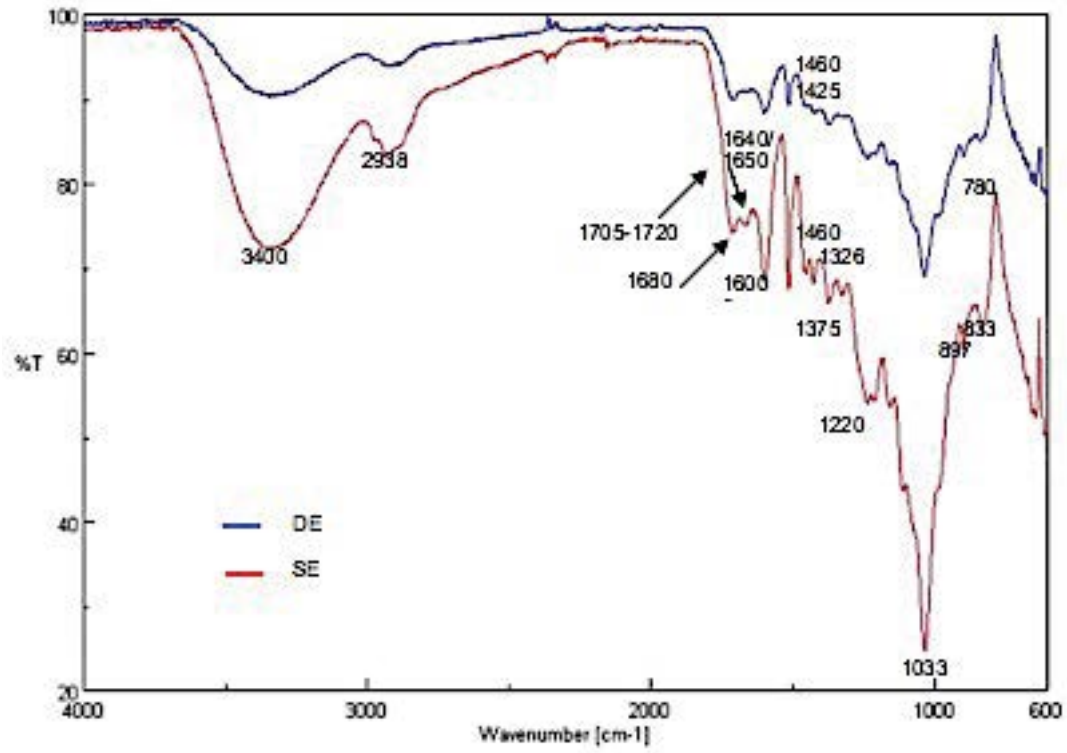

Figure 4.15. FTIR spectra for dried supernatant of DE and SE.

4.3.5.5 Spectra of *MxG* Fibre as Starting Material Before Delignification

Generally, the spectra for material obtained from DE had a stronger intensity than from SE; as illustrated in Figure 4.16.

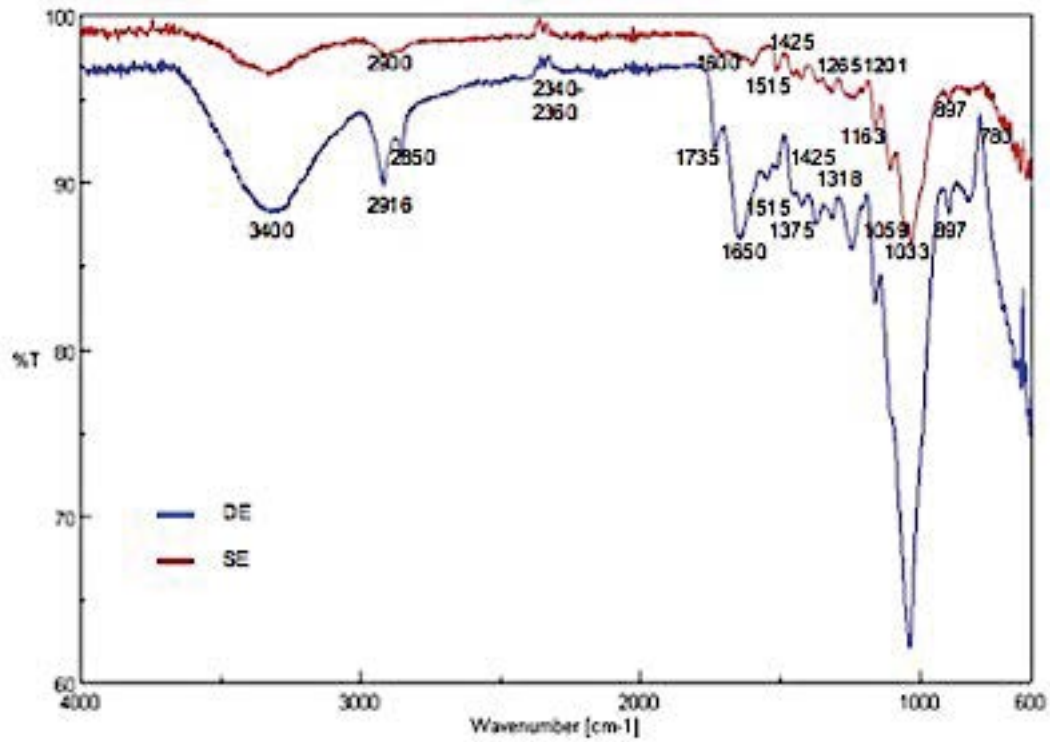

Figure 4.16. FTIR spectra for *MxG* fibre as starting material before delignification of DE and SE.

MxG fibres used for DE were from material that did not undergo any pretreatments whereas *MxG* for SE was used material that underwent pretreatments at 120°C and 180°C. Both materials showed the characteristic lignin, cellulose or hemicellulose bands. In comparison with the spectra of SE fibre, the spectra of DE fibre had obvious peaks at a wavenumber of 2916, 2850, 1650 and 897 cm^{-1}. Peaks of 2916 and 2850 cm^{-1} from DE material indicate CH stretching in aliphatic methylene groups which also may originate from fatty acids present in the lignin preparations. This is because the *MxG* fibre used for DE contains extractives including fatty acids whereas *MxG* fibre used for SE had these removed by the first step of SE process (120°C). There were carbonyl moieties (unconjugated C=O in xylans (hemicellulose) at wavenumber 1650 cm^{-1} for DE material. In addition, the spectra of 897 cm^{-1} of DE also had high intensity that relates to hemicellulose linkages. This

shows that the *MxG* fibre used in DE was contaminated with large amounts of hemicellulose. Even though, the lignin peak at 1033 cm^{-1} (G–type aromatic C-H) intensity was strongly enhanced in DE compared with SE, the purity of lignin for DE is lower than SE due to contamination of lignin with other components such as cellulose and hemicellulose.

4.3.5.6 Spectra of *MxG* Fibre After Delignification

MxG fibre or cellulose after delignification was analysed and the following typical cellulose peaks at wavenumbers: 3400, 2900, 1640, 1430, 1375, 1318, 1201, 1163, 1110, 1030, 1059, 897 and 670 cm^{-1} were identified (Pandey, 1999). When comparisons were made between cellulose fibres of DE and SE in Figure 4.17, it showed that the spectra of cellulose fibres of DE were sharper than for SE at 1059, 1030 and 1110 cm^{-1}, indicating more purity of cellulose fibres obtained by DE. Besides, the percentage of Klason lignin for cellulose fibres in SE revealed that there is more residual lignin remaining in the cellulose fibres that made the cellulose fibres less pure in terms of cellulose characteristics.

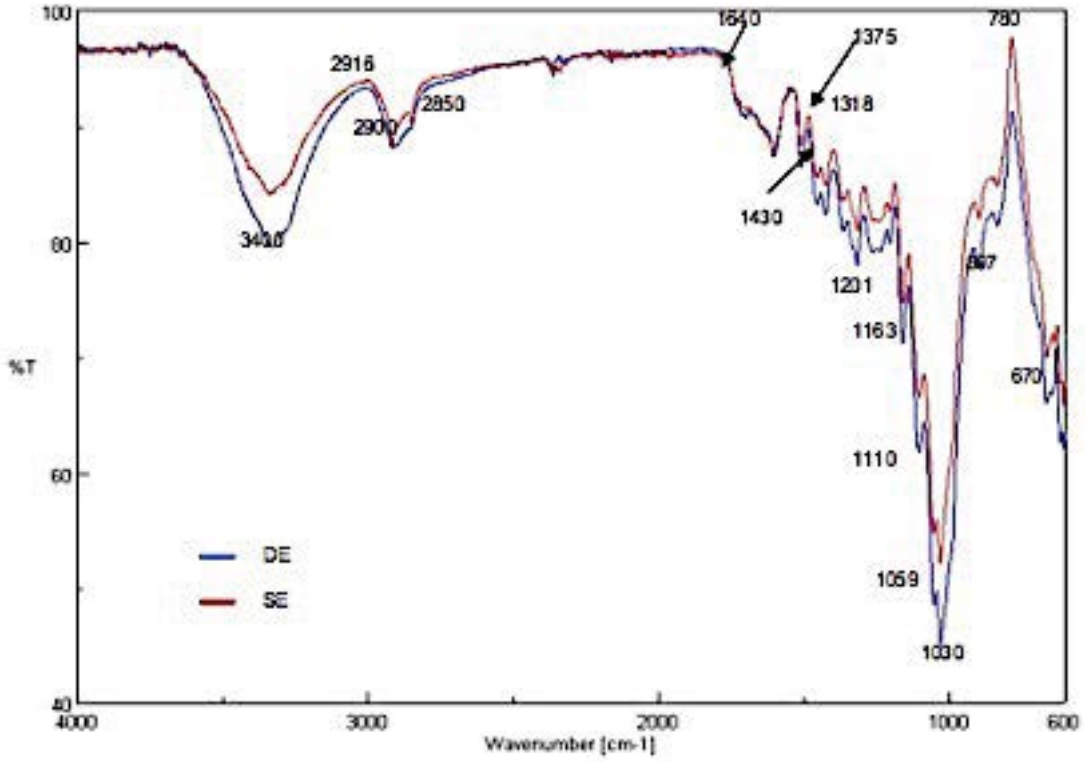

Figure 4.17. FTIR spectra for *MxG* fibre after delignification of DE and SE.

In addition, the deposited lignin in cellulose fibres could have a negative impact on the further enzymatic cellulose fermentation for subsequent bioethanol production (Selig *et al.*, 2007). The most important peak at 897 cm^{-1} shows the amorphous type cellulose concentration in SE had increased, and further hydrolysis of the cellulose to glucose by enzymatic hydrolysis was efficient compared to crystalline cellulose. It has also been postulated that the lower the value of cellulose crystallinity index, the higher will be the sugar yield and the faster will be the hydrolysis rate (Li *et al.*, 2014).

Nevertheless, the effect of lignin recovery and crystallinity index towards glucose production for subsequent enzymatic deconstruction were very complicated and difficult to understand as it remains unclear at what

conditions the glucose production would prevail depending on various factors such as processing parameters, chemical bonding and materials itself. Ishizawa *et al.* (2009) suggested that moderate lignin removal by organosolv pretreatment and retaining few lignin will necessitate the cell wall structure of biomass with least disruption of polysaccharides, further improved cellulose enzymatic digestibility.

Several line of evidence established that lignin removal was not significantly affected the enzymatic hydrolysis process. In the study of the cell wall changes of *Populus* biomass in hydrothermally-pretreated biomass of different times at 180°C, DeMartini *et al.* (2011) reported that glucose yield via enzymatic hydrolysis enhanced even though lignin removal during hydrothermal process was minimal. In another finding within same group assessing SCW for cellulose hydrolysis and glucose production from *MxG* via DE and SE approach, although the crystallinity index of cellulose fibres after delignification for SE was higher than DE, the results demonstrated that SE fibres generated higher glucose production than DE. Thus the cellulose fibres were more accessible for fermentative ethanol production (Barros, 2016). It is therefore likely that such lignin content per se in the cellulose fibres did not influence biomass recalcitrance, instead the association of lignin and polysaccharides within the cell wall, and their associations with one another and with other wall components also affected the enzymatic hydrolysis process (DeMartini *et al.*, 2011; Pu *et al.*, 2013).

The peaks at 2916 and 2850 cm^{-1} are clearly broader in DE rather than SE which the peaks referred to CH stretching in aliphatic methylene group

that can originate from fatty acids present in the lignin preparations. The broad peak of DE may be due to that the cellulose fibres of DE contain higher proportion of extractives such as sucrose, fructose, pectins and fatty acids compared to SE from which the extractives were removed at previous step prior to delignification process.

4.4 Conclusions

The impact of process parameters upon lignin extracted from *MxG* on the efficacy of DE and SE methods was evaluated. The findings showed that for both, the percentage of lignin recovery ($p=0.4$) were not significantly different. However, there was a significant difference in the percentage of solubilisation, delignification and lignin purity ($p<0.05$). Hydrolysis of *MxG* under a modified organosolv extraction resulted in the higher percentage of solubilisation for SE (45.6%) in comparison to DE (35.6%). Similar findings were achieved for purity of lignin and lignin derived from dried supernatant as SE showed higher purity of lignin (91.5% and 23.7%, respectively) than DE which gave 88.4% and 14.1%, respectively. However, percentage of delignification for SE (58.0%) was lower than DE (81.5%).

FTIR results revealed that lignin extracted from *MxG* which is subjected to sequential SCW mediated hydrolysis indicated high purity of lignin with less contamination of other components. Result of a preliminary study indicated that SE is a feasible method for delignification as it had positive effect especially on lignin purity.

The SE method offers valuable insight into biomass fractionation to recover high quality streams of each of the biomass major components whereby lignin and hemicelluloses were hydrolysed and could recover from the liquid fraction, leading to a relatively effective fractionation of cellulose-rich solid fibres (Sannigrahi and Ragauskas, 2013). In contrast, DE produced a liquid fraction that comprised various components including extractives, lignin, hemicellulose and sugar degradation products such as furfural and hydroxymethylfurfural are released as water-soluble fraction. The major challenge of DE processing route is the hemicellulose recovery during separation process while maintaining the lignin structure as well as maximising the lignin recovery (Lee *et al.*, 2014).

In summary, lignin derived from the SE processing routes demonstrated high lignin purity and high availability hydroxyl groups based on preliminary analysis via FTIR, making the lignin produced had suitable characteristics for subsequent lignin modification corresponding to lignin value-added bio-based materials. The plentiful of hydroxyl groups on lignin molecule which are reactive could act as local centres of high polarity capable of hydrogen bonding (Duval and Lawoko, 2014; Sivasankarapillai and McDonald, 2011). Modification of hydroxyl group helps to improve the solubility of lignin, thus modified lignin enhances lignin dispersion into the polymer matrix of bio-based materials (Buono *et al.*, 2016).

CHAPTER 5: AN ASSESSMENT OF ETHANOL CONCENTRATION EFFECT UPON FORMATION OF ORGANOSOLV LIGNIN AGGREGATES FROM *MISCANTHUS X GIGANTEUS*

5.1 Introduction

Lignin isolated via different extraction methods can vary widely in terms of chemical composition and molecular structure. The differences also affect the physical properties such as solubility and molecular weight (Bruijnincx *et al.*, 2016). Therefore, in the context of the growing interest in developing value added uses for lignin, this chapter examines the characterisation of lignin extracted via a SCW method; with particular emphasis on the formation of lignin aggregates.

There is insufficient information available to describe the association behaviour of lignin macromolecules in solution as this depends on the solvent conditions and lignin structure (Ratnaweera *et al.*, 2015). But an understanding of the formation and assembly of lignin aggregates in solution are relevant and significant, as the heterogeneity and complex lignin structure become the greatest bottleneck in lignin utilisation for bio-based materials (Baker and Rials, 2013; Vishtal and Kraslawski, 2011).

Numerous studies on lignin aggregates have been conducted in conjunction with different methods and sources of lignin such as aggregation and assembly of alkali lignin in iodine (Deng *et al.*, 2011), the impact of lignin source on its self assembly in dimethyl sulfoxide solution (Ratnaweera *et al.*, 2015) and the aggregation of acetylated lignins in *N,N*-dimetylacetamide

(Clauss *et al.*, 2015). Indeed, a crucial physicochemical property of organosolv lignin is that it has has a tendency to aggregate in most solvents, and this affects the lignin recovery process, the biodegradation processes and the preparation of lignin-based materials (Deng *et al.*, 2011; Norgren *et al.*, 2002). To date, there are only a few reports concerning the solubility of lignin in ethanol-water mixtures (Ni and Hu, 1995; Schuerch, 1952; Xu *et al.*, 2007). However, there is still no report pointing to the study of aggregation behaviour for organosolv lignin in ethanol-water solution especially on the structural morphology.

Here, a soluble lignin extract from the delignification process was fractionated according to ethanol solubility, with precipitates recovered via centrifugation leaving supernatant fraction. Characterisation of the resulting fractions was carried out by Klason lignin assay, FTIR, SEM, LM and particle size analysis. This chapter examines the purity, lignin recovery, chemical structure and especially, particle size and morphology characterisation for resulting soluble lignin fractions at different ethanol concentrations.

5.2 Material and Methods

5.2.1 Biomass Hydrolysis

Materials used in this work have been described in section 3.2. Biomass hydrolysis of *MxG* was performed using SE method explained in section 4.2.3.

5.2.2 Lignin Precipitation

The 50% ethanol concentration soluble lignin extract from biomass hydrolysis (section 4.2.3) was placed in a freezer at -20°C for 2 hours, after which the ethanol concentration was adjusted to either; 10% and 25% by adding distilled water; and 75% by adding ethanol. Lignin was recovered via method stated in 4.2.4. Percentage of lignin recovery was calculated using Eq 4.2 (section 4.2.5).

5.2.3 Klason Lignin Quantification

Klason lignin determination was performed for precipitated lignin and dried supernatant following the Determination of Structural Carbohydrates and Lignin in Biomass Laboratory Analytical Procedure (NREL/TP-510-42618) described in detail section 3.3.4.

5.2.4 FTIR Analysis

FTIR analysis was subjected to method mentioned in section 3.4.3. FTIR analysis was carried out for precipitated lignin and dried supernatant of 10%, 25% and 50% ethanol concentration.

5.2.5 SEM Analysis

SEM imaging analysis of lignin, dried supernatant and soluble lignin extract from each ethanol concentration (50%, 25% and 10%) were performed using method mentioned in section 3.5.4.

5.2.6 Particle Size Analysis

The precipitated lignin and dried supernatant was dispersed at 10 $mgmL^{-1}$ based on initial concentration of ethanol-water solutions (10, 25 and 50% ethanol concentration). The particle size of precipitated lignin and dried supernatant was determined as the following methods described in section 3.5.2 and 3.5.3.

Further study on particle size analysis was to study the aggregation behaviour of lignin aggregates in different ethanol concentrations of soluble lignin extract. The soluble lignin extract as a function of ethanol concentration without undergoing centrifugation were analysed with both similar methods in different ranges using Zetasizer Nano ZS and Mastersizer.

5.2.7 LM Analysis

Images of the soluble lignin extract at different ethanol concentrations were captured following method stated in section 3.5.5.

5.2.8 ImageJ Analysis

Subsequently, 10 recorded images from LM analysis were processed via ImageJ software (1.50v) according to method described in section 3.5.6.

5.2.9 Statistical Analysis

SPSS software (Version 22) was used to carry out statistical analysis. The result of one-way analysis of variance showed that there is significance difference on percentage of lignin purity, lignin derived from dried supernatant and lignin recovery since $p<0.05$. The results from the one-way ANOVA do not indicate which of the three groups differ from one another, so, in many cases, it is of interest to conduct the analysis with post hoc tests among particular means. If several comparisons between pairs of means are made, post hoc tests by Tukey's Honest Significant Difference (HSD) and Bonferroni test were conducted at $\alpha = 0.05$ to determine if the results obtained at each ethanol concentration were significantly different. One-way ANOVA statistical analysis were also performed at $\alpha = 0.05$ for imageJ analysis.

5.3 Results and Discussion

5.3.1 Percentage of Lignin Recovery

Figure 5.1 shows an increasing trend on percentage of lignin recovery as the ethanol co-solvent becomes more dilute. The post hoc tests analysis illustrated that percentage of lignin recovery using 25% ethanol concentration

(71.4%) did not differ significantly from 10% ethanol concentration (75.8%), at a 95% confidence level. Lignin precipitation using 50% ethanol concentration only recovered 25.1% lignin. Further increase of ethanol concentration to 75% led to zero recovery.

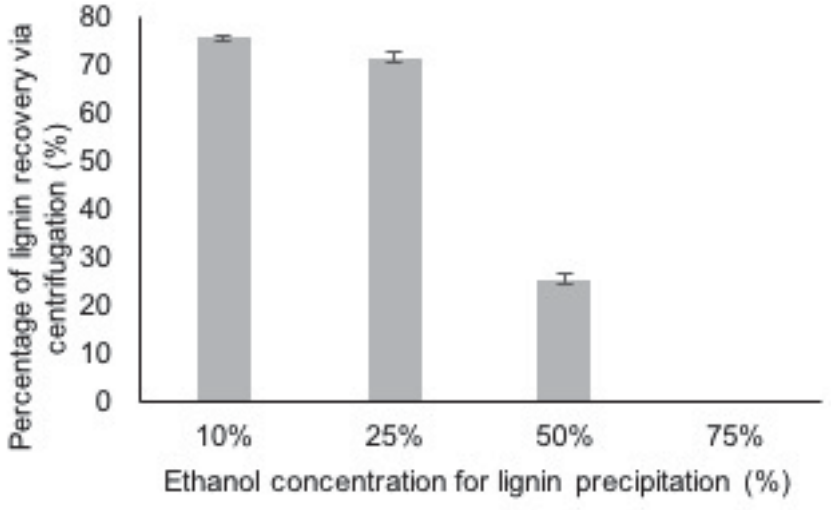

Figure 5.1. Percentage of lignin recovery at different ethanol concentrations.

A critical precaution need to be taken into consideration if water is added as the mixture of solution for delignification process. The addition of water could reduce the capability of solvent in terms of lignin dissolving capacity (Pasquini *et al.*, 2005). High water content in the mixture of solution for delignification may have demonstrated negative effects on delignification due to the nature of hydrophobic biopolymer of lignin that could trigger adsorption of lignin fragments onto the surface of biomass fibers (Tu *et al.*, 2008). A suitable concentration of water-ethanol mixtures is desirable to avoid lignin re-precipitation onto the biomass fibers, thereby reducing the efficacy of delignification. Based on the previous study within research group shown the optimum delignification was achieved using ethanol-water ratio (1:1) (Roque

et al., 2012) and the similar condition was used for delignification process in this study. Therefore, a new experiment looked at the addition of water to the soluble lignin extract was carried out after delignification for the purpose of lignin recovery study via centrifugation.

In the lignin precipitation of ethanol pulping, the removal of lignin also depends on the capacity of aqueous ethanol solution to solubilise lignin fragments (Pasquini *et al.*, 2005; Xu *et al.*, 2007). According to Wang *et al.* (2011), the ability to dissolve lignin increased with increased solvent capacity to form hydrogen bonds. Therefore, the presence of both nucleophilic agents; water and ethanol produces a good solvent for lignin recovery.

In a study with Alcell lignin and its solubility in ethanol-water mixtures, it was demonstrated that lignin solubility increased as the ethanol concentration increased until a maximum was reached at 70% ethanol concentration (Ni and Hu, 1995). When lignin precipitation is conducted by diluting the liquor with water that decreased the amount of organic solvent, the solubility of lignin decreased, thus more lignin was recovered (Fernando, 2010; Ortega, 2015; Xu *et al.*, 2007). The findings were in agreement with Sun's *et al.* statement where addition of anti-solvent such as ethanol, 1-propanol, 2-propanol and 1-butanol decreases the lignin solubility in the resultant system, therefore lead to a higher lignin recovery (Sun *et al.*, 2016). In general, it seems that a 10% ethanol concentration could be proposed ethanol concentration for lignin recovery since there was no significant difference between lignin recovery using 25% and 10% ethanol addition.

5.3.2 Percentage of Lignin Purity

The resulting soluble lignin extract after delignification was fractionated according to different ethanol concentrations, under centrifugation thereby generating two fractions, a precipitated and supernatant fraction. Both fractions were analysed by Klason lignin assay to reveal the purity of lignin. A comparison between the three different ethanol concentrations is presented in Figure 5.2.

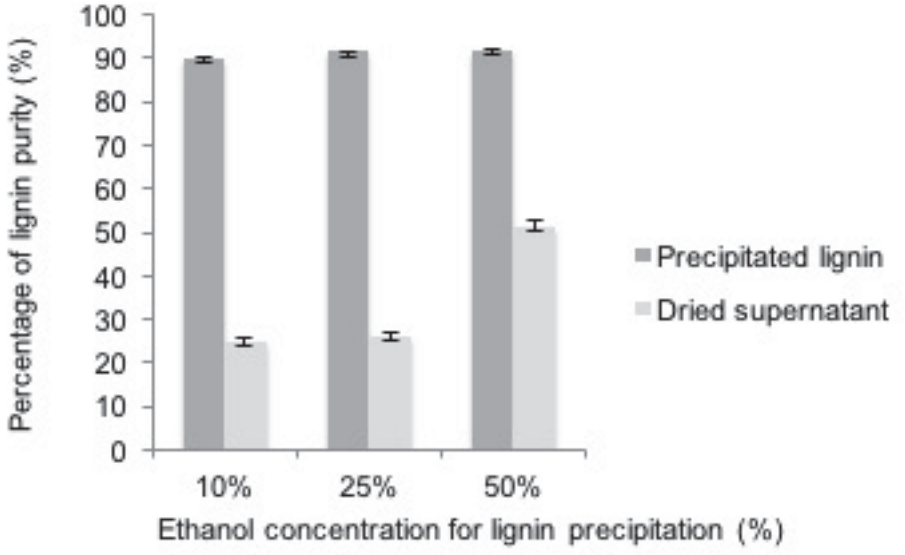

Figure 5.2. Percentage of lignin purity at different ethanol concentrations.

The purity of precipitated lignin for 50%, 25% and 10% ethanol concentration was 91.6%, 91.5% and 89.8%, respectively and did not exhibit a significant difference ($p>0.05$) for 50% and 25% ethanol concentration. Lignin derived from dried supernatant exhibited 51.6%, 26.0% and 24.7% of lignin purity for 50%, 25% and 10% ethanol concentration, respectively. According to post hoc tests analysis, ethanol concentration of 25% and 10%

were found not to have a significant influence on purity of lignin derived from dried supernatant.

Overall, the purity of precipitated lignin obtained consistently demonstrated a high purity (≥90%). Such high purity lignin has enormous possibilities for use in several industrial applications such as polymer blends, adhesive and corrosion inhibitors (Audu *et al.*, 2012; Brosse *et al.*, 2011). A few studies have also reported high purity of lignin from the organosolv method, for instance, 95.4% for sugarcane bagasse (Vallejos *et al.*, 2011), 91.9% for *MxG* (Bauer *et al.*, 2012) as well as 96.5% for shrub willow (Stewart, 2015).

As can be seen from Figure 5.2, the purity of lignin derived from dried supernatant obtained at 50% ethanol concentration is considerably higher than at 25% and 10%. When ethanol concentration increased, more lignin is solubilised in the solution, this could have resulted in low lignin recovery and the high purity of lignin remained in the supernatant. According to Derjaguin, Landau, Vervey, and Overbeek (DLVO) theory, the stability of lignin colloids in solution is interaction of attractive and repulsive forces. If the attractive forces, including Van der Waals and other hydrophobic forces dominate, then aggregation is favoured, lignin colloids become unstable and thereby lignin precipitation occurs (Zhu, 2013). Otherwise, lignin is stable in the solution and will not precipitate as the repulsive forces between lignin colloids dominate. Taking into account of high dilution may lead to excessive energy costs in process if using 50% and 25% ethanol concentration, it is recommended that 10% ethanol concentration is used for lignin precipitation.

5.3.3 FTIR Analysis

5.3.3.1 PCA of Precipitated Lignin and Dried Supernatant

There is a need to interpret the explained variance plot to identify the optimal number components in the model as the explained variance describes the variation in the data in a model. Figure 5.3 presents the PCA explained variance plot for precipitated lignin and dried supernatant. Two principal components verified the optimal numbers of the components of the model which described 93% of the validated variance and 95% of the calibrated variance data. The calibrated variance explained the same data to build and assess the model whereas the validated variance measure of model to explain new data (Cao, 2013).

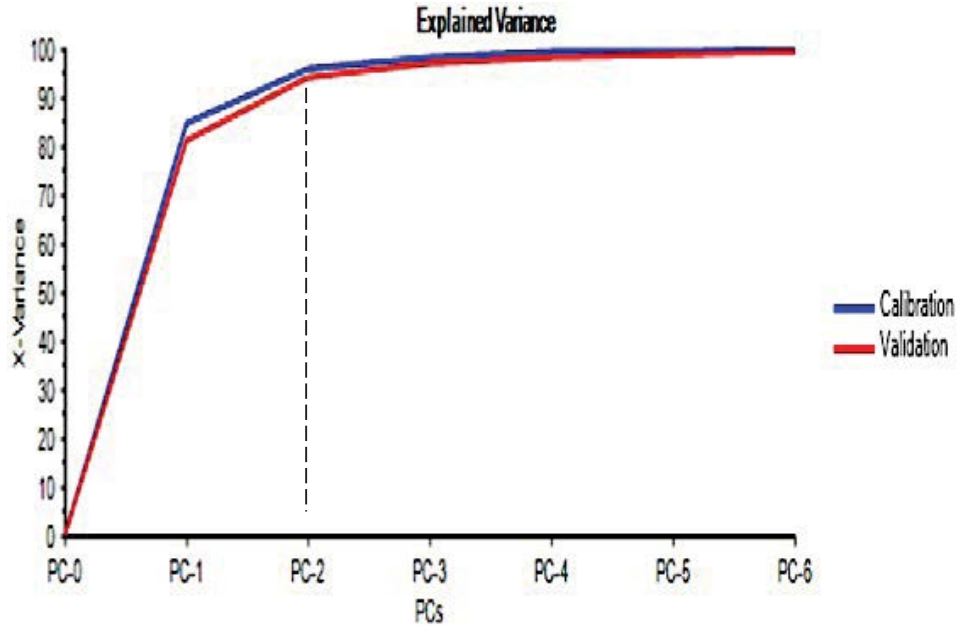

Figure 5.3. PCA explained variance plot at different ethanol concentration.

Overall, the score plot for the dataset as functions, whose first two principles components explained 84% and 11% of the spectral variance,

respectively. Figure 5.4 of PCA scores plot for precipitated lignin and dried supernatant elucidated that there were two definite clusters observed and were distinguishable within each other. At the top are the spectra for the precipitated lignin at different ethanol concentrations. A second cluster at the bottom, consists of spectra for the dried supernatant.

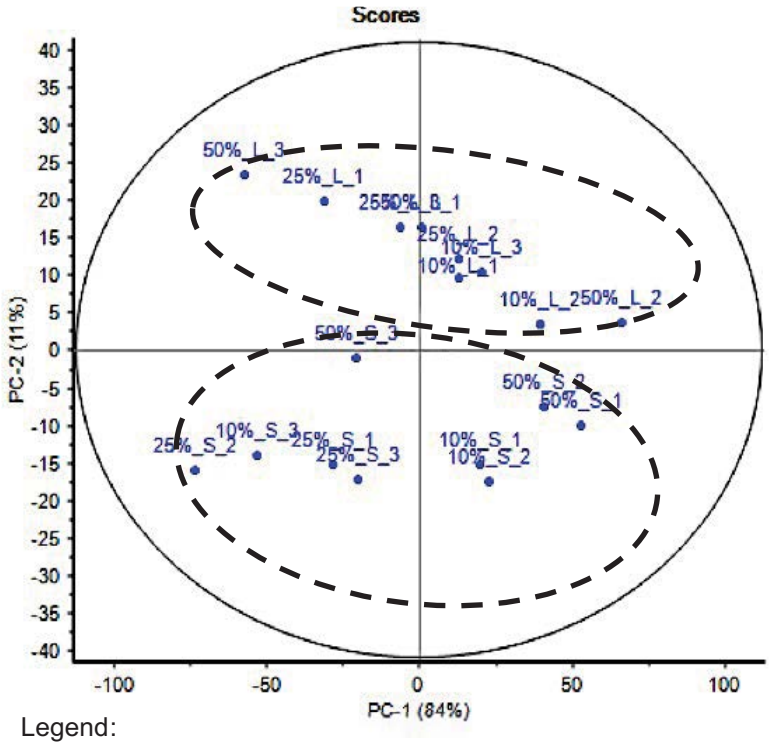

Legend:
10%_L: Precipitated lignin of 10% ethanol concentration
25%_L: Precipitated lignin of 25% ethanol concentration
50%_L: Precipitated lignin of 50% ethanol concentration
10%_S: Dried supernatant of 10% ethanol concentration
25%_S: Dried supernatant of 25% ethanol concentration
50%_S: Dried supernatant of 50% ethanol concentration
**1,2,3- repetition of spectra

Figure 5.4. PCA scores plot at different ethanol concentration.

When comparison was made between similar type of spectra within samples, scores of precipitated lignin (10%_L_1 and 10%_L3, 25%_L_1 and 25%_L_3, 50%_L_1 and 50%_L_2) and scores of dried supernatant (10%_S_1 and 10%_S_2, 25%_S_1 and 25%_S_3, 50%_S_1 and 50%_S_2) were close within each other, indicating that the samples within similar type of spectra possess similar composition. Thus, only a spectra was chosen from

spectra that have similar chemical composition to be analysed for FTIR analysis.

PCA correlation loadings are shown in Figure 5.5. Two wavenumbers, 2340 and 780 cm^{-1} were far apart compared with other wavenumbers which had influence the result of PCA score plot. The wavenumbers of 2340 and 780 cm^{-1} were correlated negatively as both wavenumber near to the center and far from the center of 100% explained variance.

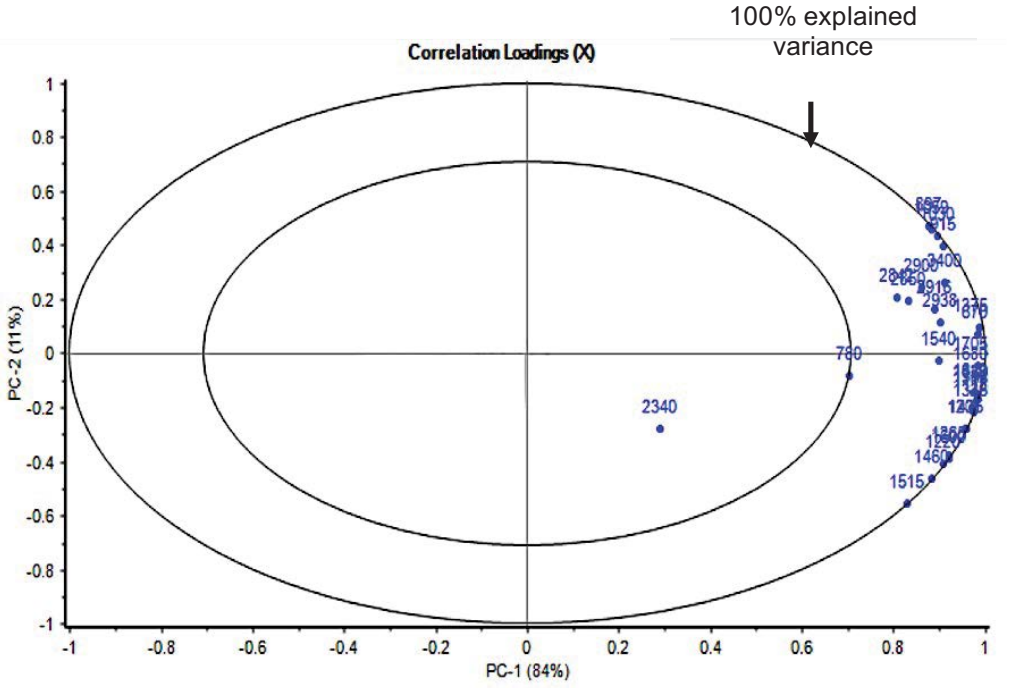

Figure 5.5. PCA correlation loadings plot at different ethanol concentration.

5.3.3.2 Spectra of Precipitated Lignin

The FTIR spectra of precipitated lignin at different ethanol concentration were shown in Figure 5.6. The indicative wavenumbers apportioned to lignin are found: 1705 to 1720, 1680, 1640, 1515, 1460, 1425, 1326, 1265, 1220, 1118, 1030, 915 and 833 cm^{-1}. The details of

wavenumbers and their interpretations are outlined in Table 4.3 (section 4.3.5.3). When comparison is made between the three spectra at different ethanol concentrations, the spectra at 50% ethanol concentration had high intensity peak rather than the other two spectra at 25% and 10%, suggesting that a high intensity in a peak indicated high purity of precipitated lignin.

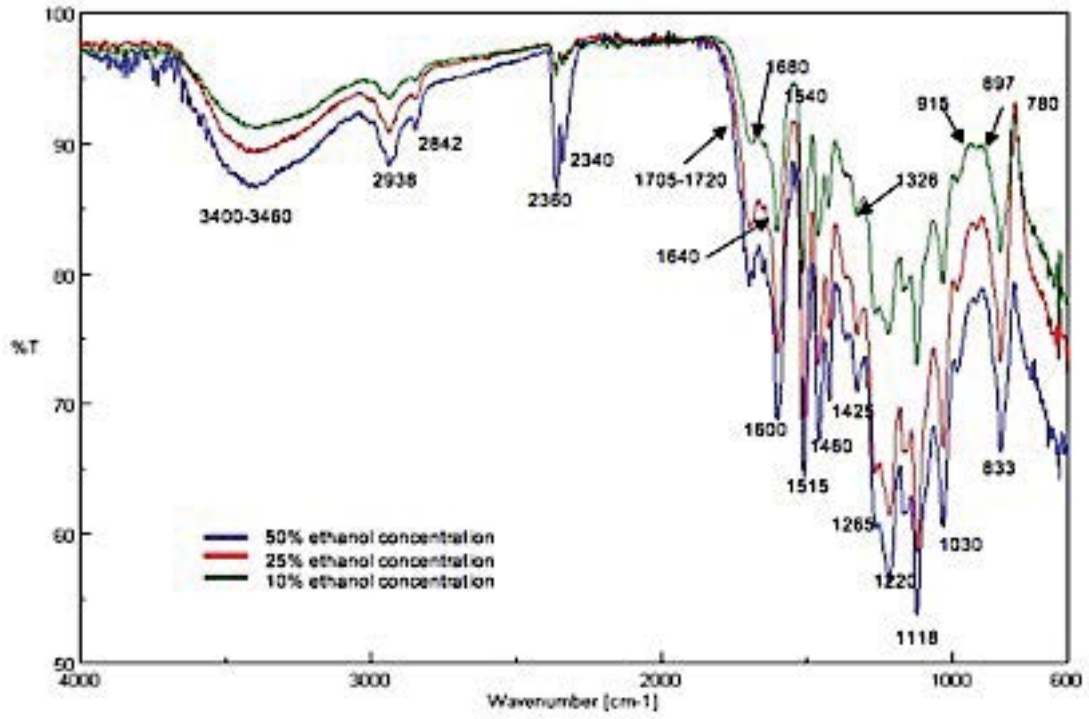

Figure 5.6. FTIR spectra for precipitated lignin from different ethanol concentrations.

The wavenumbers of 2938 and 2842 cm^{-1} are attributed to CH stretching in aromatic methoxyl groups and in methyl and methylene groups of side chains (Boeriu *et al.*, 2004). An asymmetry and broadening of the peaks at 1705 and 1600 cm^{-1} result from the weak absorption around 1640 cm^{-1} and may originate from both protein impurity and water associated with lignin, respectively (Boeriu *et al.*, 2004). The appearance of wavenumber at

1220 cm^{-1} are caused by the extraction process due to the hot water cleaved hemiacetal linkages, thus, liberated acids during biomass treatment which facilitate the breakage of ether linkages in biomass (Behera *et al.*, 2014).

However, cellulose and hemicellulose appeared as contaminants as indicated by spectra wavenumbers at 897 and 1705 to 1720 cm^{-1}. A wavenumber of 897 cm^{-1} represents amorphous cellulose which aids hydrolysis of the cellulose to glucose if enzymatic hydrolysis occurs (Ibrahim *et al.*, 2011). The wavenumbers of 1705 to 1720 cm^{-1} are attributed to ester carbonyl vibration in acetyl, feryloyl, p-coumaryl groups in hemicelluloses (Pandey, 1999). Wavenumber of 2340 to 2360 cm^{-1} was found in all spectra and is related to OH stretching from strong H-bonded-COOH (Davis *et al.*, 1999).

In general, hardwoods or angiosperms are made up of guaiacyl (G) and syringl (S) units, while softwoods or gymnosperms contain only G units. Besides, grasses contain a variety of acidic guaiacyl units attached as esters and demonstrate more substitution of *p*-hydroxyphenyl units (H) such as ferulic, hydroxycinnamic and *p*-coumaric acids (Holladay *et al.*, 2007). Lignin extracted from *Miscanthus* sp. contain all three lignin monomers, G, H and S units (Guo *et al.*, 2014; Lewandowski *et al.*, 2000; Savy *et al.*, 2015). This data showed that the wavenumbers related to G, H and S units could be at 1326 cm^{-1}(G-S units), 1265, 1030, 915 cm^{-1} (G units), 1118, 833 cm^{-1} (S units), 1705-1720 cm^{-1}(H units) and 2938, 2842 cm^{-1} for H-S units.

5.3.3.3 Spectra of Dried Supernatant

Supernatant obtained from the fractionation of resulting soluble lignin extract at different ethanol concentrations after centrifugation were dried for FTIR analysis. The following typical wavenumbers as apportioned to lignin as seen above in section 5.3.3.2 were identified in dried supernatant: 1705 to 1720, 1680, 1640, 1600, 1515, 1460, 1425, 1326, 1265, 1220, 1118, 1030 and 833 cm^{-1} as illustrated in Figure 5.7. The details of wavenumbers and their interpretations are presented in Table 4.3 (section 4.3.5.3).

In general, the spectra of 50% ethanol concentration had broader intensity than 25% and 10% especially for wavenumber apportioned to lignin. In fact, it is suggested that the dried supernatant had highest purity of lignin (51.6 %). The peaks for the dried supernatant related to lignin including wavenumbers of 2842, 2340, 2360, 1680, 1640 and 1326 cm^{-1} were in weaker intensity compared with peaks of precipitated lignin. The weak intensity and absence of peak (915 cm^{-1}) related to lignin were due to more lignin precipitated and thus less lignin composition appeared in dried supernatant.

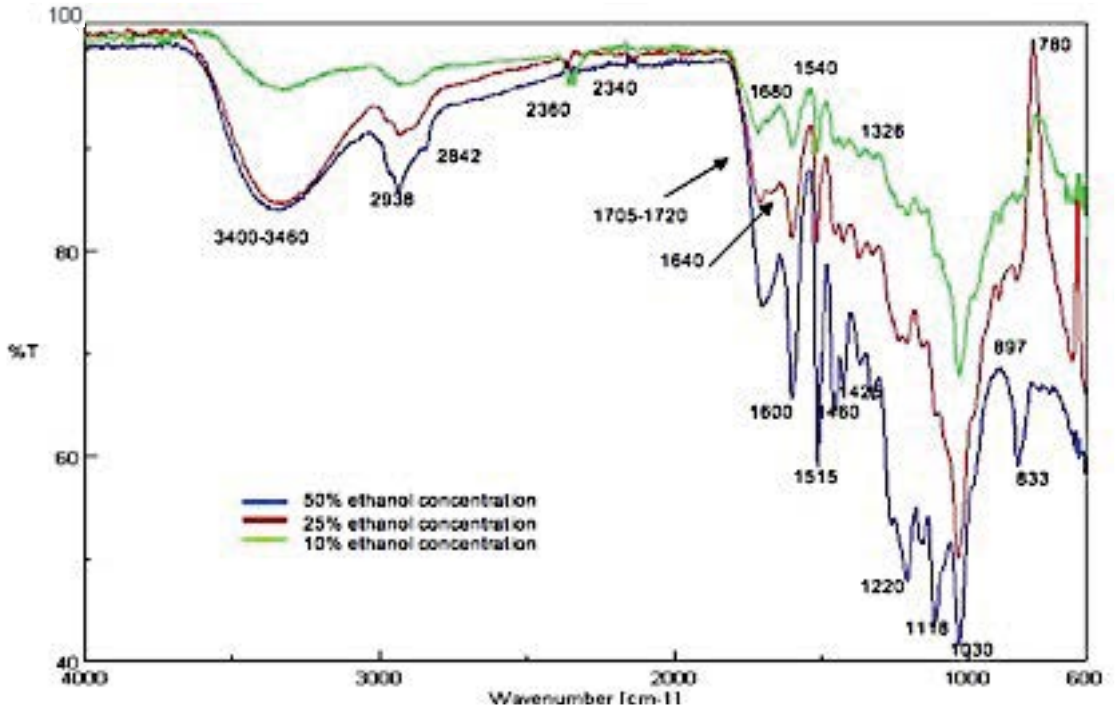

Figure 5.7. FTIR spectra for dried supernatant from different ethanol concentrations.

A new distinct peak of 1540 cm^{-1}, related to an aromatic ring stretching in lignin, was found in both spectra for the precipitated lignin and the dried supernatant (Radotić *et al.*, 2012). In summary, from the spectra in Figure 5.7, it is apparent that wavenumbers of 897 and 1705 to 1720 cm^{-1} related to the contamination of cellulose and hemicellulose were in high intensity and broader peak at 50% ethanol concentration than 25 and 10% ethanol concentration, thus less purity of lignin derived from supernatant was obtained.

5.3.4 SEM Analysis

The structural morphology of precipitated lignin and dried supernatant were examined by SEM imaging. A structural organisation of lignin appears as globular form of layered structures and the globules associated to form large macromolecular structure (Micic *et al.*, 2004; Radotić *et al.*, 2005).

5.3.4.1 Precipitated Lignin

Compared with three samples of precipitated lignin at different ethanol concentrations, SEM images showed similarity in the presence of lignin macromolecule globule structure of spherical balls or droplets. The shape of lignin macromolecule was not identical in terms of size, as shown in Figure 5.8. 5.9 and 5.10 for precipitated lignin from 50%, 25% and 10% ethanol concentration, respectively. Precipitated lignin at 50% ethanol concentration had larger lignin macromolecule than at 25% and 10%. On the other hand, precipitated lignin at 25% and 10% of ethanol concentration exhibited mixture of large and small lignin macromolecules. In addition, it formed more colloidal and amorphous lignin macromolecule structure.

This is associated with the effect of surface area and particle size. Surface area is inversely proportional to particle size (Dubois and Holgersson, 2010). In a study of the effect of calcium chlorides on the solubility of lignin in the black liquor of pre-hydrolysis kraft pulping, as the calcium chlorides concentration increased, the particle size of lignin increased, hence solubility of lignin decreased due to increasing of coagulation in the black liquor (He *et al.*, 2014). It is suggested that large particle size of lignin exerted a negative

impact on the surface area for reactions resulting in the precipitation process, thereby less lignin is recovered.

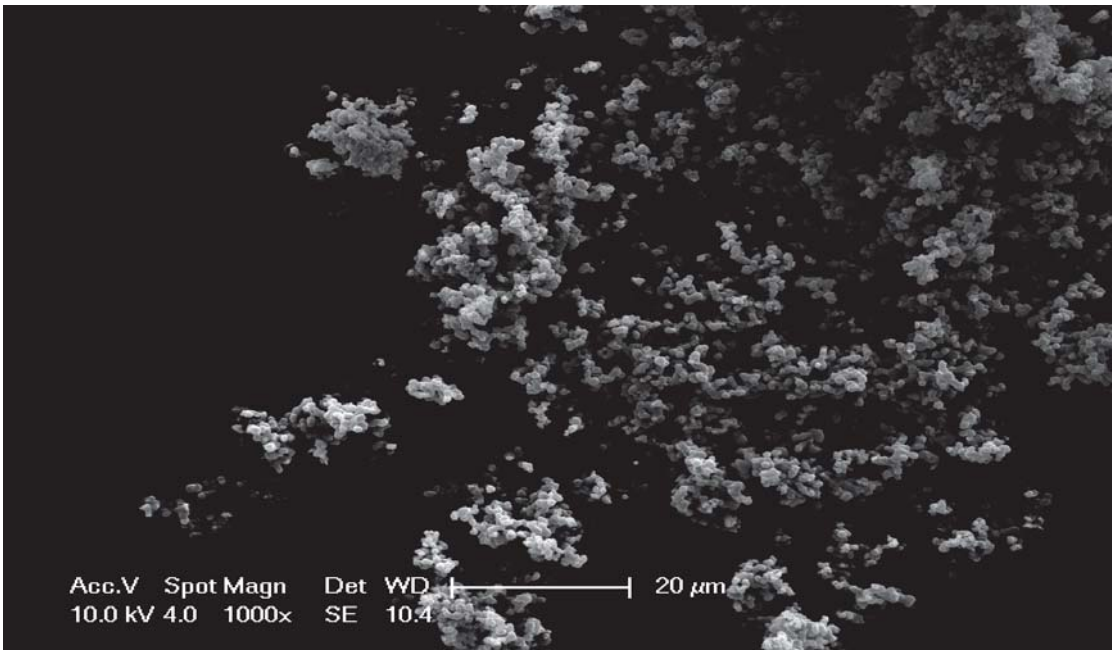

Figure 5.8. SEM image of precipitated lignin at 50% ethanol concentration.

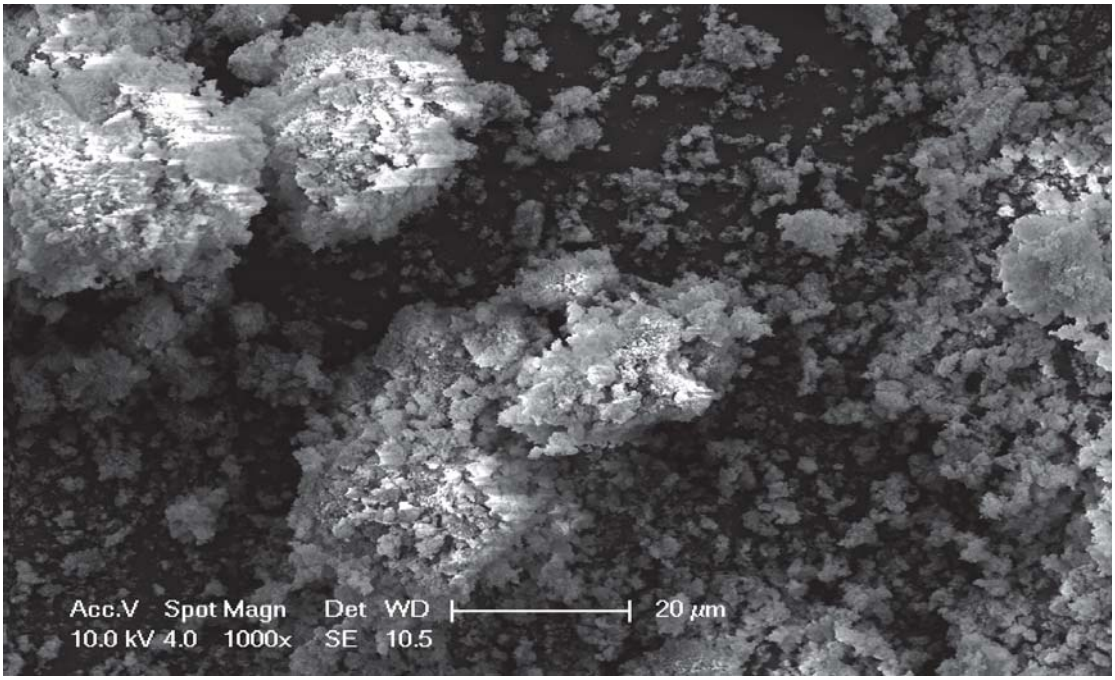

Figure 5.9. SEM image of precipitated lignin at 25% ethanol concentration.

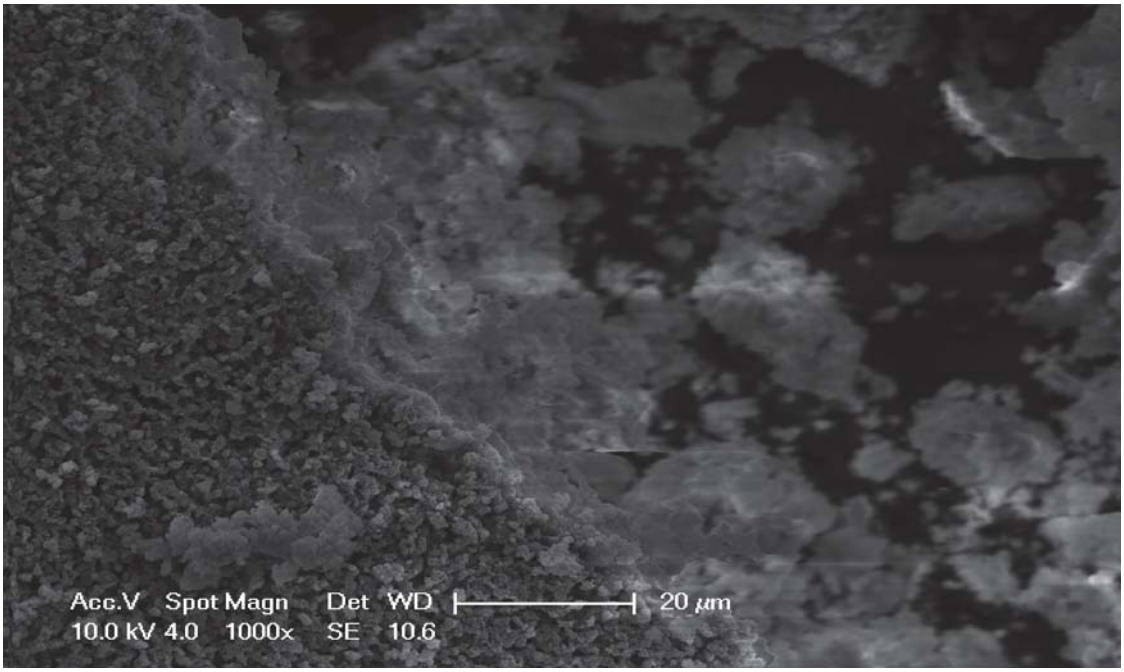

Figure 5.10. SEM image of precipitated lignin at 10% ethanol concentration.

5.3.4.2 Dried Supernatant

A representative of SEM images of dried supernatant are exhibited in Figure 5.11, 5.12 and 5.13 for dried supernatant at 50%, 25% and 10% ethanol concentration, respectively. SEM image at 50% ethanol concentration for dried supernatant revealed that crystalline structure was observed in the dried supernatant rather than at 25% and 10%. The dried supernatant at 25% and 10% ethanol concentration had less crystalline and smooth surface than at 50%.

The literature has emphasised the importance of ethanol concentration on lignin depolymerisation. The findings have revealed that there has been a significant increase in liquid separation from 41 to 65.5% by increasing ethanol concentration from 0 to 65 volume %. Nevertheless, the solid residue yields decreased steadily from 39 to 17% (Ye *et al.*, 2012). The high ethanol

concentration exerted negative impact on the recovery of solid residue in lignin depolymerisation and the results are similar to the effect of ethanol concentration on lignin precipitation in this study.

An increased of ethanol concentration resulted in low lignin recovery. The low lignin recovery may be caused by an addition of ethanol in ethanol-water mixture, which helps to dissolve lignin, lignin degraded intermediates and inhibit condensation of lignin degraded intermediates (Yuan *et al.*, 2010), thus, it reduced the precipitated lignin and lignin remained in the supernatant. This finding is linked with the percentage of lignin recovery at 50% ethanol concentration which was lower than at 25 and 10% as have been reported in section 5.3.1.

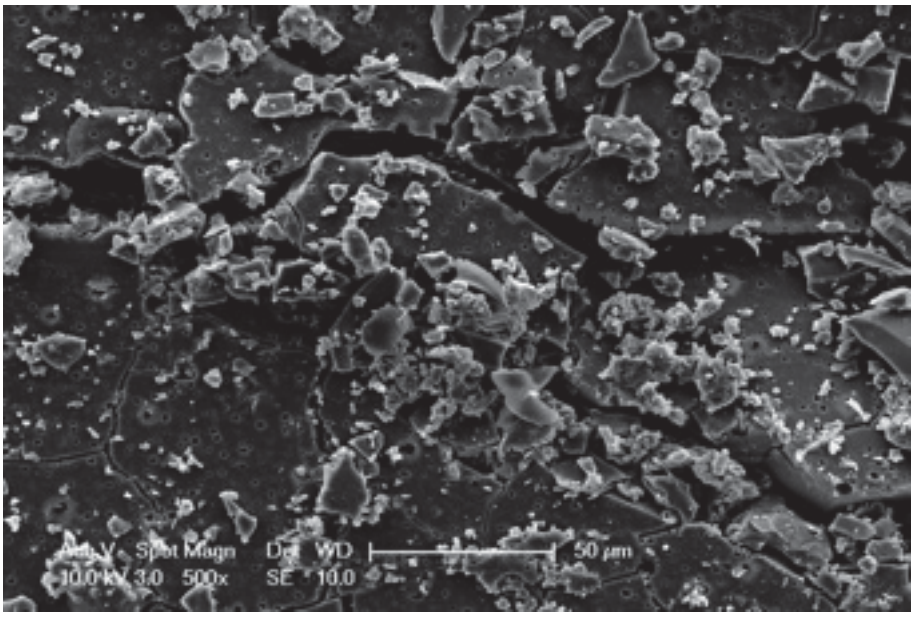

Figure 5.11. SEM image of dried supernatant at 50% ethanol concentration.

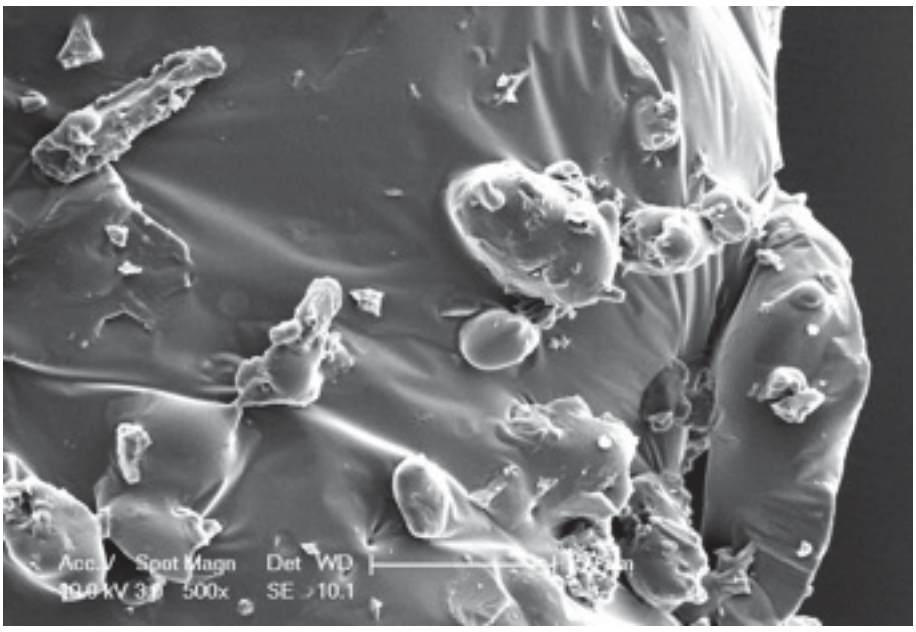

Figure 5.12. SEM image of dried supernatant at 25% ethanol concentration.

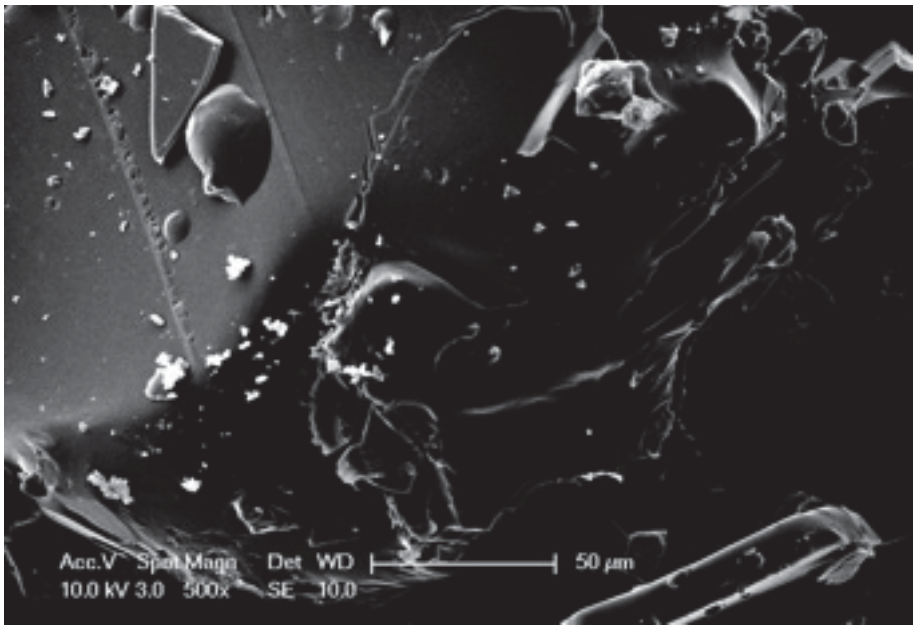

Figure 5.13. SEM image of dried supernatant at 10% ethanol concentration.

5.3.4.3 Soluble Lignin Extract

SEM images provided insignificant results for the morphology of soluble lignin extract as shown in Figure 5.14, 5.15 and 5.16 for soluble lignin extract at 50%, 25% and 10% ethanol concentration, respectively. Overall, the

morphological study of the soluble lignin extract showed discrepancy between the SEM and the particle size analysis.

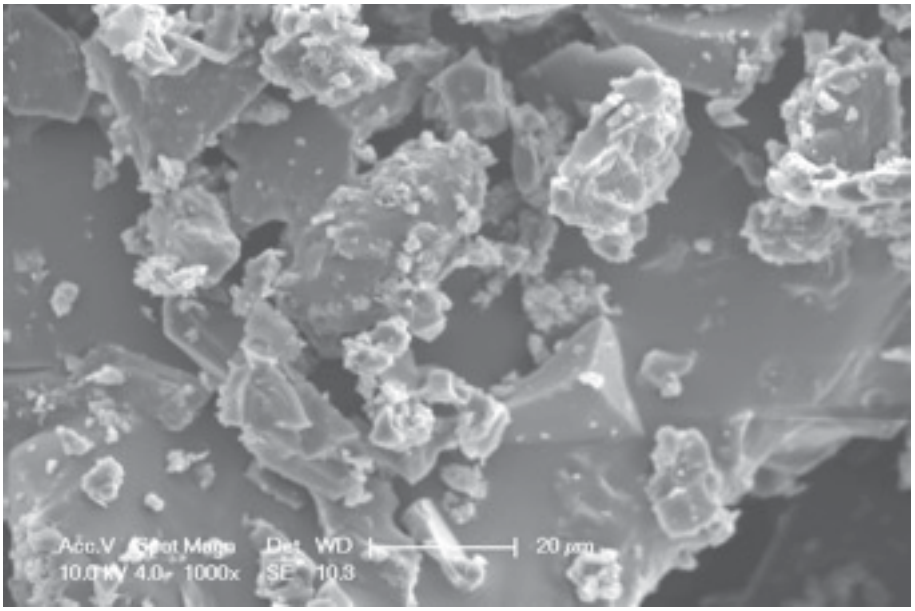

Figure 5.14. SEM image of soluble lignin extract at 50% ethanol concentration.

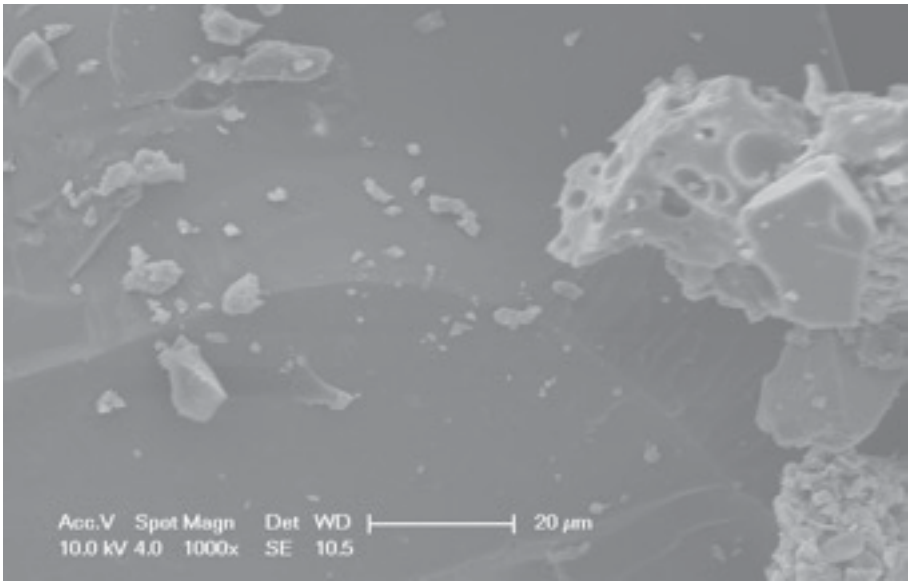

Figure 5.15. SEM image of soluble lignin extract at 25% ethanol concentration.

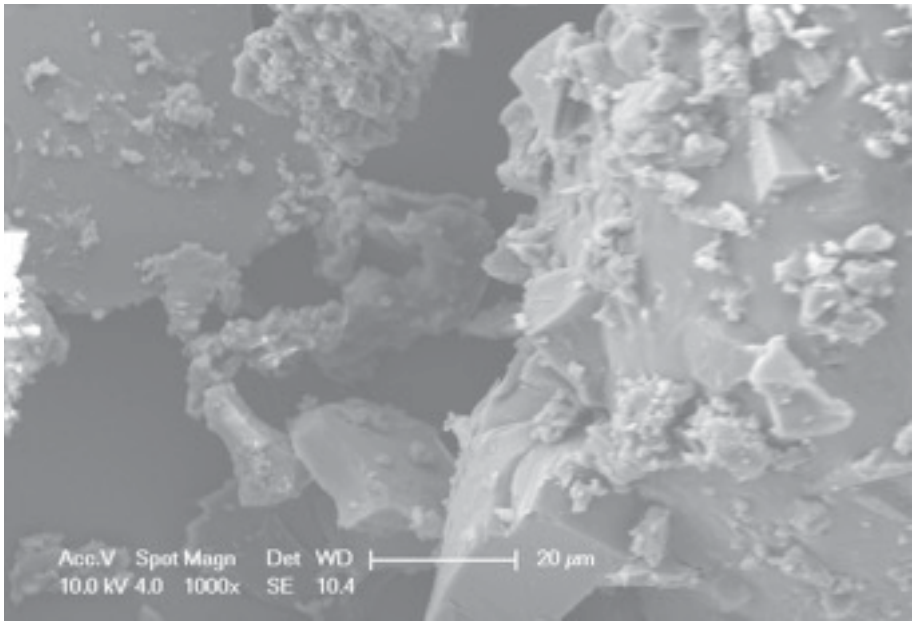

Figure 5.16. SEM image of soluble lignin extract at 10% ethanol concentration.

In hind sight the apparent aggregation of lignin with reducing ethanol concentration, observed by SEM analysis, may have been due to the sample preparation process for SEM as plant species need to be in native-hydrated state which the drying method to remove water sample may cause collapse, shrinkage and distortion of the cell and change the original form and structure of soluble lignin extract (Golding *et al.*, 2016; Moran and Coats, 2012; Pathan *et al.*, 2010). Furthermore, dehydration and coating of the cell prior to SEM also stimulated aggregation, thus the sample preparation affected the nature of colloids and particles (Doucet *et al.*, 2005). Therefore, in an attempt to visualise the lignin aggregates morphology in solution, LM is explored in section 5.3.6 and 5.3.7.

5.3.5 Particle Size Analysis of Precipitated Lignin and Supernatant

Isolation of lignin by different chemical procedures resulted in a material of different lignin complexity. Due to complex interaction between

monomers, lignin had random polymer globule structure with non-linearly and random cross-linked with other constituents, and the structure of lignin is not as the other two main components of lignocellulosic biomass, cellulose and hemicellulose which has a more linear shape structure (Chen, 2014). A schematic representation of lignin globule structure is illustrated in Figure 5.17.

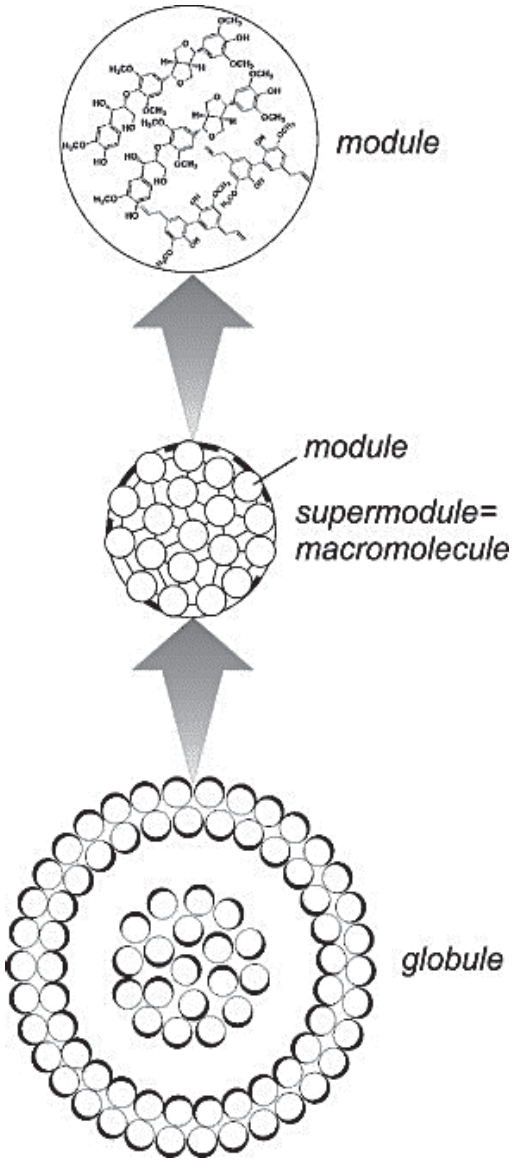

Figure 5.17. Schematic representation of lignin globule structure. (Source: Adapted from Micic *et al.*, 2004; Radotić *et al.*, 2005).

The scheme shown in Figure 5.17 is a series of steps starting from globule to the presumed molecular structure of the first stage of polymerisation (module). Thick and thin lines indicated hydrophilic and hydrophobic regions, respectively (Micic *et al.*, 2004; Radotić *et al.*, 2005). In lignin synthesis, the formation of lignin globule began with modules that consist of various monomers. Then, the polymerisation of monomers formed supermodules and globules that made up of a large number of supermodules (Radotić *et al.*, 2006).

In lignin aggregation, Norgren *et al.* (2002) suggested that the modes of aggregation starting from macromolecular lignin and the final product of fractal lignin clusters that has non-integer dimensionality of complex structures. The modes of aggregation presented as dissolved macromolecules and few steps occurred during aggregation including lignin self-associates and colloidal lignin particles. Figure 5.18 showed a schematic representation of the modes aggregation in lignin solution system. Thus, it is suggested that comparison of aggregation behaviour for organosolv lignin in different ethanol concentrations of precipitated lignin, supernatant and lignin soluble extract were studied by two different instruments, namely, Zetasizer Nano ZS and Mastersizer 2000.

Samples measured by light scattering of Zetasizer Nano ZS preferably the intensity distribution as those data are closest to what is really measured and do not involve Mie scattering function such as refractive index and absorption (Malvern, 2014). Zetasizer Nano ZS uses Mie theory by default to convert intensity distribution into volume distribution for particles within the

range of the instruments (Malvern, 2014). Nevertheless, the Mastersizer 2000 gave volume-weighted distribution, which within the relative volume contribution is proportional to size of particles (Malvern, 2012).

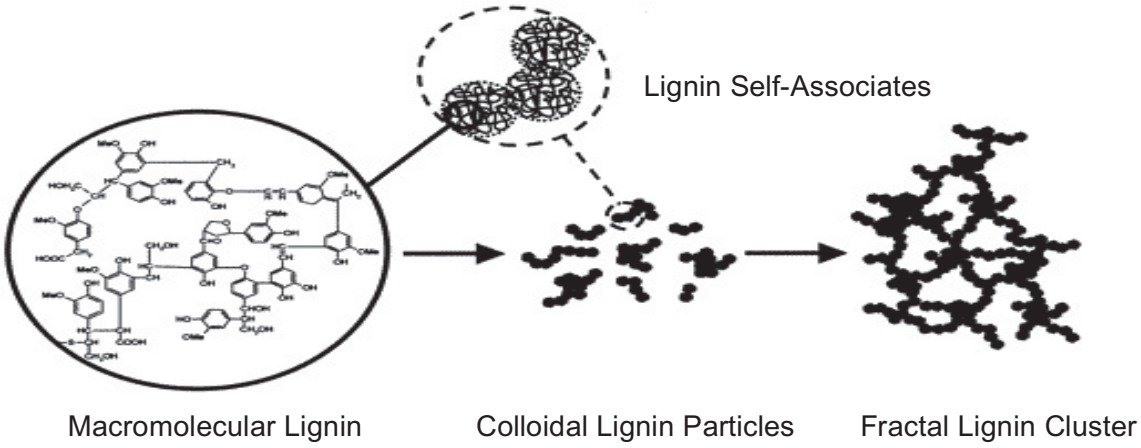

Figure 5.18. A schematic representation of the modes of aggregation in lignin solution system (Source: Adapted and modified from Norgren *et al.*, 2002).

All in all, the two sets of data obtained by Zetasizer Nano ZS and Mastersizer 2000 had common similarities on explaining the behaviour of lignin macromolecules of precipitated lignin and supernatant as well as lignin aggregates in ethanol-water solution. The surface weighted mean diameter by Mastersizer 2000 was reported in terms of the $D_{3,2}$ values. The $D_{3,2}$ refers to the diameter of a sphere of equivalent volume to surface area ratio of the particles in the sample. The value of surface weighted mean was indicative of phenomenon of particle aggregation (McClements, 2015). Decreasing aggregate sizes were found very effective on decreasing the aggregate stability and weighted mean diameter (An *et al.*, 2013; Yonter, 2015). Thus, it suggested that the surface weighted mean obtained is the size of lignin macromolecules in precipitated lignin, supernatant and soluble lignin extract.

5.3.5.1 Zetasizer

Table 5.1 shows that average particle size of precipitated lignin increased as ethanol concentration increased. In contrast, average particle size of dried supernatant decreased as ethanol concentration increased.

Table 5.1. Average particle size of precipitated lignin and dried supernatant at different ethanol concentrations by Zetasizer.

Ethanol concentration (%)	Precipitated lignin (nm)	Dried supernatant (nm)
10	306.2 ± 4.0	1598.3 ± 20.3
25	391.7 ± 6.6	1197.3 ± 65.5
50	2050.0 ± 103.7	875.1± 60.2

A comparison between the three different ethanol concentrations illustrated that lignin precipitation at 50% ethanol concentration had highest average particle size (2050.0 nm) rather than 25% (391.7 nm) and 10% (306.2 nm) and left the remaining dried supernatant with the lowest average particle size (875.1 nm) rather than 25% (1197.3 nm) and 10% (1598.3 nm). The particle size of respective lignin macromolecules can be linked and explained by SEM image analysis (Figure 5.8 to 5.10) especially SEM image of precipitated lignin of 50% ethanol concentration that clearly shows lignin macromolecules have regular, uniform and large shapes compared with 25% and 10%.

The particle size distribution of precipitated lignin and dried supernatant as a function of ethanol concentration were shown in Figure 5.19 and 5.20, respectively. The 50% and 25% ethanol concentration had bimodal

distribution whereas 10% ethanol concentration of precipitated lignin had multimodal distribution. As shown in Figure 5.19, precipitated lignin at 25% and 10% contains both nano-(<100 nm) and micro-size particles. The precipitated lignin of 50% ethanol concentration had only micro-size particles.

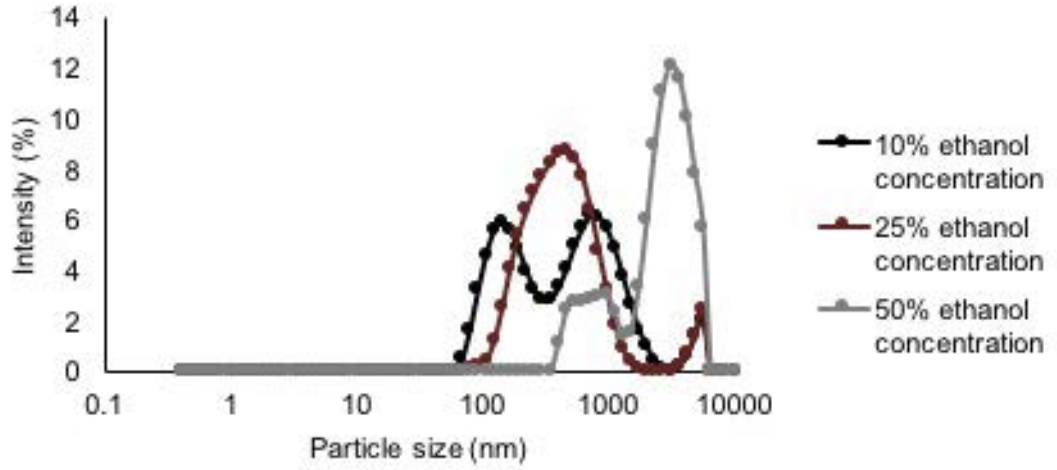

Figure 5.19. Particle size distribution at 50%, 25% and 10% ethanol concentration of precipitated lignin by Zetasizer.

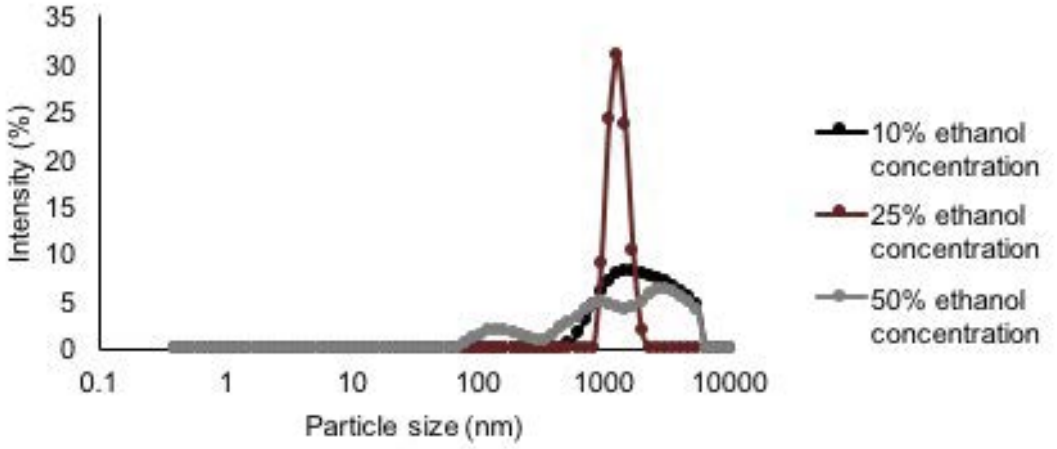

Figure 5.20. Particle size distribution at 50%, 25% and 10% ethanol concentration of dried supernatant by Zetasizer.

The measured size of dried supernatant particles of 10% and 25% ethanol concentration had a monomodal distribution whereas at 50% ethanol

concentration, the dried supernatant showed a multimodal distribution as shown in Figure 5.20. The dried supernatant of 25% and 10% ethanol concentration only had micro-particles whereby dried supernatant of 50% ethanol concentration contained both nano- and micro-particles. Results of different particle size distributions for both precipitated lignin and dried supernatant may be due to the changes of physical and chemical properties; i.e. the samples in a dried form, dispersed in the solution that rearranged lignin macromolecules in the solution and the formation of new self-assembled structures (Shulga and Vitolina, 2012).

Precipitated lignin that had low average particle size with high surface area for precipitation process resulted in high lignin recovery and left the other fraction of high average particle size remaining in the supernatant. Highest average particle size of precipitated lignin at 50% ethanol concentration also may be explained due to the agglomeration of the particles which reduces the surface area available for precipitation reaction (Allen *et al.*, 2001; Sayyar *et al.*, 2009). The surface area available during precipitation may influence the interaction of attractive and repulsive forces that further affected the lignin stability in solution and lignin recovery process.

5.3.5.2 Comparison of Zetasizer with Mastersizer

The data characterising physicochemical properties of lignin and supernatant in different ethanol concentration are presented in Table 5.2. Overall, the results of the particle size diameter of Mastersizer correlated with the patterns of particle size distribution of Zetasizer for both precipitated lignin

and dried supernatant. In general, modification of 50% to 25% ethanol concentration via Zetasizer was responsible for a shift towards the low range of particle size distribution and indicated that the particle size of lignin particles reduced for precipitated lignin and the results were vice versa for supernatant.

Table 5.2. Comparison of particle sizes of precipitated lignin and supernatant from different ethanol concentrations by Zetasizer and Mastersizer.

Sample	Ethanol concentration (%)	Particle size					
		Particle diameter from Zetasizer Nano ZS (nm)		Particle diameter from Mastersizer 2000 (μm)			
		Particle size distribution	Particle size	D_{v10}	D_{v50}	D_{v90}	$D_{3,2}$
Lignin	50	342.0-1281.0 1281.0-6439.0	2050.0	5.5	98.2	257.7	18.3
	25	91.3-1718.0 3580.0-6439.0	391.7	7.0	36.2	131.7	8.6
	10	58.8-295.3 295.3-2669.0 3580.0-6439.0	306.2	3.8	67.8	300.2	11.1
Supernatant	50	68.1-295.3 295.3-1484.0 1484.0-6439.0	875.1	4.5	13.3	239.6	10.3
	25	825.0-2305.0	1197.3	3.0	9.3	86.3	6.9
	10	531.2-6439.0	1598.3	4.1	40.7	275.6	12.6

*E.g. D=diameter, v = volume, D_{v10}= the maximum particle diameter below which 10% of the sample volume exists

A further reduction to 10% ethanol concentration showed that the distribution tends to move towards right position of the distribution,

demonstrating that the lignin particles tend to form population of large particles within precipitated lignin and dried supernatant. The results linked with overall particle size diameter of Mastersizer and verified that the particle size diameters decreased in 50% to 25% ethanol concentration and increased from 25% to 10% ethanol concentration.

According to the data presented in Table 5.2, further distribution of Mastersizer results for precipitated lignin and dried supernatant were discussed. For precipitated lignin, reduction of 50% to 25% ethanol concentration showed that D_{v10} increased from 5.5 µm to 7.0 µm and decreased to 3.8 µm at 10% ethanol concentration, this means that reduction of ethanol concentration from 50 to 10% ethanol concentration created large population of small particles. In contrast, D_{v50} and D_{v90} of particles population exhibited different trends, which reduction of ethanol concentration showed descending trend in size of lignin particles from 50 to 25% ethanol concentration and ascending trend at 10% ethanol concentration. This showed that the re-aggregation of lignin particles occurred or lignin tended to form large particles at 10% ethanol concentration for D_{v50} and D_{v90} of particles population (67.8 µm and 300.2 µm, respectively).

Similar findings were also revealed for D_{v50} and D_{v90} of particles population for supernatant, which showed increment of lignin particle size at 10% ethanol concentration in comparison to 25% and 50% ethanol concentration. D_{v10} of particles population showed similar trends for supernatant. The particle size of D_{v10} of particles population decreased from 4.5 µm (50% ethanol concentration) to 3.0 µm (25% ethanol concentration)

and increased to 4.1 μm (10% ethanol concentration). This may owe to re-arrangement of lignin macromolecules in the supernatant (Shulga and Vitolina, 2012) or effect of drying prior to the measurement. The conversion of intensity distribution to volume distribution for precipitated lignin and supernatant given by Zetasizer Nano ZS in comparison with the volume distribution given directly by Mastersizer 2000 instrument were presented in Figure 5.21 and Figure 5.22, respectively.

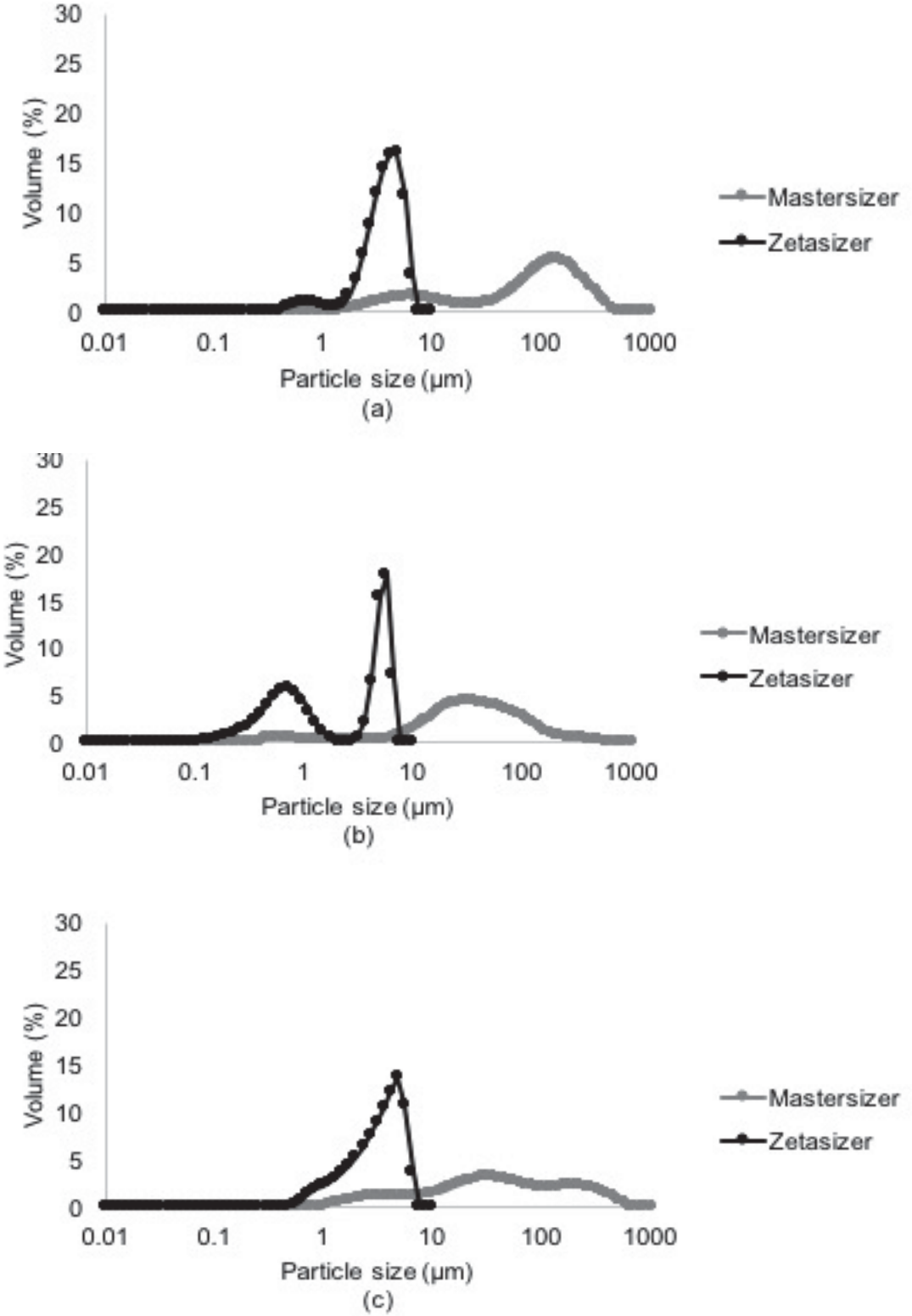

Figure 5.21. Comparison of volume distribution of precipitated lignin for Mastersizer and Zetasizer at (a) 50%, (b) 25% and (c) 10% ethanol concentration.

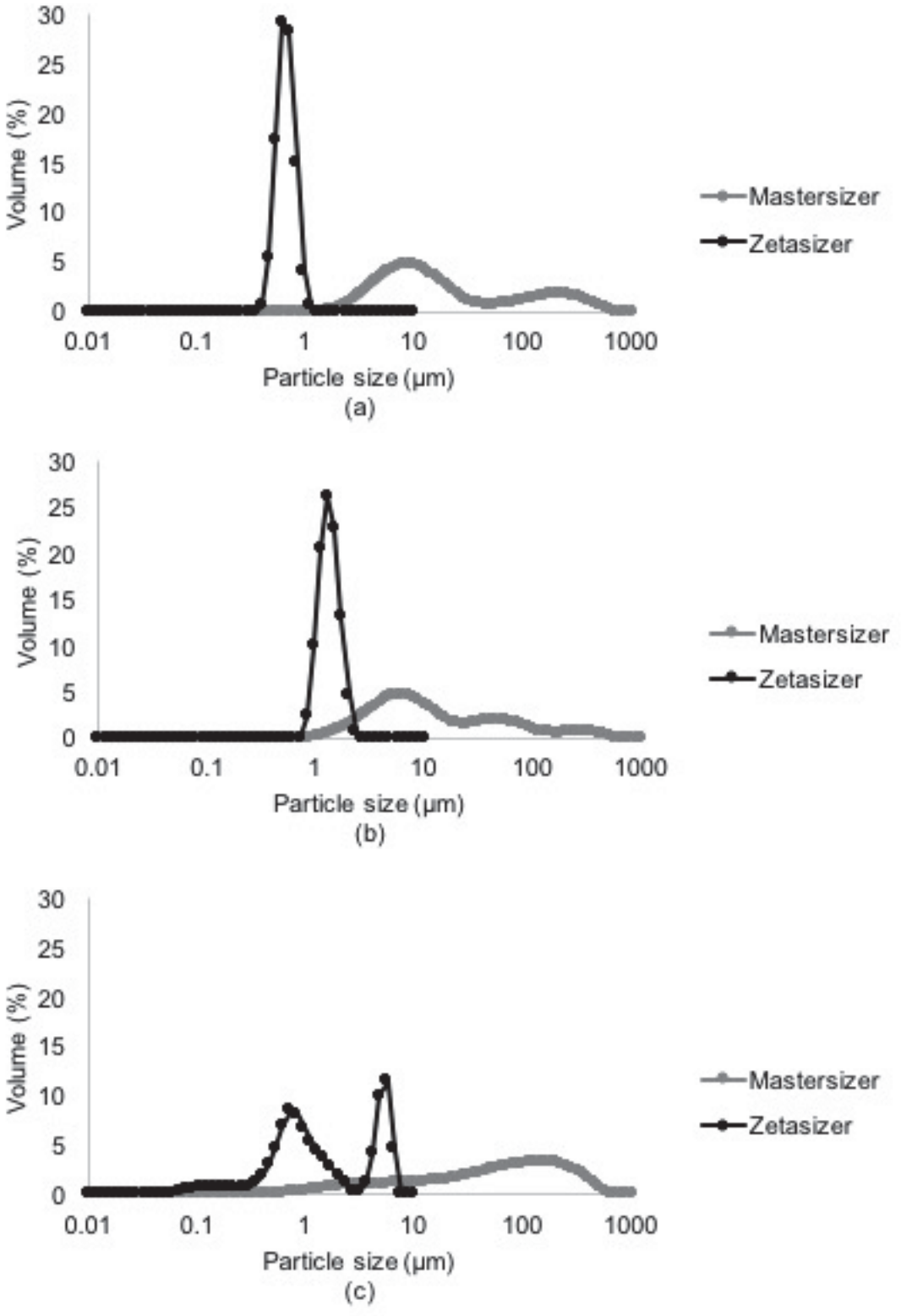

Figure 5.22. Comparison of volume distribution of dried supernatant for Mastersizer and Zetasizer at (a) 50%, (b) 25% and (c) 10% ethanol concentration.

Here, the focus has been to compare the similar particle size distribution with different particle analysis methods. In this study, volume weighted distribution was examined which the contribution of each particle in the distribution relates to the volume of that particle (Malvern, 2012). Findings showed that the notable and considerable differences between volume distribution of different instruments, Zetasizer and Mastersizer.

It is difficult and challenging to compare both volume distributions. This may due to the area where the significant differences have been observed is the particle size that could be instruments threshold. The Zetasizer instrument detects particle size only up to 10 μm in comparison to the Mastersizer instrument which measures larger particle size up to 2000 μm.

The principles of operation of instruments also differed. The Zetasizer uses dynamic light scattering technique that measures Brownian motion and relates the motion to the particles size suspended within a liquid (Malvern, 2011). On the other hand, Mastersizer uses static light scattering such as laser diffraction that measures particle size distribution by measuring the angular variation in intensity of light scattered through a dispersed particulate sample (Malvern, 2012). Even though direct conversion from instruments available to convert one type of weighting to another, the results calculated may be different, especially in the case of intensity-weighting due to the Mie assumptions that need to be considered and different principles of operation of instruments (Particle Sciences, 2009).

5.3.6 Preliminary Study of Particle Size Analysis of Soluble Lignin Extract

5.3.6.1 Zetasizer

Table 5.3 summarised the average particle size of lignin at different ethanol concentrations of soluble lignin extract. Overall, a descending trend was observed for reduction of ethanol concentration from 50% to 10%.

Table 5.3. Average particle size of soluble lignin extract at different ethanol concentrations by Zetasizer.

Ethanol concentration (%)	Particle size (nm)
10	441.5 ± 17.2
25	1077.0 ± 43.4
50	1768.2 ± 45.2

Irrespective of particle size distribution at different ethanol concentration, which are shown in Figure 5.23, 50% ethanol concentration of soluble lignin extract had a monomodal distribution whereas 25% and 10% showed a bimodal and multimodal distribution, respectively.

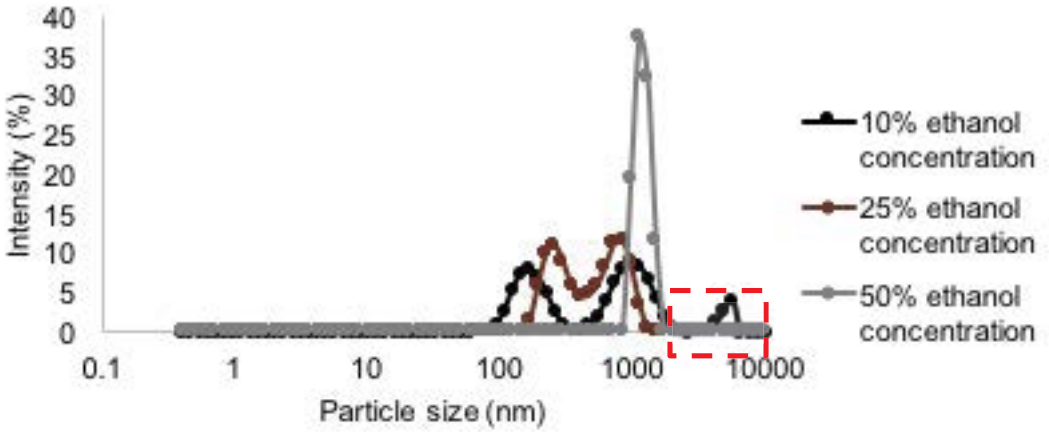

Figure 5.23. Particle size distribution at 50%, 25% and 10% ethanol concentration of soluble lignin extract by Zetasizer.

The fact that the resulted bimodal and multimodal distribution attributed to the mixture of particles including clusters of aggregates from the soluble lignin extract (Jesionowski *et al.*, 2014). Overall, 50% ethanol concentration of soluble lignin extract exhibited population of large particle between 825 and 1990 nm. Population of large particle aggregates was verified with the morphology characterisation shown in Figure 5.24. When reducing the ethanol concentration of soluble lignin extract, it resolved population of large particle into sub-population of small particle. Reduction of 50% ethanol concentration of soluble lignin extract to 25%, population of large particle began to dissociate gently into sub-population of small particle aggregates between 141.8 and 396.1 nm, as well as between 458.7 and 1281.0 nm. Figure 5.25 presented the sub-population of lignin aggregates.

The particle size distribution at 10% ethanol of soluble lignin extract showed a distinct population of particles, specifically, the lignin macromolecule in the 10% ethanol of soluble lignin extract tend to form large aggregates between sub-population of 3580 and 6439 nm (dashed red line – Figure 5.23). Figure 5.26 proved that the sub-population of small particles within population at 10% ethanol concentration of soluble lignin extract reduced and particles may be tending towards re-aggregation.

Theoretically, an increase of ethanol concentration resulted in more dispersion or aggregation of particles in the ethanol-water mixture (Claverie *et al.*, 2010; Dan *et al.*, 2009). As dispersion increases, the particle size of molecules decreases (Bergeret and Gallezot, 2008; Dan *et al.*, 2009). High dispersion of lignin macromolecules also has a broad particle size distribution. However, the findings in this study were contradictory with the theory. The

reason for this rather contradictory result is still not entirely clear, but interestingly, the preliminary study of LM images and particle size distribution have proven that aggregation of lignin occurs at low ethanol concentration. Furthermore, formation of lignin aggregates at low ethanol concentration produced more rounder or sphere particles as have been discussed in section 5.3.7. A possible explanation of contradict lignin aggregates behaviour may be that lignin is an amphiphilic polymer that contains both hydrophobic and hydrophilic segments besides possesses self-assembly behaviour (Xiong *et al.*, 2017). The hydrophilic segments of lignin macromolecules had an affinity to ethanol, whereas the hydrophobic segments of dissociated lignin aggregate into spherical or rounder shape in the ethanol-water mixture (Li *et al.*, 2016; Qian *et al.*, 2014; Rao *et al.*, 2017; Xiong *et al.*, 2017).

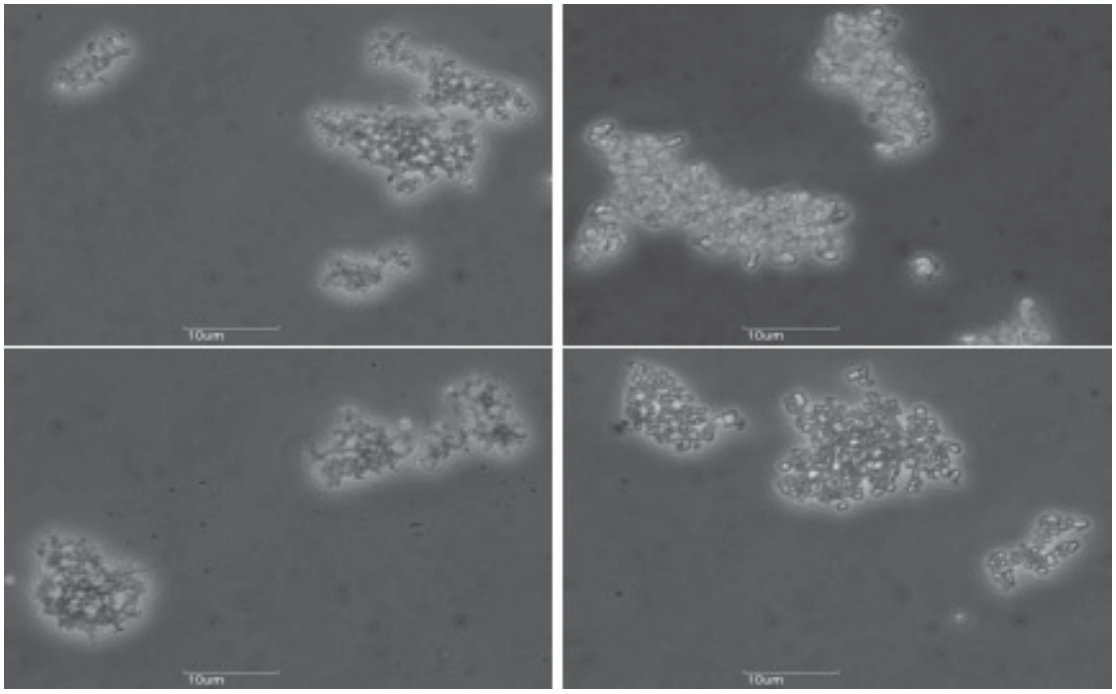

Figure 5.24. LM images of soluble lignin extract at 50% ethanol concentration.

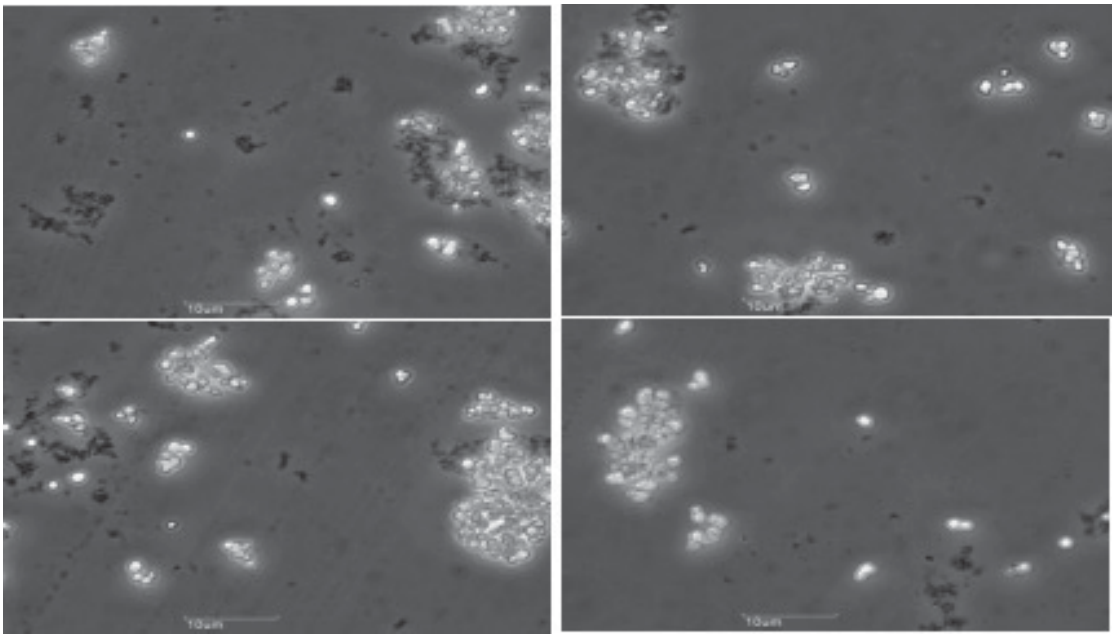

Figure 0.25. LM images of soluble lignin extract at 25% ethanol concentration.

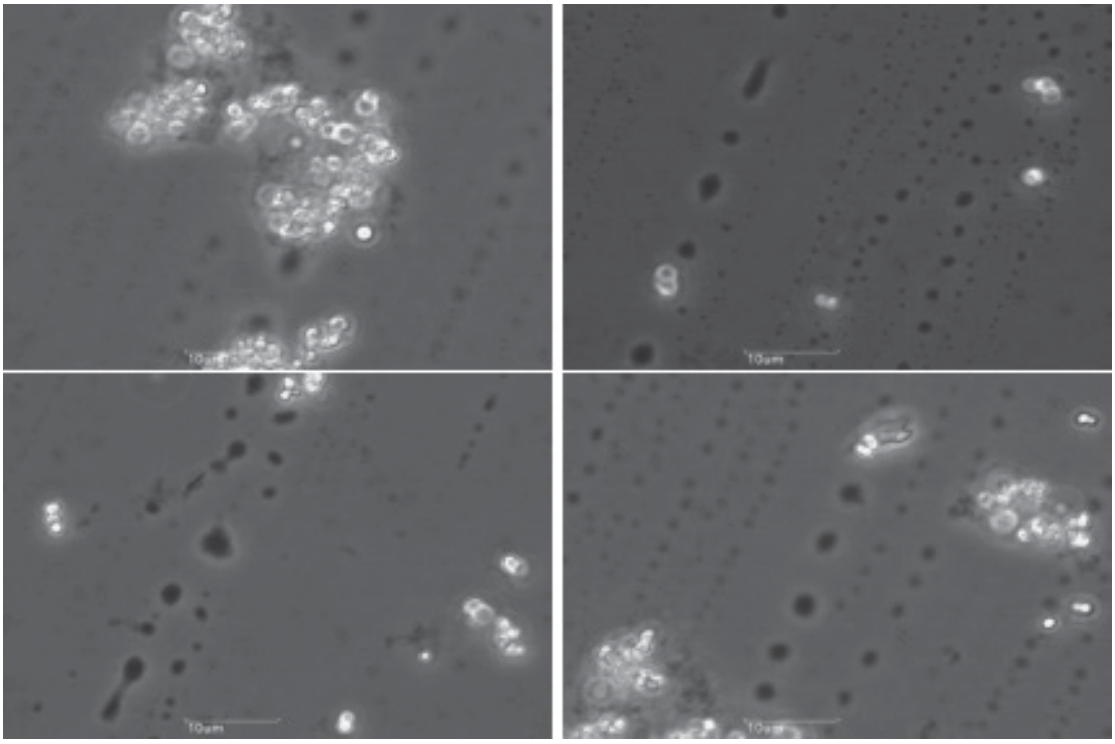

Figure 5.26. LM images of soluble lignin extract at 10% ethanol concentration.

5.3.6.2 Comparison of Zetasizer with Mastersizer

Table 5.4 presents the data characterising physicochemical properties of lignin aggregates in different ethanol concentration of soluble lignin extract.

In general, the particle size distribution could give useful information about the behaviour of lignin aggregates in soluble lignin extract (Klapiszewski *et al.*, 2012).

The results of particle size distribution of Zetasizer was comparable to that particle size given by Mastersizer. Overall, particle size distribution of Zetasizer showed that reduction of ethanol concentration from 50% to 10% resulted in the formation of population of small particles. However, the formation of distinct population of large particles (3580 to 6439 nm) for soluble lignin extract at 10% ethanol concentration shown by Zetasizer was associated with the result of particle size via Mastersizer which highest particle size was reported (6.1 μm).

Table 5.4. Comparison of particle sizes of soluble lignin extract at different ethanol concentrations by Zetasizer and Mastersizer.

Sample	Soluble lignin extract at different ethanol concentration (%)	Particle sizes					
		Particle diameter from Zetasizer Nano ZS (nm)		Particle diameter from Mastersizer 2000 (μm)			
		Particle size distribution	Particle size	D_{v10}	D_{v50}	D_{v90}	$D_{3,2}$
1	50	825.0-1990.0	1768.7	1.9	3.8	8.0	3.3
2	25	141.8-396.1 458.7-1281.0	1077.1	2.1	4.7	9.6	4.0
3	10	78.8-342.0 396.1-2305.0 3580.0-6439.0	441.5	2.6	9.7	30.1	6.1

*E.g. D=diameter, v = volume, D_{v10}= the maximum particle diameter below which 10% of the sample volume exists.

As follows from the Mastersizer 2000 results, an ascending trend was observed in which the $D_{3,2}$, surface weighted mean increased by decreasing the amount of ethanol concentration in soluble lignin extract. The lowest surface weighted mean or aggregates size was obtained from the soluble lignin extract of 50% ethanol concentration, 3.3 μm rather than 25% (4 μm) and 10% (6.1 μm). Overall, the particle size distribution recorded on Mastersizer 2000 indicated that D_{v10}, D_{v50} and D_{v90} of particles population increased as the ethanol concentration reduced, suggesting that the particles exhibited a tendency to form aggregates and the tendency is greater with decreasing of ethanol concentration. The peculiar behaviour of lignin aggregates was observed at D_{v90} of 10% ethanol concentration, which the lignin had diameter smaller than 30.1 μm.

Figure 5.27 showed the volume distribution given by Mastersizer 2000 and Zetasizer instrument involves Mie properties. The volume distribution analysed by both instruments has a discrepancy, which could be due to factors described in section 5.3.5.2.

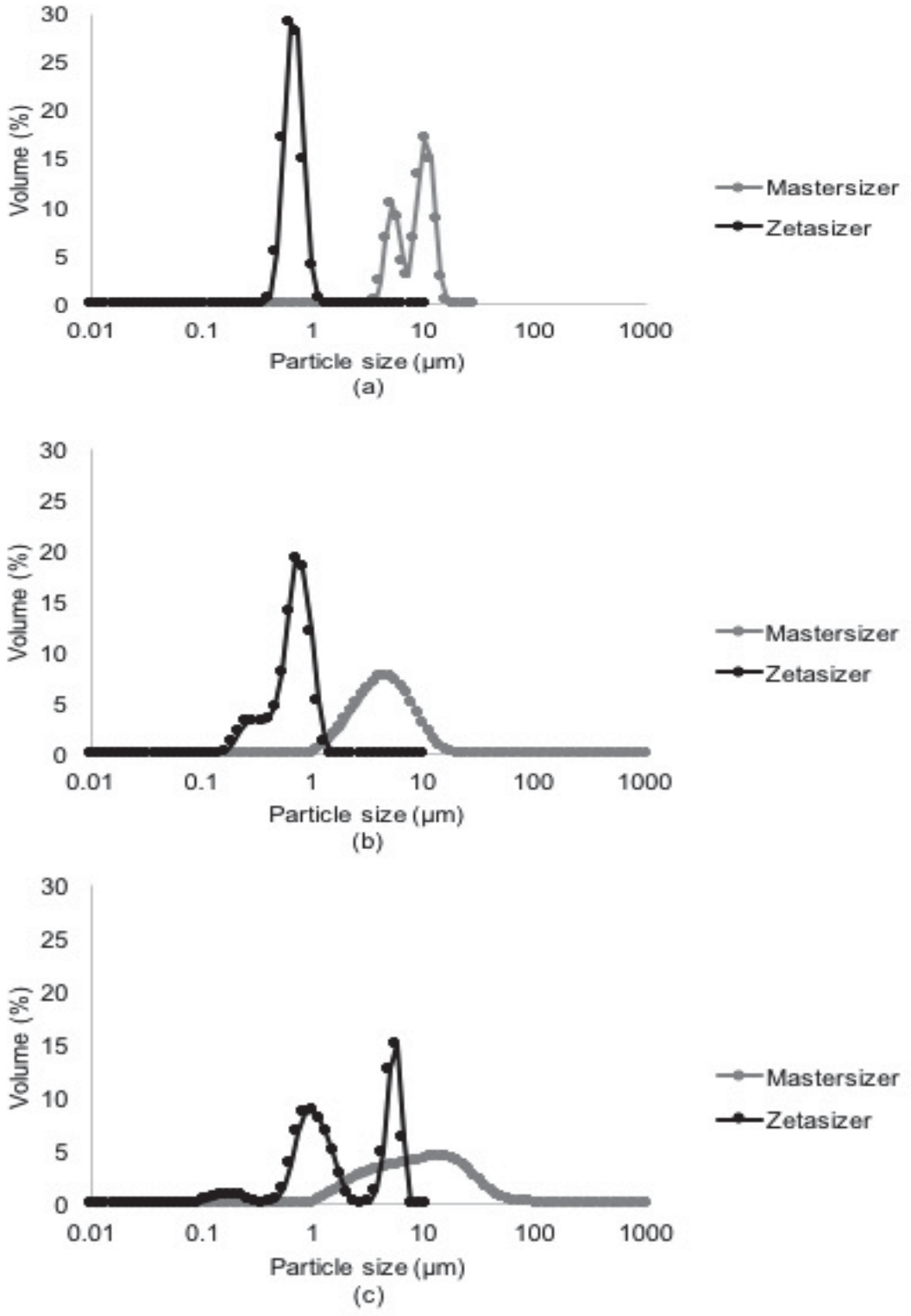

Figure 5.27. Comparison of volume distribution for Mastersizer and Zetasizer of soluble lignin extract at (a) 50%, (b) 25% and (c) 10% ethanol concentration.

5.3.7 Image Analysis

The overall global effects for particle size of lignin macromolecules was investigated via Malvern instruments either Zetasizer or Mastersizer. The particle size distribution via Malvern instruments was characterised using the concept of equivalent spheres. The results presented in terms of volume or intensity produced different results even though the data obtained from the same physico-chemical material (Nobbmann and Morfesis, 2009). Moreover, interpreting particles can be complex due to the particles may be characterised as identical though the particles had very different shapes.

Therefore, image analysis via LM is suggested to characterise individual characteristics of the particles from a 2-dimensional image, from which it determines different size and shape factors such as circularity and circle equivalent diameter. The imaging analysis inspected visually as data in pictorial form could be used as indicator to verify the particle size of particles (Gao *et al.*, 2005; North, 2006; Vaux, 2012; Wilt *et al.*, 2009).

As a function of ethanol concentration, soluble lignin extract images captured by LM were further analysed using ImageJ. Average circle equivalent diameter and average circularity versus ethanol concentration was presented in Figure 5.28. Overall, the average circle equivalent diameter and average circularity appeared to be significantly different ($p<0.05$) of all ethanol concentration studied. Figure 5.28 showed that there has been a sharp drop in the average circle equivalent diameter from 50% (7.62 μm) to 25% ethanol concentration (2.90 μm), and a slight increase at 10% ethanol concentration

(3.02 μm). The average circularity showed a gradual increase from 50% (0.62 μm) to 25 (0.81 μm) and 10% ethanol concentration (0.86 μm).

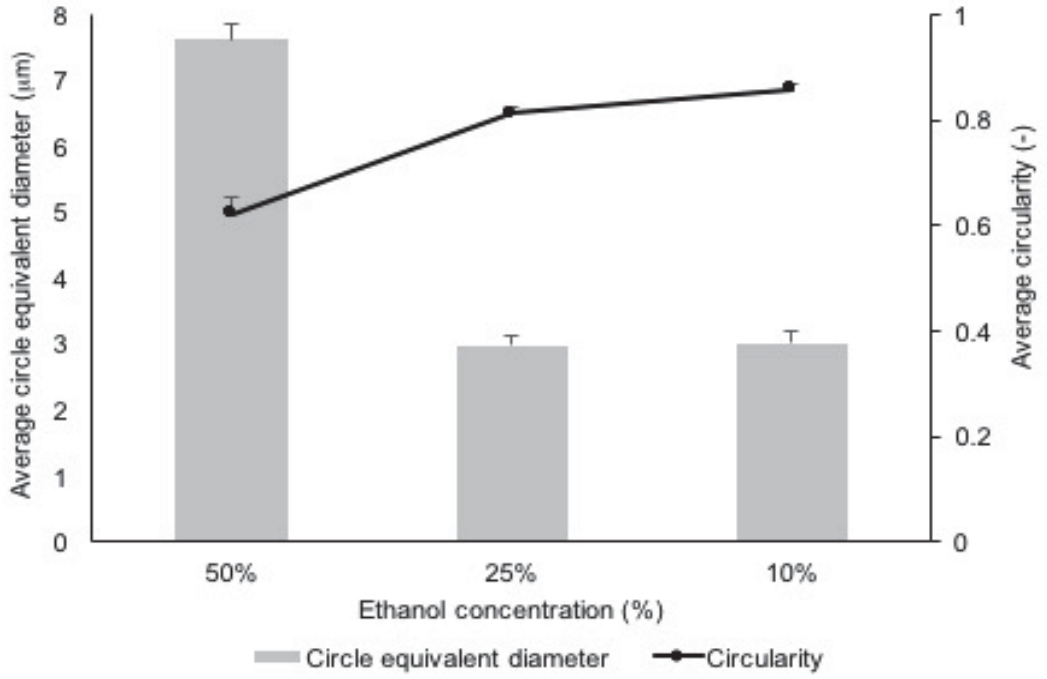

Figure 5.28. Average circle equivalent diameter and average circularity at different ethanol concentrations by ImageJ.

In general, when the ethanol concentration was reduced from 50% to 25% and 10% ethanol concentration of the soluble lignin extract, the big lumps of lignin macromolecules broke into smaller and rounder pieces of particles. Therefore, small particles result in an increase in the reaction rate for downstream processes due to the greater surface area with more exposed particles (Khadka *et al.*, 2014).

5.3.8 Conclusions

Finally, the focus of this preliminary study was primarily try to understand the behaviour of lignin aggregates in soluble lignin extract and the study has raised important question whether the effect of ethanol concentration influenced the behavior of lignin aggregates. Basically, in this chapter, it is hypothesised that water had influence on hygroscopic solvents, i.e. different ethanol concentration that has different ability to attract and hold water molecules from surrounding environment (Ghosh and Hallenbeck, 2012). Solvation of ethanol and water creates non-covalent interactions, such as hydrogen, Van der Waals and hydrophobic bonding that have a strong tendency to form aggregates with other molecules (Contreras *et al.*, 2008).

Nevertheless, the results of preliminary study via LM to study the effect of ethanol concentration showed that the ethanol concentration affected the behaviour of lignin aggregates in ethanol-water solution. Therefore, the study would have been more relevant if a wider range of ethanol concentration had been explored in order to understand the driving forces behind the dispersion or aggregation of lignin. The good dispersion state of lignin macromolecules was also responsible for an excellent compatibility of lignin in polymer matrices of bio-composites (Tian *et al.*, 2017). The experimental work on the next chapter also will look into the effect of different lignin concentration using similar ethanol concentration in the soluble lignin extract on the efficacy of lignin esterification.

CHAPTER 6: THE INFLUENCE OF CHEMICAL PROPERTIES OF ORGANOSOLV LIGNIN AGGREGATES AT DIFFERENT LIGNIN CONCENTRATION ON THE EFFICACY OF LIGNIN ESTERIFICATION

6.1 Introduction

The solvent concentration had an influence on the lignin purity and recovery as well the other physical, chemical and structural properties of precipitated lignin, supernatant and soluble lignin fraction. The relationship between the solvent concentration and the resultant lignin macromolecules' is complex, therefore the investigation presented in the previous preliminary study is imperative and could facilitate improved understanding of structural complexity of lignin for lignin obtained via the sub-critical water extraction.

The complex behaviour of lignin aggregates may result also from the interaction of the solute with a solvent containing two components with different concentrations (Da Silva *et al.*, 2002; Maitra and Bagchi, 2008). Associations of the lignin molecule under different conditions vary: the rearrangement of the hydrogen bonds of hydroxyl group play major role and the availability of the hydroxyl group in soluble lignin extract could influence the physicochemical properties of lignin aggregates in modifying and converting lignin into useful renewable materials (Bevilaqua *et al.*, 2006; Buhvestov *et al.*, 1998).

The aim of this chapter was using extracts obtained from sequential extraction that had high purity of lignin and abundance of hydroxyl groups (Chapter 4) in the study of the effect of wider range of ethanol concentration

on lignin aggregation behaviour. Subsequently, the effect of two different solute or lignin concentrations using similar ethanol concentration on the esterification efficacy was examined. This work is very important since there are no studies available in the literature concerning the use of soluble lignin extract directly after delignification or without recovering the lignin for lignin modification process. The later was obtained by exploring the changes in chemical structure of modified lignin after esterification under different lignin concentrations, the variation in the chemical properties of lignin macromolecule was tentatively related to the replacement of hydroxyl groups by ester substituent (Cachet *et al.*, 2014). This reduces the number of hydrogen bonds and causes an increase in the free volume in the molecule, imparting mobility of the chains on the ester group (Lisperguer *et al.*, 2009). Information on the chemical characteristics of modified lignin should shed light on enhancing its potential uses in value-added polymeric materials.

6.2 Material and Methods

6.2.1 Lignin Aggregation Behaviour at Wider Range of Different Ethanol Concentration

6.2.1.1 Particle Size Analysis

Soluble lignin extract containing 50% (by volume) of ethanol from the delignification process was used as starting material and diluted with water to different ethanol concentrations as shown in Figure 6.1. The samples' particle

size analysis was obtained using the Zetasizer Nano ZS and Mastersizer, following methods described in section 3.5.2 and 3.5.3, respectively.

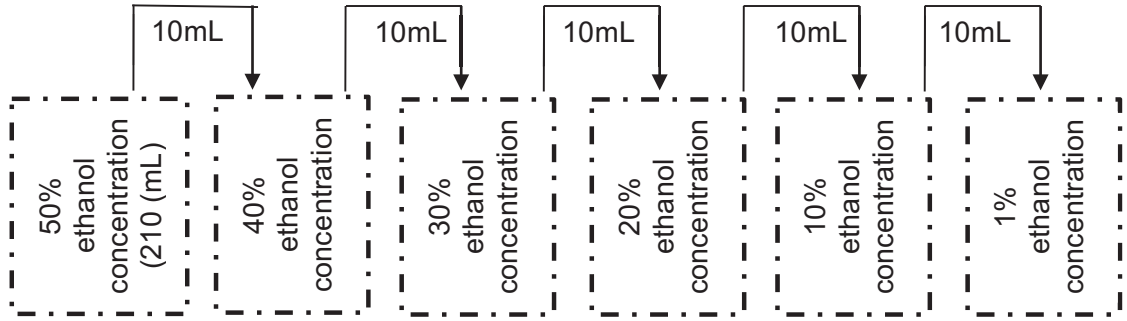

Figure 6.1. Scheme of dilution of soluble lignin extract.

6.2.1.2 LM Analysis

Images of the soluble lignin extract at different ethanol concentrations were captured following method mentioned in section 3.5.5.

6.2.1.3 ImageJ Analysis

Subsequently, 15 recorded images from LM analysis of three different microscope slides were analysed via ImageJ freeware (1.50v) according to method explained in section 3.5.6.

6.2.2 Synthesis of Lignin Fatty Acid Derivatives at Different Lignin Concentration

6.2.2.1 Preparation of Soluble Lignin Extract at Different Lignin Concentration

Soluble lignin extract containing 50% (by volume) of ethanol from the delignification process in Chapter 4 was used as starting material and diluted to different lignin concentration as shown in Figure 6.2. Two different lignin concentrations were chosen as the sample comparison for this study. The lignin concentration in the starting material was calculated using the method described in section 3.3.6, which gave 5 mg/mL. The preparation of lignin concentration for diluted sample, 1 mg/mL using the similar ethanol concentration (50%) by volume was obtained using Eq. 6.1.

$$V2 = \frac{(\mathrm{M1.V1})}{\mathrm{M2}} \tag{6.1}$$

Where M_1 is the lignin concentration of soluble lignin extract at 50% ethanol concentration (5 mg/mL); V_1 is the volume of soluble lignin extract at 50% ethanol concentration (15 mL); M_2 is the lignin concentration of soluble lignin extract (1 mg/mL) and V_2 is the volume of soluble lignin extract at 50% ethanol concentration for 1 mg/mL, mL.

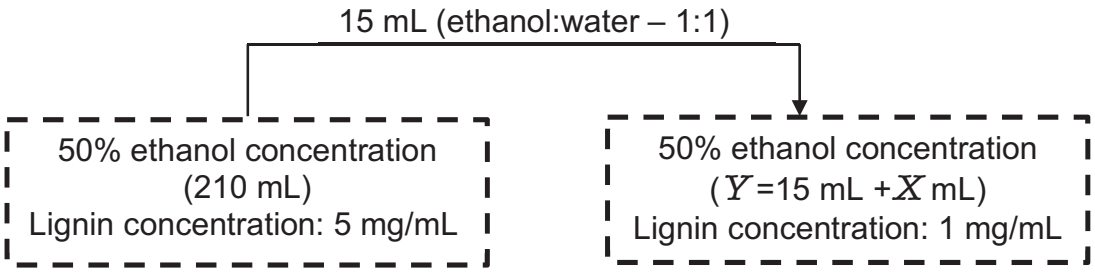

Where Y mL is the volume of soluble lignin extract at 50% ethanol concentration for 1 mg/mL (V_2); and X mL is the amount of ethanol-water mixture (1:1) need to be added to the soluble lignin extract.

Figure 6.2. Scheme of dilution of soluble lignin extract of 5 and 1 mg/mL.

6.2.2.2 Lignin Esterification

Lignin-fatty acid derivatives were synthesised using a method described by (Gordobil *et al.*, 2016) with modification, which the soluble lignin extract was used directly for analysis. Lignin esterification was performed for 5 and 1 mg/mL of soluble lignin extract to enable comparison of the chemical properties of esterified lignin at both these concentrations. 15 mL of soluble lignin extract was placed into a 250 mL beaker and stirred with a magnetic stirrer. Pyridine (2.75 mL) (Sigma-Aldrich, United Kingdom) was used as catalyst and dodecanoyl chloride (0.9 mL) (Sigma-Aldrich, United Kingdom) was added into the soluble lignin extract. The reaction was carried out at 20°C for two hours, after which the solution was decanted directly into 650 mL of 2% ice-cold hydrochloric acid (VWR, United Kingdom) and stirred for five minutes, resulting formation of a brownish ester layer at the top of a yellowish solution, mainly consisting of the excess acid, alcohol and water which separated under the ester layer. The ester layer was separated via a Buchner funnel with filter paper (Fisher Scientific, Qualitative, 150mm), and washed

with excess distilled water and ethanol (1:1) to remove unreacted fatty acids. Then, the esterified lignin was further directly analysed for its chemical structure characterisation via FTIR. The esterification reaction is shown in Figure 6.3.

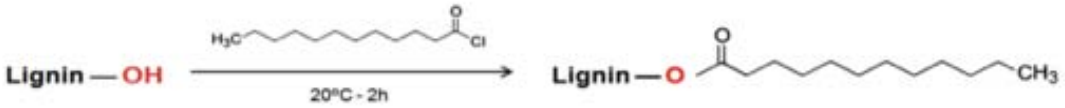

Figure 6.3. Reaction of scheme of lignin-fatty acid derivatives. (Source: Adapted from Gordobil *et al.*, 2016).

6.2.2.3 FTIR Analysis

FTIR analysis was performed on the unmodified and modified lignin samples at different lignin concentration without any pre-treatment for the samples containing 5 and 1 mg/mL lignin concentration. The IR spectra measurements were taken via a Nicolet 380 FTIR-Thermo Electron Corporation over a spectral range from 4000 to 600 cm^{-1} with resolution of 4 cm^{-1} and accumulation of 32 scans. The experiments were done in triplicate for each sample. Area-normalised and smoothed spectra in the regions of 4000 to 600 cm^{-1} were subjected to PCA using Unscrambler^{TM} software (Version 10.3, CAMO). For comparison study, FTIR analysis also was carried out on water, ethanol, water-ethanol (50% by volume), filtrate, blank solution prior esterification (mixture of ethanol:water (1:1), pyridine (2.75 mL), dodecanoyl chloride (0.9 mL), 2% ice cold hydrochloric acid (650 mL)) and dodecanoyl chloride.

6.2.3 Statistical Analysis

SPSS software (Version 22) was used for statistical analysis. One way analysis of variance was carried out at α = 0.05 to analyse the significance difference of imageJ analysis.

6.3 Results and Discussion

6.3.1 Lignin Aggregation Behaviour at Different Ethanol Concentration

6.3.1.1 Particle Size Analysis by Zetasizer

Figure 6.4 shows a gradual decrease in the average particle size of lignin macromolecules as ethanol concentration is decreased.

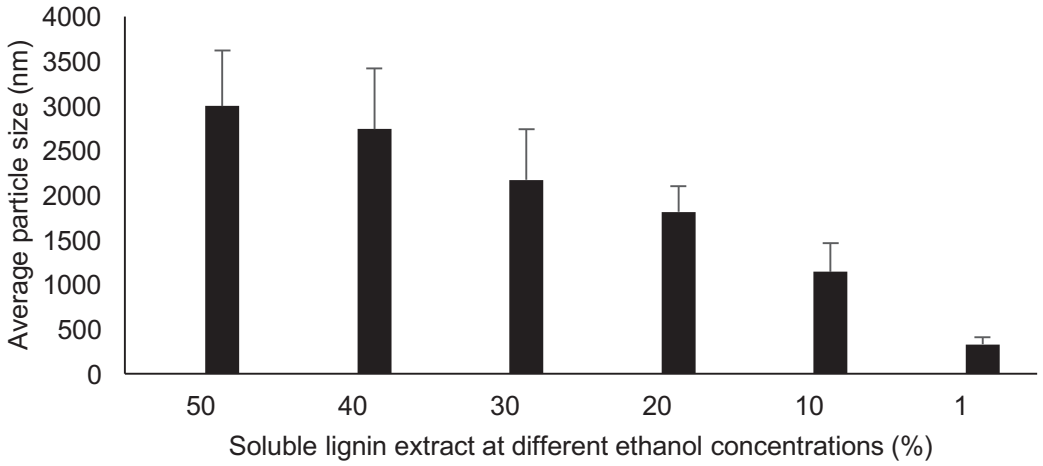

Figure 6.4. Average particle size at different ethanol concentrations of soluble lignin extract by Zetasizer.

Particle size distributions are shown in Figure 6.5 and 6.6 for ethanol concentrations of 50%, 40% and 30%; and 20%, 10%, and 1% ethanol

concentrations of soluble lignin extract, respectively. The behavior is complex: bimodal distributions are obtained at 50% and 10% ethanol concentration, multimodal distributions are observed at 40% and 30% ethanol concentration whereas, 20% and 1% ethanol concentration have a unimodal distribution, respectively. To elucidate the features of the particles in more detail, microscopy was carried out and is described further below.

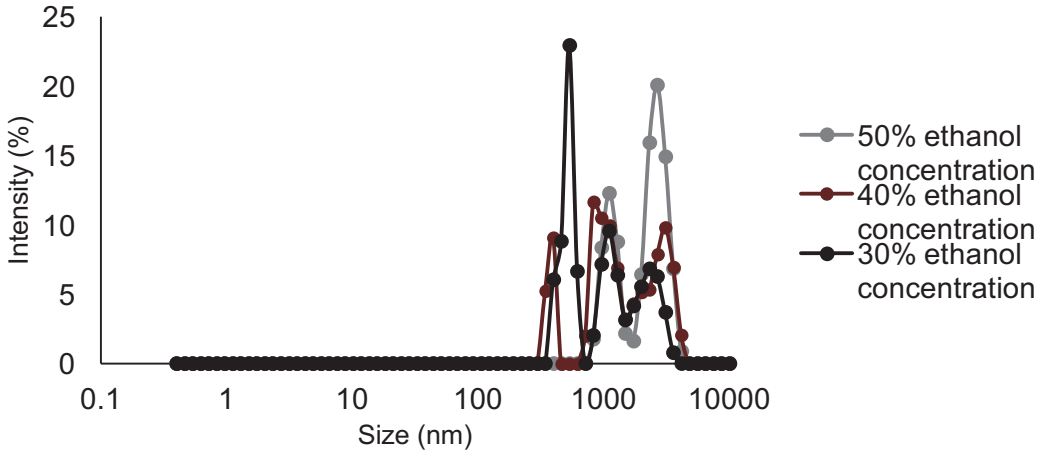

Figure 6.5. Particle size distribution at 50, 40 and 30% ethanol concentration of soluble lignin extract by Zetasizer.

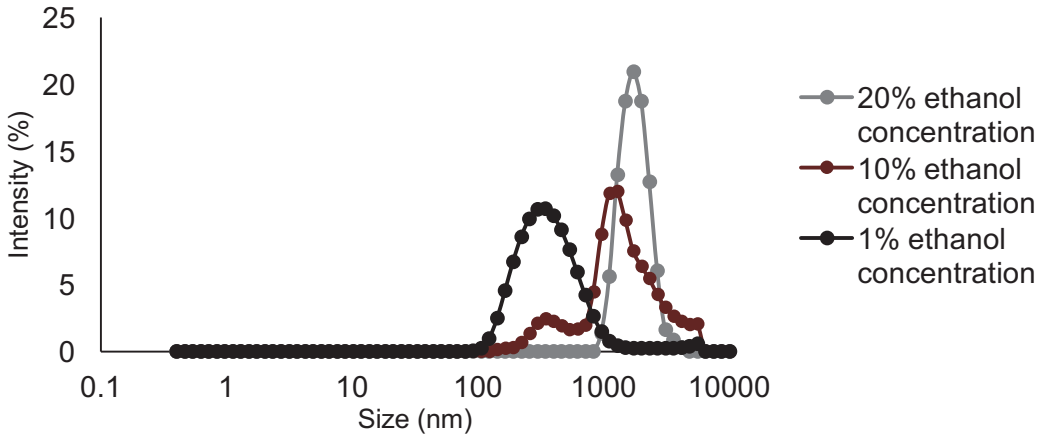

Figure 6.6. Particle size distribution at 20%, 10% and 1% ethanol concentration of soluble lignin extract by Zetasizer.

At 50% ethanol concentration of soluble lignin extract, the particle size distribution showed population of large particle size between 712 and 4801

nm. Figure 6.7 of LM images showed that population of large particles also were observed.

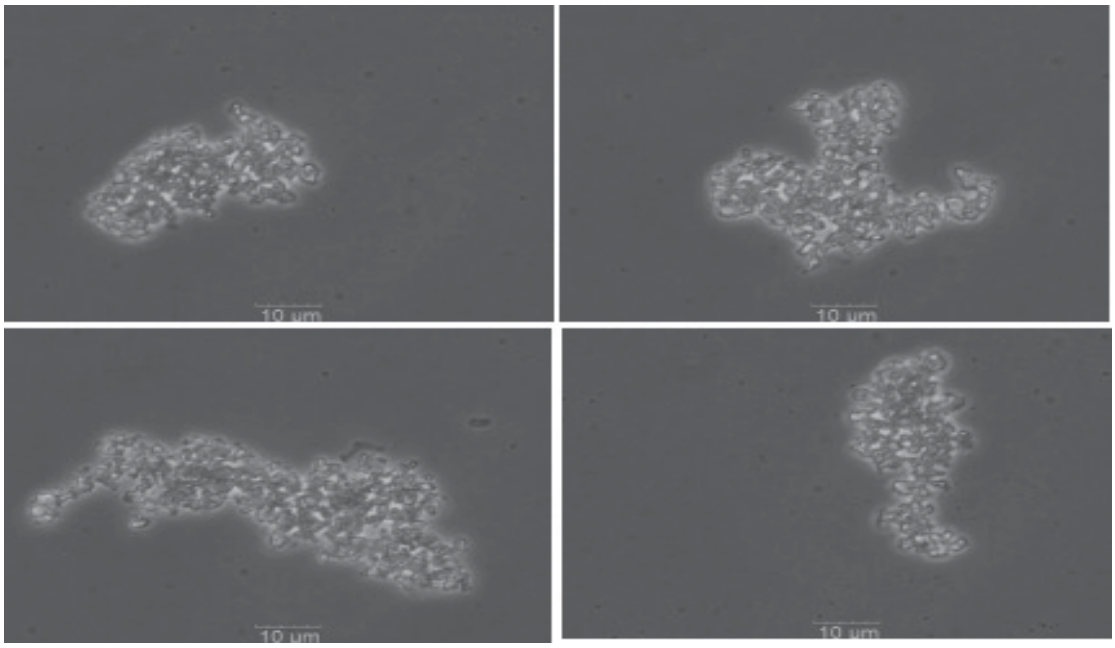

Figure 6.7. LM images of the 50% ethanol concentration of soluble lignin extract.

Whilst the overall trend appears to be a reduction of particle size with reducing ethanol concentration, at 40% ethanol concentration, two different particle populations are observed; a population of large particle between 615 and 4801 nm, and a population of small particle between 295 and 459 nm. Figure 6.8 illustrated the evolution of lignin aggregates behaviour (dotted circle–small particles) of 40% ethanol concentration of soluble lignin extract.

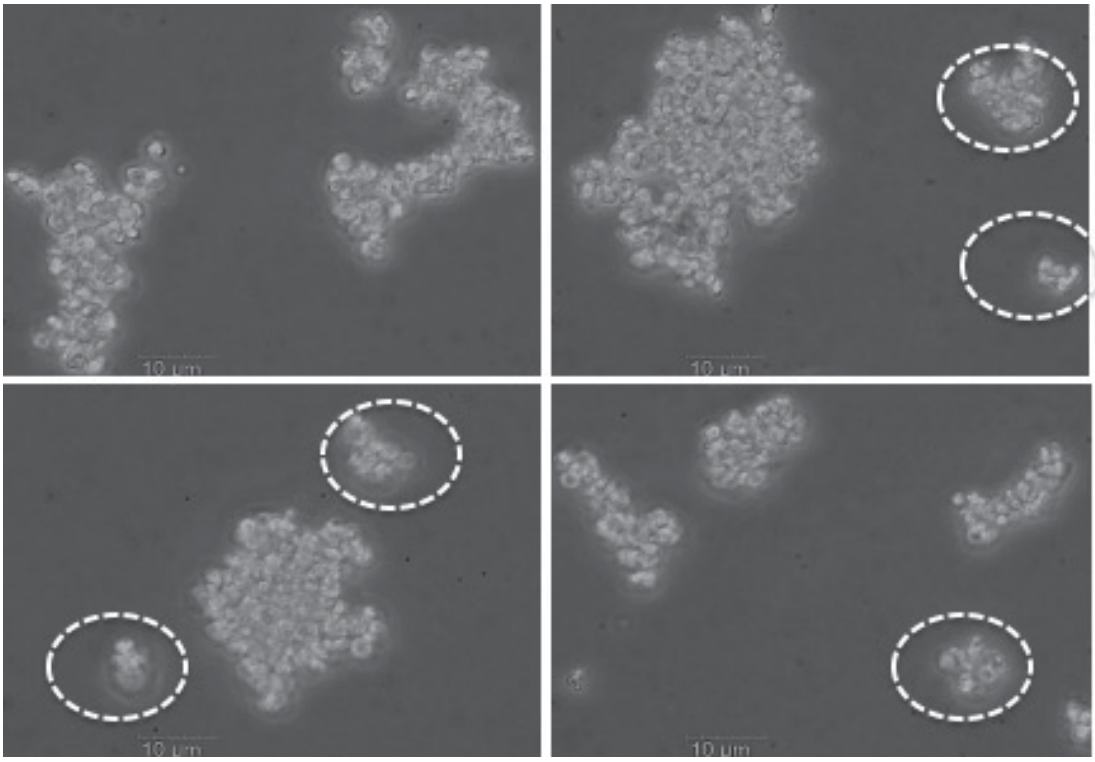

Figure 6.8. LM images of the 40% ethanol concentration of soluble lignin extract.

When reducing from 40% to 30% ethanol concentration of soluble lignin extract, the partitioning behaviour of lignin aggregates can be distinguished, where population of large particle segregated into sub-population of smaller particle (712 and 4145 nm; 342 and 712 nm). However, at 30% ethanol concentration large aggregates are observed, which is in accordance with the fact that the range of population of small particle increase from 295 and 459 nm (40% ethanol concentration of soluble lignin extract) to, 342 and 712 nm. LM results for the 30% ethanol concentration of soluble lignin extract are given in Figure 6.9, showing both large and small aggregates.

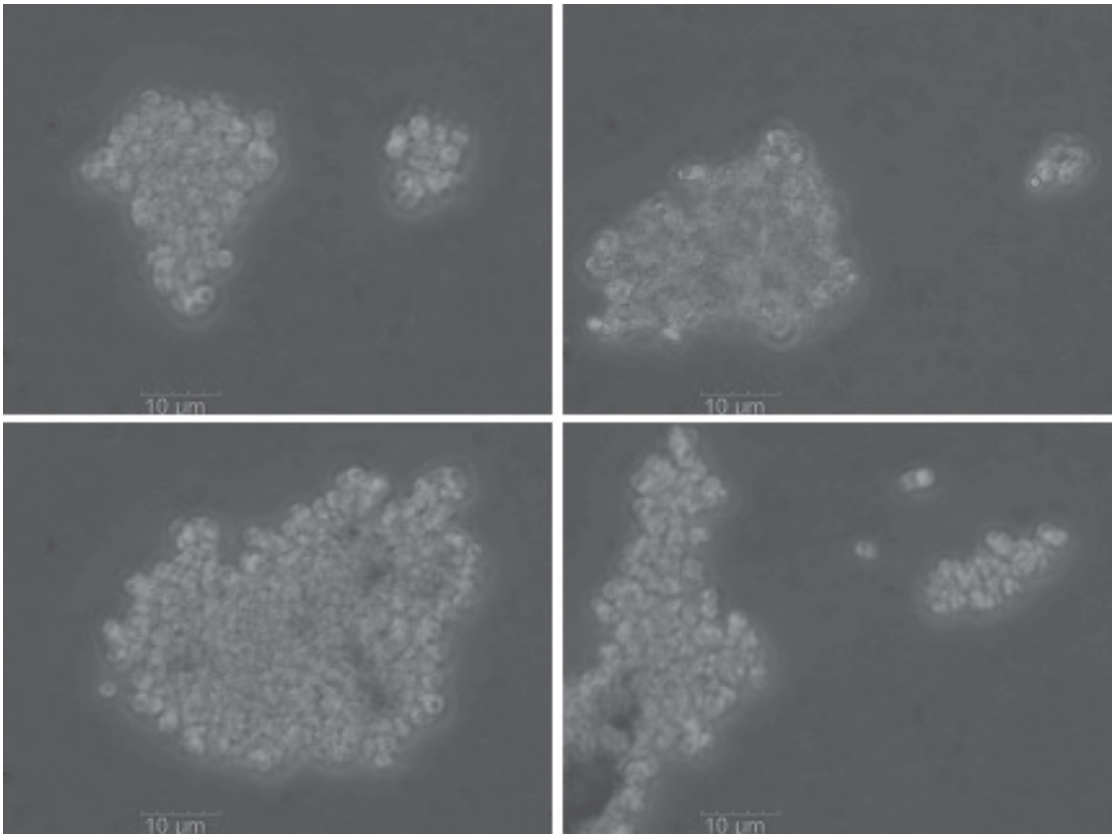

Figure 6.9. LM images of 30% ethanol concentration of soluble lignin extract.

20% ethanol concentration of soluble lignin extract exhibited particle size distribution with a population of large particle between 825 and 4801 nm, probably mainly reflecting that the particle population appear surprisingly large and the behavior of lignin aggregates at concentration of 20% ethanol concentration was inexplicable phenomena. The eccentric behavior of 20% ethanol concentration of soluble lignin extract was to found to be in agreement with the optical microscopy imaging analysis depicted in Figure 6.10.

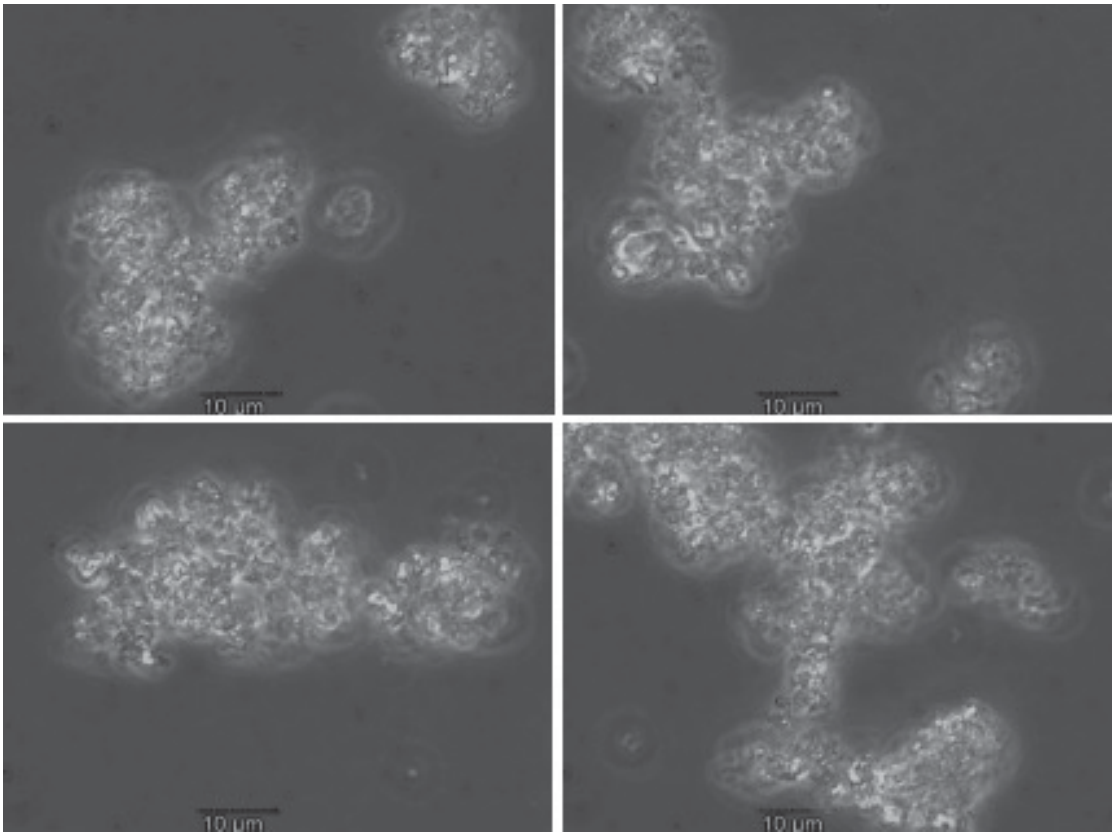

Figure 6.10. LM images of 20% ethanol concentration of soluble lignin extract.

The particle size distribution at 10% ethanol concentration of soluble lignin extract showed a population of small and large aggregates, with populations between of 164 and 6439 nm (Figure 6.11). Figure 6.12 shows optical images of 1% ethanol concentration of soluble lignin extract, where the particle sizes obtained by Zetasizer were between 106 and 1281 nm. The range of particle size for lignin aggregates of 1% ethanol concentration was apparently smaller in comparison to the lignin aggregates of 10% ethanol concentration of soluble lignin extract. Different range of particle size and aggregation behavior was observed in this study compared with the preliminary study reported in section 5.3.6 may due to the different batch *MxG* used in the work and the different volume used for dilution process that affected the lignin aggregation behavior.

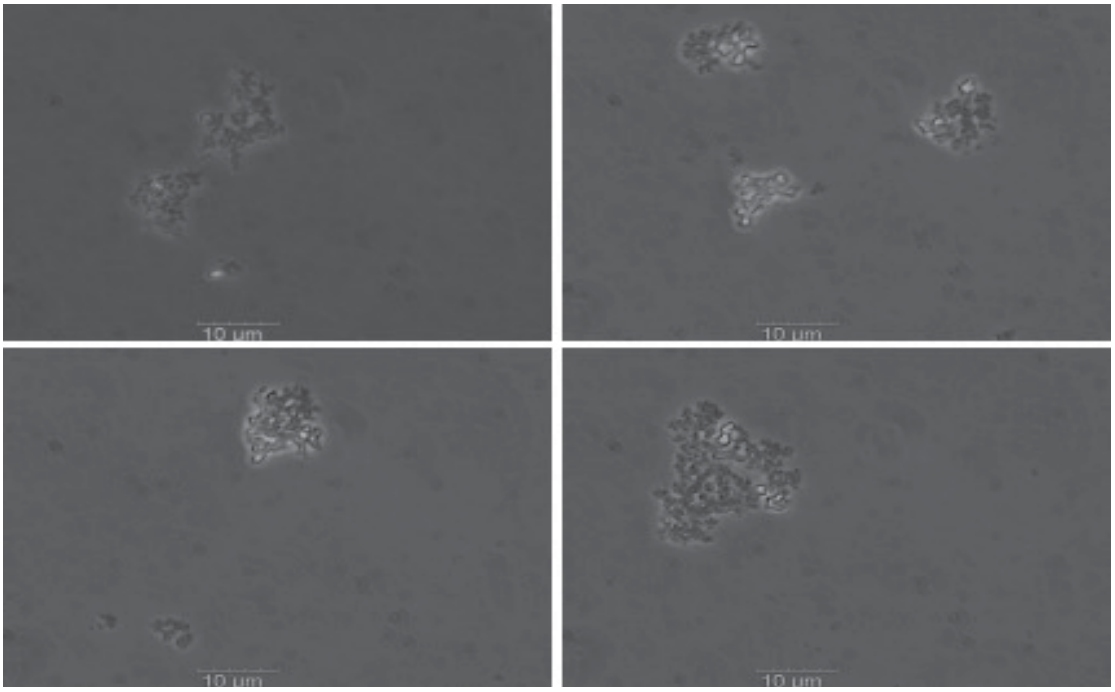

Figure 6.11. LM images of 10% ethanol concentration of soluble lignin extract.

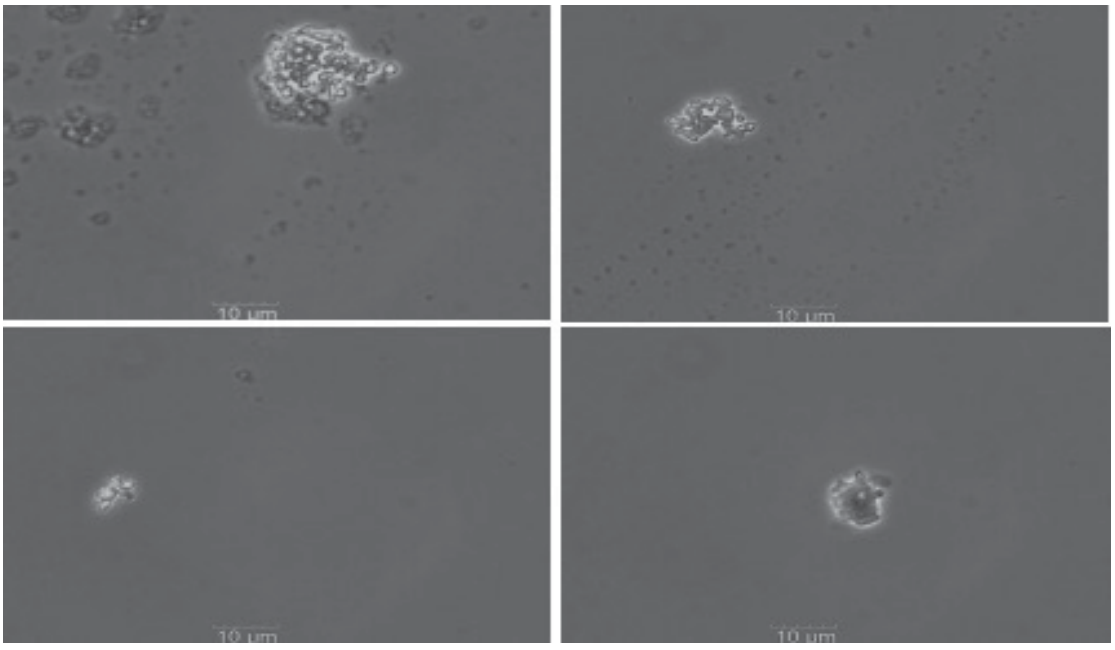

Figure 6.12. LM images of 1% ethanol concentration of soluble lignin extract.

6.3.1.2 Comparison of Zetasizer with Mastersizer

In attempt to capture the significance and comparable findings between the particle size analysis of Zetasizer with other instruments, a series of analysis for each of soluble lignin extract at different ethanol concentrations was performed via Mastersizer. Detailed information regarding the particle sizes of soluble lignin extract at different ethanol concentrations, is reported in Table 6.1.

Table 6.1. Comparison of particle sizes of soluble lignin extract at different ethanol concentrations by Zetasizer and Mastersizer.

Soluble lignin extract at different ethanol concentration (%)	Particle size					
	Particle diameter from Zetasizer Nano ZS (nm)		Particle diameter from Mastersizer 2000 (μm)			
	Particle size distribution	Particle size	D_{v10}	D_{v50}	D_{v90}	$D_{3,2}$
50	712.4-1718.0 1718.0-4801.0	3001.8	3.0	6.7	13.4	5.4
40	295.3-458.7 615.1-1484.0 1484.0-4801.0	2743.6	7.9	16.3	29.3	3.6
30	342.0-712.4 712.4-1484.0 1484.0-4145.0	2172.9	6.0	13.1	25.8	3.7
20	825.0-4801.0	1815.7	3.5	7.10	13.2	6.0
10	164.2-531.2 531.2-6439.0	1144.9	1.9	5.9	15.0	4.8
1	105.7-1281.0	331.7	0.1	2.2	13.0	0.4

*E.g. D=diameter, v = volume, D_{v10}= the maximum particle diameter below which 10% of the sample volume exists.

The Sauter mean diameter $D_{3,2}$, obtained from Mastersizer also shows a downward trend with decreasing ethanol concentration apart from a local increase at 10% and 20% ethanol concentration. There is a remarkable drop at 1% ethanol concentration; the value here approaches the resolution limit of the instrument; thus it fails to provide an accurate result.

While surface weighted mean follows a decreasing trend of average particle size from 50% to 30% ethanol concentration due to breakdown of large particles into population of small particles of lignin aggregates, at 20% ethanol concentration the value increased up to 6.0 μm as the population of large lignin aggregates increased. The other two fractions at 10% and 1% ethanol concentration of soluble lignin extract showed a marked drop; it may be speculated that the low ethanol concentration resemble complex formation of lignin aggregates, which affected the measurement of particle size analysis via Mastersizer.

The 50% ethanol concentration of soluble lignin extract showed that D_{v10} of particles population have the diameter smaller than 3.0 μm, while D_{v90} of particles population have the diameter smaller than 13.4 μm. The particles exhibited a tendency to form aggregates which increases with decrease of ethanol concentration from 50% to 40% ethanol concentration. The particle size distribution recorded on Mastersizer 2000 for 40% ethanol concentration of soluble lignin extract indicated that D_{v10} of the sample had diameter smaller than 7.9 μm whereas D_{v90} of the sample had diameter smaller than 29.3 μm.

The data of Mastersizer in Table 6.1 indicated that there has a gradual decrease in particle diameter for D_{v10} of the sample from 30% to 1% ethanol

concentration of soluble lignin extract. Nevertheless, D_{v90} of the sample showed a decrease in particle diameter from 30% to 20% ethanol concentration, slight increase from 20% to 10% ethanol concentration, and slight decrease from 10% to 1% ethanol concentration of soluble lignin extract. The variation in the trends in the particle diameter profile might be explained by the aggregation or disaggregation due to the change on the particles and their subsequent interactions with the solvent. This includes the motion of solvent relative to the particles that affected the breakage of particle (Jackson and Burd, 1998).

Although the Zetasizer and Mastersizer have different size detection ranges of 0.3 nm to 10 μm and in the ranges of 0.02 to 2000 μm, respectively; it is nevertheless of interest to compare the results directly. Indeed, this may highlight that a combined approach is needed to fully characterise the size of all particles in the samples. This comparison is shown in Figure 6.13 on a volume basis. Overall, the volume particle size distributions of different methods have been unable to demonstrate the similarities of lignin aggregates behaviour, that could be attributed to the justification discussed in section 5.3.5.2 including different size detection ranges and different principles operation of instrument.

Overall, the results in this study also showed discrepancies with the theory as have been described in section 5.3.6.1. The results were not expected which a decrease of ethanol concentration resulted in more dispersion or aggregation of lignin in the ethanol-water mixture of soluble lignin extract. The reasons for this result are not yet wholly understood due to

the facts that nature of lignin as an amphiphilic polymer that consists both hydrophobic and hydrophilic segments (Xiong et al., 2017) and the interaction between amphiphilic properties of lignin and mixture of solvents was very selective and complicated (Da Silva *et al.*, 2002; Maitra and Bagchi, 2008).

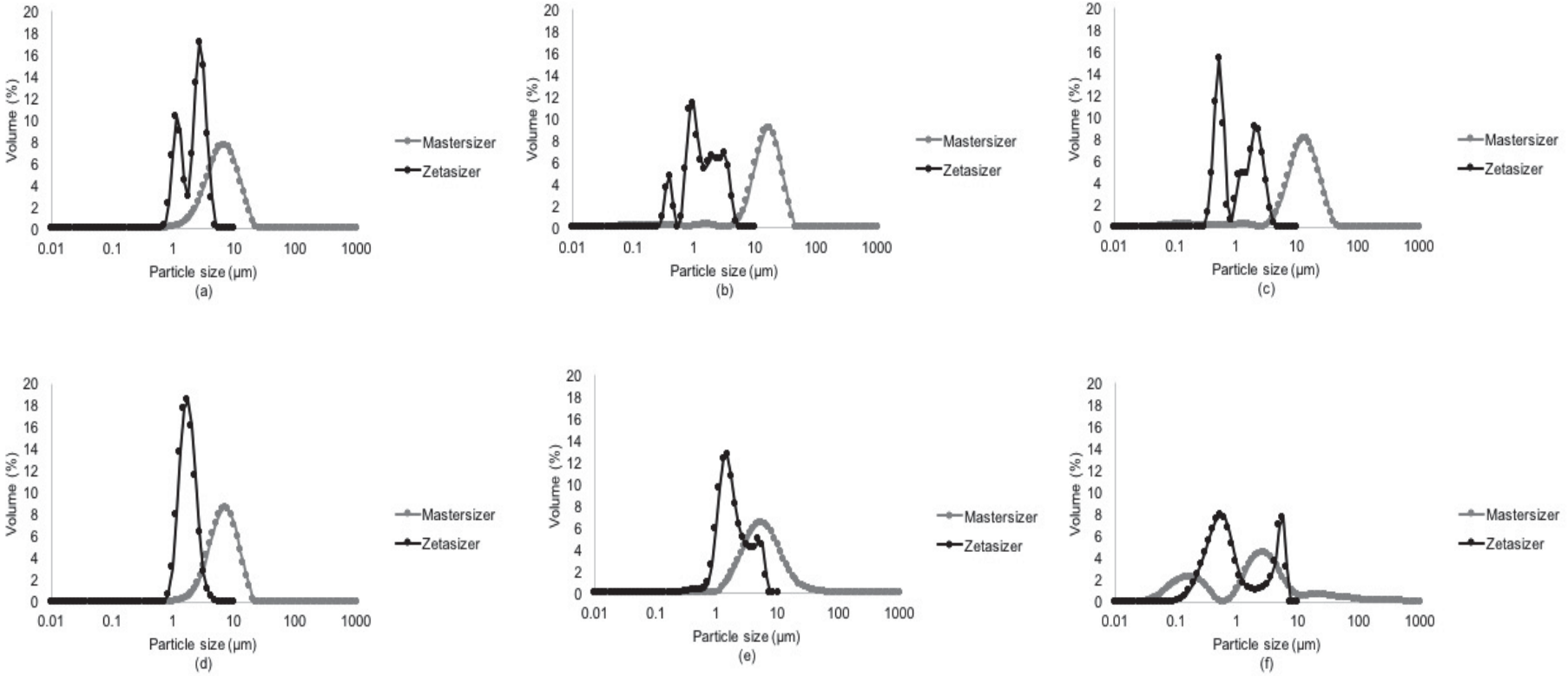

Figure 6.13. Comparison of volume distribution of the soluble lignin extract for Mastersizer and Zetasizer at (a) 50%, (b) 40%, (c) 30%, (d) 20%, (e) 10%, and (f) 1%, ethanol concentration.

6.3.1.3 Image Analysis

In an attempt to evaluate the relationship between different ethanol concentrations with average circle equivalent diameter and circularity of lignin aggregates, analysis of microscopy images was carried out via the freeware ImageJ. The lignin aggregates behaviour, therefore need to be interpreted with caution since the lignin aggregation was very selective according to the particular ethanol concentrations. Figure 6.14 shows the average circle equivalent diameter and circularity against ethanol concentrations of soluble lignin extract. The results were significantly different ($p<0.05$).

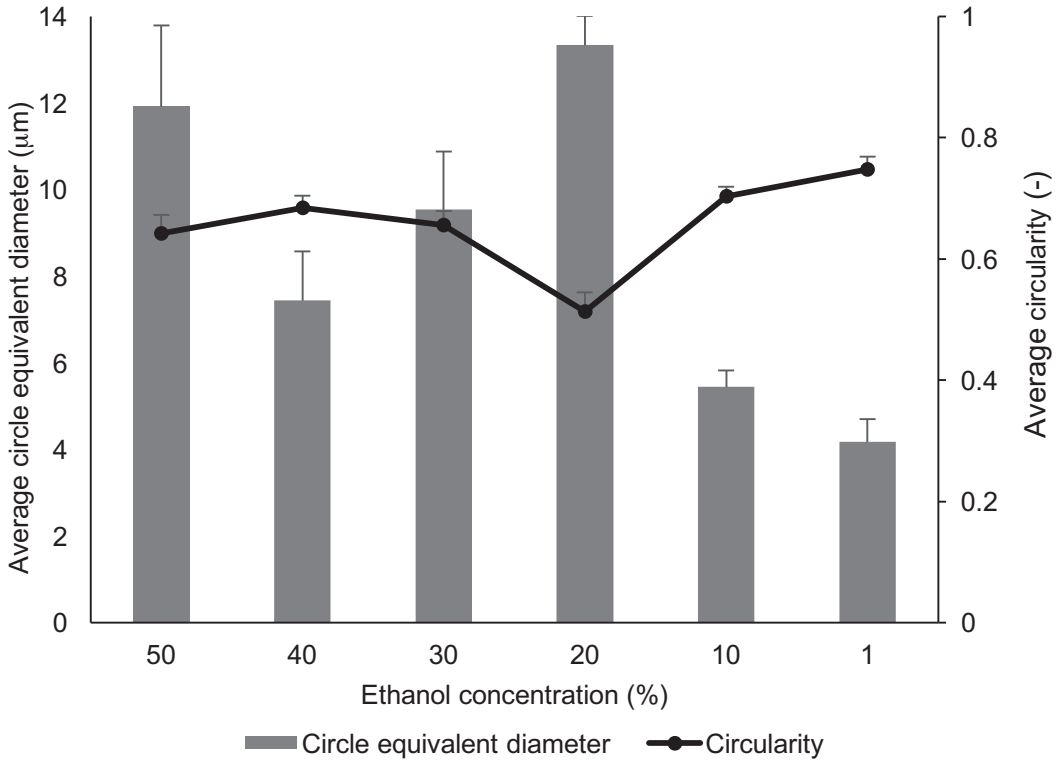

Figure 6.14. Average circle equivalent diameter and average circularity at different ethanol concentrations by ImageJ.

Generally, 11.91 μm of average circle equivalent diameter were observed for 50% ethanol concentration and the average circle equivalent diameter was reduced at 40% ethanol concentration of soluble lignin extract (7.43 μm). However, the reduction of ethanol concentration from 40% to 30% and 20% of soluble lignin extract showed a slight rise in the average of circle equivalent diameter of 9.54 and 13.34 μm, respectively. A decrease in the average circle equivalent diameter was identified towards lowest ethanol concentration from 10% to 1% of soluble lignin extract, 5.45 and 4.18 μm, respectively. The explanation for the distinct aggregation phenomena due to the selective stability of particulate matter when dissolved within a mixture of solvent environment (Snowden *et al.*, 2008). The various aggregation driven at different solute concentrations affected by particle size, shape, flexibility the interaction between the particles as well as particles and solvent (Amin *et al.*, 2014; Lomakin *et al.*, 2005).

Overall, the solvation of solute including solute-solvent and solvent-solvent interactions affect lignin aggregates' behavior. Furthermore, there was difference in specificities in the interaction of the lignin with two constituent solvents, ethanol and water (Maitra and Bagchi, 2008). The interaction of lignin aggregates was very complicated: either the solute could be demonstrated to be responsible for the aggregates clustering with one component of solvent mixture or solvating in the mixture of solvent aggregates (Bevilaqua *et al.*, 2006). There are various factors that drive particle aggregation including the type and concentration of solutes in solution as well

as others environmental conditions, i.e. temperature, solvent type, pH, and ionic strength (Jones and McClements, 2010). Another important factor that influence the tendency of particle aggregation is the attractive and repulsive colloidal interactions between aggregates such as van der Waals, steric, electrostatic, and hydrophobic forces (Jones and McClements, 2010; McClements, 2005).

The average circularity parameter determines the divergence of a particle from a circle (C=1) due to the change of particle elongation or increase of surface area (Liu *et al.*, 2015). Therefore, the average circularity describes the particle morphology of lignin macromolecules at different ethanol concentration. The low circularity value indicates that the lignin macromolecules are misshapen and irregular lumps rather than defined circular particles. The average circularity increased from 50 to 40% ethanol concentration of soluble lignin extract (0.65 to 0.68), indicating the breaking of large lumps into small pieces. There was a steady decreased in the average circularity from 30% to 20% ethanol concentration of soluble lignin extract (0.66 to 0.51) due to the re-aggregation of particles creating more large lumps. An upward trend in the average circularity was observed towards reduction of ethanol concentration from 10% to 1% ethanol concentration of soluble lignin extract, 0.70 and 0.75, respectively, which showed that the lignin macromolecules are more small and round.

When comparisons were made between the highest ethanol concentration (50%) and lowest ethanol concentration (1%) of soluble lignin extract, the findings showed that dilution of soluble lignin extract from 50% to

1% decreased the average circle equivalent diameter and increased the circularity. The diluted soluble lignin extract used by adding more water into the mixture of ethanol and water solution of soluble lignin extract could disrupt the aggregates stability, facilitate and break up the proportion of large lumps of lignin macromolecules to small fragments of aggregates. Hence, the reducing of lignin macromolecules can increase the surface area and more particles are available to react, thus speeding up the reaction rate for chemical processes (Fu *et al.*, 2014).

Here, it has been suggested that the molecular structure of lignin is highly polar with a large number of hydroxyl (-OH) groups, have tendency for particle aggregation due to the interaction of hydrogen-bonded complexes such as the O-H stretching bands, O-H bond of phenols and alcohol as well as C=O stretching that would affected the lignin and solvent interaction (Da Silva *et al.*, 2002). Given that the fact this study was only a preliminary attempt to assess the effect of ethanol concentration on lignin aggregation behaviour, it is hardly surprising that the results showed a complex structural lignin macromolecules dispersion or assembly.

Therefore, the study would more convincing if a firm knowledge of the hydrogen bonding properties of hydroxyl group in lignin aggregates and their potential interactions with different ethanol concentrations in addition to structural assembly mechanism could be approached. It is worthwhile if the validation of availability of phenolic hydroxyl groups in the soluble lignin extract at different ethanol concentrations also could be performed via various methods such as potentiometric titration, ultraviolet-visible spectroscopy or

nuclear magnetic resonance spectroscopy in future prior to lignin modification via esterification process.

Esterification of lignin was expected to be an easy route to improve the physico-chemical properties of lignin, thus significantly expanding lignin potential for various industrial applications (Bridson *et al.*, 2013). In lignin modification processes, it might be postulated that the high content of free hydroxyl groups in lignin could be substituted by ester groups, to provide more reactive sites for lignin reactivity.

The usual approach to modify lignin via esterification is to dissolve lignin in a powder form into various solutions such as dimethylformamide and dioxane prior to synthesis of esterified lignin (Gordobil *et al.*, 2016; Pawar *et al.*, 2016). Here, a less costly approach is suggested to use directly soluble lignin extract of water-ethanol mixture (50% by volume of ethanol) after delignification of SE processing routes in Chapter 4 for lignin modification process. The lignin concentration of soluble lignin extract after delignification for SE processing routes was 5 mg/mL. It was recommended that the comparison for the esterification study was conducted between 5 mg/mL and lower lignin concentration than 5 mg/mL of soluble lignin extract using similar ethanol-water composition (50% by volume), 1 mg/mL. The comparison of esterification reaction between different lignin concentration attempted to demonstrate the effect of different availability of hydroxyl groups on chemical properties of esterified lignin.

6.3.2 Synthesis of Lignin Fatty Acid Derivatives at Different Lignin Concentration

An infrared spectrum includes a large number of wavenumbers that are challenging to interpret. It was a *priori* questionable whether the repetition analysis of FTIR spectra within similar lignin concentrations consists of similar chemical structure characteristics. Therefore, chemometrics of PCA was performed to determine the main source of variation in the FTIR spectra data (Cordella, 2012; Hori and Sugiyama, 2003). The results obtained from PCA analysis are presented in terms of explained variance, scores and loadings plot.

Here, the first two principal component (PC) showed the majority of variance (99%) in the original dataset, where the samples are grouped in the score plot according to the first two PC scores. Figure 6.15 presents the PCA explained variance plot for unmodified and modified lignin at different lignin concentration. Although Figure 6.15 clearly showed that PC1 (dotted line) explained the maximum variance in the data set (plateau line), PC2 was chosen as the optimal number of the principal components since there is remaining variance in the PC2 (1%). The calibration and validation data cannot be distinguished, due to overlapping of the red and blue line (dotted circle) means that there is a small variation in the dataset between calibration and validation data.

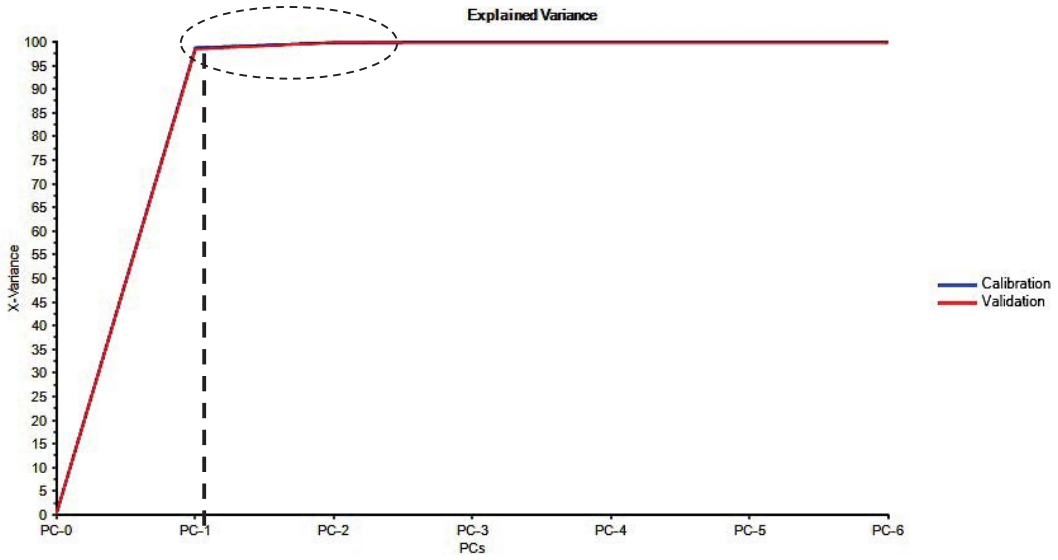

Figure 6.15. PCA explained variance plot of unmodified and modified lignin at different lignin concentration.

The score plot of PC1 (variability; 99%) x PC2 (variability; 1%) is shown in Figure 6.16. The score plot gave information of the data structure by interpreting similarity between samples as well as revealing the detection of deviating spectra (Nieuwoudt *et al.*, 2004). In short, four definite groups are observed. On the first quadrant were the spectra for unmodified lignin at 5 mg/mL whereas the fourth quadrant on the right hand side, consists of spectra for unmodified lignin at 1 mg/mL. The modified lignin at 1 mg/mL was located at second quadrant, and the third quadrant comprises of modified lignin at 5 mg/mL. This separate clusters showed that the chemical structures were differed significantly. In the plot PC1 against PC2, the closer the spectra in the same quadrant within the same samples denoting the spectra were similar in chemical composition or structure. Table 6.2 showed the spectra that have similar chemical structure. Any spectra that showed similar structure was chosen for general comparison analysis.

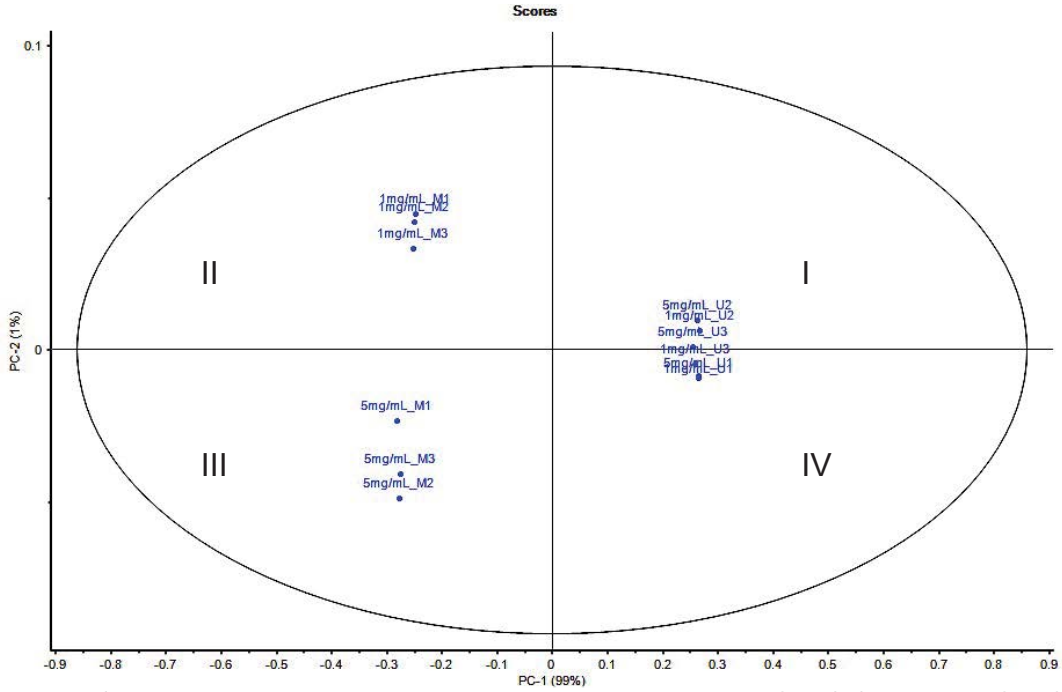

Xmg/mL_AB whereby X is the lignin concentration, A is modified (M) or unmodified (U) lignin and B is repetition of spectra.

Figure 6.16. PCA scores plot of unmodified and modified lignin at different lignin concentration.

Table 6.2. Scores table for similar chemical composition of unmodified and modified lignin at different lignin concentration.

Lignin concentration (mg/mL)	Type of lignin	Spectra of similar chemical composition
5	Unmodified	5mg/mL_U2, 5mg/mL_U3
	Modified	5mg/mL_M2, 5mg/mL_M3
1	Unmodified	1mg/mL_U3,1mg/mL_U1
	Modified	1mg/mL_M1, 1mg/mL_M2

The scores plot of PC2 against PC1 shown in Figure 6.16 illustrates the groupings, however the interpretation of the correlation loadings plot was not straightforward and complicated. The correlation loadings plot in Figure 6.17 showed the specific wavenumbers that influenced the scores plot.

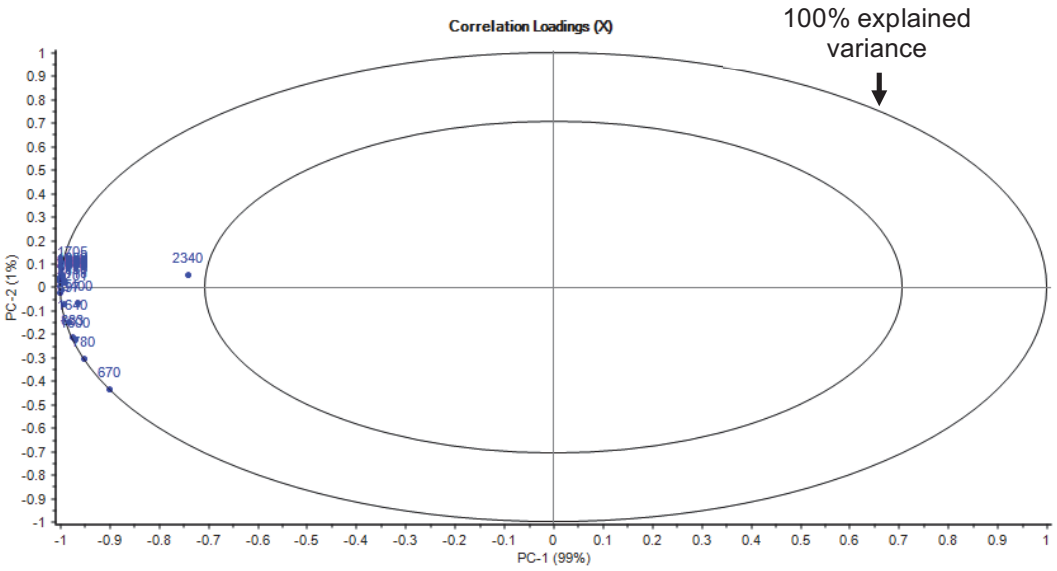

Figure 6.17. PCA correlation loadings plot of unmodified and modified lignin at different lignin concentration.

All wavenumbers related to lignocellulosic biomass identified by FTIR in the range from 4000 to 600 cm^{-1} were correlated positively as the wavenumbers very close to 100% explained variance except for wavenumber of 2340 cm^{-1}. The wavenumber of 2340 cm^{-1} contributed the most variability that affect the position of the samples. The wavenumber at 2340 cm^{-1} referred to OH stretch from strong H-bonded-COOH (Davis *et al.*, 1999). The location of wavenumbers either in positive or negative loadings in quadrant is not clearly explained. Even though the loadings plot could not have explained clearly what PC2 and PC1 describe, the scores plot can differentiate the spectra of samples according to different lignin concentration.

6.3.2.1 Comparison Between Unmodified Soluble Lignin Extract at Different Lignin Concentration and Blank Solution (Ethanol-Water Mixture)

Here, the FTIR spectra of unmodified lignin were obtained using a spectra manipulation technique where the absorbance of a blank solution of ethanol-water mixture (contains 50% by volume of ethanol) was subtracted from the absorbance of a sample spectra (soluble lignin extract at 5 or 1 mg/mL). Figure 6.18 illustrated the spectra of a blank solution and sample spectra prior to spectra subtraction method for both lignin concentration, 5 and 1 mg/mL.

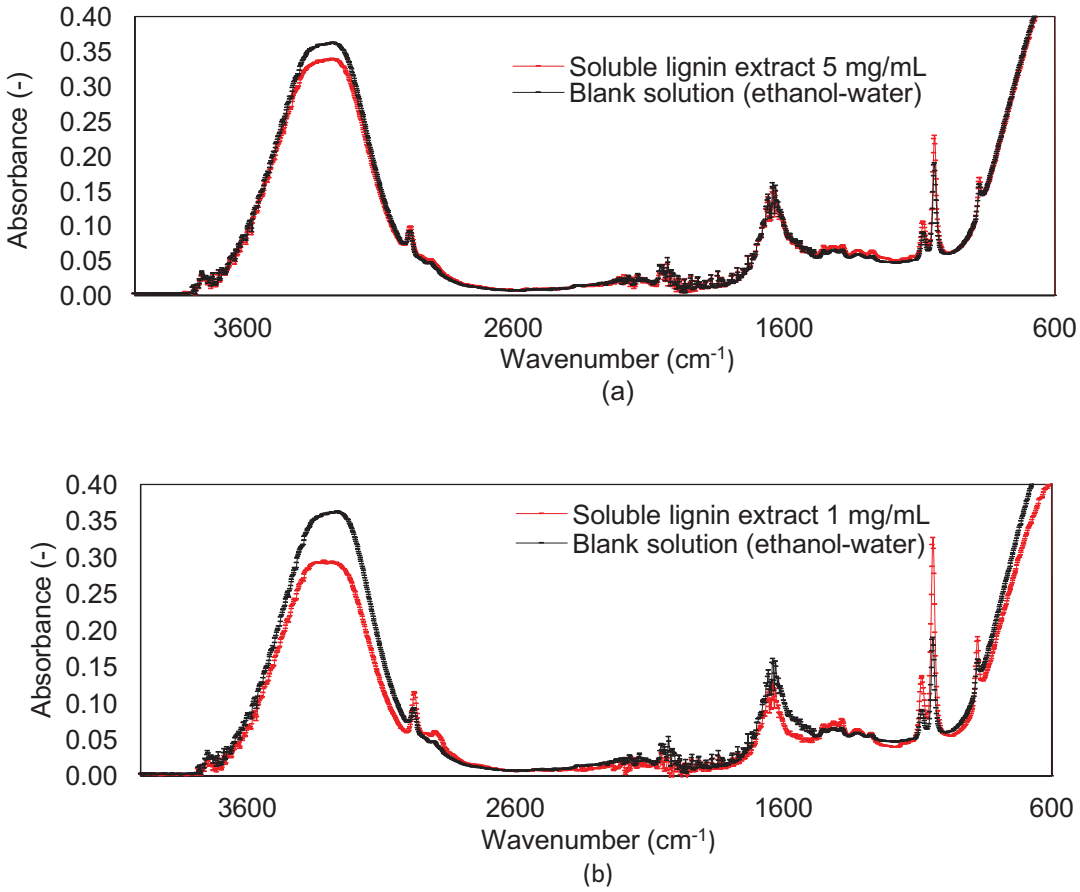

Figure 6.18. FTIR spectra of blank solution (ethanol-water) and soluble lignin at (a) 5 mg/mL and (b) 1 mg/mL lignin concentration.

A representative FTIR spectra of unmodified soluble lignin extract at 5 and 1 mg/mL lignin concentration after spectra subtraction can be seen in Figure 6.19.

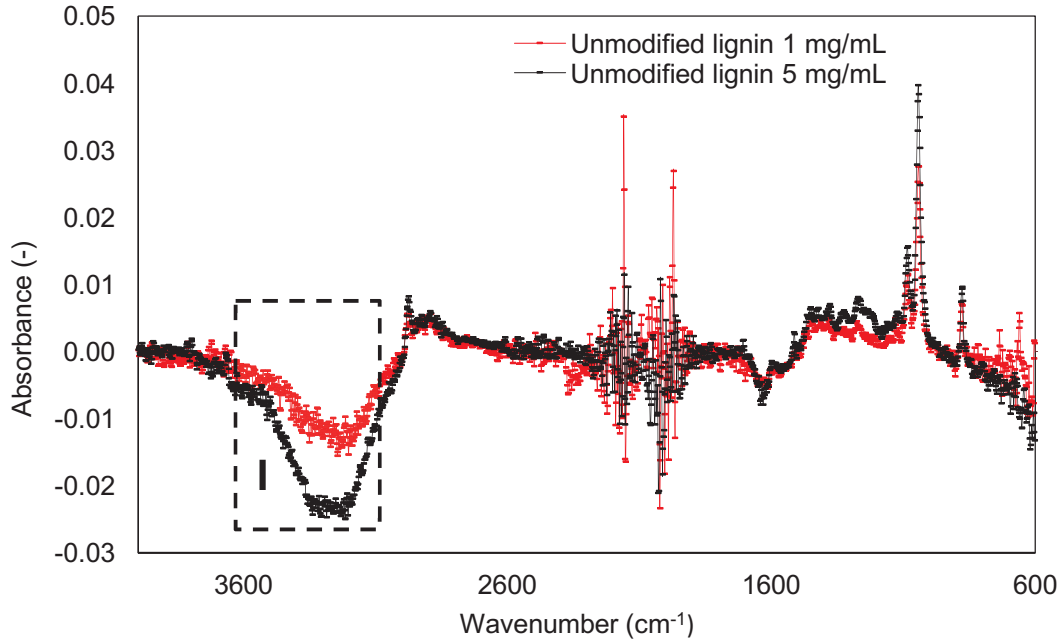

Figure 6.19. FTIR spectra of unmodified lignin at 5 and 1 mg/mL lignin concentration.

Even though the spectra subtraction method is quite useful for most applications using IR accessories, an attempt to remove the water spectra from FTIR spectra will be complicated in most cases (Nishikida *et al.*, 1995). A representative of specific fingerprint around 3400 cm^{-1} attributed to O-H stretching vibrations in aromatic and aliphatic hydroxyl groups can be seen in Figure 6.19 (labeled as I). Initially, as anticipated, the absorbance of unmodified lignin at 5 mg/mL was stronger than 1 mg/mL; indicating the high availability hydroxyl groups of intramolecular and intermolecular hydrogen bonding formed and existed between lignin and dual solvent in the soluble

lignin extract (Wang *et al.*, 2016). The source of O-H bonds could be originated from water, ethanol and lignin.

However, a more careful analysis revealed that the negative value of absorbance especially in the region I (Figure 6.19) corresponds to the stretch of O-H bonds in water molecules causes dominant absorbance in the wavenumber of 3400 cm^{-1} (Zaiqun, 2007). The finding appears to be well supported by Barth (2007) which the strong absorbance of water in the IR spectra region overlaps with sample modes of interest. Figure 6.20 has proved that the peak at 3400 cm^{-1} of water (labeled as II) had strong absorption (0.39) rather than ethanol (0.15).

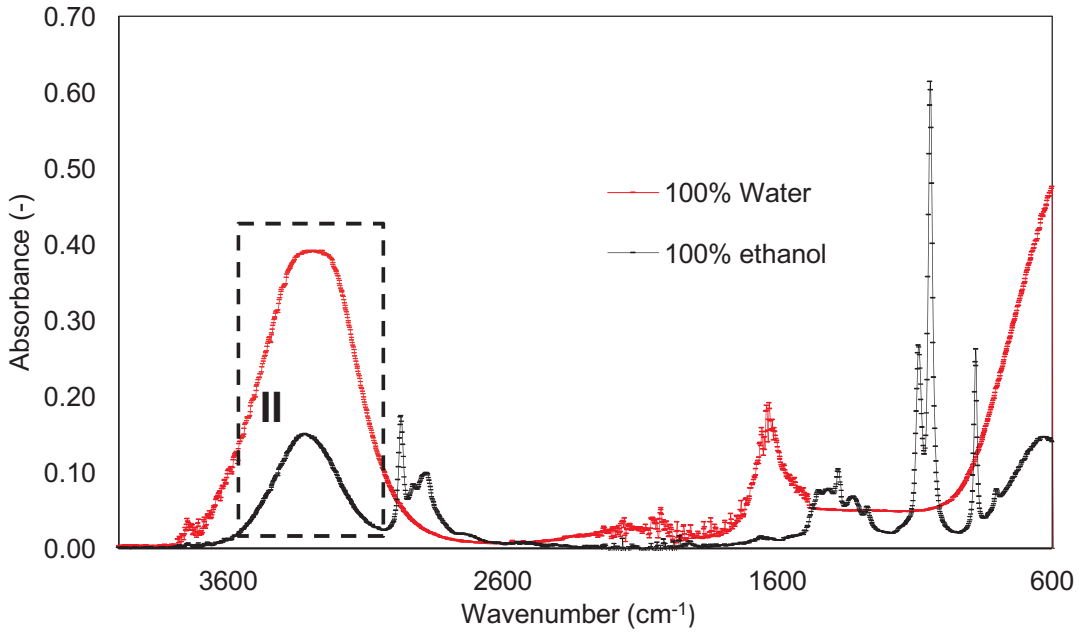

Figure 6.20. FTIR spectra of water and ethanol.

Therefore, when the hydroxyl groups wavenumber is of interest, the strong water absorption in the aqueous samples could have influenced the results obtained and in turn, relatively led into misinterpretation of the data.

Despite the limitation of this method, and consequently the poor results in the analysis of unmodified lignin samples, the findings do however suggest that dehydration of sample could be conducted or the precipitated lignin used for analysis in future to reduce the intense IR absorption of water (Trenerry and Rochfort, 2010). Therefore, the spectra of unmodified lignin based on the spectra subtraction method could not be comparable with the spectra of modified lignin.

6.3.2.2 Comparison of Modified Lignin at Different Lignin Concentration

Figure 6.21 provides the schematic diagram of sample analysed via FTIR for esterification study.

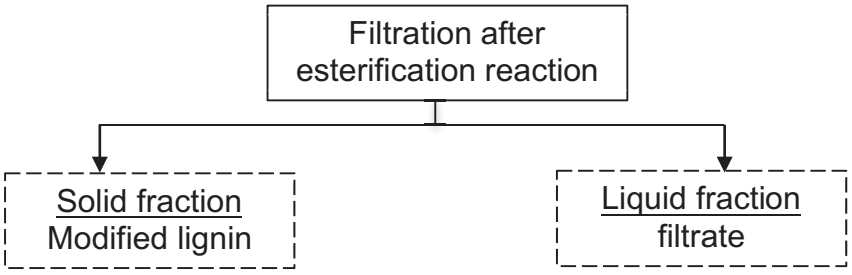

*Additional sample analysed for comparison study (1) dodecanoyl chloride (2) blank solution contains ethanol-water mixture (50% by volume), pyridine, dodecanoyl chloride and 2% of ice-cold hydrochloric acid.

Figure 6.21. Schematic diagram of sample analysed via FTIR for esterification study.

The FTIR spectra of the resulting modified lignin at 5 and 1 mg/mL lignin concentration were compared in Figure 6.22. The wavenumbers at 3400, 2938, 2850, 1800, 1760, 1740, and 1700 cm^{-1} of FTIR spectra could be used as physiological fingerprints to assess the efficacy of esterification process.

The presence of 3400 cm^{-1} (region I) was noted with broad intensity at 5 mg/mL (0.04) rather than 1 mg/mL (0.03), and the wavenumber of 3400cm^{-1} was attributed to O-H stretching of aromatic and aliphatic hydroxyl groups (Alriols *et al.*, 2010; Boeriu *et al.*, 2014; Pandey, 1999). The peak of 3400 cm^{-1} at 1 mg/mL become more flattened. As hypothesised, the findings showed that more material or lignin concentration in the soluble lignin extract, the more source of O-H bonds in the esterified lignin.

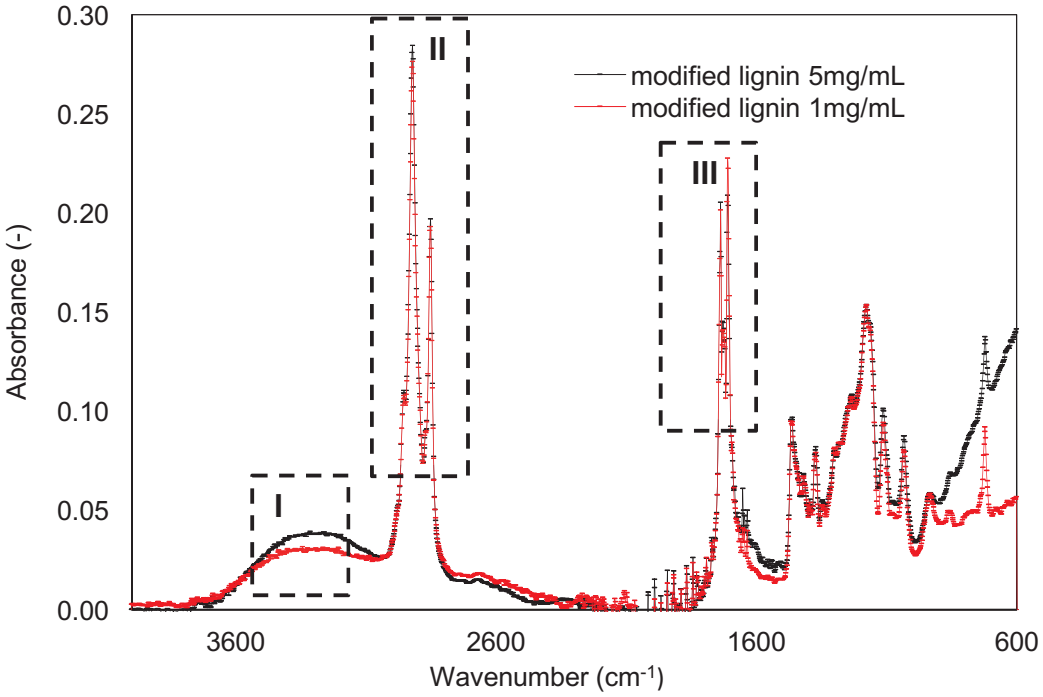

Figure 6.22. FTIR spectra of modified lignin at different ethanol concentration.

When comparison was made to modified lignin prepared to 1 mg/mL, the region II and III in Figure 6.22 of modified lignin from 5 mg/mL showed no difference in intensity of the peaks around 2938, 2850, 1760 and 1740 cm^{-1}. Strong absorptions at 2938 and 2850 cm^{-1} of modified lignin (region II) at both lignin concentrations arise from long chain alkyl groups (aliphatic carbon) which are present in fatty acid chloride, dodecanoyl chloride (Gordobil *et al.*,

2016), and the CH stretching vibrations in methyl and methylene groups (Szczepkowski *et al.*, 2007). A clear evidence of a sharp intensity peak at 1760 and 1740 cm^{-1} (region III) at both lignin concentrations that related to aromatic and aliphatic ester bonds were observed (Pawar *et al.*, 2016). This indicates that the esterification process was successful.

Given that the findings of modified lignin showed the esterification was successfully conducted at both lignin concentrations, the results from such FTIR analysis should thus consequently be compared with the filtrate, dodecanoyl chloride and blank solution of FTIR spectra to support the evidence of esterification efficacy. Dodecanoyl chloride is the C_{12} fatty acid chloride that reacted with lignin to form ester. Upon filtration after esterification process, esterified lignin was separated from the filtrate. The filtrate may consist of ethanol, water and 2% of ice-cold hydrochloric acid. The chemical modification via esterification was confirmed by FTIR and the spectra of the filtrate, dodecanoyl chloride and blank solution of each lignin concentration were shown in Figure 6.23.

The spectra between modified lignin at both concentrations were compared with the spectra of dodecanoyl chloride. The disappearance peak of dodecanoyl chloride, 1800 cm^{-1} associated to COCl and 1700 cm^{-1} referred to dodecanoyl acid in Figure 6.23 (labeled as I), strongly support that the modified lignins do not contain any traces of unreacted fatty acid (Gordobil *et al.*, 2016). Figure 6.23 showed that the spectra of filtrate had a similar chemical characterisation with the spectra of blank solution. Both spectra, filtrate and blank solution were dominated by water at 5 and 1 mg/mL lignin

concentration, in turn the spectra produced were similar with the spectra of water and overlap with other modes of interest as have been shown previously in Figure 6.20.

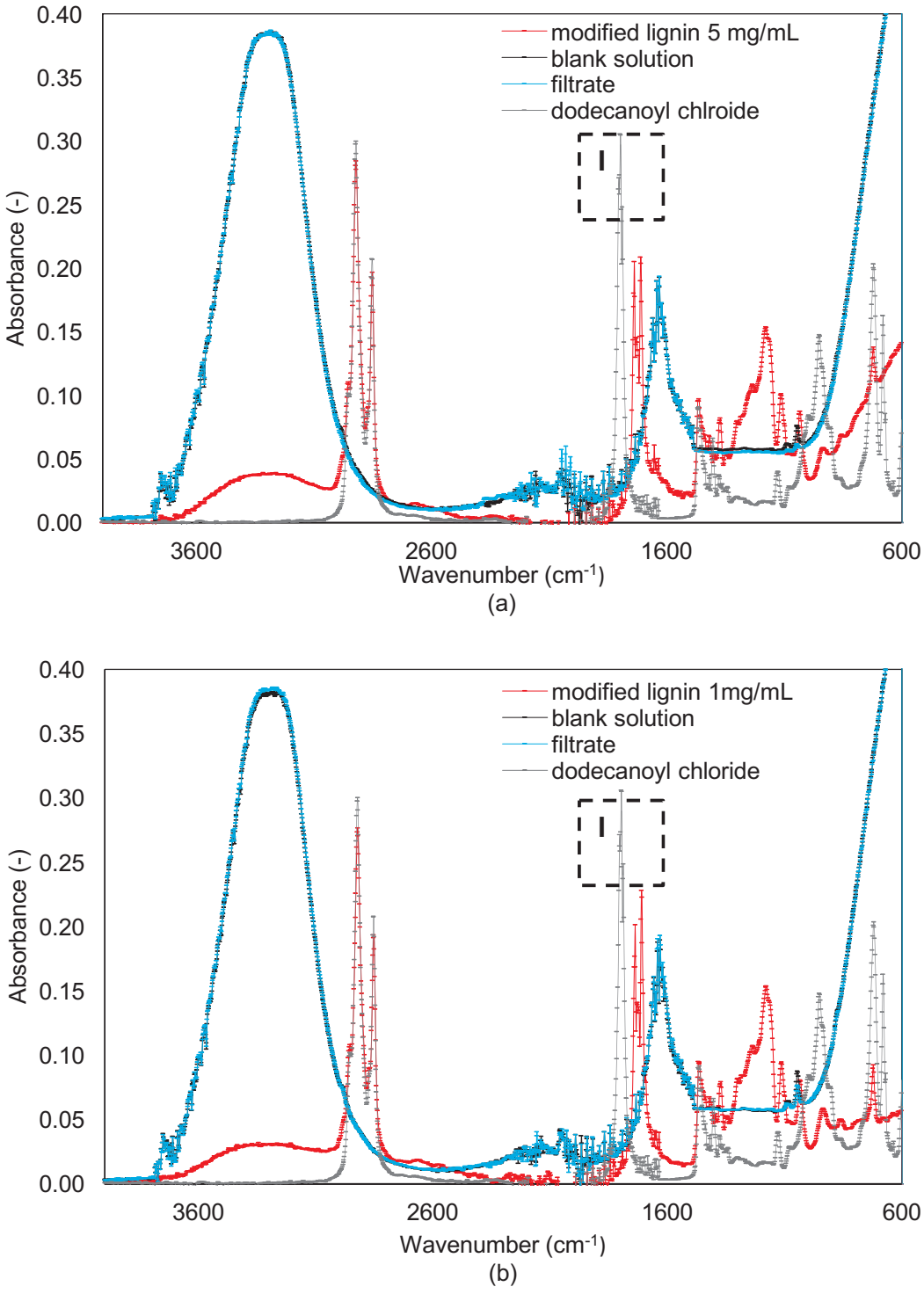

Figure 6.23. FTIR spectra of modified lignin, blank solution, filtrate and dodecanoyl chloride at (a) 5 and (b) 1 mg/mL lignin concentration.

In general, the findings of this study implied that esterification works well with both lignin concentration, 5 and 1 mg/mL of soluble lignin extract. However, the utilisation of 1 mg/mL lignin concentration of soluble lignin extract is not feasible for lignin modification process. Taking into account of high dilution may lead to exessive energy costs in process if using 1 mg/mL lignin concentration of soluble lignin extract, it is recommended the soluble lignin extract produced from SE processing routes that had 5 mg/mL lignin concentration is used directly for lignin modification process.

6.3.2.3 Comparison of Unmodified Lignin and Modified Lignin

Overall, the comparison of unmodified and modified lignin at both lignin concentration, 5 and 1 mg/mL have been unable to demonstrate the efficacy of esterification reaction at different lignin concentration due to the justification discussed in section 6.3.2.1. However, an assumption that unmodified lignin produced in Chapter 5 had 5 mg/mL or more lignin material seem to be realistic and acceptable if the comparison between unmodified lignin and modified lignin has to be made for the soluble lignin extract within similar ethanol concentration (50% ethanol concentration by volume). A representative FTIR spectra between unmodified and derivatised lignin esters or modified lignin can be seen in Figure 6.24.

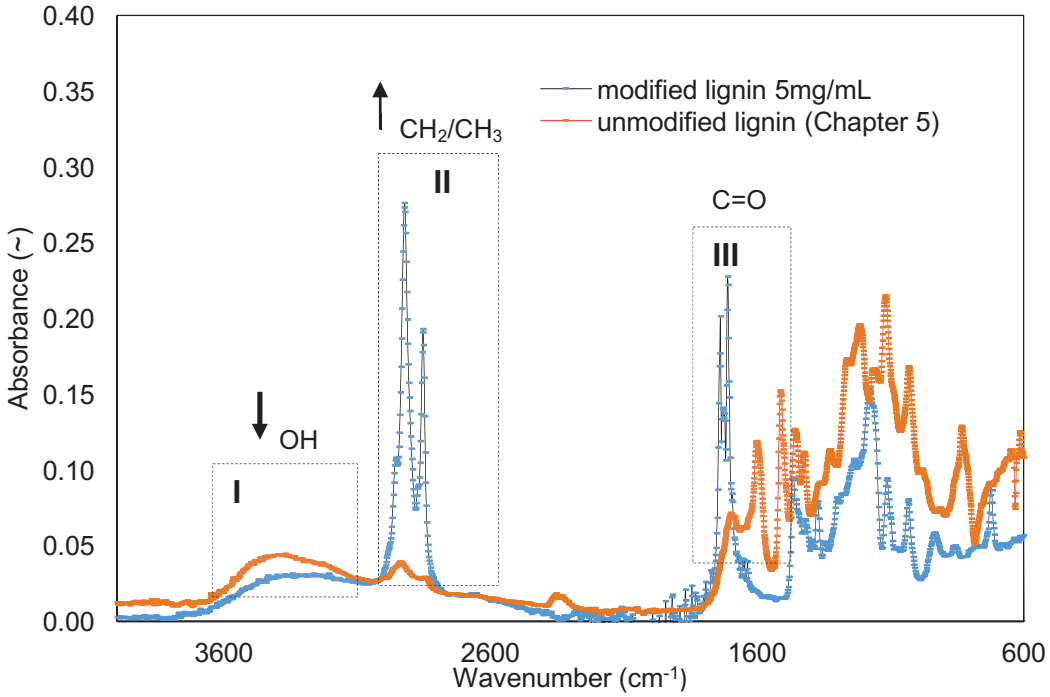

Figure 6.24. FTIR spectra of unmodified lignin and modified lignin.

Here, the esterification was assessed by FTIR which also focused on the absorbance data for quantitative analysis (Gallignani *et al.*, 2014; Khanmohammadi *et al.*, 2009). The esterification can be clearly examined by the incremental decline of the hydroxyl group at wavenumber at 3400 cm^{-1}, the incremental increase of aliphatic CH stretching from the ester groups at 2938 and 2850 cm^{-1}, and the incremental appearance of ester bonds at 1760 and 1740 cm^{-1} (phenolic and aliphatic, respectively) with a degree of added C_{12} fatty acid chloride (Koivu *et al.*, 2016; Pawar *et al.*, 2016). The dotted line in Figure 6.24 showed the specific fingerprints I, II, and III (hydroxyl group, CH stretching and ester bonds, respectively) that could be further focused for the efficacy of lignin esterification.

Overall, modified lignin showed that a decrease in the intensity of the OH stretching band in aromatic and aliphatic hydroxyl groups at 3400 cm^{-1}

(region I), indicating that the lignin esterification reduced the availability of hydroxyl groups in the lignin macromolecules for modified lignin (Lisperguer *et al.*, 2009). Upon derivatisation, the appearance of two peaks in region III strongly confirm the formation of lignin esters (Chen *et al.*, 2014; Namazi *et al.*, 2011). The peaks that originated from CH_2 and CH_3 stretching at region II were also increased in absorption after modification reaction (Chen *et al.*, 2014). The absence of wavenumbers at 1800 cm^{-1} that related to the carbonyl stretch of dodecanoyl chloride exhibited that the modified lignin was free from unreacted acyl chloride (COCl) (Gordobil *et al.*, 2016; Massaro *et al.*, 1995). The disappearance of peak at 1700 cm^{-1} (COOH) in the spectra of modified lignin also validated that the modified lignin does not contain traces of dodecanoyl acid, by-product formed of acyl chloride hydrolysis (Cao *et al.*, 2015; Dawodu *et al.*, 2014). The washing method after filtration was efficient to remove impurities from the end product (Gordobil *et al.*, 2016).

The esterification conversion was evaluated according to the absorbance changes which were denoted to conversion, by measuring the height of the hydroxyl group at 3400 cm^{-1} stretching band, H_{OH} and normalising with the height of C=C aromatic skeletal vibrations band at 1515 cm^{-1}, which was taken as reference, H_{ref} (Cachet *et al.*, 2014). Esterification conversion (*A*) was calculated from the Eq. 6.2 (Passauer *et al.*, 2016; Saralegi *et al.*, 2013) measuring H_{OH} and H_{ref} at reaction time, t = 2 hr and at the beginning, t = 0.

$$A = 1 - \left[\frac{\left({}^{H_{OH}}/_{H_{ref}}\right)_{t-2h}}{\left({}^{H_{OH}}/_{H_{ref}}\right)_{t=0}}\right] x\ 100\% \qquad (6.2)$$

The esterification conversion achieved was 81.2% and the esterification conversion is almost similar to that esterification of Eucalyptus and Spruce organosolv lignins with fatty acid (dodecanoyl chloride), resultant values were 82% and 80%, respectively (Gordobil *et al.*, 2016).

6.4 Conclusion

This study provided the understanding of microscopic properties and structural insights of lignin aggregates at wider range of ethanol concentration. Detailed analysis on particle size determination was conducted and the findings of average particle size correlated well with the microscopy images at different ethanol concentrations. Contrary to theoretical, the finding in this study showed that dispersion of lignin aggregates occurred at low ethanol concentration in the ethanol-water mixture. However, the conclusion of the findings should be treated with cautions, as the findings related to particle size and the availability of hydroxyl groups at different ethanol concentrations can be validated by various methods in future such as size exclusion chromatography and potentiometric titration, respectively.

The efficacy of the lignin modification via esterification was evidenced directly via FTIR using the similar ethanol concentration of soluble lignin extract at different lignin concentration. The most obvious findings to emerge from this study is the water that had strong absorption peaks causing overlapping the absorption of interest wavenumbers. Therefore, the FTIR method by spectra subtraction method failed to provide accurate spectra for

unmodified lignin, which in turn unable to find a comparison between unmodified and modified lignin's spectra. Despite the limitation and the poor results by spectra subtraction method, findings do however suggest that the comparison between modified lignin and unmodified lignin (Chapter 5) achieved. The esterified lignin derived at 5 mg/mL is suggested to expand greater lignin functionality in the preparation of lignin bio-based materials.

CHAPTER 7: CONCLUSIONS AND RECOMMENDATIONS FOR FUTURE WORK

7.1 Conclusions

The development of economically feasible second-generation bioethanol offers promising source of energy to reduce the world's dependence on fossil fuels throughout diverse efficient separation technologies. The emerging of biorefinery concept for second-generation bioethanol produces a multitude of different valuable building blocks, namely hemicellulose, cellulose and lignin from lignocellulosic biomass. In this study, the biomass fractionation was carried out via SCW mediated hydrolysis, in which the study focused on the developing novel approaches to support enhanced added value applications of lignin.

The impact of SCW mediated hydrolysis of two different lignin extraction processing routes, DE and SE were assessed with regards to physical and chemical properties of lignin macromolecules. An assessment on percentage of delignification from DE was 81.5% whereas the SE yielded 58.0%. Although the SE showed lower efficacy of delignification than DE, the lignin macromolecules of SE exhibited higher purity of lignin and lignin derived from dried supernatant than DE. The percentage of lignin recovery was not significantly different for both lignin extraction processing routes. The FTIR analysis demonstrated that the lignin obtained by different processing routes had different chemical compositions. Overall, even though SE exerted negative impact specifically on percentage of delignification, the SE process

has potential to produce quality streams of fractionated biomass, which successfully evokes the concept of biorefining in second-generation bioethanol process. In addition, the lignin produced from SE processing routes had abundance of hydroxyl groups, indicating that lignin recovered can be a good alternative to polyols in the production of lignin bio-based materials. The soluble lignin extract from SE process were used as the starting materials to assess the lignin aggregation behavior, as well to characterise the derived lignin fractions in terms of particle size, degree of substitution and therefore reactivity prior to lignin modification and utilisation.

In the present study, the effect on ethanol concentrations (10%, 25%, 50% and 75%) was investigated on lignin recovery, particle size, chemical structure and microscopy imaging properties. Findings showed that the lignin recovery increased as the ethanol concentration decreased. Since the purity of precipitated lignin was not significant using 50% and 25% ethanol concentration, it is suggested that 10% ethanol concentration is used for lignin recovery. Moreover, the purity of precipitated lignin at 10% ethanol concentration demonstrated a high purity (≥90%). The results of lignin purity correlated well with chemical structure analysis via FTIR. The morphology images captured via SEM imaging revealed the findings of particle size analysis.

Despite the lignin recovery study having the prevailing consensus that lignin could be recovered by the centrifugation process with certain conditions, the underlying driving forces of lignin association behind the centrifugation process remain unclear. Thereby, further study of soluble lignin extract

without centrifugation at different ethanol concentrations was carried out, focusing on particle size and LM images. LM method was more preferable than SEM due to effect of drying changed the morphology of lignin macromolecules, thus the difference in morphology cannot be observed via SEM imaging method. The aggregation behavior study of soluble lignin extract at wider ranges of different ethanol concentrations via LM images was comparable to the particle size analysis.

Low average particle size could be effectively produced at lowest ethanol concentration of soluble lignin extract. Nevertheless, these findings need to be interpreted with caution due to the dispersion cannot lead to particle size or molecular weight reduction. However, findings by LM showed that the lignin aggregates appeared to be disaggregated from population of large aggregates to population of sub-population of small aggregates when the ethanol concentration reduced. The appearance of sub-population of small lignin aggregates can thus be suggested, de-blocking the available hydroxyl groups and creating more hydroxyl groups especially phenolic hydroxyl groups, the most reactive functional group in the soluble lignin extract. Nevertheless, the specific area of the availability of hydroxyl group remains unclear and further studies will need to be undertaken.

Given that the main aim was to utilise the soluble lignin extract directly from SE processing routes without the normal practice to recover the lignin prior to lignin modification process, a strategy to attach fatty acid molecules to organosolv lignin using simple esterification was reported. The success of the modification reaction of lignin was confirmed with FTIR. The modification

involves a significant decrease in hydroxyl group and increases considerably the CH stretching and C=O ester bonds. Saturated C_{12} fatty acid were substituted on organosolv lignin to prepare lignin ester with the esterification conversion rate of 81.2%.

In summary, the present study makes noteworthy contributions that an efficient process for completely separating main biomass components in a biorefinery approach produces soluble lignin extract that provides high availability of hydroxyl groups in addition to hemicellulose and celluloce recovery. The available reactive hydroxyl groups in lignin offers exciting possibilities for lignin chemical modification. Moreover, a less time consuming and less costly method to use directly the soluble lignin extract instead to dissolve lignin powder in the solvent, is recommended for lignin chemical modification. The modified lignin under esterification derived using the soluble lignin extract directly from SE (5 mg/mL) could be used further with increased functionalities in the bio-replacement ratios and facilitated the chemical transformation of lignin stream in bio-based industrial applications.

7.2 Recommendations for Future Work

Considerably more work will need to be done in several areas with regards to extraction and modification of lignin to support enhanced lignin utilisation using critical fluids.

The use of SE showed potential for lignin fractionation, in addition to other main components of lignocellulosic biomass, hemicellulose and cellulose. The optimum conditions achieved by delignification of DE was

applied to delignification of SE and the findings demonstrated that the experimental conditions used for delignification of SE was too severe for the *MxG* pre-processed fibres. The optimisation of delignification of SE needs to be carried out, so that high delignification could be achieved by SCW mediated hydrolysis with associated modifiers. The processing parameters for delignification of SE that could be examined including temperature, reaction time and pressure. However, with the assessment of delignification experimental conditions, caution must be applied, as the delignification process will disrupt the structure of cellulose fibres and further influence the cellulose enzymatic digestibility for bioethanol production.

Lignin recovery via centrifugation method also could be another research area deserving further investigation especially the lignin aggregation behavior in separation process. In the centrifugation method, it would be interesting to assess the effects of temperature, time and acceleration rate towards lignin recovery process. Further LM analysis could also be conducted to examine the differences of lignin macromolecules in the soluble lignin extract before the centrifugation process. The findings before the centrifugation process also could be compared with the lignin and supernatant morphology structure after centrifugation process at different process parameters for lignin recovery. In a study of lignin aggregation behaviour at different ethanol concentration, the reduction of particle size and the availability of hydroxyl group has thrown up many questions in need of further investigation. Future research should therefore concentrate on the validation of particle size and determination of hydroxyl groups via different established methods. In addition, the effect of lignin concentration may affect the whole

behaviour of lignin aggregates in the ethanol-water mixture. Future research regards to behaviour is suggested to be conducted using the similar ethanol concentration at different lignin concentration.

Preliminary study of lignin modification via esterification was demonstrated in order to evaluate the feasibility of using soluble lignin extract after SCW mediated hydrolysis with associated modifiers. Future work should focus on enhancing the efficacy of esterification process by optimising the esterification experimental condition such as the amount of acyl chloride required in the reaction, reaction time and temperature prior to lignin valorisation. After lignin modification, further recommendations also have been suggested to investigate the bio-replacement ratios and further scale up the process for industrial production of lignin bio-based materials.

REFERENCES

Abbas, K. A., Mohamed, A., Abdulamir, A. S., and Abas, H. A. (2008). A review on supercritical fluid extraction as new analytical method. *American Journal of Biochemistry and Biotechnology*, *4*(4), 345–353.

Abdel-Ghani, N. T., El-Chaghaby, G. A., and Helal, F. S. (2014). Individual and competitive adsorption of phenol and nickel onto multiwalled carbon nanotubes. *Journal of Advanced Research*, *6*(3), 405–415.

Abdelaziz, O. Y., Brink, D. P., Prothmann, J., Ravi, K., Sun, M., García-Hidalgo, J., … Gorwa-Grauslund, M. F. (2016). Biological valorisation of low molecular weight lignin. *Biotechnology Advances*, *34*(8), 1318–1346.

Abdelaziz, O. Y., and Hulteberg, C. P. (2017). Physicochemical characterisation of technical lignins for their potential valorisation. *Waste and Biomass Valorization*, *8*(3), 859–869.

Abdul Khalil, H. P. S., Bhat, A. H., and Ireana Yusra, A. F. (2012). Green composites from sustainable cellulose nanofibrils: A review. *Carbohydrate Polymers*, *87*(2), 963–979.

Abidi, N., Hequet, E., Cabrales, L., Gannaway, J., Wilkins, T., and Wells, L. W. (2008). Evaluating cell wall structure and composition of developing cotton fibers using Fourier transform infrared spectroscopy and thermogravimetric analysis. *Journal of Applied Polymer Science*, *107*(1), 476–486.

Abiven, S., Heim, A., and Schmidt, M. W. I. (2011). Lignin content and chemical characteristics in maize and wheat vary between plant organs and growth stages: consequences for assessing lignin dynamics in soil. *Plant Soil*, *343*(1–2), 369–378.

Achyuthan, K. E., Achyuthan, A. M., Adams, P. D., Dirk, S. M., Harper, J. C., Simmons, B. A., and Singh, A. K. (2010). Supramolecular self-assembled chaos: Polyphenolic lignin's barrier to cost-effective lignocellulosic biofuels. *Molecules*, *15*(12), 8641–8688.

Agarwal, U. P., and Atalla, R. H. (2010). Vibrational Spectroscopy. In J. Heitner, Cyril, R. Dimmer, Donald, A. Schmidt (Ed.), *Lignin and Lignans Advances in Chemistry* (pp. 104–129). Boca Raton, United States of America: CRC Press.

Agbor, V. B., Cicek, N., Sparling, R., Berlin, A., and Levin, D. B. (2011). Biomass pretreatment: Fundamentals toward application. *Biotechnology Advances*, *29*(6), 675–685.

Alberts, B., Johnson, A., Lewis, J., Raff, M., Roberts, K., and Peter Walter. (1989). Cells in Their Social Context. In *Molecular Biology of The Cell* (Fourth, Vol. 53, p. 160). New York, USA: Garland Science.

Aleš, H., Michal, J., Lenka, D., Alexandra, S., and Igor, Š. (2015). Thermal properties and size distribution of lignins precipitated with sulphuric acid. *Wood Research*, *60*(3), 375–384.

Allen, E., Paul Smith, and Henshaw, J. (2001). *A review of particle agglomeration*. Dorset, United Kingdom.

Alriols, M. G., García, A., Llano-ponte, R., and Labidi, J. (2010). Combined organosolv and ultrafiltration lignocellulosic biorefinery process. *Chemical Engineering Journal*, *157*(1), 113–120.

Alvira, P., Tomás-Pejó, E., Ballesteros, M., and Negro, M. J. (2010). Pretreatment technologies for an efficient bioethanol production process based on enzymatic hydrolysis: A review. *Bioresource Technology*, *101*(13), 4851–4861.

Amendola, D., De Faveri, D. M., Egües, I., Serrano, L., Labidi, J., and Spigno, G. (2012). Autohydrolysis and organosolv process for recovery of hemicelluloses, phenolic compounds and lignin from grape stalks. *Bioresource Technology*, *107*, 267–274.

Amin, S., Barnett, G. V., Pathak, J. A., Roberts, C. J., and Sarangapani, P. S. (2014). Protein aggregation, particle formation, characterisation and rheology. *Current Opinion in Colloid & Interface Science*, *19*(5), 438–449.

An, S., Darboux, F., and Cheng, M. (2013). Revegetation as an efficient means of increasing soil aggregate stability on the *Loess Plateau* (China). *Geoderma*, *209–210*, 75–85.

Ando, H., Sakaki, T., Kokusho, T., Shibata, M., Uemura, Y., and Hatate, Y. (2000). Decomposition behaviour of plant biomass in hot-compressed water. *Industrial and Engineering Chemistry Research*, *39*(10), 3688–3693.

Anwar, Z., Gulfraz, M., and Irshad, M. (2014). Agro-industrial lignocellulosic biomass a key to unlock the future bio-energy: A brief review. *Journal of Radiation Research and Applied Sciences*, *7*(2), 163–173.

Argyropoulos, D. S., and Menachem, S. B. (1997). Lignin. In K.-E. L. Eriksson, W. Babel, H. W. Blanch, P. D. C. L. Cooney, P. D. S.-O. Enfors, P. D. K.-E. L. Eriksson, … P. D. C. Wandrey (Eds.), *Biotechnology in the Pulp and Paper Industry* (pp. 128–151). New York, USA: Springer Berlin Heidelberg.

Asl, A. H., and Khajenoori, M. (2013). Subcritical Water Extraction. In H. Nakajima (Ed.), *Mass Transfer - Advances in Sustainable Energy and Environment Oriented Numerical Modeling* (pp. 459–487). InTech.

Audu, I. G., Brosse, N., Desharnais, L., and Rakshit, S. K. (2012). Ethanol organosolv pretreatment of *Typha Capensis* for bioethanol production and co-products. *BioResources*, *7*(4), 5917–5933.

Ayusheev, A. B., and Taran, O. P. (2016). Depolymerisation of birch-wood organosolv lignin over solid catalysts in supercritical ethanol. *Journal of Siberian Federal University*, *9*(3), 353–370.

Azizi Samir, M. A. S., Alloin, F., and Dufresne, A. (2005). Review of recent research into cellulosic whiskers, their properties and their application in nanocomposite field. *Biomacromolecules*, *6*(2), 612–626.

Baker, D. A., and Rials, T. G. (2013). Recent advances in low-cost carbon fiber manufacture from lignin. *Journal of Applied Polymer Science*, *130*(2), 713–728.

Bakiz, B., Bourja, L., Benlhachemi, A., Guinneton, F., Villain, S., Ezahri, M., and Gavarri, J.-R. (2012). Time-dependent oxidative capacities of La_2O_3, Lu_2O_3, CeO_2, Bi_2O_3 and materials interacting with air-CO or air-CH_4 flows. *ISRN Materials Science*, *2012*, 1–9.

Balat, M., and Ayar, G. (2005). Biomass energy in the world, use of biomass and potential trends. *Energy Sources*, *27*(10), 931–940.

Baptista, C., Belgacem, N., and Daurte, A. P. (2006). The Effect of Wood Extractives on Pulp Properties of Maritime Pine Kraft Pulp. *Journal of the Technical Association of the Australian and New Zealand Pulp and Paper*

Industry, *59*(4), 311–316.
Bardet, M., Energy, A., and Co, A. E. (1988). Structural changes in aspen lignin during steam explosion treatment. *Cellulose Chemistry and Technology*, *22*, 221–230.
Barros, A. M. De. (2016). *A new approach to develop cost-effective lignocellulosic bioethanol production*. PhD thesis. University of Birmingham.
Barth, A. (2007). Infrared spectroscopy of proteins. *Biochimica et Biophysica Acta - Bioenergetics*, *1767*(9), 1073–1101.
Bauer, S., Sorek, H., Mitchell, V. D., Ibáñez, A. B., and Wemmer, D. E. (2012). Characterisation of *Miscanthus* x *giganteus* lignin isolated by ethanol organosolv process under reflux condition. *Journal of Agricultural and Food Chemistry*, *60*(33), 8203–8212.
Behera, S., Arora, R., Nandhagopal, N., and Kumar, S. (2014). Importance of chemical pretreatment for bioconversion of lignocellulosic biomass. *Renewable and Sustainable Energy Reviews*, *36*, 91–106.
Bentsen, N., and Felby, C. (2012). Biomass for energy in the European Union - a review of bioenergy resource assessments. *Biotechnology for Biofuels*, *5*(1), 25.
Bergeret, G., and Gallezot, P. (2008). Particle Size and Dispersion Measurements. In *Handbook of Heterogeneous Catalysis* (pp. 738–765). WILEY-VCH Verlag GmbH &Co. KGaA.
Bevilaqua, T., Gonçalves, T. F., Venturini, C. de G., and Machado, V. G. (2006). Solute–solvent and solvent–solvent interactions in the preferential solvation of 4-[4-(dimethylamino)styryl]-1-methylpyridinium iodide in 24 binary solvent mixtures. *Spectrochimica Acta Part A: Molecular and Biomolecular Spectroscopy*, *65*(3), 535–542.
Bhat, R., Abdullah, N., Din, R. H., and Tay, G.-S. (2013). Producing novel sago starch based food packaging films by incorporating lignin isolated from oil palm black liquor waste. *Journal of Food Engineering*, *119*(4), 707–713.
Boeriu, C. G., Bravo, D., Gosselink, R. J. A., and van Dam, J. E. G. (2004). Characterisation of structure-dependent functional properties of lignin with infrared spectroscopy. *Industrial Crops and Products*, *20*(2), 205–218.
Boeriu, C. G., Fiţigău, F. I., Gosselink, R. J. A., Frissen, A. E., Stoutjesdijk, J., and Peter, F. (2014). Fractionation of five technical lignins by selective extraction in green solvents and characterisation of isolated fractions. *Industrial Crops and Products*, *62*, 481–490.
Borrega, M., Nieminen, K., and Sixta, H. (2011). Effects of hot water extraction in a batch reactor on the delignification of birch wood. *BioResources*, *6*(2), 1890–1903.
Bridson, J. H., Van De Pas, D. J., and Fernyhough, A. (2013). Succinylation of three different lignins by reactive extrusion. *Journal of Applied Polymer Science*, *128*(6), 4355–4360.
Brosse, N., Dufour, A., Meng, X., Sun, Q., and Ragauskas, A. (2012). Miscanthus: a fast-growing crop for biofuels and chemicals production. *Biofuels, Bioproducts and Biorefining*, *6*(5), 246–256.
Brosse, N., Mohamad Ibrahim, M. N., and Abdul Rahim, A. (2011). Biomass to bioethanol: initiatives of the future for lignin. *ISRN Materials Science*,

2011, 1–10.
Bruijnincx, P., Weckhuysen, B., Gruter, G.-J., Westenbroek, A., and Engelen-Smeets, E. (2016). *Lignin Valorisation The Importance of a Full Value Chain Approach*. Netherlands.
Brunow, G. (2004). Methods to Reveal the Structure of Lignin. In M. Hofrichter and A. Steinbüchel (Eds.), *Biopolymers: Lignin, Humic Substances and Coal* (pp. 89–99). Findland: Wiley.
Buhvestov, U., Rived, F., Ràfols, C., Bosch, E., and Rosés, M. (1998). Solute-solvent and solvent-solvent interactions in binary solvent mixtures. Part 7. Comparison of the enhancement of the water structure in alcohol-water mixtures measured by solvatochromic indicators. *Journal of Physical Organic Chemistry*, *11*(3), 185–192.
Buono, P., Duval, A., Verge, P., Averous, L., and Habibi, Y. (2016). New insights on the chemical modification of lignin: Acetylation versus silylation. *ACS Sustainable Chemistry & Engineering*, *4*(10), 5212–5222.
Byrt, C. S., Grof, C. P. L., and Furbank, R. T. (2011). C4 plants as biofuel feedstocks: Optimising biomass production and feedstock quality from a lignocellulosic perspective. *Journal of Integrative Plant Biology*, *53*(2), 120–135.
Cabeza, A., Piqueras, C. M., Sobrón, F., and García-Serna, J. (2016). Modeling of biomass fractionation in a lab-scale biorefinery: Solubilisation of hemicellulose and cellulose from holm oak wood using subcritical water. *Bioresource Technology*, *200*, 90–102.
Cachet, N., Camy, S., Benjelloun-Mlayah, B., Condoret, J.-S., and Delmas, M. (2014). Esterification of organosolv lignin under supercritical conditions. *Industrial Crops and Products*, *58*, 287–297.
Campbell, M. M., and Sederoff, R. R. (1996). Variation in lignin content and composition. *Plant Physiology*, *110*(1), 3–13.
Canilha, L., Silva, J., Felipe, M., and Carvalho, W. (2003). Batch xylitol production from wheat strawhemicellulosic hydrolysate using Candida guilliermondii in a stirred tank reactor. *Biotechnology Letters*, *25*, 1811–1814.
Cao, N. (2013). *Calibration optimisation and efficiency in near infrared spectroscopy*. PhD thesis. Iowa State University.
Cao, S., Pu, Y., Studer, M., Wyman, C., Ragauskas, A. J., Ragauskas, A. J., … Lundquist, K. (2012). Chemical transformations of *Populus trichocarpa* during dilute acid pretreatment. *RSC Advances*, *2*(29), 10925–10936.
Cao, X., Fesinmeyer, R. M., Pierini, C. J., Siska, C. C., Litowski, J. R., Brych, S., … Kleemann, G. R. (2015). Free fatty acid particles in protein formulations, Part 1: Microspectroscopic identification. *Journal of Pharmaceutical Sciences*, *104*(2), 433–446.
Carr, A. G., Mammucari, R., and Foster, N. R. (2011). A review of subcritical water as a solvent and its utilisation for the processing of hydrophobic organic compounds. *Chemical Engineering Journal*, *172*(1), 1–17.
Cateto, C. A., Barreiro, M. F., Rodrigues, A. E., and Belgacem, M. N. (2009). Optimisation study of lignin oxypropylation in view of the preparation of polyurethane rigid foams. *Industrial and Engineering Chemistry Research*, *48*(5), 2583–2589.
Çetin, N. S., and Özmen, N. (2002). Use of organosolv lignin in phenol–formaldehyde resins for particleboard production. *International Journal of*

Adhesion and Adhesives, *22*(6), 477–480.
Chen, H. (2014). Chemical Composition and Structure of Natural Lignocellulose. In *Biotechnology of Lignocellulose* (pp. 25–71). China: Springer.
Chen, L., Carpita, N. C., Reiter, W.-D., Wilson, R. H., Jeffries, C., and McCann, M. C. (1998). A rapid method to screen for cell-wall mutants using discriminant analysis of Fourier transform infrared spectra. *The Plant Journal*, *16*(3), 385–392.
Chen, Y., Stark, N. M., Cai, Z., Frihart, C. R., Lorenz, L. F., and Ibach, R. E. (2014). Chemical modification of kraft lignin: Effect on chemical and thermal properties. *Bioresources*, *9*(3), 5488–5500.
Chiou, T.-Y., Neoh, T. L., Kobayashi, T., and Adachi, S. (2012). Properties of extract obtained from defatted rice bran by extraction with aqueous ethanol under subcritical conditions. *Food Science and Technology Research*, *18*(1), 37–45.
Chung, J.-H., and Kim, D.-S. (2012). Miscanthus as a potential bioenergy crop in East Asia. *Journal of Crop Science and Biotechnology*, *15*(2), 65–77.
Cigolotti, V. (2012). Biomass and Waste as Sustainable Resources. In S. J. McPhail, V. Cigolotti, and A. Moreno (Eds.), *Fuel Cells in the Waste-to-Energy Chain. Green Energy and Technology.* (Vol. 45, pp. 23–44). London, United Kingdom: Springer.
Ciobanu, C., Ungureanu, M., Ignat, L., Ungureanu, D., and Popa, V. I. (2004). Properties of lignin–polyurethane films prepared by casting method. *Industrial Crops and Products*, *20*(2), 231–241.
Clauss, M. M., Weldin, D. L., Frank, E., Giebel, E., and Buchmeiser, M. R. (2015). Size-exclusion chromatography and aggregation studies of acetylated lignins in N,N-dimethylacetamide in the presence of salts. *Macromolecular Chemistry and Physics*, *216*(20), 2012–2019.
Claverie, J., Marie-Thérèse Charreyre, and Pichot, C. (2010). *Polymers in Dispersed Media I: International Conference on Polymers in Dispersed Media (Macromolecular Symposia)*. (I. Miesel and S. Spiegel, Eds.). France: Wiley-VCH Verlag GmbH & Co. KGaA.
Coates, J. (2000). *Interpretation of Infrared Spectra , A Practical Approach Interpretation of Infrared Spectra , A Practical Approach*. (R. A. Meyers, Ed.)*Encyclopedia of Analytical Chemistry*. Chichester, UK: John and Wiley Sons, Inc.
Constant, S., Wienk, H. L. J., Frissen, A. E., Peinder, P. de, Boelens, R., van Es, D. S., … Bruijnincx, P. C. A. (2016). New insights into the structure and composition of technical lignins: a comparative characterisation study. *Green Chem.*, *18*(9), 2651–2665.
Contreras, S., Gaspar, A. R., Guerra, A., Lucia, L. A., & Argyropoulos, D. S. (2008). Propensity of lignin to associate: Light scattering photometry study with native lignins. *Biomacromolecules*, *9*(12), 3362–3369.
Cordella, C. B. Y. (2012). *PCA : The Basic Building Block of Chemometrics*. (I. S. Krull, Ed.)*Analytical chemistry*. Croatia: InTech.
Cox, B. J., Jia, S., Zhang, Z. C., and Ekerdt, J. G. (2011). Catalytic degradation of lignin model compounds in acidic imidazolium based ionic liquids: Hammett acidity and anion effects. *Polymer Degradation and Stability*, *96*(4), 426–431.
Cumpstey, I. (2013). Chemical Modification of Polysaccharides. *ISRN Organic*

Chemistry, 1–27.
Cybulska, I., Brudecki, G. P., Zembrzuska, J., Schmidt, J. E., Lopez, C. G.-B., and Thomsen, M. H. (2017). Organosolv delignification of agricultural residues (date palm fronds, *Phoenix dactylifera* L.) of the United Arab Emirates. *Applied Energy*, *185*(2), 1040–1050.
Da Silva, D. C., Ricken, I., Silva, M. A. D. R., and Machado, V. G. (2002). Solute-solvent and solvent-solvent interactions in the preferential solvation of Brooker's merocyanine in binary solvent mixtures. *Journal of Physical Organic Chemistry*, *15*(7), 420–427.
Dan, X., Kuanjun, F., and Shaohai, F. (2009). Effects of ethanol on the stability of pigment colloidal dispersion. *Journal of Dispersion Science and Technology*, *30*(4), 510–513.
Davis, W. M., Erickson, C. L., Johnston, C. T., Delfino, J. J., and Porter, J. E. (1999). Quantitative Fourier Transform Infrared spectroscopic investigation humic substance functional group composition. *Chemosphere*, *38*(12), 2913–2928.
Dawodu, F. A., Ayodele, O., Xin, J., Zhang, S., and Yan, D. (2014). Effective conversion of non-edible oil with high free fatty acid into biodiesel by sulphonated carbon catalyst. *Applied Energy*, *114*, 819–826.
De Gonzalo, G., Colpa, D. I., Habib, M. H. M., and Fraaije, M. W. (2016). Bacterial enzymes involved in lignin degradation. *Journal of Biotechnology*, *236*, 110–119.
DeMartini, J. D., Pattathil, S., Avci, U., Szekalski, K., Mazumder, K., Hahn, M. G., and Wyman, C. E. (2011). Application of monoclonal antibodies to investigate plant cell wall deconstruction for biofuels production. *Energy Environ. Sci.*, *4*(10), 4332–4339.
Demirbas, A. (2009). Biomass Feedstocks. In *Biofuels: Securing the Planet's Future Energy Needs* (pp. 45–85). London: Springer.
Deng, Y., Feng, X., Zhou, M., Qian, Y., Yu, H., and Qiu, X. (2011). Investigation of aggregation and assembly of alkali lignin using iodine as a probe. *Biomacromolecules*, *12*(4), 1116–1125.
Dinc, I., Sigdel, M., Dinc, S., Sigdel, M. S., Pusey, M. L., and Aygun, R. S. (2014). Evaluation of normalisation and PCA on the performance of classifiers for protein crystallisation images. In *Conference Proceedings - IEEE Southeastcon* (pp. 1–19).
Doherty, W. O. S., Mousavioun, P., and Fellows, C. M. (2011). Value-adding to cellulosic ethanol: Lignin polymers. *Industrial Crops and Products*, *33*(2), 259–276.
Donaldson, L. A. (1985). Critical assessment of interference microscopy as a technique for measuring lignin distribution in cell walls. *New Zealand Journal of Forestry Science*, *15*(3), 349–360.
Doucet, F. J., Lead, J. R., Maguire, L., Achterberg, E. P., and Millward, G. E. (2005). Visualisation of natural aquatic colloids and particles - a comparison of conventional high vacuum and environmental scanning electron microscopy. *Journal of Environmental Monitoring*, *7*(2), 115.
Dowell, F., and Wang, D. (2013). Qualitative and quantitative analysis of lignocellulosic biomass using infrared techniques : A. *Applied Energy*, *104*, 801–809.
Duff, S. J. B., and Murray, W. D. (1996). Bioconversion of forest products industry waste cellulosics to fuel ethanol: A review. *Bioresource*

Technology, *55*(1), 1–33.
Duku, M. H., Gu, S., and Hagan, E. Ben. (2011). A comprehensive review of biomass resources and biofuels potential in Ghana. *Renewable and Sustainable Energy Reviews*, *15*(1), 404–415.
Duval, A., and Lawoko, M. (2014). A review on lignin-based polymeric, micro- and nano-structured materials. *Reactive and Functional Polymers*, *85*, 78–96.
Edvardsson, K. (2010). *Evaluation of Dust Suppressants for Gravel Roads : Methods Development and Efficiency Studies*. *PhD Thesis*. Royal Institute of Technology (KTH).
Effendi, A., Gerhauser, H., and Bridgwater, A. V. (2008). Production of renewable phenolic resins by thermochemical conversion of biomass: A review. *Renewable and Sustainable Energy Reviews*, *12*(8), 2092–2116.
Eggert, C., Temp, U., Eriksson, K. E., Eggert, C., and Temp, U. (1996). The ligninolytic system of the white rot fungus *Pycnoporus cinnabarinus* : purification and characterisation of the laccase. *Applied and Environmental Microbiology*, *62*(4), 1151–1158.
El Hage, R., Chrusciel, L., Desharnais, L., and Brosse, N. (2010). Effect of autohydrolysis of *Miscanthus* x *giganteus* on lignin structure and organosolv delignification. *Bioresource Technology*, *101*(23), 9321–9329.
El Mansouri, N. E., Yuan, Q., and Huang, F. (2011). Characterisation of alkaline lignins for use in phenol-formaldehyde and epoxy resins. *BioResources*, *6*, 2647–2662.
Eriksson, L., Johansson, E., Kettaneh-Wold, N., Trygg, C., Wikström, C., and Wold, S. (2006). PCA. In *Multi- and Megavariate Data Analysis Part 1, Basic Principles and Applications* (3rd ed., pp. 39–62). MKS Umetrics AB.
Esbensen, K. H., Guyot, D., Westad, F., and Houmøller, L. P. (2002). *Multivariate Data Analysis: In Practice : an Introduction to Multivariate Data Analysis and Experimental Design* (5th ed.). Oslo: CAMO.
Espinoza-Acosta, J. L., Torres-Chavez, P. I., Carvajal-Millan, E., Ramirez-Wong, B., Bello-Perez, L. A., and Montano-Leyva, B. (2014). Ionic liquids and organic solvents for recovering lignin from lignocellulosic biomass. *BioResources*, *9*(2), 3660–3687.
Falter, C., Zwikowics, C., Eggert, D., Blümke, A., Naumann, M., Wolff, K., … Voigt, C. A. (2015). Glucanocellulosic ethanol: the undiscovered biofuel potential in energy crops and marine biomass. *Scientific Reports*, *5*, 1–9.
FAO. (2010). *Global Forest Resources Assessment*. Rome.
Faruk, O., Obaid, N., Tjong, J., and Sain, M. (2015). *Lignin Reinforcement in Thermoplastic Composites*. *Lignin in Polymer Composites*. Elsevier Inc.
Ferdosian, F., Yuan, Z., Anderson, M., and Xu, C. (Charles). (2016). Synthesis and characterisation of hydrolysis lignin-based epoxy resins. *Industrial Crops and Products*, *91*, 295–301.
Ferdosian, F., Yuan, Z., Anderson, M., and Xu, C. C. (2012). Chemically modified lignin through epoxidation and its thermal properties. *J-For*, *2*(4), 11–15.
Fernando, E. F. (2010). Lignin recovery from spent liquors from ethanol-water fractionation of sugar cane bagasse. *Cellulose Chemistry and Technology*, *44*(9), 311–318.
Filly, A., Fabiano-Tixier, A. S., Louis, C., and Fernandez, X. (2016). Water as a green solvent combined with different techniques for extraction of

essential oil from lavender flowers. *Comptes Rendus Chimie*, *19*(6), 707–717.

FitzPatrick, M., Champagne, P., Cunningham, M. F., and Whitney, R. A. (2010). A biorefinery processing perspective: Treatment of lignocellulosic materials for the production of value-added products. *Bioresource Technology*, *101*(23), 8915–8922.

Francisco G. Calvo-Flores, Dobado, J. A., Isac-Garcia, J., and Francisco J. Martin-Martinez. (2015). *Lignin and Lignans as Renewable Raw Materials* (1st ed.). United Kingdom: John and Wiley Sons, Inc.

Frankó, B., Carlqvist, K., Galbe, M., Lidén, G., and Wallberg, O. (2017). Removal of Water-Soluble Extractives Improves the Enzymatic Digestibility of Steam-Pretreated Softwood Barks. *Applied Biochemistry and Biotechnology*, 1–17.

Frigerio, P., Zoia, L., Orlandi, M., Hanel, T., and Castellani, L. (2014). Application of sulphur-free lignins as a filler for elastomers: Effect of hexamethylenetetramine treatment. *BioResources*, *9*(1), 1387–1400.

Fu, Q.-S., Xue, Y.-Q., Cui, Z.-X., and Wang, M.-F. (2014). Study on the size-dependent oxidation reaction kinetics of nanosized zinc sulfide. *Journal of Nanomaterials*, *2014*, 1–8.

Fukushima, R. S., Kerley, M. S., Ramos, M. H., Porter, J. H., and Kallenbach, R. L. (2015). Comparison of acetyl bromide lignin with acid detergent lignin and Klason lignin and correlation with in vitro forage degradability. *Animal Feed Science and Technology*, *201*, 25–37.

Gallignani, M., Rondón, R. A., Ovalles, J. F., and Brunetto, M. R. (2014). Transmission FTIR derivative spectroscopy for estimation of furosemide in raw material and tablet dosage form. *Acta Pharmaceutica Sinica B*, *4*(5), 376–383.

Gan, M., Pan, J., Zhang, Y., Dai, X., Yin, Y., Qu, Q., and Yan, Y. (2014). Molecularly imprinted polymers derived from lignin-based Pickering emulsions and their selectively adsorption of lambda-cyhalothrin. *Chemical Engineering Journal*, *257*, 317–327.

Gao, N., Wang, S. C., Ubhi, H. S., and Starink, M. J. (2005). A comparison of grain size determination by light microscopy and EBSD analysis. *Journal of Materials Science*, *40*(18), 4971–4974.

Ghaffar, S. H., and Fan, M. (2014). Lignin in straw and its applications as an adhesive. *International Journal of Adhesion and Adhesives*, *48*, 92–101.

Ghosh, D., and Hallenbeck, P. C. (2012). Advanced Bioethanol Production. In P. C. Hallenbeck (Ed.), *Microbial Technologies in Advanced Biofuels Production* (pp. 165–182). New York, USA: Springer.

Golding, C. G., Lamboo, L. L., Beniac, D. R., and Booth, T. F. (2016). The scanning electron microscope in microbiology and diagnosis of infectious disease. *Scientific Reports*, *6*(February), 26516.

Gordobil, O., Egüés, I., and Labidi, J. (2016). Modification of Eucalyptus and Spruce organosolv lignins with fatty acids to use as filler in PLA. *Reactive and Functional Polymers*, *104*, 45–52.

Gordobil, O., Moriana, R., Zhang, L., Labidi, J., and Sevastyanova, O. (2016). Assesment of technical lignins for uses in biofuels and biomaterials: Structure-related properties, proximate analysis and chemical modification. *Industrial Crops and Products*, *83*, 155–165.

Gosselink, R. J. A., Teunissen, W., van Dam, J. E. G., de Jong, E.,

Gellerstedt, G., Scott, E. L., and Sanders, J. P. M. (2012). Lignin depolymerisation in supercritical carbon dioxide/acetone/water fluid for the production of aromatic chemicals. *Bioresource Technology*, *106*, 173–177.

Grootveld, M. (2012). Introduction to the Applications of Chemometric Techniques in 'Omics' Research: Common Pitfalls, Misconceptions and 'Rights and Wrongs'. In D. Anderson, M. Waters, and T. C. Marrs (Eds.), *Metabolic Profiling: Disease and Xenobiotics* (pp. 1–34). Cambridge, United Kingdom: Royal Society of Chemistry.

Guo, F., Shi, W., Sun, W., Li, X., Wang, F., Zhao, J., and Qu, Y. (2014). Differences in the adsorption of enzymes onto lignins from diverse types of lignocellulosic biomass and the underlying mechanism. *Biotechnology for Biofuels*, *7*(1), 38.

Gupta, S. K. (2008). *Isolation, Cloning and characterisation of Lignin Biosynthesis Pathway Gene(s) 4-Coumarate Co A Ligase (4-CL) from Leucaena leucocephala*. *PhD Thesis*. University of Pune.

Haghighi Mood, S., Hossein Golfeshan, A., Tabatabaei, M., Salehi Jouzani, G., Najafi, G. H., Gholami, M., and Ardjmand, M. (2013). Lignocellulosic biomass to bioethanol, a comprehensive review with a focus on pretreatment. *Renewable and Sustainable Energy Reviews*, *27*, 77–93.

Hall, M., Bansal, P., Lee, J. H., Realff, M. J., and Bommarius, A. S. (2010). Cellulose crystallinity - A key predictor of the enzymatic hydrolysis rate. *FEBS Journal*, *277*(6), 1571–1582.

Hamaguchi, M., Cardoso, M., and Vakkilainen, E. (2012). Alternative technologies for biofuels production in kraft pulp mills—Potential and prospects. *Energies*, *5*(12), 2288–2309.

Harkin, J. M. (1969). *Lignin and its Uses*. Wisconsin, USA.

Hasegawa, I., Tabata, K., Okuma, O., and Mae, K. (2004). New pretreatment methods combining a hot water treatment and water/acetone extraction for thermo-chemical conversion of biomass. *Energy and Fuels*, *18*(3), 755–760.

Hatakeyama, H., Nakayachi, A., and Hatakeyama, T. (2005). Thermal and mechanical properties of polyurethane-based geocomposites derived from lignin and molasses. *Composites Part A: Applied Science and Manufacturing*, *36*(5), 698–704.

Hatfield, R., and Fukushima, R. S. (2005). Can lignin be accurately measured? *Crop Science*, *45*(3), 832–839.

Hattori, T., and Morita, S. (2010). Energy crops for sustainable bioethanol production; which, where and how? *Plant Production Science*, *13*(3), 221–234.

Havlík, P., Schneider, U. A., Schmid, E., Böttcher, H., Fritz, S., Skalský, R., … Obersteiner, M. (2011). Global land-use implications of first and second generation biofuel targets. *Energy Policy*, *39*, 5690–5702.

He, L., Liu, Q., Song, Y., and Deng, Y. (2014). Effects of metal chlorides on the solubility of lignin in the black liquor of prehydrolysis kraft pulping. *BioResources*, *9*(2), 4636–4642.

Heaton, E. A., Dohleman, F. G., & Long, S. P. (2008). Meeting US biofuel goals with less land: The potential of Miscanthus. *Global Change Biology*, *14*, 2000–2014.

Henriksson, G. (2009). Lignin. In M. Ek, G. Gellerstedt, and G. Henriksson

(Eds.), *Wood Chemistry and Wood Biotechnology* (pp. 121–146). Berlin, Germany: Walter de Gruyter GmbH and Co.

Holladay, J. E., White, J. F., Bozell, J. J., and Johnson, D. (2007). *Top Value-Added Chemicals from Biomass Volume II — Results of Screening for Potential Candidates from Biorefinery Lignin* (Vol. II). Virginia, United States of America.

Hori, R., and Sugiyama, J. (2003). A combined FT-IR microscopy and principal component analysis on softwood cell walls. *Carbohydrate Polymers*, *52*(4), 449–453.

Hosseinaei, O., Harper, D. P., Bozell, J. J., and Rials, T. G. (2017). Improving processing and performance of pure lignin carbon fibers through hardwood and herbaceous lignin blends. *International Journal of Molecular Sciences*, *18*(7).

Hsu, T. ., Ladisch, M. ., and Tsao, G. T. (1980). Alcohol from Cellulose. *ChemTech*, 315–319.

Hu, F., Jung, S., and Ragauskas, A. (2012). Pseudo-lignin formation and its impact on enzymatic hydrolysis. *Bioresource Technology*, *117*, 7–12.

Hu, L., Pan, H., Zhou, Y., and Zhang, M. (2011). Methods to improve lignin's reactivity as a phenol substitute and as replacement for other phenolic compounds: a brief review. *Bioresources*, *6*(3), 3515–3525.

Hu, Z.-H., Yue, Z.-B., and Yu, H.-Q. (2010). Anaerobic Digestion of Lignocellulosic Wastes by Rumen Microorganisms: Chemical and Kinetic Analyses. In H. H.P. Fang (Ed.), *Environmental Anaerobic Technology: Applications and New Developments* (pp. 259–275). London: Imperial College Press.

Huijgen, W. J. J., Smit, A. T., de Wild, P. J., and den Uil, H. (2012). Fractionation of wheat straw by prehydrolysis, organosolv delignification and enzymatic hydrolysis for production of sugars and lignin. *Bioresource Technology*, *114*, 389–398.

Ibrahim, M. M., El-Zawawy, W. K., Abdel-Fattah, Y. R., Soliman, N. A., and Agblevor, F. A. (2011). Comparison of alkaline pulping with steam explosion for glucose production from rice straw. *Carbohydrate Polymers*, *83*(2), 720–726.

IEA Bioenergy. (2009). *Biorefineries: adding value to the sustainable utilisation of biomass*. New Zealand: IEA Bioenergy Secretariat.

Ignat, L., Ignat, M., Ciobanu, C., Doroftei, F., and Popa, V. I. (2011). Effects of flax lignin addition on enzymatic oxidation of poly(ethylene adipate) urethanes. *Industrial Crops and Products*, *34*(1), 1017–1028.

Ionescu, M. (2005). *Chemistry and Technology of Polyols for Polyurethane*. Shropshire, United Kingdom: Rapra Technology Limited.

Ishizawa, C. I., Jeoh, T., Adney, W. S., Himmel, M. E., Johnson, D. K., and Davis, M. F. (2009). Can delignification decrease cellulose digestibility in acid pretreated corn stover? *Cellulose*, *16*(4), 677–686.

Jackson, G. A, and Burd, A. B. (1998). Critical Review Aggregation in the Marine Environment. *Environmental Science and Technology*, *32*(19), 2805–2814.

Jahan, M. S., Rawsan, S., Chowdhury, D. A. N., and Al-Maruf, A. (2008). Alternative pulping process for producing dissolving pulp from jute. *BioResources*, *3*(4), 1359–1370.

Jain, M. (2006, October). The Boundary Around The Plant Cell. *Pratiyogita*

Darpan Group, 1088–1090.
Jeffries, T. W. (1994). Biodegradation of Lignin and Hemicelluloses. In C. Ratledge (Ed.), *Biochemistry of microbial degradation* (pp. 233–277). United Kingdom: Springer Science+Business Media, B.V.
Jesionowski, T., Klapiszewski, Ł., and Milczarek, G. (2014). Kraft lignin and silica as precursors of advanced composite materials and electroactive blends. *Journal of Materials Science*, *49*(3), 1376–1385.
Jones, E. (1984). The Infrared Spectrum of Spruce Native Lignin. *Journal of the American Chemical Society*, *70*, 1984–1985.
Jones, O. G., and McClements, D. J. (2010). Functional biopolymer particles: Design, fabrication, and applications. *Comprehensive Reviews in Food Science and Food Safety*, *9*(4), 374–397.
Jönsson, L. J., and Martín, C. (2016). Pretreatment of lignocellulose: Formation of inhibitory by-products and strategies for minimising their effects. *Bioresource Technology*, *199*, 103–112.
Jørgensen, U. (2011). Benefits versus risks of growing biofuel crops: the case of Miscanthus. *Current Opinion in Environmental Sustainability*, *3*(1–2), 24–30. http://doi.org/10.1016/j.cosust.2010.12.003
Juhascik, M., Gleba, J., and Jenkins, A. (2012). Formation of benzoylecgonine isopropyl ester following solid-phase extraction. *Journal of Analytical Toxicology*, *36*(2), 141–143.
Jung, H. J. G., Varel, V. H., Weimer, P. J., and Ralph, J. (1999). Accuracy of Klason lignin and acid detergent lignin methods as assessed by bomb calorimetry. *Journal of Agricultural and Food Chemistry*, *47*(5), 2005–2008.
Kai, D., Tan, M. J., Chee, P. L., Chua, Y. K., Yap, Y. L., and Loh, X. J. (2016). Towards lignin-based functional materials in a sustainable world. *Green Chemistry*, *18*(5), 1175–1200.
Kelly, R. N., DiSante, K. J., Stranzl, E., Kazanjian, J. A., Bowen, P., Matsuyama, T., and Gabas, N. (2006). Graphical comparison of image analysis and laser diffraction particle size analysis data obtained from the measurements of nonspherical particle systems. *AAPS PharmSciTech*, *7*(3), 1–14.
Khadka, P., Ro, J., Kim, H., Kim, I., Kim, J. T., Kim, H., … Lee, J. (2014). Pharmaceutical particle technologies: An approach to improve drug solubility, dissolution and bioavailability. *Asian Journal of Pharmaceutical Sciences*, *9*(6), 304–316.
Khanal, S. K., Surampalli, R. Y., Zhang, T. C., Lamsal, B. P., and Tyagi, R. D. (2010). *Bioenergy and Biofuel from Biowastes and Biomass*. United States of America: American Society of Civil Engineers.
Khanmohammadi, M., Mobedi, H., Mobedi, E., Kargosha, K., Bagheri Garmarudi, A., and Ghasemi, K. (2009). Quantitative determination of naltrexone by attenuated total reflectance-FTIR spectrometry using partial least squares (PLS) wavelength selection. *Spectroscopy*, *23*(2), 113–121.
Kindermann, G. E., Mccallum, I., Fritz, S., and Obersteiner, M. (2008). A global forest growing stock, biomass and carbon map based on FAO statistics. *Silva Fennica*, *42*(3), 387–396.
King, J. W., and Grabiel, R. D. (2007). US Patent 7,2008,181 B1. United States of America.

Klapiszewski, L., Madrawska, M., and Jesionowski, T. (2012). Preparation and characterisation of hydrated silica/lignin biocomposites. *Physicochemical Problems of Mineral Processing*, *48*(2), 463–473.

Kline, L. M., Hayes, D. G., Womac, A. R., and Labbe, N. (2010). Simplified determination of lignin content in hard and soft woods via UV-spectrophotometric analysis of biomass dissolved in ionic liquids. *BioResources*, *5*(3), 1366–1383.

Kogel-Knobner, I. (2002). The macromolecular organic composition of plant and microbial residues as inputs to soil organic matter. *Soil Biology and Biochemistry*, *34*, 139–162.

Koivu, K. A. Y., Sadeghifar, H., Nousiainen, P. A., Argyropoulos, D. S., and Sipilä, J. (2016). Effect of fatty acid esterification on the thermal properties of softwood kraft lignin. *ACS Sustainable Chemistry and Engineering*, *4*(10), 5238–5247.

Kosa, M., and Ragauskas, A. J. (2013). Lignin to lipid bioconversion by oleaginous Rhodococci. *Green Chemistry*, *15*(8), 2070–2074.

Kryževičienė, A. (2011). Cultivation of *Miscanthus× giganteus* for biofuel and its tolerance of Lithuania's climate. *Zemdirbyste= Agriculture*, *98*(3), 267–274.

Kumar, P., Barrett, D. M., Delwiche, M. J., and Stroeve, P. (2009). Methods for pretreatment of lignocellulosic biomass for efficient hydrolysis and biofuel production. *Industrial and Engineering Chemistry Research*, *48*(8), 3713–3729.

Kummamuru, B. V, Lang, A., Calderon, C., Bradley, D., Gauthier, G., Farouk, H., … Uyar, T. S. (2015). *WBA Global Bioenergy Statistics 2015*. *World Bioenergy Association*. Stockholm, Sweden.

Kutscha, N. P., and Gray, J. R. (1970, March). The Potential of Lignin Research. *Maine Agricultural Experiment Station*, 1–21.

Labbé, N., Harper, D., and Rials, T. (2006). Chemical structure of wood charcoal by infrared spectroscopy and multivariate analysis. *Journal of Agricultural and Food Chemistry*, *54*(10), 3492–3497.

Landová, H., Vetchý, D., Gajdziok, J., Doležel, P., Muselík, J., Dvořáčková, K., … Knotek, Z. (2014). Evaluation of the influence of formulation and process variables on mechanical properties of oral mucoadhesive films using multivariate data analysis. *BioMed Research International*, 1–9.

Lange, H., Decina, S., and Crestini, C. (2013). Oxidative upgrade of lignin – Recent routes reviewed. *European Polymer Journal*, *49*(6), 1151–1173.

Lapierre, C. (2010). 'Determining Lignin Structure by Chemical Degradations. In J. Heitner, Cyril, R. Dimmer, Donald, A. Schmidt (Ed.), *Lignin and Lignans Advances in Chemistry* (pp. 11–48). Boca Raton, United States of America: CRC Press.

Laurichesse, S., and Avérous, L. (2014). Chemical modification of lignins: Towards biobased polymers. *Progress in Polymer Science*, *39*(7), 1266–1290.

Lee Black, D., McQuay, M. Q., and Bonin, M. P. (1996). Laser-based techniques for particle-size measurement: A review of sizing methods and their industrial applications. *Progress in Energy and Combustion Science*, *22*(3), 267–306.

Lee, H. V., Hamid, S. B. A., and Zain, S. K. (2014). Conversion of lignocellulosic biomass to nanocellulose: Structure and chemical process.

Scientific World Journal, *2014*, 1–21.
Leisola, M., Pastinen, O., and Axe, D. D. (2012). Lignin-designed randomness. *BIO-Complexity*, *2012*(3), 1–11.
Lewandowski, I., Clifton-Brown, J. C., Scurlock, J. M. O., and Huisman, W. (2000). Miscanthus: European experience with a novel energy crop. *Biomass and Bioenergy*, *19*(4), 209–227.
Li, H., Deng, Y., Liu, B., Ren, Y., Liang, J., Qian, Y., … Zheng, D. (2016). Preparation of Nanocapsules via the Self-Assembly of Kraft Lignin: A Totally Green Process with Renewable Resources. *ACS Sustainable Chemistry and Engineering*, *4*(4), 1946–1953.
Li, J., Henriksson, G., and Gellerstedt, G. (2005). Carbohydrate reactions during high-temperature steam treatment of aspen wood. *Applied Biochemistry and Biotechnology*, *125*, 175–188.
Li, J., Henriksson, G., and Gellerstedt, G. (2007). Lignin depolymerisation/repolymerisation and its critical role for delignification of aspen wood by steam explosion. *Bioresource Technology*, *98*(16), 3061–8.
Li, L., Zhou, W., Wu, H., Yu, Y., Liu, F., and Zhu, D. (2014). Relationship between crystallinity index and enzymatic hydrolysis performance of celluloses separated from aquatic and terrestrial plant materials. *BioResources*, *9*(3), 3993–4005.
Li, M.-F., Fan, Y.-M., Xu, F., Sun, R.-C., and Zhang, X.-L. (2010). Cold sodium hydroxide/urea based pretreatment of bamboo for bioethanol production: Characterisation of the cellulose rich fraction. *Industrial Crops and Products*, *32*(3), 551–559.
Li, Y., Jia, H., Ruxianguli, R., Yin, H., and Zhang, Q. (2015). Extraction of lignin from wheat straw by catalysts in 1,4-butanediol medium under atmospheric pressure. *BioResources*, *10*(1), 1085–1098.
Li, Y., and Sarkanen, S. (2005). Miscible blends of kraft lignin derivatives with low-Tg polymers. *Macromolecules*, *38*(6), 2296–2306.
Ligero, P., Kolk, J. C. van der, Vega, A. de, and Dam, J. E. G. van. (2011). Production of xylo-oligosaccharides from *Miscanthus* x *giganteus* by autohydrolysis. *BioResources*, *6*(4), 4417–4429.
Lisperguer, J., Perez, P., and Urizar, S. (2009). Structure and thermal properties of lignins: Characterisation by infrared spectroscopy and differential scanning calorimetry. *Journal of the Chilean Chemical Society*, *54*(4), 460–463.
Liu, E. J., Cashman, K. V., and Rust, A. C. (2015). Optimising shape analysis to quantify volcanic ash morphology. *GeoResJ*, *8*, 14–30.
Lomakin, A., Teplow, D. B., and Benedek, G. B. (2005). Quasielastic light scattering for protein assembly studies. *Methods in Molecular Biology*, *299*, 153–174.
Lora, J. (2008). Industrial Commercial Lignins : Sources, Properties and Applications. In M. N. Belgacem and A. Gandini (Eds.), *Monomers, Polymers and Composites from Renewable Resources* (1st editio, pp. 225–241). United Kingdom: Elsevier.
Lora, J. ., and Wayman, M. (1978). Delignification of hardwoods by autohydrolysis and extraction. *Tappi [Technical Association of the Pulp and Paper Industry]*, *61*, 47–50.
Lora, J. H., and Glasser, W. G. (2002). Recent industrial applications of lignin:

A sustainable alternative to nonrenewable materials. *Journal of Polymers and the Environment*, *10*(1), 39–48.
Lu, F., and Ralph, J. (2011). Solution-state NMR of lignocellulosic biomass. *Journal of Biobased Materials and Bioenergy*, *5*(2), 169–180.
Lü, H., Ren, M., Zhang, M., and Chen, Y. (2013). Pretreatment of corn stover using supercritical CO_2 with water-ethanol as co-solvent. *Chinese Journal of Chemical Engineering*, *21*(5), 551–557.
Lupoi, J. S., Singh, S., Simmons, B. A., and Henry, R. J. (2013). Assessment of Lignocellulosic Biomass Using Analytical Spectroscopy: an Evolution to High-Throughput Techniques. *BioEnergy Research*, *7*(1), 1–23.
Luthria, D. L., Mukhopadhyay, S., Lin, L., and Harnly, J. M. (2013). A comparison of analytical and data preprocessing methods for spectral fingerprinting. *Applied Spectroscopy*, *65*(3), 250–259.
Ma, Z., Merkus, H. G., de Smet, J. G. A. ., Heffels, C., and Scarlett, B. (2000). New developments in particle characterisation by laser diffraction: size and shape. *Powder Technology*, *111*(1), 66–78.
Macfarlane, A. L., Prestidge, R., Farid, M. M., and Chen, J. J. J. (2009). Dissolved air flotation: A novel approach to recovery of organosolv lignin. *Chemical Engineering Journal*, *148*(1), 15–19.
Mahmood, N., Yuan, Z., Schmidt, J., and Xu, C. (2016). Depolymerisation of lignins and their applications for the preparation of polyols and rigid polyurethane foams: A review. *Renewable and Sustainable Energy Reviews*, *60*, 317–329.
Maitra, A., and Bagchi, S. (2008). Study of solute–solvent and solvent–solvent interactions in pure and mixed binary solvents. *Journal of Molecular Liquids*, *137*(1), 131–137.
Malvern. (2011). *Dynamic Light Scattering : An Introduction in 30 Minutes*. *Technical Note*. Worcestershire, UK.
Malvern. (2012). *A Basic Guide to Particle Characterization*. *White Paper*. Worcestershire, UK.
Malvern. (2014). *Intensity - Volume - Number*. Worcestershire, UK.
Malvern Instruments Ltd. (2000). *Integrated Systems for Particle Sizing*. Worcestershire, UK.
Mankar, S. S., Chaudhari, A. R., & Soni, I. (2012). Lignin in phenol-formaldehyde resins. *International Journal of Knowledge Engineering*, *3*(1), 116–118.
Manley, M. (2014). Near-infrared spectroscopy and hyperspectral imaging: non-destructive analysis of biological materials. *Chemical Society Reviews*, *43*, 8200–8214.
Manorach, K., Poonsrisawat, A., Viriya-empikul, N., and Laosiripojana, N. (2015). Optimisation of Sub-Critical Water Pretreatment for Enzymatic Hydrolysis of Sugarcane Bagasse. In *Energy Procedia* (Vol. 79, pp. 937–942). Elsevier.
Mansouri, N.-E. El, Pizzi, A., and Salvado, J. (2007). Lignin-based polycondensation resins for wood adhesives. *Journal of Applied Polymer Science*, *103*(3), 1690–1699.
Mansouri, N.-E. El, and Salvadó, J. (2006). Structural characterisation of technical lignins for the production of adhesives: Application to lignosulfonate, kraft, soda-anthraquinone, organosolv and ethanol process lignins. *Industrial Crops and Products*, *24*(1), 8–16.

Massaro, M., Grudey, G., and Ilardi, L. (1995). Compositions comprising fatty acid esters of alkoxylated isethionic acid and process for making. USA: Feb 2, 1994.
Matsushita, Y. (2015). Conversion of technical lignins to functional materials with retained polymeric properties. *Journal of Wood Science*, *61*(3), 230–250.
Matsushita, Y., and Yasuda, S. (2003). Reactivity of a condensed – type lignin model compound in the Mannich reaction and preparation of cationic surfactant from sulfuric acid lignin. *Journal of Wood Science*, *49*(2), 166–171.
Maurya, D. P., Singla, A., and Negi, S. (2013). An overview of key pretreatment processes for biological conversion of lignocellulosic biomass to bioethanol. *3 Biotech*, *3*(5), 415–431.
McClements, D. J. (2005). *Food Emulsions Principles, Practices, and Techniques* (2nd ed.). United States of America: CRC Press.
McClements, D. J. (2015). *Nanoparticle- and Microparticle-based Delivery Systems: Encapsulation, Protection and Release of Active Compounds*. Boca Raton, Fl: CRC Press.
Meng, C., Lin, W., and Guo, X. U. E. (2016). Depolymerisation mechanism of alkali lignin in sub- and supercritical ethanol. *Journal of Fuel Chemistry and Technology*, *44*(10), 1203–1210.
Micic, M., Radotic, K., Jeremic, M., Djikanovic, D., and Kämmer, S. B. (2004). Study of the lignin model compound supramolecular structure by combination of near-field scanning optical microscopy and atomic force microscopy. *Colloids and Surfaces B: Biointerfaces*, *34*(1), 33–40.
Mohammad, A. M. (2008). *Recovery of Hemicelluloses from Wood Hydrolysates by Membrane Filtration*. Lappeenranta University of Technology, Finland.
Morais, A. R. C., Da Costa Lopes, A. M., and Bogel-Łukasik, R. (2015). Carbon dioxide in biomass processing: Contributions to the green biorefinery concept. *Chemical Reviews*, *115*(1), 3–27.
Moran, P., and Coats, B. (2012). Biological sample preparation for SEM imaging of porcine retina. *Microscopy Today*, *20*(2), 28–31.
Moriarty, P., and Honnery, D. (2012). What is the global potential for renewable energy? *Renewable and Sustainable Energy Reviews*, *16*(1), 244–252.
Mosier, N., Wyman, C., Dale, B., Elander, R., Lee, Y. Y., Holtzapple, M., and Ladisch, M. (2005). Features of promising technologies for pretreatment of lignocellulosic biomass. *Bioresource Technology*, *96*(6), 673–86.
Mulder, W. J., Gosselink, R. J. A., Vingerhoeds, M. H., Harmsen, P. F. H., and Eastham, D. (2011). Lignin based controlled release coatings. *Industrial Crops and Products*, *34*(1), 915–920.
Mustafa, A., and Turner, C. (2011). Pressurised liquid extraction as a green approach in food and herbal plants extraction: A review. *Analytica Chimica Acta*, *703*(1), 8–18.
Myburg, A. A., Lev-Yadun, S., and Sederoff, R. R. (2013). Xylem Structure and Function. In *Encyclopedia of Life Sciences* (pp. 1–9). Nature Publishing Group.
Namazi, H., Fathi, F., and Dadkhah, A. (2011). Hydrophobically modified starch using long-chain fatty acids for preparation of nanosized starch

particles. *Scientia Iranica*, *18*(3), 439–445.
Naseem, A., Tabasum, S., Zia, K. M., Zuber, M., Ali, M., and Noreen, A. (2016). Lignin-derivatives based polymers, blends and composites: A review. *International Journal of Biological Macromolecules*, *93*, 296–313.
Ni, Y., and Hu, Q. (1995). Alcell lignin solubility in ethanol-water mixtures. *Journal of Applied Polymer Science*, *57*(12), 1441–1446.
Nicolet, T. (2001). *Introduction to Fourier Transform Infrared Spectrometry*. United States of America: Thermo Nicolet Corporation.
Nieuwoudt, H. H., Prior, B. A., Pretorius, I. S., Manley, M., and Bauer, F. F. (2004). Principal component analysis applied to Fourier transform infrared spectroscopy for the design of calibration sets for glycerol prediction models in wine and for the detection and classification of outlier samples. *Journal of Agricultural and Food Chemistry*, *52*(12), 3726–3735.
Nishikida, K., Nishio, E., and Hannah, R. W. (1995). Features and Operation Techniques of the Infrared Accessories. In *Selected Applications of Modern FT-IR Techniques* (pp. 19–56). Tokyo: Gordon and Breach Publishers.
Nitsos, C., Stoklosa, R., Karnaouri, A., Voros, D., Lange, H., Hodge, D., … Christakopoulos, P. (2016). Isolation and characterisation of organosolv and alkaline lignins from hardwood and softwood biomass. *ACS Sustainable Chemistry and Engineering*, *4*(10), 5181–5193.
Nobbmann, U., and Morfesis, A. (2009). Light scattering and nanoparticles. *Materials Today*, *12*(5), 52–54.
Norgren, M., and Edlund, H. (2014). Lignin: Recent advances and emerging applications. *Current Opinion in Colloid & Interface Science*, *19*(5), 409–416.
Norgren, M., Edlund, H., and Wågberg, L. (2002). Aggregation of lignin derivatives under alkaline conditions. Kinetics and aggregate structure. *Langmuir*, *18*(7), 2859–2865.
North, A. J. (2006). Seeing is believing? A beginners' guide to practical pitfalls in image acquisition. *Journal of Cell Biology*, *172*(1), 9–18.
Núñez-Flores, R., Giménez, B., Fernández-Martín, F., López-Caballero, M. E., Montero, M. P., and Gómez-Guillén, M. C. (2013). Physical and functional characterisation of active fish gelatin films incorporated with lignin. *Food Hydrocolloids*, *30*(1), 163–172.
Olson, E. (2011). Particle shape factors and their use in image analysis-part 1: Theory. *Journal of GXP Compliance*, *15*(3), 85–96.
Ortega, J. H. (2015). *Process design of lignocellulosic biomass fractionation into cellulose, hemicellulose and lignin by prehydrolysis and organosolv process*. M.Sc. Thesis. Wageningen University.
Palma, M., Piñeiro, Z., and Barroso, C. G. (2002). In-line pressurised-fluid extraction–solid-phase extraction for determining phenolic compounds in grapes. *Journal of Chromatography A*, *968*(1), 1–6.
Palonen, H., Thomsen, A. B., Tenkanen, M., Schmidt, A. S., and Viikari, L. (2004). Evaluation of wet oxidation pretreatment for enzymatic hydrolysis of softwood. *Applied Biochemistry and Biotechnology*, *117*(1), 1–17.
Pan, Y., Birdsey, R. a., Phillips, O. L., and Jackson, R. B. (2013). The structure, distribution, and biomass of the world's forests. *Annual Review of Ecology, Evolution, and Systematics*, *44*(1), 593–622.

Panda, H. (2016). Lignin and Hemicellulose. In *Handbook on Coal , Lignin , Wood and Rosin Processing* (pp. 166–207). Delhi, India: NIIR Project Consultancy Services.

Pandey, A., Bhaskar, T., Stöcker, M. (Chemist), and Sukumaran, R. (2015). *Recent Advances in Thermochemical Conversion of Biomass*. (M. S. and R. K. S. shok Pandey, Thallada Bhaskar, Ed.). Boston: Elsevier.

Pandey, K. K. (1999). A study of chemical structure of soft and harwood and wood polymers by FTIR spectrscopy. *Journal of Applied Polymer Science*, *71*(12), 1969–1975.

Pandey, M. P., and Kim, C. S. (2011). Lignin depolymerisation and conversion: A review of thermochemical methods. *Chemical Engineering and Technology*, *34*(1), 29–41.

Parikka, M. (2004). Global biomass fuel resources. *Biomass and Bioenergy*, *27*(6), 613–620.

Particle Sciences. (2009). *Considerations in Particle Sizing. Part 1: Classification of the Various Sizing Techniques*. *Particle Sciences* (Vol. 6). Pennsylvania, USA.

Pasquini, D., Pimenta, M. T. B., Ferreira, L. H., and Curvelo, A. A. da S. (2005). Extraction of lignin from sugar cane bagasse and Pinus taeda wood chips using ethanol–water mixtures and carbon dioxide at high pressures. *The Journal of Supercritical Fluids*, *36*(1), 31–39.

Passauer, L., Salzwedel, K., Struch, M., Herold, N., and Appelt, J. (2016). Quantitative analysis of the etherification degree of phenolic hydroxyl groups in oxyethylated lignins: Correlation of selective aminolysis with FTIR spectroscopy. *ACS Sustainable Chemistry and Engineering*, *4*(12), 6629–6637.

Pathan, A. K., Bond, J., and Gaskin, R. E. (2010). Sample preparation for SEM of plant surfaces. *Materials Today*, *12*, 32–43.

Pauly, M., Gille, S., Liu, L., Mansoori, N., de Souza, A., Schultink, A., and Xiong, G. (2013). Hemicellulose biosynthesis. *Planta*, *238*(4), 627–642.

Pawar, S. N., Venditti, R. A., Jameel, H., Chang, H.-M., and Ayoub, A. (2016). Engineering physical and chemical properties of softwood kraft lignin by fatty acid substitution. *Industrial Crops and Products*, *89*, 128–134.

Peng, F., Peng, P., Xu, F., and Sun, R.-C. (2012). Fractional purification and bioconversion of hemicelluloses. *Biotechnology Advances*, *30*(4), 879–903.

Peterson, A. A., Vogel, F., Lachance, R. P., Fröling, M., Antal, Jr., M. J., and Tester, J. W. (2008). Thermochemical biofuel production in hydrothermal media: A review of sub- and supercritical water technologies. *Energy and Environmental Science*, *1*(1), 32.

Pielhop, T., Larrazábal, G. O., Studer, M. H., Brethauer, S., Seidel, C.-M., and Rudolf von Rohr, P. (2015). Lignin repolymerisation in spruce autohydrolysis pretreatment increases cellulase deactivation. *Green Chem.*, *17*(6), 3521–3532.

Piñeiro, Z., Palma, M., and Barroso, C. G. (2004). Determination of catechins by means of extraction with pressurized liquids. *Journal of Chromatography A*, *1026*(1), 19–23.

Ping, L., Brosse, N., Sannigrahi, P., and Ragauskas, A. (2011). Evaluation of grape stalks as a bioresource. *Industrial Crops and Products*, *33*(1), 200–204.

Pinto, P. C. R., and Borges, E. A. (2011). Insights into oxidative conversion of lignin to high-added-value phenolic aldehydes. *Industrial and Engineering Chemistry Research*, *50*(2), 741–748.

Plaza, M., and Turner, C. (2015). Pressurised hot water extraction of bioactives. *TrAC Trends in Analytical Chemistry*, *71*, 39–54.

Popp, J., Lakner, Z., Harangi-Rákos, M., and Fári, M. (2014). The effect of bioenergy expansion: Food, energy, and environment. *Renewable and Sustainable Energy Reviews*, *32*, 559–578.

Potumarthi, R., Mekala, N. K., Baadhe, R. R., and Gupta, V. K. (2014). Current bioenergy researches: strengths and future challenges. In V. K. Gupta, M. G. Tuohy, C. P. Kubicek, J. Saddler, and F. Xu (Eds.), *Bioenergy research: advances and applications* (pp. 1–18). United Kingdom: Elsevier B.V.

Pu, Y., Hu, F., Huang, F., Davison, B. H., and Ragauskas, A. J. (2013). Assessing the molecular structure basis for biomass recalcitrance during dilute acid and hydrothermal pretreatments. *Biotechnology for Biofuels*, *6*(15), 1–13.

Pyter, R., Voigt, T., Heaton, E., Dohleman, F., and Long, S. (2007). Giant Miscanthus : Biomass Crop for Illinois. In J. J. and W. A. (Eds.), *Issues in New Crops and New Uses* (pp. 39–42). Alexandria, VA: ASHS Press.

Qian, Y., Deng, Y., Qiu, X., Li, H., and Yang, D. (2014). Formation of uniform colloidal spheres from lignin, a renewable resource recovered from pulping spent liquor. *Green Chemistry*, *16*(4), 2156.

Qiao, W., Li, S., Guo, G., Han, S., Ren, S., and Ma, Y. (2014). Synthesis and characterisation of phenol-formaldehyde resin using enzymatic hydrolysis lignin. *Journal of Industrial and Engineering Chemistry*, *21*, 1417–1422.

Radotić, K., Micić, M., and Milorad, J. (2005). New insights into the structural organisation of the plant polymer lignin. *Annals of the New York Academy of Sciences*, *104*(1), 215–229.

Radotić, K., Micić, M., and Milorad, J. (2006). Scanning Probe Microscopy of Plant Cell Wall and its Constituents. In B. P. Jena and H. J. K. Horber (Eds.), *Force Microscopy: Applications in Biology and Medicine* (p. 303). United States of America: John and Wiley Sons, Inc.

Radotić, K., Roduit, C., Simonović, J., Hornitschek, P., Fankhauser, C., Mutavdžić, D., … Kasas, S. (2012). Atomic force microscopy stiffness tomography on living arabidopsis thaliana cells reveals the mechanical properties of surface and deep cell-wall layers during growth. *Biophysical Journal*, *103*(3), 386–394.

Rao, X., Liu, Y., Zhang, Q., Chen, W., Liu, Y., and Yu, H. (2017). Assembly of Organosolv Lignin Residues into Submicron Spheres: The Effects of Granulating in Ethanol/Water Mixtures and Homogenisation. *ACS Omega*, *2*(6), 2858–2865.

Ratnaweera, D. R., Saha, D., Pingali, S. V., Labbé, N., Naskar, A. K., and Dadmun, M. (2015). The impact of lignin source on its self-assembly in solution. *RSC Advances*, *5*(82), 67258–67266.

Reid, I. D., and Paice, M. G. (1994). Effect of residual lignin type and amount on bleaching of kraft pulp by Trametes versicolor. *Applied and Environmental Microbiology*, *60*(5), 1395–1400.

Rencoret, J., Gutiérrez, A., Nieto, L., Jiménez-Barbero, J., Faulds, C. B., Kim, H., … Del Río, J. C. (2011). Lignin composition and structure in young

versus adult Eucalyptus globulus plants. *Plant Physiology*, *155*(2), 667–82.

Rinaldi, R., Jastrzebski, R., Clough, M. T., Ralph, J., Kennema, M., Bruijnincx, P. C. A., and Weckhuysen, B. M. (2016). Paving the way for lignin valorisation: Recent advances in bioengineering, biorefining and catalysis. *Angewandte Chemie International Edition*, *55*(29), 8164–8215.

Rodriguez-Saona, L. E., and Allendorf, M. E. (2011). Use of FTIR for rapid authentication and detection of adulteration of food. *Annual Review of Food Science and Technology*, *2*(1), 467–483.

Rogalinski, T., Liu, K., Albrecht, T., and Brunner, G. (2008). Hydrolysis kinetics of biopolymers in subcritical water. *Journal of Supercritical Fluids*, *46*(3), 335–341.

Roque, R. M. N. (2013). *Hydrolysis of lignocellulosic biomass by a modified organosolv Method on a biorefinery perspective - example of Miscanthus x giganteus*. PhD Thesis. University of Birmingham.

Roque, R. M. N., Baig, M. N., Leeke, G. A., Bowra, S., and Santos, R. C. D. (2012). Study on sub-critical water mediated hydrolysis of Miscanthus a lignocellulosic biomass. *Resources, Conservation and Recycling*, *59*, 43–46.

Rubin, E. M., Himmel, M. E., Ding, S., Johnson, D. K., and Adney, W. S. (2007). Biomass recalcitrance : Engineering plants and enzymes for biofuels production. *Nature*, *315*, 804–807.

Ruiz, H. A., Rodríguez-Jasso, R. M., Fernandes, B. D., Vicente, A. A., and Teixeira, J. A. (2013). Hydrothermal processing, as an alternative for upgrading agriculture residues and marine biomass according to the biorefinery concept: A review. *Renewable and Sustainable Energy Reviews*, *21*, 35–51.

Sadeghifar, H., Cui, C., and Argyropoulos, D. S. (2012). Toward thermoplastic lignin polymers. Part 1. Selective masking of phenolic hydroxyl groups in kraft lignins via methylation and oxypropylation chemistries. *Industrial and Engineering Chemistry Research*, *51*(51), 16713–16720.

Saha, B. C. (2003). Hemicellulose bioconversion. *Journal of Industrial Microbiology and Biotechnology*, *30*(5), 279–291.

Sahoo, S., Misra, M., and Mohanty, A. K. (2013). Effect of compatibiliser and fillers on the properties of injection molded lignin-based hybrid green composites. *Journal of Applied Polymer Science*, *127*(5), 4110–4121.

Salleh, L. M., Rahman, R. A., Selamat, J., Hamid, A., and Sarker, M. Z. I. (2013). Optimisation of extraction condition for supercritical carbon dioxide ($SCCO_2$) extraction of *Strobhilantes crispus* (Pecah Kaca) leaves by response surface methodology. *Journal of Food Processing and Technology*, *4*(1), 1–6.

Sannigrahi, P., Kim, D. H., Jung, S., and Ragauskas, A. (2011). Pseudo-lignin and pretreatment chemistry. *Energy & Environmental Science*, *4*(4), 1306.

Sannigrahi, P., and Ragauskas, A. J. (2013). Fundamentals of Biomass Pretreatment by Fractionation. In C. V. Stevens (Ed.), *Aqueous Pretreatment of Plant Biomass for Biological and Chemical Conversion to Fuels and Chemicals* (pp. 201–222). Chichester, UK: John and Wiley Sons, Inc.

Saralegi, A., Rueda, L., Fernández-D'Arlas, B., Mondragon, I., Eceiza, A., and

Corcuera, M. A. (2013). Thermoplastic polyurethanes from renewable resources: Effect of soft segment chemical structure and molecular weight on morphology and final properties. *Polymer International*, *62*(1), 106–115.
Sasaki, K., Okamoto, M., Shirai, T., Tsuge, Y., Teramura, H., Sasaki, D., … Kondo, A. (2015). Precipitate obtained following membrane separation of hydrothermally pretreated rice straw liquid revealed by 2D NMR to have high lignin content. *Biotechnology for Biofuels*, *8*(1), 88.
Savy, D., Mazzei, P., Roque, R., Nuzzo, A., Bowra, S., and Santos, R. (2015). Structural recognition of lignin isolated from bioenergy crops by subcritical water: ethanol extraction. *Fuel Processing Technology*, *138*, 637–644.
Savy, D., and Piccolo, A. (2014). Physical–chemical characteristics of lignins separated from biomasses for second-generation ethanol. *Biomass and Bioenergy*, *62*, 58–67.
Sayyar, S., Abidin, Z. Z., Yunus, R., and Muhammad, A. (2009). Extraction of oil from Jatropha seeds-optimisation and kinetics. *American Journal of Applied Sciences*, *6*(7), 1390–1395.
Scheller, H. V., and Ulvskov, P. (2010). Hemicelluloses. *Annual Review of Plant Biology*, *61*(1), 263–289.
Schou, A., Jager, D. de, Maniatis, K., and Kwant, K. (2010). *Better Use of Biomass for Energy*. *IEA RETD and IEA Bioenergy*. Germany.
Schuerch, C. (1952). The solvent properties of liquids and their relation to the solubility, swelling, isolation and fractionation of lignin. *Journal of the American Chemical Society*, *74*(20), 5061–5067.
Scurlock, J. M. O. (1999). *A review of European experience with a novel energy crop* (Vol. ORNL/TM-13). Oak Ridge, TN, USA.
Selig, M. J., Viamajala, S., Decker, S. R., Tucker, M. P., Himmel, M. E., and Vinzant, T. B. (2007). Deposition of lignin droplets produced during dilute acid pretreatment of maize stems retards enzymatic hydrolysis of cellulose. *Biotechnology Progress*, *23*(6), 1333–1339.
Shulga, G., and Vitolina, S. (2012). Lignin separated from the hydrolysate of the hydrothermal treatment of birch wood and its surface properties. *Cellulose Chemistry and Technology*, *46*, 307–318.
Sim, S., Mohamed, M., and Lu, N. (2012). Analysis of Fourier Transform Infrared (FTIR) spectra for characterisation of various treated and untreated agriculture. *BioResources*, *7*, 5367–5380.
Sims, R., Taylor, M., Saddler, J., and Mabee, W. (2008). *From 1st to 2nd Generation Bio Fuel Technologies: An overview of current industry and RD&D activities*. Paris, France.
Sindhu, R., and Pandey, A. (2016). Biological pretreatment of lignocellulosic biomass – An overview. *Bioresource Technology*, *199*, 76–82.
Sivasankarapillai, G., and McDonald, A. G. (2011). Synthesis and properties of lignin-highly branched poly (ester-amine) polymeric systems. *Biomass and Bioenergy*, *35*(2), 919–931.
Sixta, H. (2006). Part I Chemical Pulping. In H. Sixta (Ed.), *Handbook of Pulp* (pp. 1–20). Weinheim, Germany: WILEY-VCH Verlag GmbH &Co. KGaA.
Slade, R., Saunders, R., Gross, R., and Bauen, A. (2011). *Energy from biomass : the size of the global resource*. London.
Sluiter, A., Hames, B., Ruiz, R., Scarlata, C., Sluiter, J., Templeton, D., and

Crocker, D. (2012). *Determination of Structural Carbohydrates and Lignin in Biomass*. *Laboratory Analytical Procedure (LAP)*. Colorado.
Sluiter, A., Ruiz, R., Scarlata, C., Sluiter, J., Templeton, D., Sluiter, A., … Templeton, D. (2008). *Determination of Extractives in Biomass Laboratory Analytical Procedure*. Colorado.
Smith, R. M. (2006). Superheated water: The ultimate green solvent for separation science. *Analytical and Bioanalytical Chemistry*, *385*(3), 419–421.
Smolarski, N. (2012). *High-Value Opportunities for Lignin : Unlocking its Potential Lignin potential*. Paris.
Snowden, M. J., Gracra, L. H., and Nur, H. (2008). Heteroflocculation Studies of Colloidal Poly(N-isopropylacrylamide) Microgels with Polystryrene Latex Particles: Effect of Particle Size, Temperature and Surface Charge. In S. Biggs, T. Cosgrove, and P. Dowding (Eds.), *New Frontiers in Colloid Science: A Celebration of the Career of Brian Vincent* (pp. 149–164). RSC Publishing.
Snowdon, M. R., Mohanty, A. K., and Misra, M. (2014). A study of carbonised lignin as an alternative to carbon black. *ACS Sustainable Chemistry and Engineering*, *2*(5), 1257–1263.
Stewart, H. E. (2015). *Development of food-grade microparticles from lignin*. PhD Thesis. Massey University, New Zealand.
Sticklen, M. B. (2008). Plant genetic engineering for biofuel production: Towards affordable cellulosic ethanol. *Nature Reviews Genetics*, *9*(6), 433–443.
Stuart, B. (2004). *Infrared spectroscopy: Fundamentals and applications*. *Journal of Chemical Information and Modeling* (Vol. 53). United Kingdom: John and Wiley Sons, Inc.
Suhas, Gupta, V. K., Carrott, P. J. M., Singh, R., Chaudhary, M., and Kushwaha, S. (2016). Cellulose: A review as natural, modified and activated carbon adsorbent. *Bioresource Technology*, *216*, 1066–1076.
Sun, J., Dutta, T., Parthasarathi, R., Kim, K. H., Tolic, N., Chu, R. K., … Singh, S. (2016). Rapid room temperature solubilization and depolymerisation of polymeric lignin at high loadings. *Green Chem.*, *18*(22), 6012–6020.
Sun, Y., and Cheng, J. (2002). Hydrolysis of lignocellulosic materials for ethanol production: a review. *Bioresource Technology*, *83*(1), 1–11.
Šurina, I., Jablonskỳ, M., Ház, A., Sladková, A., Briškárová, A., Kačík, F., and Šima, J. (2015). Characterisation of non-wood lignin precipitated with sulphuric acid of various concentrations. *BioResources*, *10*(1), 1408–1423.
Swain, P. K., Das, L. M., and Naik, S. N. (2011). Biomass to liquid: A prospective challenge to research and development in 21st century. *Renewable and Sustainable Energy Reviews*, *15*(9), 4917–4933.
Szczepkowski, A., Nicewicz, D., and Koczon, P. (2007). The relationship between tree health and chemical composition of beech (*Fagus sylvatica* L.) and oak (*Quercus robur* L.) wood of polish provenances. *Acta Scientiarum Polonorum - Silvarum Colendarum Ratio et Industria Lignaria*, *6*(3), 77–88.
Taherzadeh, M. J., and Karimi, K. (2008). Pretreatment of lignocellulosic wastes to improve ethanol and biogas production: A review. *International*

Journal of Molecular Sciences, *9*(9), 1621–1651.
Tarabanko, V. E., and Petukhov, D. V. (2003). Study of mechanism and improvement of the process of oxidative cleavage of lignins into the aromatic aldehydes. *Chemistry for Sustainable Development*, *11*, 655–667.
Tejado, A., Peña, C., Labidi, J., Echeverria, J. M., and Mondragon, I. (2007). Physico-chemical characterisation of lignins from different sources for use in phenol-formaldehyde resin synthesis. *Bioresource Technology*, *98*(8), 1655–63.
Thakur, V. K., Thakur, M. K., Raghavan, P., and Kessler, M. R. (2014). Progress in green polymer composites from lignin for multifunctional applications: A review. *ACS Sustainable Chemistry and Engineering*, *2*(5), 1072–1092.
Thielemans, W., and Wool, R. P. (2005). Lignin esters for use in unsaturated thermosets: lignin modification and solubility modeling. *Biomacromolecules*, *6*(4), 1895–905.
Thompson, W., and Meyer, S. (2013). Second generation biofuels and food crops: Co-products or competitors? *Global Food Security*, *2*(2), 89–96.
Thring, R. W., Vanderlaan, M. N., and Griffin, S. L. (1997). Polyurethanes from Alcell® lignin. *Biomass and Bioenergy*, *13*(3), 125–132.
Tiainen, E., Drakenberg, T., Tamminen, T., Kataja, K., and Hase, A. (1999). Determination of phenolic hydroxyl groups in lignin by combined use of H-1 NMR and UV spectroscopy. *Holzforschung*, *53*(5), 529–533.
Tian, D., Hu, J., Bao, J., Chandra, R. P., Saddler, J. N., and Lu, C. (2017). Lignin valorisation: lignin nanoparticles as high-value bio-additive for multifunctional nanocomposites. *Biotechnology for Biofuels*, *10*(1), 192.
Timilsena, Y. P., Audu, I. G., Rakshit, S. K., and Brosse, N. (2013). Impact of the lignin structure of three lignocellulosic feedstocks on their organosolv delignification. Effect of carbonium ion scavengers. *Biomass and Bioenergy*, *52*, 151–158.
Tong, Z., Cheng, N., and Pullammanappallil, P. (2013). *Pretreatment of Ligno-cellulosic Biomass for Biofuels and Bioproducts*. Gainesville, Florida: Department of Agricultural and Biological Engineering, Florida Cooperative Extension Service, Institute of Food and Agricultural Sciences, University of Florida.
Toor, S. S., Rosendahl, L., and Rudolf, A. (2011). Hydrothermal liquefaction of biomass: A review of subcritical water technologies. *Energy*, *36*(5), 2328–2342.
Trenerry, V. C., and Rochfort, S. J. (2010). Natural Products Research and Metabolomics. *Comprehensive Natural Products II, Modern Methods in Natural Products Chemistry*, *9*, 595–628.
Tu, Q., Fu, S., Zhan, H., Chai, X., and Lucia, L. A. (2008). Kinetic modeling of formic acid pulping of bagasse. *Journal of Agricultural and Food Chemistry*, *56*(9), 3097–3101.
Tumuluru, J. S., Wright, C. T., Hess, J. R., and Kenney, K. L. (2011). A review of biomass densification systems to develop uniform feedstock commodities for bioenergy application. *Biofuels, Bioproducts and Biorefining*, *5*, 683–707.
Ummartyotin, S., and Manuspiya, H. (2015). A critical review on cellulose: From fundamental to an approach on sensor technology. *Renewable and*

Sustainable Energy Reviews, *41*, 402–412.
Upton, B. M., and Kasko, A. M. (2015). Strategies for the conversion of lignin to high-value polymeric materials: Review and perspective. *Chemical Reviews*, *116*, 2275–2306.
Vallejos, M. E., Felissia, F. E., Curvelo, A. A. S., Zambon, M. D., Ramos, L., and Area, M. C. (2011). Chemical and physico-chemical characterisation of lignins obtained from ethanol-water fractionation of bagasse. *BioResources*, *6*(2), 1158–1171.
van Dam, J., Faaij, A. P. C., Lewandowski, I., and Fischer, G. (2007). Biomass production potentials in Central and Eastern Europe under different scenarios. *Biomass and Bioenergy*, *31*(6), 345–366.
Van Walsum, G. P. (2001). Severity function describing the hydrolysis of xylan using carbonic acid. *Applied Biochemistry and Biotechnology*, *91–93*, 317–329.
Van Walsum, G. P., Garcia-Gil, M., Chen, S. F., and Chambliss, K. (2007). Effect of dissolved carbon dioxide on accumulation of organic acids in liquid hot water pretreated biomass hydrolyzates. *Applied Biochemistry and Biotechnology*, *137–140*(1–12), 301–311.
Vanholme, R., Demedts, B., Morreel, K., Ralph, J., and Boerjan, W. (2010). Lignin biosynthesis and structure. *Plant Physiology*, *153*(3), 895–905.
Vaux, D. L. (2012). Know when your numbers are significant. *Nature*, *492*, 180–181.
Vippola, M., Valkonen, M., Sarlin, E., Honkanen, M., and Huttunen, H. (2016). Insight to nanoparticle size analysis—Novel and convenient image analysis method versus conventional techniques. *Nanoscale Research Letters*, *11*(169), 1–9.
Vishtal, A., and Kraslawski, A. (2011). Challenges in industrial applications of technical lignins. *BioResources*, *6*(3), 3547–3568.
Wahid, R., Nielsen, S. F., Hernandez, V. M., Ward, A. J., Gislum, R., Jørgensen, U., and Møller, H. B. (2015). Methane production potential from Miscanthus sp.: Effect of harvesting time, genotypes and plant fractions. *Biosystems Engineering*, *133*, 71–80.
Walter, A., Dolzan, P., and Piacente, E. (2006). Biomass energy and bio-energy trade: historic developments in Brazil and current opportunities. *Country Report: Brazil–Task*, (October 2016), 40.
Wang, C., Guo, L., Li, Y., and Wang, Z. (2012). Systematic comparison of C3 and C4 plants based on metabolic network analysis. *BMC Systems Biology*, *6*(S9), 1–14.
Wang, C., Kelley, S. S., and Venditti, R. A. (2016). Lignin-based thermoplastic materials. *ChemSusChem*, *9*(8), 770–783.
Wang, D., Naidu, S. L., Portis, A. R., Moose, S. P., and Long, S. P. (2008). Can the cold tolerance of C4 photosynthesis in *Miscanthus* x *giganteus* relative to Zea mays be explained by differences in activities and thermal properties of Rubisco? *Journal of Experimental Botany*, *59*(7), 1779–1787.
Wang, H., Chen, W., Zhang, X., Liu, C., and Sun, R. (2017). Esterification Mechanism of Bagasse Modified with Glutaric Anhydride in 1-Allyl-3-methylimidazolium Chloride. *Materials*, *10*(8), 966.
Wang, H., Tucker, M., and Ji, Y. (2013). Recent development in chemical depolymerisation of lignin: A review. *Journal of Applied Chemistry*, *2013*,

1–9.
Wang, Q., Chen, K., Li, J., Yang, G., Liu, S., and Xu, J. (2011). The solubility of lignin from bagasse in a 1,4-butanediol/water system. *Bioresources*, *6*(3), 3034–3043.
Wang, W., Zhuang, X., Yuan, Z., Qi, W., Yu, Q., and Wang, Q. (2016). Structural changes of lignin after liquid hot water pretreatment and its effect on the enzymatic hydrolysis. *BioMed Research International*, *2016*, 1–8.
Wang, Z.-W., Zhu, M.-Q., Li, M.-F., Wang, J.-Q., Wei, Q., Sun, R.-C., … Tschaplinski, T. (2016). Comprehensive evaluation of the liquid fraction during the hydrothermal treatment of rapeseed straw. *Biotechnology for Biofuels*, *9*(142), 1–16.
Watkins, D., Nuruddin, M., Hosur, M., Tcherbi-Narteh, A., and Jeelani, S. (2015). Extraction and characterisation of lignin from different biomass resources. *Journal of Materials Research and Technology*, *4*(1), 26–32.
Wild, P. J. de, Huijgen, W. J. J., Linden, R. van der, Uil, H. den, Snelders, J., and Benjelloun-Mlayah, B. (2015). *Organosolv fractionation of lignocellulosic biomass for an integrated biorefinery*. Netherlands.
Willen, U. (2008). Automation in image analysis for particle size and shape measurement. *G.I.T. Laboratory Journal*, *7*(8), 34–36.
Wilt, B. A., Burns, L. D., Wei Ho, E. T., Ghosh, K. K., Mukamel, E. A., & Schnitzer, M. J. (2009). Advances in light microscopy for neuroscience. *Annual Review of Neuroscience*, *32*(1), 435–506.
World Bioenergy Association. (2016). *Global Biomass Potential Towards 2035*. Stockholm, Sweden.
World Energy Balances 2009. (2009). Paris.
Wu, M., Zhao, D., Pang, J., Zhang, X., Li, M., Xu, F., and Sun, R. (2015). Separation and characterisation of lignin obtained by catalytic hydrothermal pretreatment of cotton stalk. *Industrial Crops and Products*, *66*, 123–130.
Xi, Q., and Jezowski, S. (2004). Plant resources of Triarrhena and Miscanthus species in china and its meanning for Europe. *Plant Breeding and Seed Science*, *49*, 63–75.
Xiao, L.-P., Sun, Z.-J., Shi, Z.-J., Xu, F., and Sun, R. (2011). Impact of hot compressed water pretreatment on the structural changes of woody biomass for bioethanol production. *BioResources*, *6*(2), 1576–1598.
Xiong, F., Han, Y., Wang, S., Li, G., Qin, T., Chen, Y., and Chu, F. (2017). Preparation and formation mechanism of size-controlled lignin nanospheres by self-assembly. *Industrial Crops and Products*, *100*, 146–152.
Xu, C., Arneil, R., Arancon, D., Labidi, J., and Luque, R. (2014). Lignin depolymerisation strategies: towards valuable chemicals and fuels. *Chem. Soc. Rev. Chem. Soc. Rev*, *43*(43), 7485–7500.
Xu, F., Yu, J., Tesso, T., Dowell, F., and Wang, D. (2013). Qualitative and quantitative analysis of lignocellulosic biomass using infrared techniques: A mini-review. *Applied Energy*, *104*, 801–809.
Xu, W., Miller, S. J., Agrawal, P. K., and Jones, C. W. (2012). Depolymerisation and hydrodeoxygenation of switchgrass lignin with formic acid. *ChemSusChem*, *5*(4), 667–675.
Xu, Y., Li, K., and Zhang, M. (2007). Lignin precipitation on the pulp fibers in

the ethanol-based organosolv pulping. *Colloids and Surfaces A: Physicochemical and Engineering Aspects*, *301*(1–3), 255–263.
Yang, D., Qiu, X., Pang, Y., and Zhou, M. (2008). Physicochemical properties of calcium lignosulfonate with different molecular weights as dispersant in aqueous suspension. *Journal of Dispersion Science and Technology*, *29*(9), 1296–1303.
Yasarla, L. R., and Ramarao, B. V. (2013). Lignin removal from lignocellulosic hydrolysates by flocculation with polyethylene oxide. *Journal of Biobased Materials and Bioenergy*, *7*(6), 684–689.
Ye, Y., Zhang, Y., Fan, J., and Chang, J. (2012). Novel method for production of phenolics by combining lignin extraction with lignin depolymerisation in aqueous ethanol. *Industrial and Engineering Chemistry Research*, *51*(1), 103–110.
Yedro, F. M., García-Serna, J., Cantero, D. A., Sobrón, F., and Cocero, M. J. (2014). Hydrothermal fractionation of grape seeds in subcritical water to produce oil extract, sugars and lignin. *Catalysis Today*, *257*(2), 160–168.
Yesodharan, S. (2002). Supercritical water oxidation: An environmentally safe method for the disposal of organic wastes. *Current Science*, *82*(9), 1112–1122.
Yokoo, T., and Miyafuji, H. (2014). Reaction behavior of wood in an ionic liquid, 1-ethylpyridinium bromide. *Journal of Wood Science*, *60*(5), 339–345.
Yokoyama, S., and Matsumura, Y. (2008). *The Asian Biomass Handbook: A Guide for Biomass Production and Utilization*. Japan: The Japan Institute of Energy.
Yonter, G. (2015). A study on the effects of the aggregate size on erosion by runoff and splash under simulated rainfall conditions. *Ekoloji Dergisi*, *24*(97), 45–53.
Yuan, T.-Q., Xu, F., and Sun, R.-C. (2013). Role of lignin in a biorefinery: separation characterisation and valorisation. *Journal of Chemical Technology & Biotechnology*, *88*(3), 346–352.
Yuan, Z., Cheng, S., Leitch, M., and Xu, C. C. (2010). Hydrolytic degradation of alkaline lignin in hot-compressed water and ethanol. *Bioresource Technology*, *101*(23), 9308–13.
Zaiqun, Y. (2007). *Particle engineering in anti-solvent crystallisation*. PhD Thesis. National University of Singapore.
Zakaria, S. M., and Kamal, S. M. M. (2016). Subcritical water extraction of bioactive compounds from plants and algae: Applications in pharmaceutical and food ingredients. *Food Engineering Reviews*, *8*(1), 23–34.
Zhao, L., Grius, B. F., Chen, C., Gratzl, J. S., and Yun, H. (1994). Utilisation of softwood kraft lignin as adhesive for the manufacture of reconstituted wood. *Journal of Wood Chemistry and Technology*, *14*(1), 127–145.
Zhao, X., Cheng, K., and Liu, D. (2009). Organosolv pretreatment of lignocellulosic biomass for enzymatic hydrolysis. *Applied Microbiology and Biotechnology*, *82*(5), 815–827.
Zheng, Y., Lin, H. M., and Tsao, G. T. (1998). Pretreatment for cellulose hydrolysis by carbon dioxide explosion. *Biotechnology Progress*, *14*(6), 890–896.
Zheng, Y., Zhao, J., Xu, F., and Li, Y. (2014). Pretreatment of lignocellulosic

biomass for enhanced biogas production. *Progress in Energy and Combustion Science*, *42*, 35–53.
Zhu, W. (2013). *Equilibrium of lignin precipitation*. Degree of Licentiate of Engineering. Chalmers University of Technology, Sweden.
Zobel, B. J., and Buijtenen, J. P. van. (1989). *Wood Variation Its Causes and Control* (1st ed.). Berlin, Heidelberg: Springer.

APPENDICES

Appendix A

Table A1. Analysis of variance of SE and DE.

ANOVA

		Sum of Squares	df	Mean Square	F	Sig.
Purity of lignin derived supernatant	Between Groups	138.817	1	138.817	107.581	.000
	Within Groups	5.161	4	1.290		
	Total	143.978	5			
Purity of precipitated lignin	Between Groups	14.045	1	14.045	264.508	.000
	Within Groups	.212	4	.053		
	Total	14.258	5			
Percentage of delignification	Between Groups	827.905	1	827.905	3741.662	.000
	Within Groups	.885	4	.221		
	Total	828.790	5			
Percentage of lignin recovery	Between Groups	1.540	1	1.540	.956	.383
	Within Groups	6.442	4	1.610		
	Total	7.982	5			
Percentage of biomass solubilisation	Between Groups	142.984	1	142.984	229.669	.000
	Within Groups	2.490	4	.623		
	Total	145.474	5			

Appendix B

Table B1. Analysis of variance for an assessment of ethanol concentrations.

ANOVA

		Sum of Squares	df	Mean Square	F	Sig.
Percentage of purity precipitated lignin	Between Groups	4.527	2	2.263	21.504	.007
	Within Groups	.421	4	.105		
	Total	4.948	6			
Percentage of purity dried supernatant	Between Groups	975.795	2	487.897	387.032	.000
	Within Groups	5.042	4	1.261		
	Total	980.837	6			
Percentage of lignin recovery	Between Groups	4741.364	2	2370.682	505.553	.000
	Within Groups	28.136	6	4.689		
	Total	4769.500	8			

Table B2. Analysis of post hoc tests for an assessment of ethanol concentrations

Multiple Comparisons

Dependent Variable		(I) percentage of ethanol concentration	(J) percentage of ethanol concentration	Mean Difference (I-J)	Std. Error	Sig.	95% Confidence Interval Lower Bound	95% Confidence Interval Upper Bound
Percentage of purity precipitated lignin	Tukey HSD	50% ethanol concentration	25% ethanol concentration	.16000	.29616	.857	-.8955	1.2155
			10% ethanol concentration	1.87000	.32442	.010	.7138	3.0262
		25% ethanol concentration	50% ethanol concentration	-.16000	.29616	.857	-1.2155	.8955
			10% ethanol concentration	1.71000	.29616	.010	.6545	2.7655
		10% ethanol concentration	50% ethanol concentration	-1.87000	.32442	.010	-3.0262	-.7138
			25% ethanol concentration	-1.71000	.29616	.010	-2.7655	-.6545
	Bonferroni	50% ethanol concentration	25% ethanol concentration	.16000	.29616	1.000	-1.0130	1.3330
			10% ethanol concentration	1.87000	.32442	.013	.5850	3.1550
		25% ethanol concentration	50% ethanol concentration	-.16000	.29616	1.000	-1.3330	1.0130
			10% ethanol concentration	1.71000	.29616	.013	.5370	2.8830

		10% ethanol concentration	50% ethanol concentration	-1.87000	.32442	.013	-3.1550	-.5850
			25% ethanol concentration	-1.71000	.29616	.013	-2.8830	-.5370
Percentage of purity dried supernatant	Tukey HSD	50% ethanol concentration	25% ethanol concentration	-1.71000	.29616	.013	-2.8830	-.5370
			10% ethanol concentration	26.83500	1.12277	.000	22.8335	30.8365
		25% ethanol concentration	50% ethanol concentration	-25.63000	1.02494	.000	-29.2829	-21.9771
			10% ethanol concentration	1.20500	1.02494	.525	-2.4479	4.8579
		10% ethanol concentration	50% ethanol concentration	-26.83500	1.12277	.000	-30.8365	-22.8335
			25% ethanol concentration	-1.20500	1.02494	.525	-4.8579	2.4479
	Bonferroni	50% ethanol concentration	25% ethanol concentration	25.63000	1.02494	.000	21.5704	29.6896
			10% ethanol concentration	26.83500	1.12277	.000	22.3879	31.2821
		25% ethanol concentration	50% ethanol concentration	-25.63000	1.02494	.000	-29.6896	-21.5704
			10% ethanol concentration	1.20500	1.02494	.915	-2.8546	5.2646
		10% ethanol concentration	50% ethanol concentration	-26.83500	1.12277	.000	-31.2821	-22.3879
			25% ethanol concentration	-1.20500	1.02494	.915	-5.2646	2.8546

Percentage of lignin recovery	Tukey HSD	50% ethanol concentration	25% ethanol concentration	-46.31000	1.76810	.000	-51.7350	-40.8850
			10% ethanol concentration	-50.76333	1.76810	.000	-56.1884	-45.3383
		25% ethanol concentration	50% ethanol concentration	46.31000	1.76810	.000	40.8850	51.7350
			10% ethanol concentration	-4.45333	1.76810	.100	-9.8784	.9717
		10% ethanol concentration	50% ethanol concentration	50.76333	1.76810	.000	45.3383	56.1884
			25% ethanol concentration	4.45333	1.76810	.100	-.9717	9.8784
	Bonferroni	50% ethanol concentration	25% ethanol concentration	-46.31000	1.76810	.000	-52.1226	-40.4974
			10% ethanol concentration	-50.76333	1.76810	.000	-56.5759	-44.9508
		25% ethanol concentration	50% ethanol concentration	46.31000	1.76810	.000	40.4974	52.1226
			10% ethanol concentration	-4.45333	1.76810	.136	-10.2659	1.3592
		10% ethanol concentration	50% ethanol concentration	50.76333	1.76810	.000	44.9508	56.5759
			25% ethanol concentration	4.45333	1.76810	.136	-1.3592	10.2659

Appendix C

Table C1. Analysis of variance for an assessment of ethanol concentrations on imageJ analysis.

ANOVA

		Sum of Squares	df	Mean Square	F	Sig.
Circle equivalent diameter	Between Groups	741.662	2	370.831	54.432	.000
	Within Groups	1798.550	264	6.813		
	Total	2540.212	266			
Circularity	Between Groups	1.585	2	0.792	46.204	.000
	Within Groups	4.528	264	0.017		
	Total	6.113	266			

Appendix D

Table D1. Analysis of variance for an assessment of wider range of ethanol concentrations on imageJ analysis.

ANOVA

		Sum of Squares	df	Mean Square	F	Sig.
Circle equivalent diameter	Between Groups	2787.701	5	557.540	7.869	.000
	Within Groups	20760.324	293	70.854		
	Total	23548.025	298			
Circularity	Between Groups	1.321	5	0.264	10.234	.000
	Within Groups	7.566	293	0.026		
	Total	8.887	298			

LIST OF PUBLICATIONS

M.H. Hamzah, S. Bowra, M.J.H Simmons and P.W. Cox (2016). Proceedings from the 24th European Conference and Exhibition: *The Impact of Process Parameters on the Purity and Chemical Properties of Lignin Extracted from Miscanthus x giganteus* using a Modified Organosolv Method. Amsterdam, The Netherlands.

M.H. Hamzah, S. Bowra, P.W. Cox and M.J.H. Simmons (2016). Proceedings from the 4th CIGR Agricultural Engineering Conference: *The Effect of Ethanol Concentration upon Formation of Organosolv Lignin Aggregates from Miscanthus x giganteus.* Aarhus, Denmark.

CHAPTER 1: INTRODUCTION

1.1 Background

Lignin is the second most abundant natural polymer on earth after cellulose and is found in all terrestrial plants and some aquatic species. The biosphere is estimated to contain 3×10^{11} tonnes of lignin with an annual biosynthetic rate of 2×10^{10} tonnes (Argyropoulos and Menachem, 1997; Hu *et al.*, 2011). Currently, lignin is recovered in large quantities as a by-product from pulping industry (Gan *et al.*, 2014). Lignin is produced by a chemical pulping process which results in a black liquor, leaving cellulose fibres for pulp production. However, the black liquor is predominantly dewatered and burned to supplement the heat requirement of the pulping operation (Mahmood *et al.*, 2016) and only 1 to 2% of the total amount of lignin produced is used in bio-based material applications (Gordobil *et al.*, 2016).

There are two basic pulping processing 1) the sulphite process which uses a mixture of an aqueous sulphur dioxide and a base such as calcium, sodium, magnesium or ammonium bisulphide and 2) the Kraft process which is based on cooking with a sodium hydroxide and sodium sulphide (Hamaguchi *et al.*, 2012; Laurichesse and Avérous, 2014; Tarabanko and Petukhov, 2003). Lignin derived from the Kraft or the sulphite process are recovered from black liquor by acidification. Lignosulphonates contains sulfonic acid groups that makes lignin water soluble. Lignosulphonates exhibit a high molecular weight with a broad distribution of polydispersity index (around 6-8) and are the most utilised lignins with applications including

CHAPTER 2: LITERATURE REVIEW

2.1 Introduction

The literature review describes the refining of biomass (biorefining) to produce diverse marketable bio-based products and bioenergy. More importantly, the use of lignocellulosic biomass focusing on *Miscanthus x giganteus (MxG)* is explored. The various lignin extraction methods published in the available literature are discussed. Finally, methods of lignin depolymerisation and modification to alter the chemical structure of lignin and to improve lignin reactivity, therefore, the range of biochemicals produced are also discussed.

2.2 Bio-based Economy and Integrated Biorefinery

Energy and material needs play an essential role in the world's future. Currently, about 80% of the world's energy markets rely on crude oil, coal and natural gas which is expected to last for around another 60 and 120 years at the current rate of consumption (Balat and Ayar, 2005; Potumarthi *et al.*, 2014). Global energy requirements, depletion of fossil fuel reserves, high cost of fossil fuels and greenhouse effects caused by fossil fuel usage have caused workers all over the world to seek another alternative and sustainable energy sources (Duku *et al.*, 2011).

First generation biofuels were produced from sugar or starch rich food crops such as sugarcane, corn and wheat. Of major environmental and ethical

and straw contain mainly xylan (Agbor *et al*., 2011). Figure 2.6 shows the main constituents of hemicelluloses.

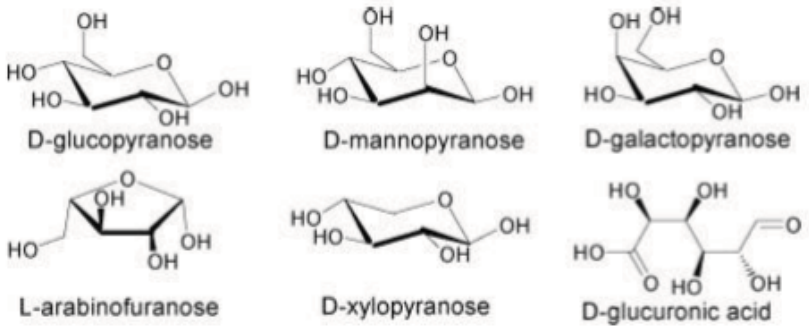

Figure 2.6. Main constituents of hemicellulose. (Source: Adapted from Mohammad, 2008).

Hemicelluloses are easily hydrolysed due to their lower molecular weight compared to cellulose and their branched structure with short lateral chain (Li *et al.*, 2010; Saha, 2003). The degree of polymerisation of hemicelluloses is between 80 to 200 sugar units and average molecular weight of < 30,000 (Anwar *et al.*, 2014; Mohammad, 2008). Substantial amount of hemicelluloses and lignin need to be removed from cellulose fibres, rendering the cellulose more accessible for enzymatic hydrolysis process (Agbor *et al*., 2011). Nevertheless, process conditions including temperature, reaction time, moisture content and pH must be carefully chosen to prevent formation of undesirable products such as fulfural and hydroxymethylfulfural that have been shown to hinder the fermentation process (Agbor *et al.*, 2011; Jönsson and Martín, 2016).

Hemicelluloses provide a renewable material supply for wide variety of industrial applications, for example, xyloglucans from hemicellulose have been used for pharmaceutical applications such as antibiotics and a treatment

for ulcers (Pauly *et al.*, 2013). Hemicellulose sugars, pentose (xylose and arabinose) and hexose (glucose, galactose and mannose) also have been utilised for conversion of lignocellulosic materials to fuel ethanol and other value added fermentation products including 5-hydroxymethylfurfural (HMF), furfural, levulinic acid, and xylitol (Canilha *et al.*, 2003; Saha, 2003). Moreover, hemicelluloses act as wet strength additives in papermaking, viscosity modifiers in food packaging film as well as tablet binders (Peng *et al.*, 2012).

2.4.3 Lignin

Lignin is built up from three different phenyl propane monomers, which form complex macromolecules, which then form an amorphous, three-dimensional polymer. The three phenyl propane monomers, namely *p*-coumaryl, coniferyl and sinapyl alcohol differ in the substitution at the 3 and 5 positions (Mansouri and Salvadó, 2006) as shown in Figure 2.7. Lignin is formed via two types of linkages; condensed linkages (e.g. 5-5 and β-1 linkages) and ether linkages (e.g. α-O-4 and β-O-4 linkages) (Abiven *et al.*, 2011; Zobel and Buijtenen, 1989). Figure 2.8 shows the structure of major bonds in lignin.

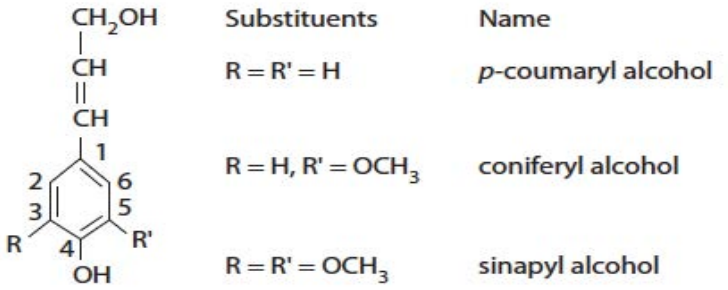

Figure 2.7. Lignin monomeric building blocks. (Source: Adapted from Lapierre, 2010).

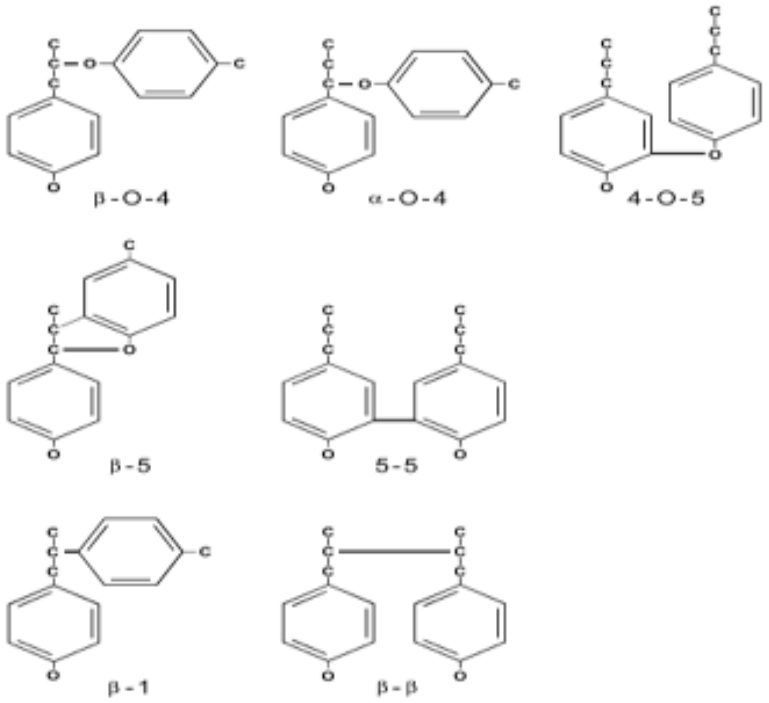

Figure 2.8. Structure of the major bonds in lignin. (Source: Adapted from Kogel-Knobner, 2002).

The starting points for the formation of guaiacyl and syringl structures of lignin are derived from coniferyl and sinapyl alcohol as outlined in Figure 2.9.

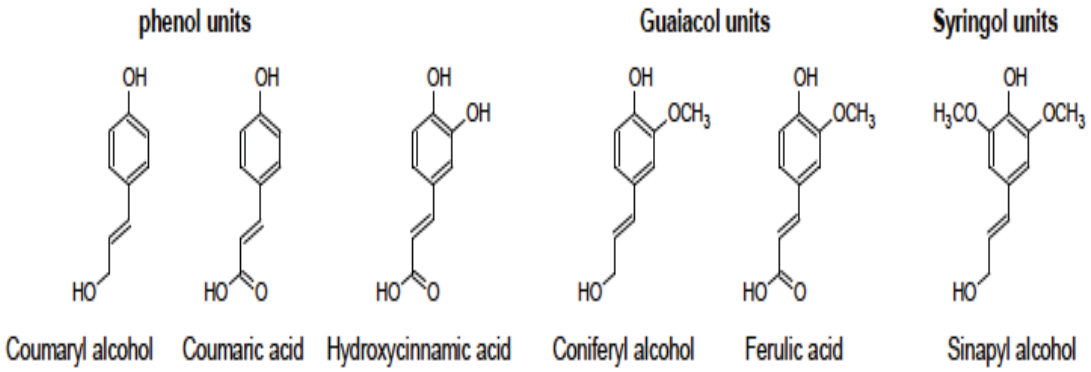

Figure 2.9. Types of phenyl propanoids units found in lignin. (Source: Adapted from Holladay *et al.*, 2007).

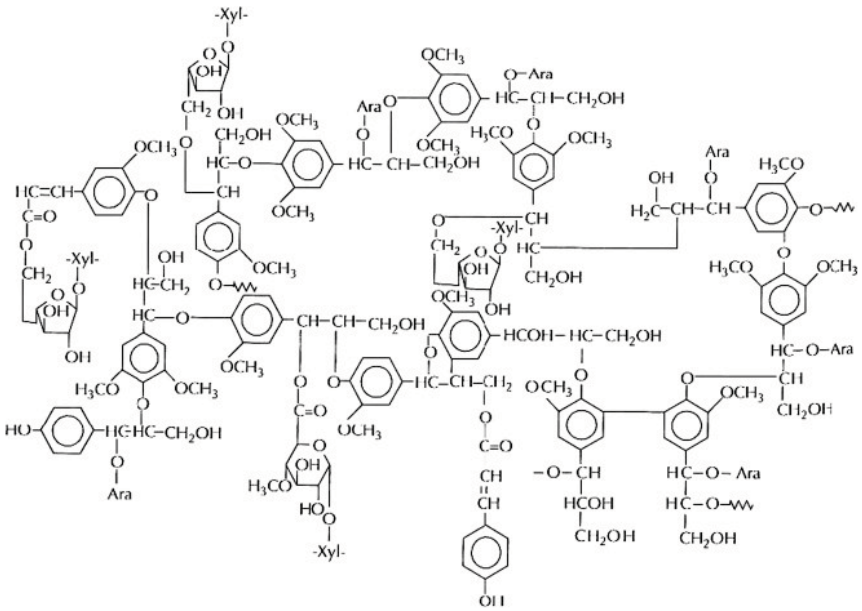

Figure 2.10. A structural model of wheat straw lignin. (Source: Adapted from Ghaffar and Fan, 2014).

Lignin plays various roles in plants, alongside the main natural components of cellulose and hemicellulose. Lignin gives stiffness and structural stability of a plant cell wall by cementing and fixating lignin with other polysaccharides in the plant cell wall (Alberts *et al.*, 1989). The presence of lignin makes the plant fibres more rigid and stiff, providing mechanical support for the stem and branches enabling healthy plant growth (Henriksson, 2009). Besides, lignin also works as glue that binds the individual plant cells and the other carbohydrate polymers in the complex secondary wall (Achyuthan *et al.*, 2010). Lignin makes the cell wall in intercellular regions of xylem by providing the hydrophobic capillary surface needed for nutrient transport (Leisola *et al.*, 2012; Myburg *et al.*, 2013). Moreover, lignin serves an essential function in plant defense. The lignified cell wall serves as a barrier against microorganisms by preventing the

from 2 to 44 tonnes/ha dry matter; yields range from 27 to 44 tonnes/ha in Europe and the USA Midwest, and from 10 to 11 tonnes/ha in Canada (Heaton *et al.*, 2008; Pyter *et al.*, 2007; Scurlock, 1999; Xi and Jezowski, 2004).

Figure 2.11. *Miscanthus* sp. energy crop. (Source: Adapted and modified from Falter *et al.*, 2015).

Miscanthus spp. originated in Japan and first cultivated in Europe in the 1930s (Brosse *et al.*, 2012). Seasonal changes and with its bioclimatic location may have affected the relative composition of biomass including *MxG* (Savy and Piccolo, 2014). Other factors that affect the biomass yield and composition of *Miscanthus* sp. are genotypes, soil types, nutrients used as well as crop age (Brosse *et al.*, 2012).

When comparisons are made with other genotypes, *MxG* has a strong range of potential benefits including the possibly unique and exclusive trait for

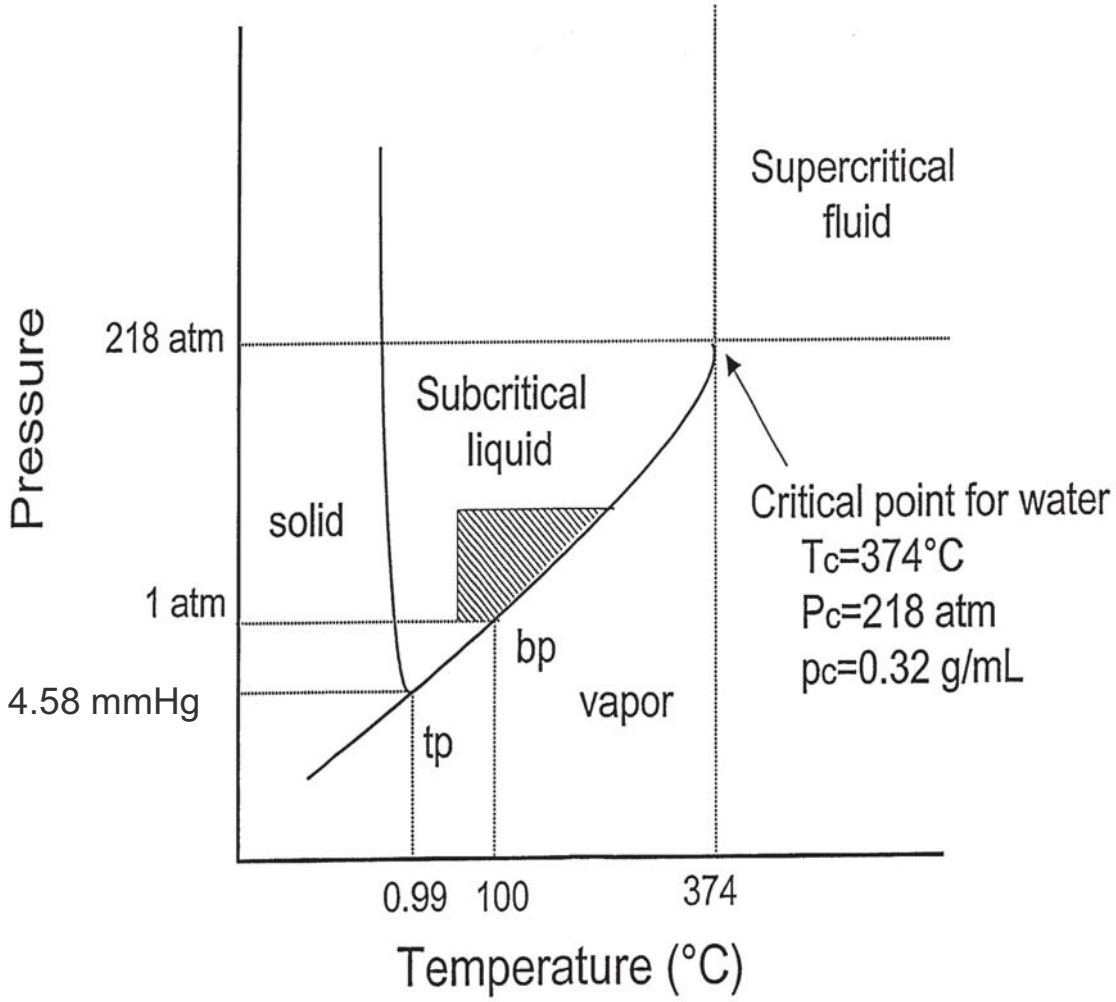

Figure 2.14. Phase diagram of water as a function of temperature and pressure. (Source: Adapted from King and Grabiel, 2007).

The SCW has several unique properties compared to water at ambient conditions especially for its dielectric strength and ionic product that causes dramatic changes in physical properties (Rogalinski *et al.*, 2008). Dramatic rise of temperature in SCW causes a decrease in permittivity, an increase in the diffusion rate and a decrease in the viscosity and surface tension (Asl and Khajenoori, 2013). As a result, more polar target materials with high solubility in water at ambient conditions are extracted most effectively at lower temperatures, while moderately polar and non-polar materials need a less polar medium influenced by elevated temperature (Asl and Khajenoori, 2013;

pulping agent, the pulping medium will become highly acidic and alkaline for sodium sulphite. The main reaction scheme for lignosulphonate formation during acid sulphite pulping is illustrated in Fig. 2.16.

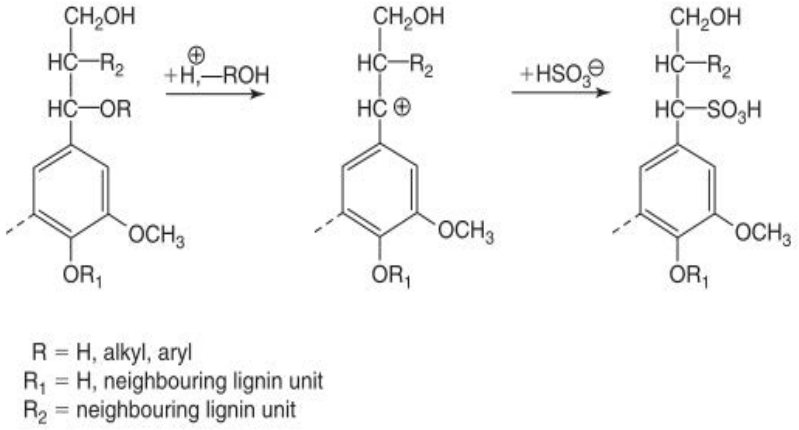

Figure 2.16. Main reaction scheme for lignosulphonate formation during acid sulphite pulping. (Source: Adapted from Lora, 2008).

Lignosulphonate has good water solubility at all values of pH and has been used by industry in a wide variety of applications. Lignosulphonate has been used as a binder or glue in pellets or compressed materials (Tumuluru *et al.*, 2011) and also used to reduce dust particles and stabilise the road surfaces (Edvardsson, 2010). This binding ability makes lignosulfphonate an essential component of materials such as ceramics, animal pellets, coal briquettes and others (Lora, 2008). In addition, lignosulphonate also acts as a dispersant especially in concrete mixes. Lignosulphonate attaches to the particle surface, keeps the particle from being attracted to the other particles and reduces the amount of water needed for cement or concrete mixes (Yang *et al.*, 2008).

ester substituent by nucleophilic substitution (Cachet *et al.*, 2014; Wang *et al.*, 2017) and thus, reduce the intermolecular interactions of hydrogen bonding, providing a plasticisation phenomena and mobility of the chains (Lisperguer *et al.*, 2009). Figure 2.17 showed the esterification mechanism of kraft lignin modified using acid chlorides that produces kraft lignin with more reactive aliphatic hydroxyl units.

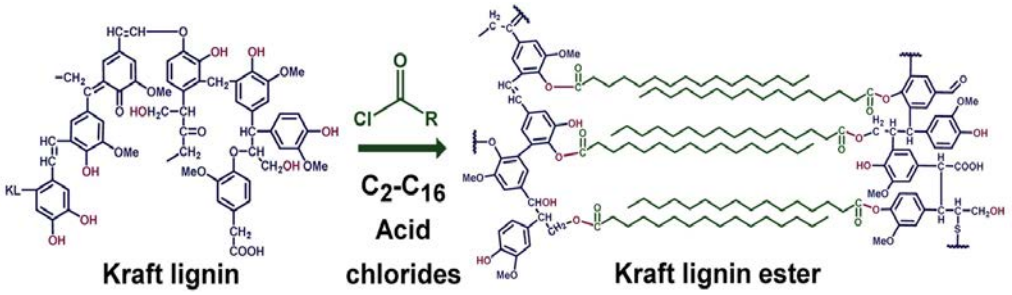

(a)

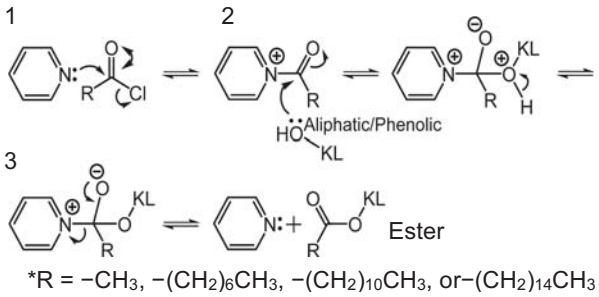

1.Addition of the nucleophile.
2.Elimination of the leaving group, forming the tetrahedral intermediate.
3.Loss of a proton.

(b)

Figure 2.17. (a) Esterification of kraft lignin using acid chlorides (b) Mechanism of pyridine catalysed klason lignin esterification with C_2–C_{16} fatty acid chlorides (Source: Adapted and modified from Koivu *et al.*, 2016).

2.9.2.1 Esterification

Esterification is one of the simplest ways to modify the hydroxyl groups within lignin and depends on the reaction parameters and reactants used

2.9.2.4 Urethanisation

The first urethane was discovered as early as 1849 by Wurtz. Works conducted by Dr. Otto Bayer at IG Farbenindustrie, Germany in 1937 synthesised the first polyurethane using the urethanisation process involving terminal hydroxyl groups in reaction with addition of di-isocyanates or polyisocyanates, forming polyurethane groups in the polymer backbone as shown in Figure 2.22 (Ionescu, 2005; Upton and Kasko, 2015).

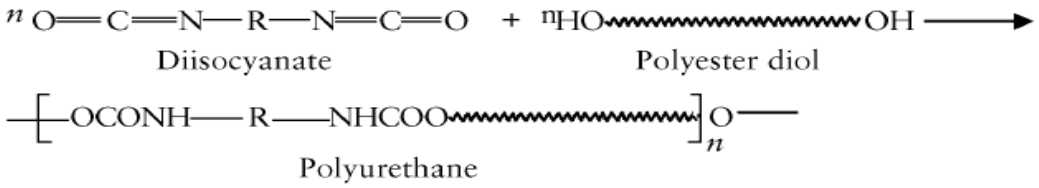

Figure 2.22. Reaction involving hydroxyl groups with isocyanate groups, active RNC=O sites to form a urethane. (Source: Ionescu, 2005).

Lignin is utilised either directly without further chemical modification or after chemical modification with different polyols to produce polyurethane; the latter approach is the most practical method for industrial applications (Laurichesse and Avérous, 2014). A study by Ciobanu *et al.* (2004) of lignin-polyurethane films reported various properties in a series of blends prepared by solvent casting technique obtained in dimethyl formamide solutions from a polyurethane elastomer and different proportions of flax/soda pulping lignin. A major finding was observed in that adding up to 5% lignin contributed to the polyurethane elastomer strength and biodegradability, simultaneously with lower decomposition temperature and elasticity. Hatakeyama *et al.* (2005) studied the mechanical properties of polyurethane-based biocomposites derived from lignin and molasses that could be applied in the field of housing

CHAPTER 3: MATERIALS AND METHOD

3.1 Introduction

This chapter describes the general materials and methods used throughout the work for characterisation and quantification analysis.

3.2 Feedstock and Reagents

Miscanthus x giganteus (*MxG*), a lignocellulosic biomass, was grown and harvested in Aberystwyth, Wales, United Kingdom and provided by the Institute of Biological, Environmental and Rural Sciences (IBERS, UK) and Phytatec (UK) Ltd. The biomass was stored dry and in the dark.

Absolute ethanol (Fisher Scientific, UK), nitrogen (compressed oxygen free nitrogen, BOC, UK) and carbon dioxide (vapour withdrawal, BOC, UK) used had ≥ 99.8% purity. 72% sulphuric acid (Fluka-Sigma Aldrich, UK), pyridine (Sigma-Aldrich, UK), dodecanoyl chloride (Sigma-Aldrich, UK), hydrochloric acid (VWR, UK), and HPLC grade water, HiPerSolv CHROMANOR® (VWR Chemicals, France) were used as reagents.

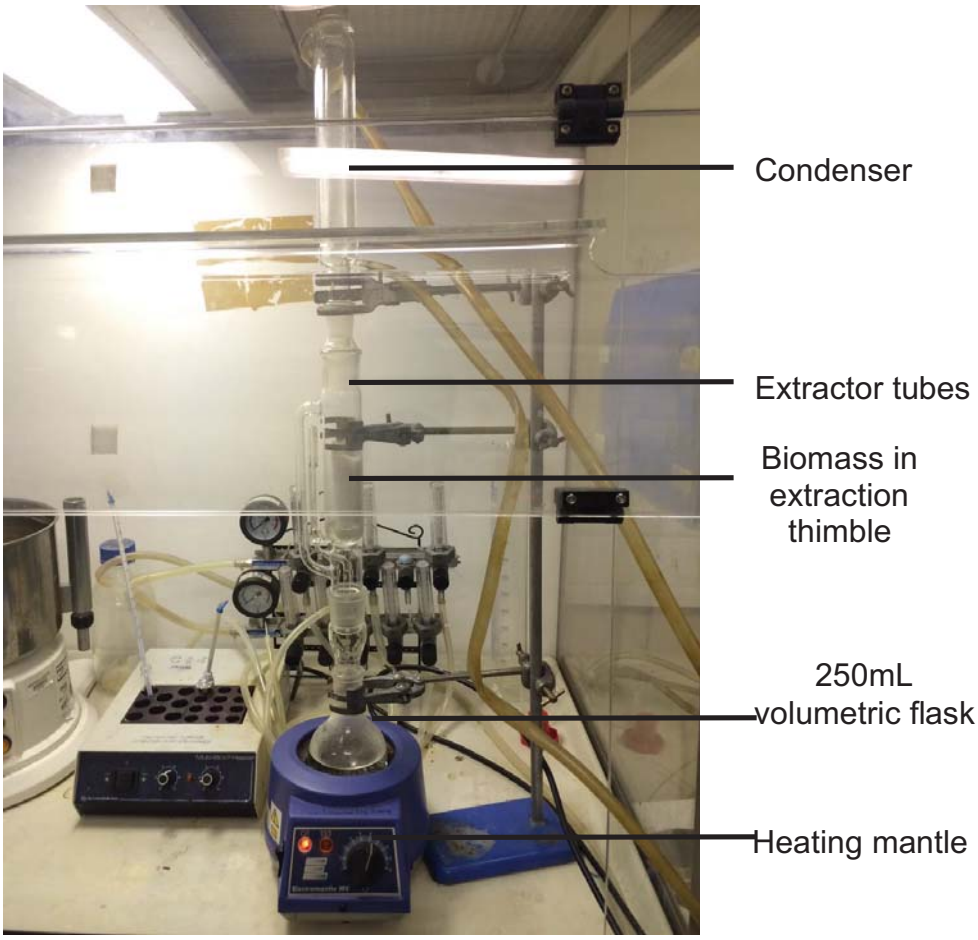

Figure 3.1. Soxhlet apparatus experimental set-up.

The thimble containing the Miscanthus biomass was placed into a Soxhlet apparatus. 200 mL of HPLC grade water added to the receiving flask before it was coupled to the Soxhlet apparatus. The water was refluxed through the biomass for 16 hours, before replacing with 200 mL ethanol. The ethanol was again refluxed for another 16 hours. At the end of ethanol extraction step, the thimble was removed from the Soxhlet apparatus and the residual biomass was filtered through a Pyrex sintered disc funnel porosity 2 using a vacuum filtration unit (VP100 High Savant Vacuum Pump). The biomass was washed three times with 100 mL of fresh ethanol and then dried

species present in the sample (Manley, 2014). Thus, it is very challenging to interpret the overlapping peaks.

In summary, FTIR spectra contain a large amount of information including chemical bonds and compositional; thus, chemometric techniques analysis, such as multivariate analysis, are promising methods for further details of spectra analysis (Xu *et al.*, 2013).

3.4.2 Principal Component Analysis (PCA) on FTIR data

PCA is an essential mathematical tool to verify the correlations that exists within multivariable data. Analysis of FTIR spectra datasets by PCA determines the differences between spectra in terms of chemical structure and composition of the samples (Chen *et al.*, 1998; Labbé *et al.*, 2006). PCA transforms a one-dimensional dataset to multi-dimensional dataset that is dependent on the projection of principal components. The principle of PCA is denoted with a matrix of data with N rows (observations) or Y and K columns (variables) or X in a multidimensional variable space as shown in Figure 3.2. Y can be analytical samples and X can be spectral origin or chromatographic origin.

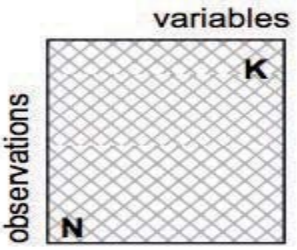

Figure 3.2. Notation used in PCA. (Source: Adapted from Eriksson *et al.*, 2006).

Each observation is represented by a point in the variable space. The whole dataset then constitutes a swarm of points in the variable space. PCA finds a line or planes in K dimensional variable space that approximates the data using the principle of least squares and statistically minimising the variance (Eriksson *et al.*, 2006). Figure 3.3 shows the derivation of a PCA model. The line is the direction of the first principal component (PC1) and points in the direction of the maximum variation.

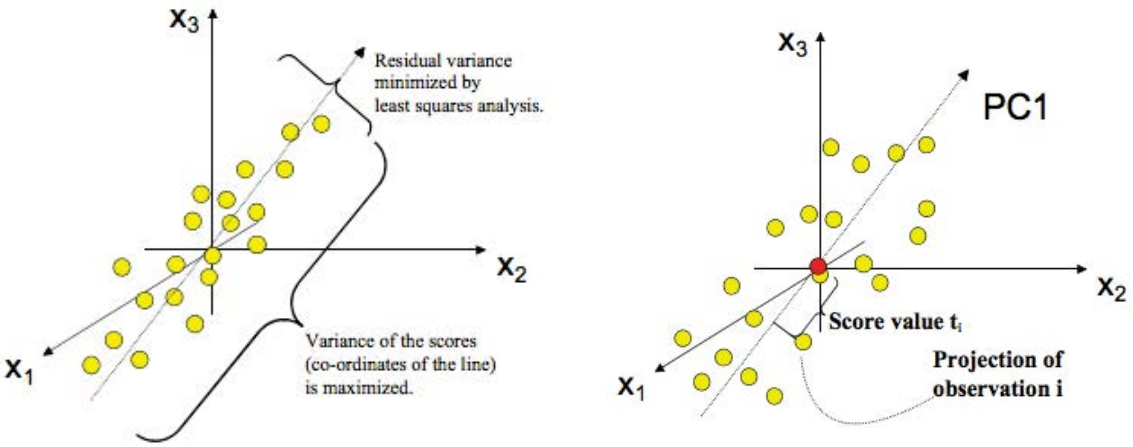

Figure 3.3. Derivation of a PC1 model. (Source: Adapted from Eriksson *et al.*, 2006).

The first principal component may not be enough to explain the data variation. By projecting the samples onto the new coordinate system, there may still unexplained variance. If the projection process is extended orthogonal to the first PC in the remaining part of the space, the second principal component (PC2) is created as shown in Figure 3.4. The process can be continued to find more PCs.

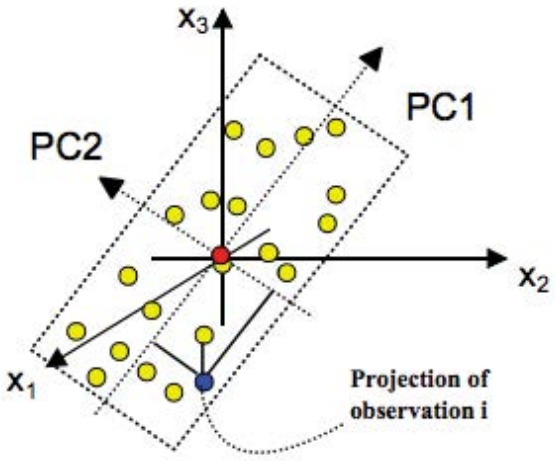

Figure 3.4. Second Principal Component (PC2). (Source: Adapted from Eriksson *et al.*, 2006).

The percentage of explained variance decreases with increasing of principal components, and could describe the variability between spectra (Grootveld, 2012). The explained variance gives the results based on calibrated and validated variance. The calibrated variance measures the model fit whereas the validated variance measures the new variance data or predicting the difference or error associated between projected and measurement data (Esbensen *et al.*, 2002).

A two-dimensional plot of the projected objects by using PC1 and PC2 create a new coordinate system and a map of objects in the principal components plot a so-called a score plot. In the case of spectra analysis, score is described by the degree of correlation for each spectra of each principal component whereas each principal component is associated with loadings that contribute by wavenumbers (Cordella, 2012; Kline *et al.*, 2010).

The score plot reveals the sample patterns, groupings, similarities and differences amongst the distribution of samples. For instance, in the

determination of lignin content in grass, hard and soft woods following analysis of biomass dissolved in ionic liquids, the cluster of grass, hard and soft wood could be observed in Figure 3.5. Thereby, spectra that cluster together on the scores plot reveal any similarity of chemical composition and structure between spectra. Thus, if the spectra from samples showed similar characteristics, these spectra were chosen for analysis.

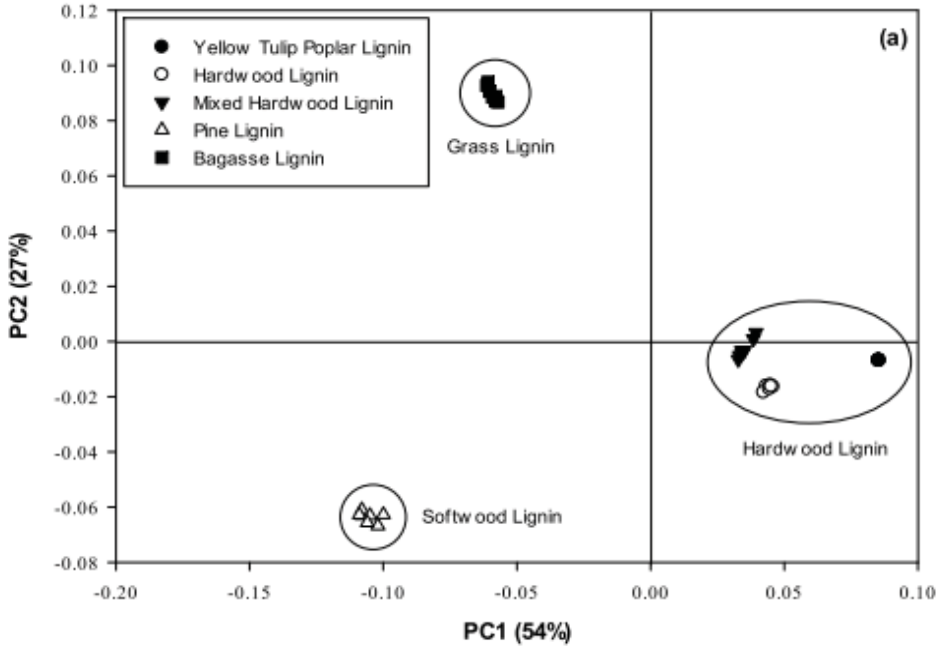

Figure 3.5. Score plot as a function of PC1 and PC2. (Source: Adapted from Kline *et al.*, 2010).

Loading plot is used to find correlation patterns among variables and the more significant variables (Lupoi *et al.*, 2013). For example, in the work to evaluate the influence of formulation and process variables on mechanical properties of oral mucoadhesive films using multivariate analysis, further analysis on data of films without a nonwoven textile were studied (Landová *et al.*, 2014). In the loading plot shown in Figure 3.6, the variables that are close to each other to the left loadings plot (dotted line of circle) and far from the center circle, very close to the 100% explained variance, which means,

therefore, they correlate positively (Cordella, 2012). Here, the analysis of the loadings plot emphasises the PC1 that captures maximum variability in the data.

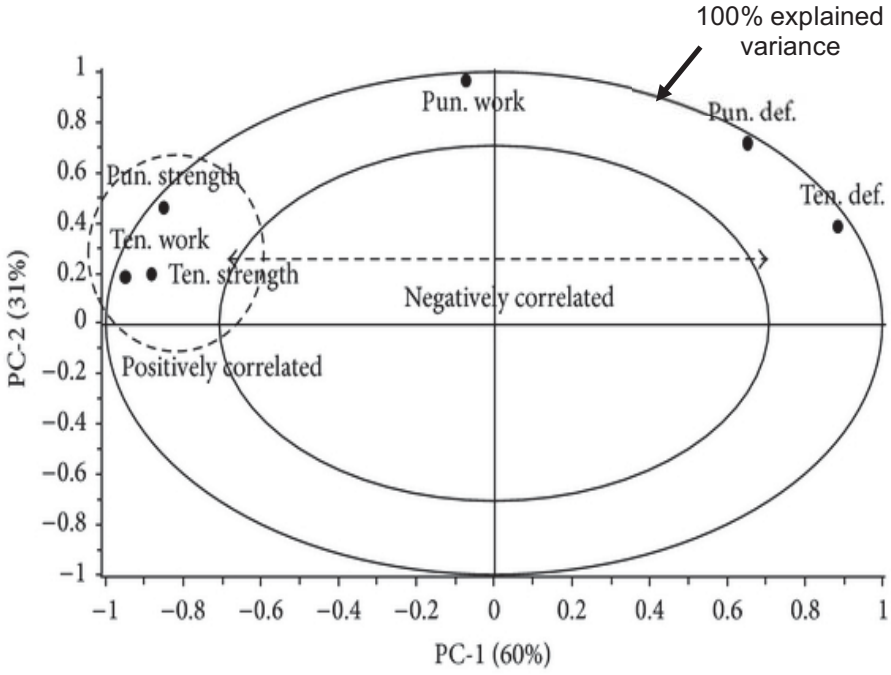

Figure 3.6. Loading plot for PC1 and PC2 for data of films without a nonwoven textile (Source: Adapted and modified from Landová *et al.*, 2014).

In general, the similarities or differences among sample and variables could not be detected easily in terms of the raw data. In practice, there is often a need to slightly modify the shape of the data to better suit an analysis, such modification is called preprocessing or pretreatment. There are various pretreatments including baseline correction, scatter correction, derivatives, normalisation or spectroscopic transformations (Luthria *et al.*, 2013).

Here, the spectra data collected was subjected to two types of pretreatment including smoothing and normalisation prior to PCA analysis. A smoothing function is to reduce noise and improve spectral resolution (Stuart, 2004). Normalisation of FTIR data transforms and maps the data into a

CHAPTER 4: AN EVALUATION OF IMPACT OF DIRECT AND SEQUENTIAL EXTRACTION PROCESSES ON THE PURITY AND CHEMICAL PROPERTIES OF LIGNIN FROM *MISCANTHUS X GIGANTEUS*

4.1 Introduction

In the biorefinery approach, lignin and carbohydrates which are the biomass recalcitrant components need to be removed, so that the cellulose fibres become more accessible and amenable for bioethanol production via enzymatic and microbial hydrolysis (Pu *et al.*, 2013). In such a context of the biorefinery approach, this work is carried out by sequential processing, thus enabling recovery of multiple naturally occurring biopolymers namely hemicellulose, cellulose and lignin which then become the feedstock for either direct application or subsequent downstream transformation.

In this chapter, sub-critical water (SCW) is applied at pressures up to 50 bar over a temperature range from 120°C to 200°C, depending on the targeted components to recover. Several studies have demonstrated that temperature has a pronounced influence on conversion rate of lignocellulosic biomass in SCW hydrolysis. The extraction temperature used is commonly within the range of 130°C to 240°C, conversion also depends on other factors such as particle size and solid to liquid ratio (Borrega *et al.*, 2011). From another point of view, Yedro *et al.* (2014) proposed that the SCW fractionation can be performed at mild conditions (<100°C) to remove the water-soluble

extraction (**DE**), *MxG* was subjected to a single treatment step which is similar to third treatment in SE by the SCW with associated modifiers.

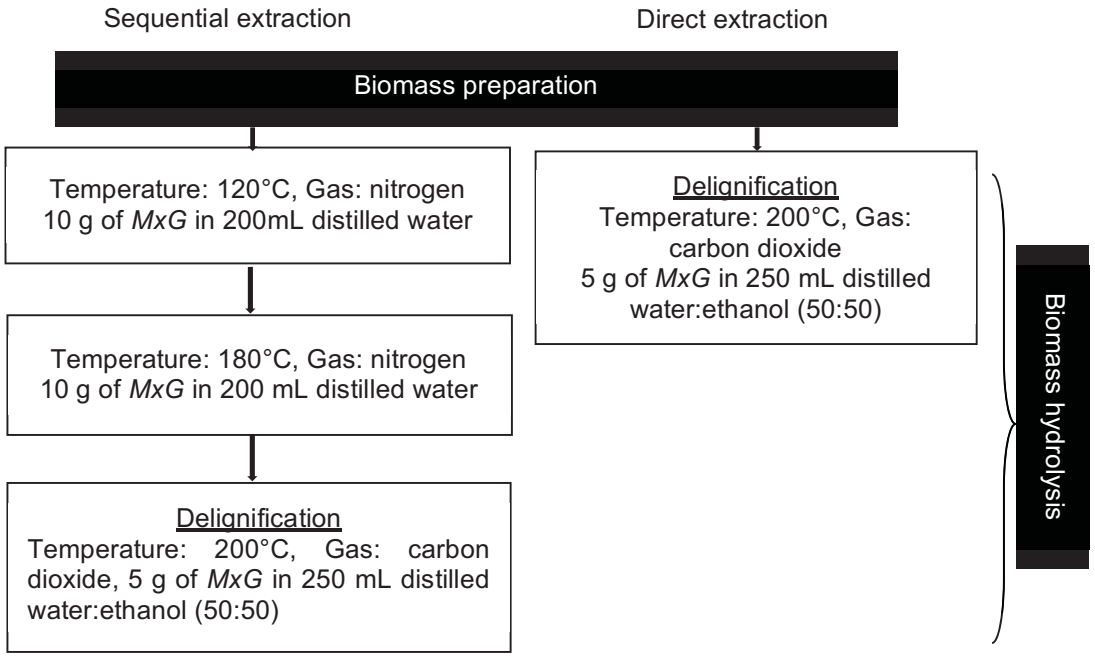

Figure 4.1. Flow chart of SE and DE.

4.2.2 Biomass Preparation

Materials used in this work are described in section 3.2. Prior to hydrolysis, the Miscanthus biomass was mixed in distilled water, then warmed to 50°C to soften the grass. The mixture was then soaked for 20 minutes to rehydrate the grass. The mixture was milled for three minutes in a domestic blender to reduce the particle size of material. The grinding conditions of temperature, soaking time, grinding time and solid:liquid ratio were previously optimised to yield an average particle size of 500 μm (Roque, 2013).

The Miscanthus biomass slurry was placed inside the reactor directly after sample preparation for SE at 120°C. Then, the sequentially processed

after cooling in a desiccator for calculation of biomass solubilisation. The percentage of biomass solubilisation was calculated using Eq 4.1.

$$\%\ \text{of biomass solubilisation} = \frac{\text{A}}{\text{B}}\ \text{x}\ 100\% \quad (4.1)$$

Where A is the weight of dried solution, g; B is the initial weight of biomass, g.

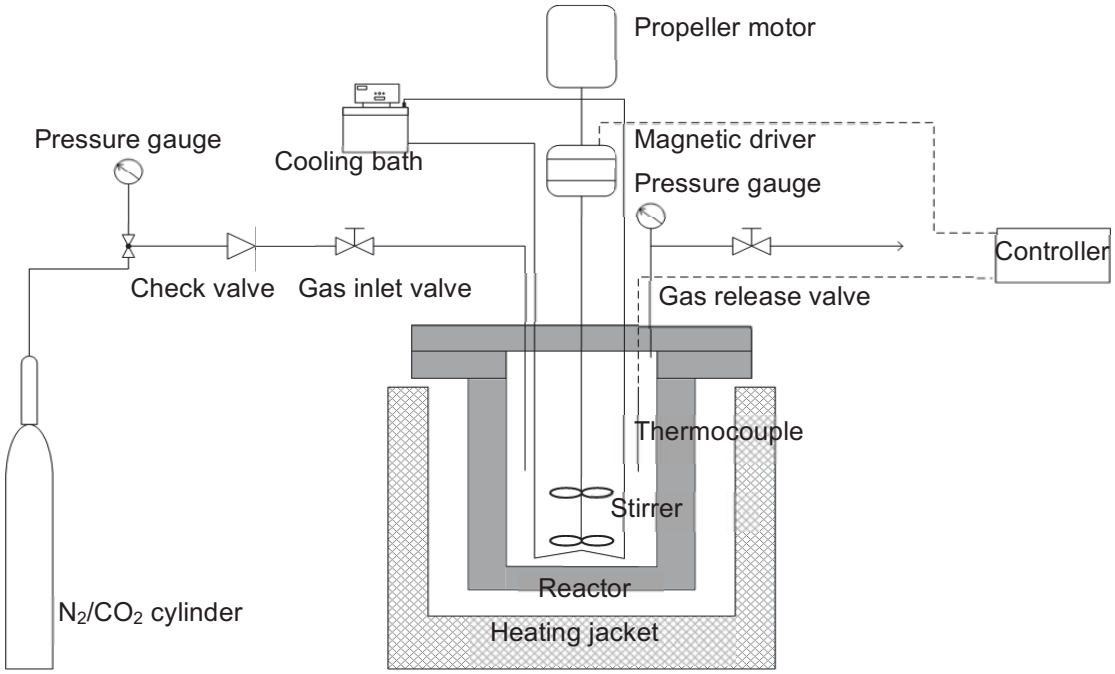

Figure 4.2. Schematic diagram of experimental set-up of Miscanthus biomass hydrolysis for DE and SE.

4.2.4 Lignin Precipitation

The filtrate from vacuum filtration was placed in a freezer at -20°C for 2 hours, after which the ethanol concentration was adjusted to 25% by adding distilled water. Lignin was recovered using a Beckman, model J2-21 centrifuge with a JA-10 rotor at 4°C and at 10,000 revolutions per minute (RPM), 17700 relative centrifugal force (RCF) for 10 minutes. The remaining supernatant was dried at 65°C for further Klason lignin assay and FTIR

MxG fibre after delignification for *MxG* which had been subjected to sequential sub-critical water mediated hydrolysis (SE). A second cluster on the right hand side, consists of the spectra for *MxG* fibre before and after delignification for DE. Thereby, Figure 4.9 shows the spectra of DE and SE were distinguishable from each other.

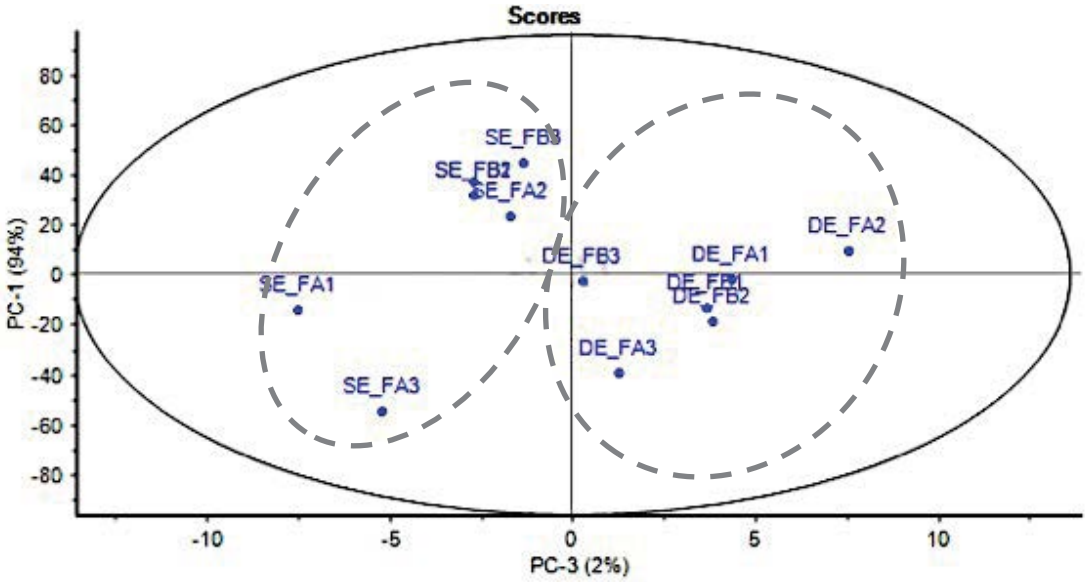

Legend:
SE_FA: Sequential extraction- *MxG* fibre after delignification
SE_FB: Sequential extraction- *MxG* fibre before delignification
DE_FA: Direct extraction- *MxG* fibre after delignification
DE_FB: Direct extraction- *MxG* fibre before delignification
**1,2,3- Repetition of spectra

Figure 4.9. PCA scores plot for solid fraction.

When comparison is made between samples among SE itself, (SE_FB1 and SE_FB2) and (SE_FA1 and SE_FA3) correlations were in the same quadrant. For DE, (DE_FB1 and DE_FB2) and (DE_FA1 and DE_FA3) correlations were in the same quadrant too. The closer the spectra are in the same quadrant; the spectra possess similar chemical composition. Thus, only a spectra was chosen from spectra that have similar chemical composition to be analysed for FTIR analysis.

Based on the correlation loadings plot in Figure 4.10, it is possible to acquire information related the chemical aspects involved in the DE and SE process. All wavenumbers related to lignocellulosic biomass as identified by FTIR (4000 to 600 cm^{-1}) have an extreme position on the top of the correlation loadings plot except for a wavenumber of 780 cm^{-1}.

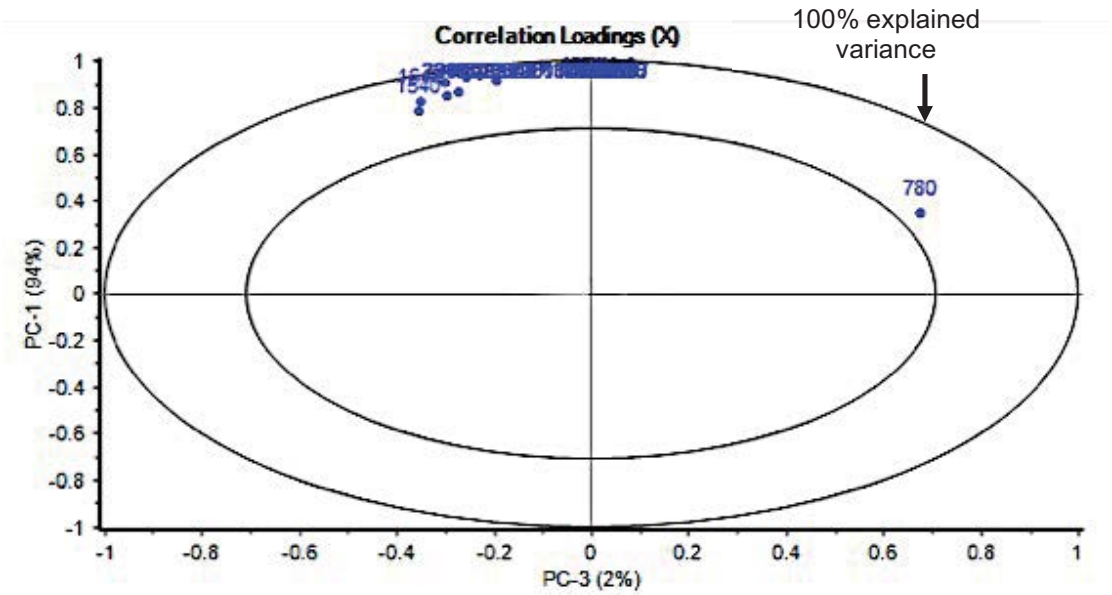

Figure 4.10. PCA correlation loadings plot for solid fraction.

The wavenumbers at the top of the plot are close to each other, and far from the centre of circle, very close to the 100% explained variance circle; they correlate positively. Wavenumber of 780 cm^{-1} which refers to 1,2-disubstitution (ortho) C-H aromatic ring (aryl) groups (Coates, 2000) had influenced the result of PCA score plot. In spite of fact that, even though the loadings plot could not explain clearly what PC1 and PC3 describes, the score plot can differentiate the samples according to different extraction methods and to answer simple questions such as if the spectra represent significant differences.

scores illustrated that the spectra possess similar chemical composition.

Table 4.2. Scores table for similar chemical composition.

Spectra category	Spectra of similar chemical composition
SE_L	SE_L2 and SE_L3
SE_S	SE_S1 and SE_S2
DE_L	DE_L1 and DE_L2
DE_S	DE_S1, DE_S2 and DE_S3

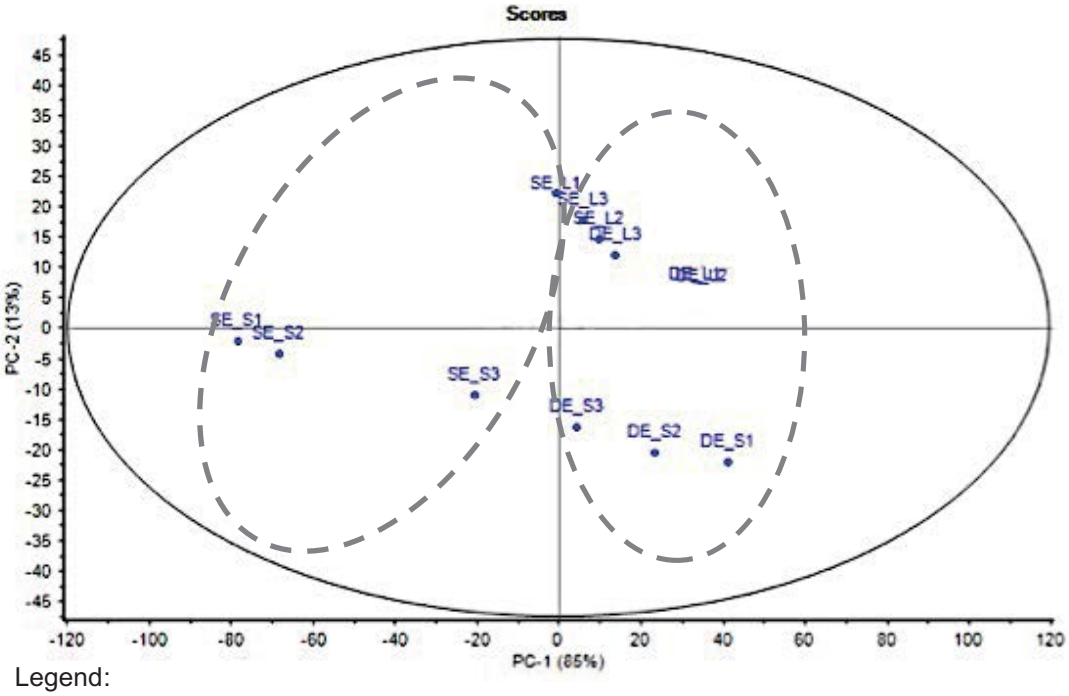

Legend:
SE_L: Sequential extraction- Precipitated lignin
SE_S: Sequential extraction- Dried supernatant
DE_L: Direct extraction- Precipitated lignin
DE_S: Direct extraction- Dried supernatant
**1,2,3-repetition of spectra

Figure 4.12. PCA scores plot for liquid fraction.

PCA correlation loadings are shown in Figure 4.13. Two wavenumbers, 2340 and 780 cm^{-1} are separated from the other wavenumbers corresponding to lignocellulosic biomass of FTIR analysis (4000 to 600 cm^{-1}) which affected the data variability of PCA. The wavenumbers of 2340 and 780 cm^{-1} are negatively correlated negatively as they are near to the centre and far from

the circle at 100% explained variance.

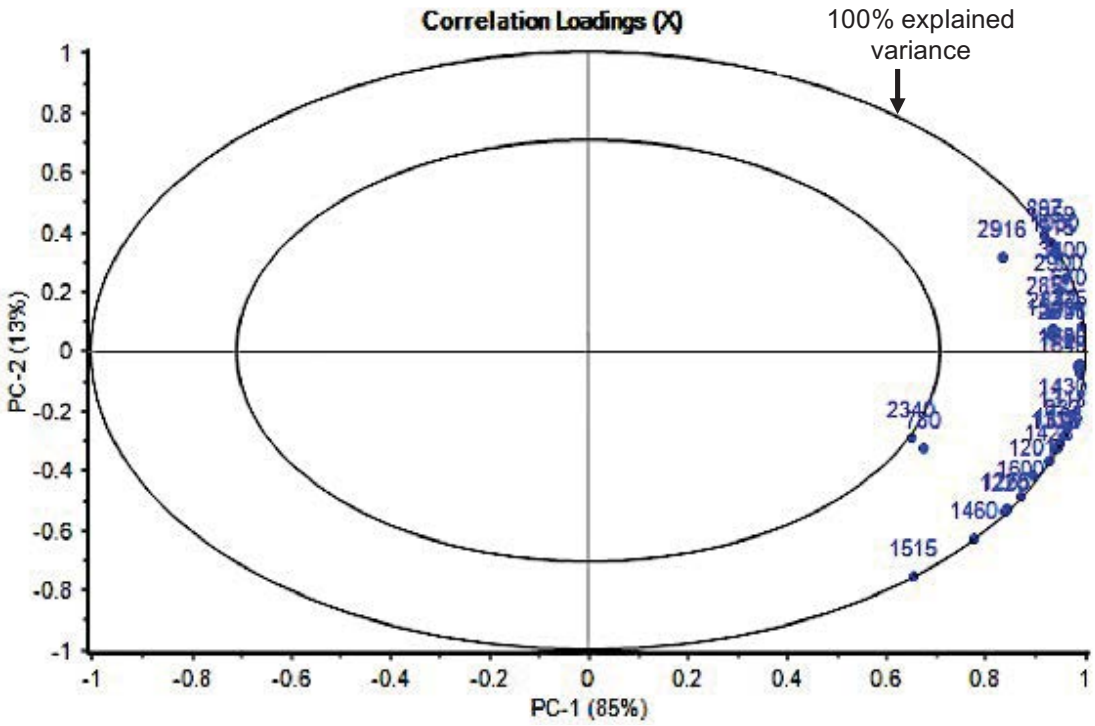

Figure 4.13. PCA correlation loadings plot for liquid fraction.

4.3.5.3 Spectra of Precipitated Lignin

Spectra of precipitated lignin, analysed by FTIR, for both DE and SE are shown in Figure 4.14. In general, spectra of precipitated lignin for SE presents stronger and broader intensity spectra than DE. The typical peaks at wavenumbers of lignin were found: 3400, 1705, 1600, 1650, 1515, 1460, 1425, 1326, 1265, 1220, 1033, 1118, 915 and 833 cm^{-1}. The details of wavenumbers and interpretations are outlined in Table 4.3.

CHAPTER 5: AN ASSESSMENT OF ETHANOL CONCENTRATION EFFECT UPON FORMATION OF ORGANOSOLV LIGNIN AGGREGATES FROM *MISCANTHUS X GIGANTEUS*

5.1 Introduction

Lignin isolated via different extraction methods can vary widely in terms of chemical composition and molecular structure. The differences also affect the physical properties such as solubility and molecular weight (Bruijnincx *et al.*, 2016). Therefore, in the context of the growing interest in developing value added uses for lignin, this chapter examines the characterisation of lignin extracted via a SCW method; with particular emphasis on the formation of lignin aggregates.

There is insufficient information available to describe the association behaviour of lignin macromolecules in solution as this depends on the solvent conditions and lignin structure (Ratnaweera *et al.*, 2015). But an understanding of the formation and assembly of lignin aggregates in solution are relevant and significant, as the heterogeneity and complex lignin structure become the greatest bottleneck in lignin utilisation for bio-based materials (Baker and Rials, 2013; Vishtal and Kraslawski, 2011).

Numerous studies on lignin aggregates have been conducted in conjunction with different methods and sources of lignin such as aggregation and assembly of alkali lignin in iodine (Deng *et al.*, 2011), the impact of lignin source on its self assembly in dimethyl sulfoxide solution (Ratnaweera *et al.*, 2015) and the aggregation of acetylated lignins in *N,N*-dimetylacetamide

respectively. Figure 5.4 of PCA scores plot for precipitated lignin and dried supernatant elucidated that there were two definite clusters observed and were distinguishable within each other. At the top are the spectra for the precipitated lignin at different ethanol concentrations. A second cluster at the bottom, consists of spectra for the dried supernatant.

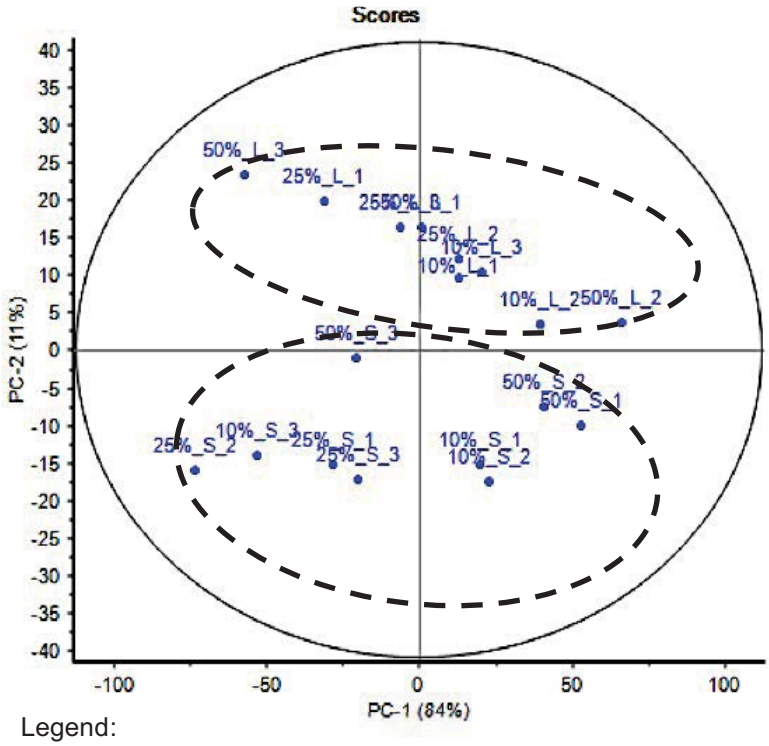

Legend:
10%_L: Precipitated lignin of 10% ethanol concentration
25%_L: Precipitated lignin of 25% ethanol concentration
50%_L: Precipitated lignin of 50% ethanol concentration
10%_S: Dried supernatant of 10% ethanol concentration
25%_S: Dried supernatant of 25% ethanol concentration
50%_S: Dried supernatant of 50% ethanol concentration
**1,2,3- repetition of spectra

Figure 5.4. PCA scores plot at different ethanol concentration.

When comparison was made between similar type of spectra within samples, scores of precipitated lignin (10%_L_1 and 10%_L3, 25%_L_1 and 25%_L_3, 50%_L_1 and 50%_L_2) and scores of dried supernatant (10%_S_1 and 10%_S_2, 25%_S_1 and 25%_S_3, 50%_S_1 and 50%_S_2) were close within each other, indicating that the samples within similar type of spectra possess similar composition. Thus, only a spectra was chosen from

spectra that have similar chemical composition to be analysed for FTIR analysis.

PCA correlation loadings are shown in Figure 5.5. Two wavenumbers, 2340 and 780 cm^{-1} were far apart compared with other wavenumbers which had influence the result of PCA score plot. The wavenumbers of 2340 and 780 cm^{-1} were correlated negatively as both wavenumber near to the center and far from the center of 100% explained variance.

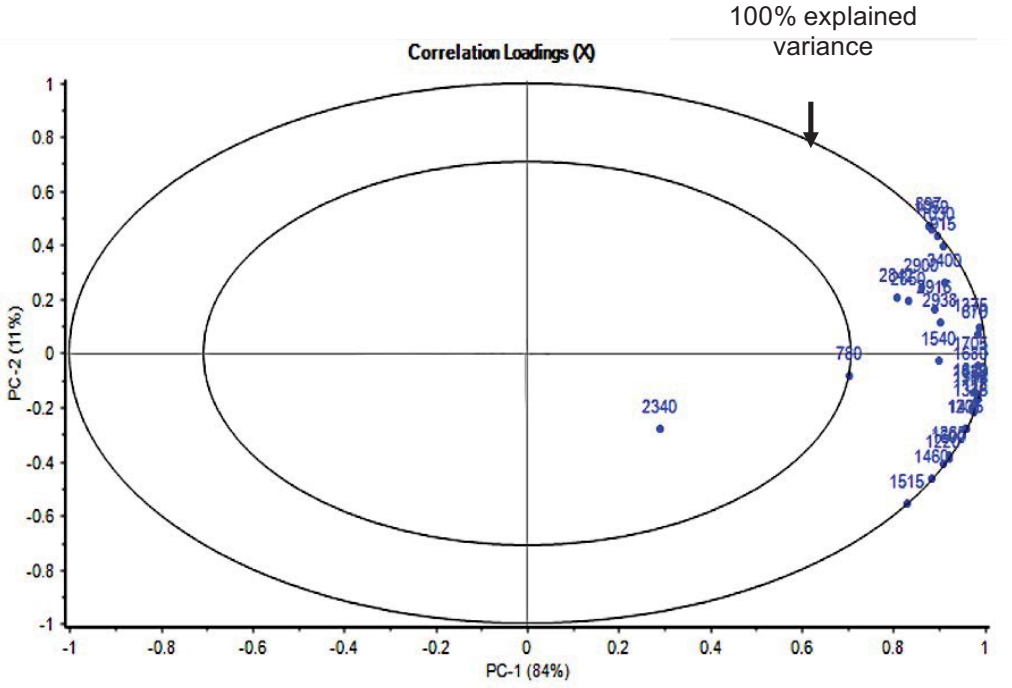

Figure 5.5. PCA correlation loadings plot at different ethanol concentration.

5.3.3.2 Spectra of Precipitated Lignin

The FTIR spectra of precipitated lignin at different ethanol concentration were shown in Figure 5.6. The indicative wavenumbers apportioned to lignin are found: 1705 to 1720, 1680, 1640, 1515, 1460, 1425, 1326, 1265, 1220, 1118, 1030, 915 and 833 cm^{-1}. The details of

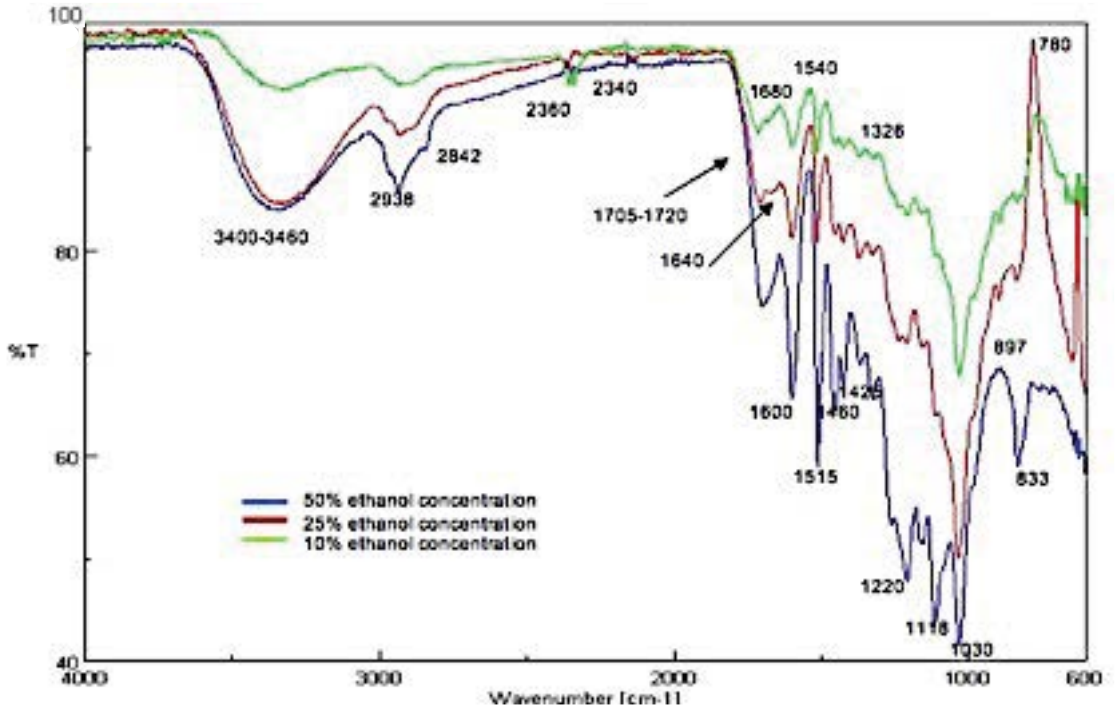

Figure 5.7. FTIR spectra for dried supernatant from different ethanol concentrations.

A new distinct peak of 1540 cm^{-1}, related to an aromatic ring stretching in lignin, was found in both spectra for the precipitated lignin and the dried supernatant (Radotić *et al.*, 2012). In summary, from the spectra in Figure 5.7, it is apparent that wavenumbers of 897 and 1705 to 1720 cm^{-1} related to the contamination of cellulose and hemicellulose were in high intensity and broader peak at 50% ethanol concentration than 25 and 10% ethanol concentration, thus less purity of lignin derived from supernatant was obtained.

monomers, lignin had random polymer globule structure with non-linearly and random cross-linked with other constituents, and the structure of lignin is not as the other two main components of lignocellulosic biomass, cellulose and hemicellulose which has a more linear shape structure (Chen, 2014). A schematic representation of lignin globule structure is illustrated in Figure 5.17.

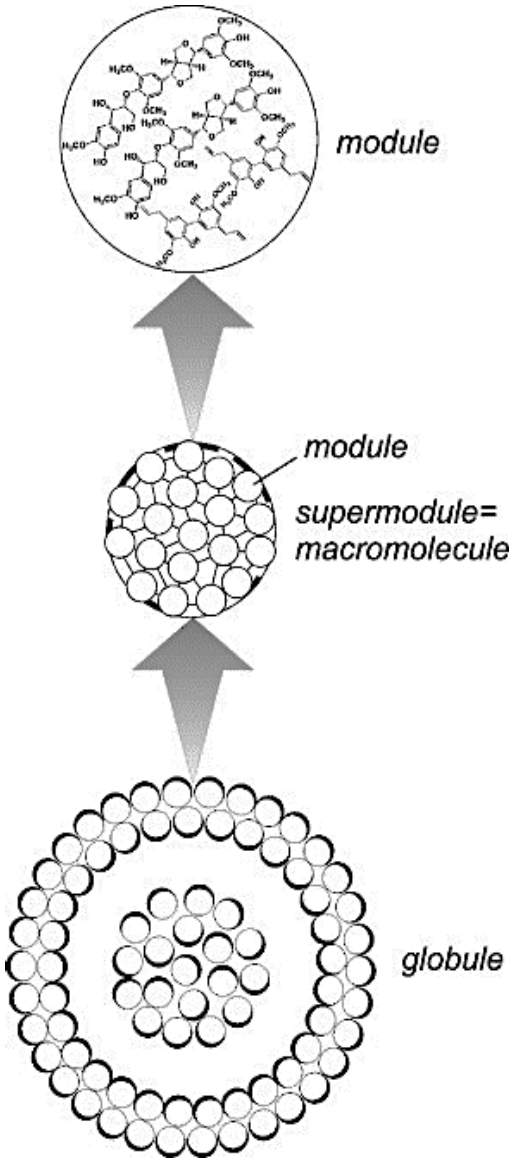

Figure 5.17. Schematic representation of lignin globule structure. (Source: Adapted from Micic *et al.*, 2004; Radotić *et al.*, 2005).

range of the instruments (Malvern, 2014). Nevertheless, the Mastersizer 2000 gave volume-weighted distribution, which within the relative volume contribution is proportional to size of particles (Malvern, 2012).

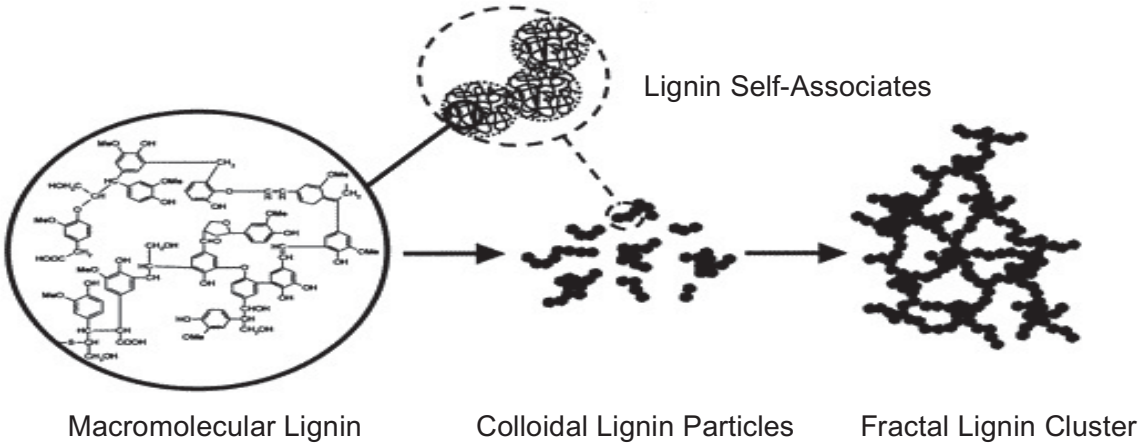

Figure 5.18. A schematic representation of the modes of aggregation in lignin solution system (Source: Adapted and modified from Norgren *et al.*, 2002).

All in all, the two sets of data obtained by Zetasizer Nano ZS and Mastersizer 2000 had common similarities on explaining the behaviour of lignin macromolecules of precipitated lignin and supernatant as well as lignin aggregates in ethanol-water solution. The surface weighted mean diameter by Mastersizer 2000 was reported in terms of the $D_{3,2}$ values. The $D_{3,2}$ refers to the diameter of a sphere of equivalent volume to surface area ratio of the particles in the sample. The value of surface weighted mean was indicative of phenomenon of particle aggregation (McClements, 2015). Decreasing aggregate sizes were found very effective on decreasing the aggregate stability and weighted mean diameter (An *et al.*, 2013; Yonter, 2015). Thus, it suggested that the surface weighted mean obtained is the size of lignin macromolecules in precipitated lignin, supernatant and soluble lignin extract.

5.3.6 Preliminary Study of Particle Size Analysis of Soluble Lignin Extract

5.3.6.1 Zetasizer

Table 5.3 summarised the average particle size of lignin at different ethanol concentrations of soluble lignin extract. Overall, a descending trend was observed for reduction of ethanol concentration from 50% to 10%.

Table 5.3. Average particle size of soluble lignin extract at different ethanol concentrations by Zetasizer.

Ethanol concentration (%)	Particle size (nm)
10	441.5 ± 17.2
25	1077.0 ± 43.4
50	1768.2 ± 45.2

Irrespective of particle size distribution at different ethanol concentration, which are shown in Figure 5.23, 50% ethanol concentration of soluble lignin extract had a monomodal distribution whereas 25% and 10% showed a bimodal and multimodal distribution, respectively.

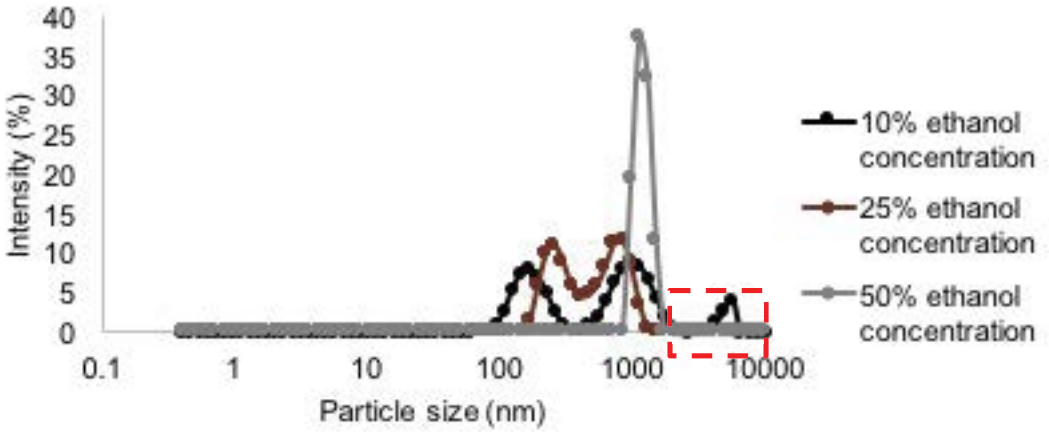

Figure 5.23. Particle size distribution at 50%, 25% and 10% ethanol concentration of soluble lignin extract by Zetasizer.

CHAPTER 6: THE INFLUENCE OF CHEMICAL PROPERTIES OF ORGANOSOLV LIGNIN AGGREGATES AT DIFFERENT LIGNIN CONCENTRATION ON THE EFFICACY OF LIGNIN ESTERIFICATION

6.1 Introduction

The solvent concentration had an influence on the lignin purity and recovery as well the other physical, chemical and structural properties of precipitated lignin, supernatant and soluble lignin fraction. The relationship between the solvent concentration and the resultant lignin macromolecules' is complex, therefore the investigation presented in the previous preliminary study is imperative and could facilitate improved understanding of structural complexity of lignin for lignin obtained via the sub-critical water extraction.

The complex behaviour of lignin aggregates may result also from the interaction of the solute with a solvent containing two components with different concentrations (Da Silva *et al.*, 2002; Maitra and Bagchi, 2008). Associations of the lignin molecule under different conditions vary: the rearrangement of the hydrogen bonds of hydroxyl group play major role and the availability of the hydroxyl group in soluble lignin extract could influence the physicochemical properties of lignin aggregates in modifying and converting lignin into useful renewable materials (Bevilaqua *et al.*, 2006; Buhvestov *et al.*, 1998).

The aim of this chapter was using extracts obtained from sequential extraction that had high purity of lignin and abundance of hydroxyl groups (Chapter 4) in the study of the effect of wider range of ethanol concentration

size analysis was obtained using the Zetasizer Nano ZS and Mastersizer, following methods described in section 3.5.2 and 3.5.3, respectively.

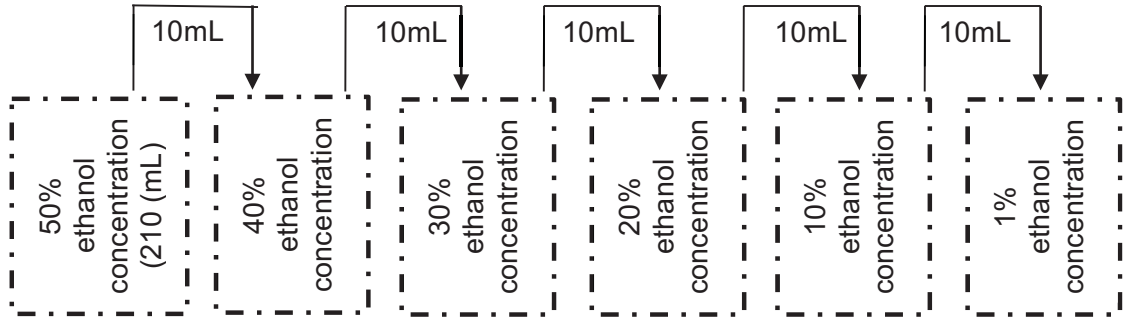

Figure 6.1. Scheme of dilution of soluble lignin extract.

6.2.1.2 LM Analysis

Images of the soluble lignin extract at different ethanol concentrations were captured following method mentioned in section 3.5.5.

6.2.1.3 ImageJ Analysis

Subsequently, 15 recorded images from LM analysis of three different microscope slides were analysed via ImageJ freeware (1.50v) according to method explained in section 3.5.6.

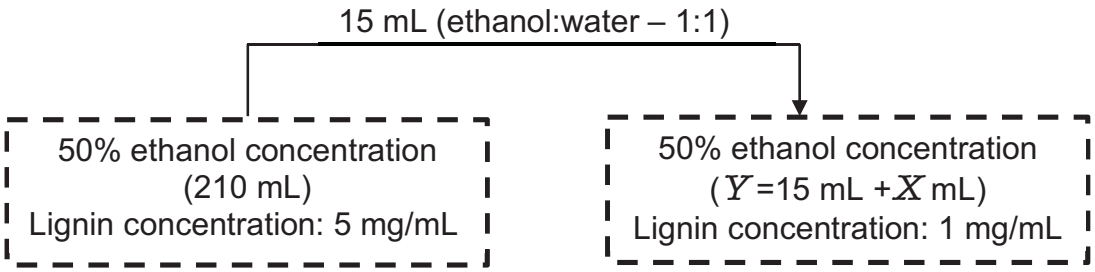

Where Y mL is the volume of soluble lignin extract at 50% ethanol concentration for 1 mg/mL (V_2); and X mL is the amount of ethanol-water mixture (1:1) need to be added to the soluble lignin extract.

Figure 6.2. Scheme of dilution of soluble lignin extract of 5 and 1 mg/mL.

6.2.2.2 Lignin Esterification

Lignin-fatty acid derivatives were synthesised using a method described by (Gordobil *et al.*, 2016) with modification, which the soluble lignin extract was used directly for analysis. Lignin esterification was performed for 5 and 1 mg/mL of soluble lignin extract to enable comparison of the chemical properties of esterified lignin at both these concentrations. 15 mL of soluble lignin extract was placed into a 250 mL beaker and stirred with a magnetic stirrer. Pyridine (2.75 mL) (Sigma-Aldrich, United Kingdom) was used as catalyst and dodecanoyl chloride (0.9 mL) (Sigma-Aldrich, United Kingdom) was added into the soluble lignin extract. The reaction was carried out at 20°C for two hours, after which the solution was decanted directly into 650 mL of 2% ice-cold hydrochloric acid (VWR, United Kingdom) and stirred for five minutes, resulting formation of a brownish ester layer at the top of a yellowish solution, mainly consisting of the excess acid, alcohol and water which separated under the ester layer. The ester layer was separated via a Buchner funnel with filter paper (Fisher Scientific, Qualitative, 150mm), and washed

with excess distilled water and ethanol (1:1) to remove unreacted fatty acids. Then, the esterified lignin was further directly analysed for its chemical structure characterisation via FTIR. The esterification reaction is shown in Figure 6.3.

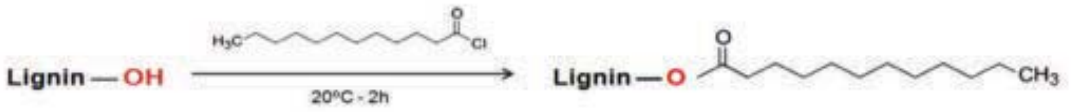

Figure 6.3. Reaction of scheme of lignin-fatty acid derivatives. (Source: Adapted from Gordobil *et al.*, 2016).

6.2.2.3 FTIR Analysis

FTIR analysis was performed on the unmodified and modified lignin samples at different lignin concentration without any pre-treatment for the samples containing 5 and 1 mg/mL lignin concentration. The IR spectra measurements were taken via a Nicolet 380 FTIR-Thermo Electron Corporation over a spectral range from 4000 to 600 cm^{-1} with resolution of 4 cm^{-1} and accumulation of 32 scans. The experiments were done in triplicate for each sample. Area-normalised and smoothed spectra in the regions of 4000 to 600 cm^{-1} were subjected to PCA using Unscrambler^{TM} software (Version 10.3, CAMO). For comparison study, FTIR analysis also was carried out on water, ethanol, water-ethanol (50% by volume), filtrate, blank solution prior esterification (mixture of ethanol:water (1:1), pyridine (2.75 mL), dodecanoyl chloride (0.9 mL), 2% ice cold hydrochloric acid (650 mL)) and dodecanoyl chloride.

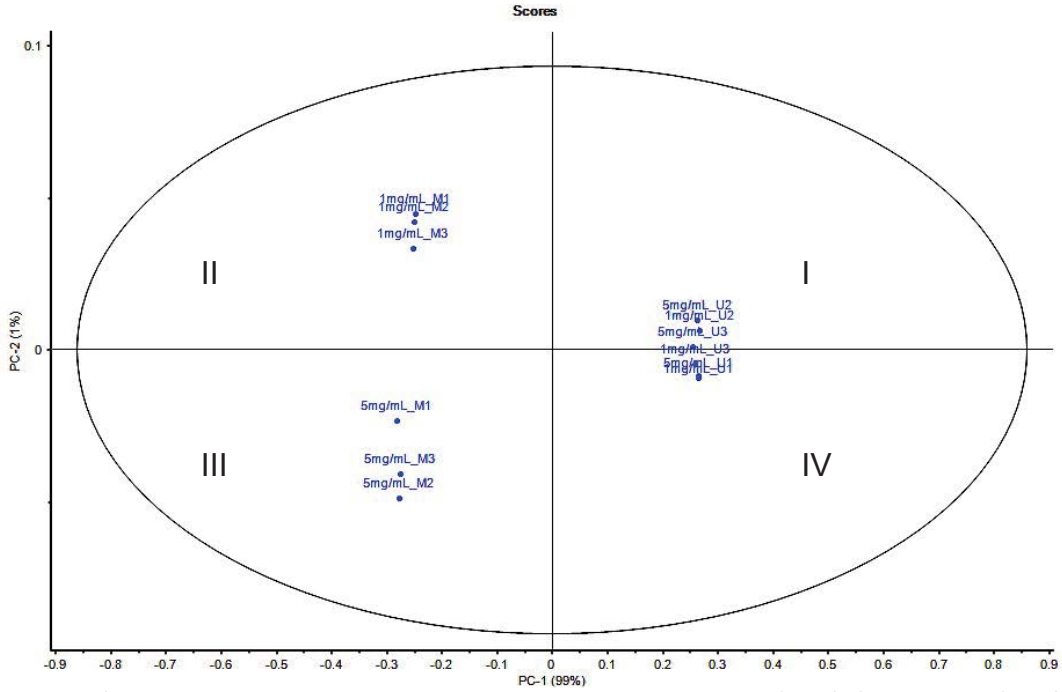

Xmg/mL_AB whereby X is the lignin concentration, A is modified (M) or unmodified (U) lignin and B is repetition of spectra.

Figure 6.16. PCA scores plot of unmodified and modified lignin at different lignin concentration.

Table 6.2. Scores table for similar chemical composition of unmodified and modified lignin at different lignin concentration.

Lignin concentration (mg/mL)	Type of lignin	Spectra of similar chemical composition
5	Unmodified	5mg/mL_U2, 5mg/mL_U3
	Modified	5mg/mL_M2, 5mg/mL_M3
1	Unmodified	1mg/mL_U3,1mg/mL_U1
	Modified	1mg/mL_M1, 1mg/mL_M2

The scores plot of PC2 against PC1 shown in Figure 6.16 illustrates the groupings, however the interpretation of the correlation loadings plot was not straightforward and complicated. The correlation loadings plot in Figure 6.17 showed the specific wavenumbers that influenced the scores plot.

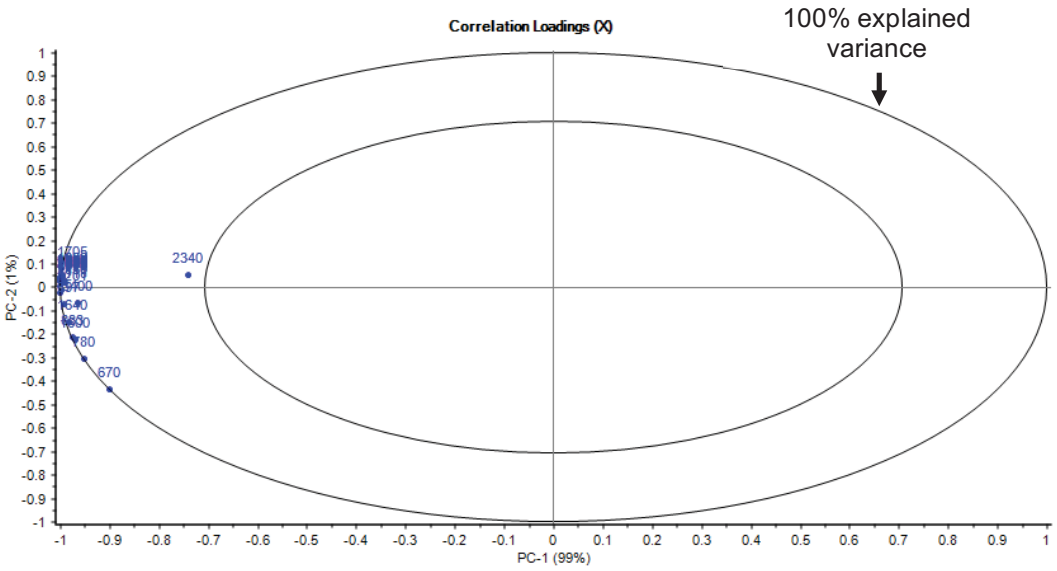

Figure 6.17. PCA correlation loadings plot of unmodified and modified lignin at different lignin concentration.

All wavenumbers related to lignocellulosic biomass identified by FTIR in the range from 4000 to 600 cm^{-1} were correlated positively as the wavenumbers very close to 100% explained variance except for wavenumber of 2340 cm^{-1}. The wavenumber of 2340 cm^{-1} contributed the most variability that affect the position of the samples. The wavenumber at 2340 cm^{-1} referred to OH stretch from strong H-bonded-COOH (Davis *et al.*, 1999). The location of wavenumbers either in positive or negative loadings in quadrant is not clearly explained. Even though the loadings plot could not have explained clearly what PC2 and PC1 describe, the scores plot can differentiate the spectra of samples according to different lignin concentration.

A representative FTIR spectra of unmodified soluble lignin extract at 5 and 1 mg/mL lignin concentration after spectra subtraction can be seen in Figure 6.19.

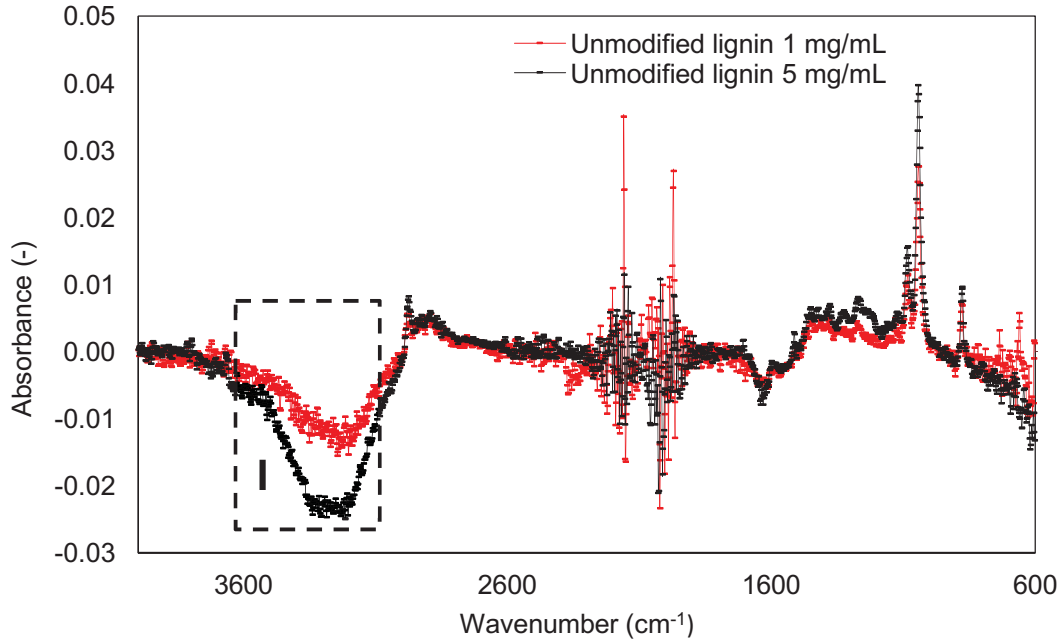

Figure 6.19. FTIR spectra of unmodified lignin at 5 and 1 mg/mL lignin concentration.

Even though the spectra subtraction method is quite useful for most applications using IR accessories, an attempt to remove the water spectra from FTIR spectra will be complicated in most cases (Nishikida *et al.*, 1995). A representative of specific fingerprint around 3400 cm^{-1} attributed to O-H stretching vibrations in aromatic and aliphatic hydroxyl groups can be seen in Figure 6.19 (labeled as I). Initially, as anticipated, the absorbance of unmodified lignin at 5 mg/mL was stronger than 1 mg/mL; indicating the high availability hydroxyl groups of intramolecular and intermolecular hydrogen bonding formed and existed between lignin and dual solvent in the soluble

lignin extract (Wang *et al.*, 2016). The source of O-H bonds could be originated from water, ethanol and lignin.

However, a more careful analysis revealed that the negative value of absorbance especially in the region I (Figure 6.19) corresponds to the stretch of O-H bonds in water molecules causes dominant absorbance in the wavenumber of 3400 cm^{-1} (Zaiqun, 2007). The finding appears to be well supported by Barth (2007) which the strong absorbance of water in the IR spectra region overlaps with sample modes of interest. Figure 6.20 has proved that the peak at 3400 cm^{-1} of water (labeled as II) had strong absorption (0.39) rather than ethanol (0.15).

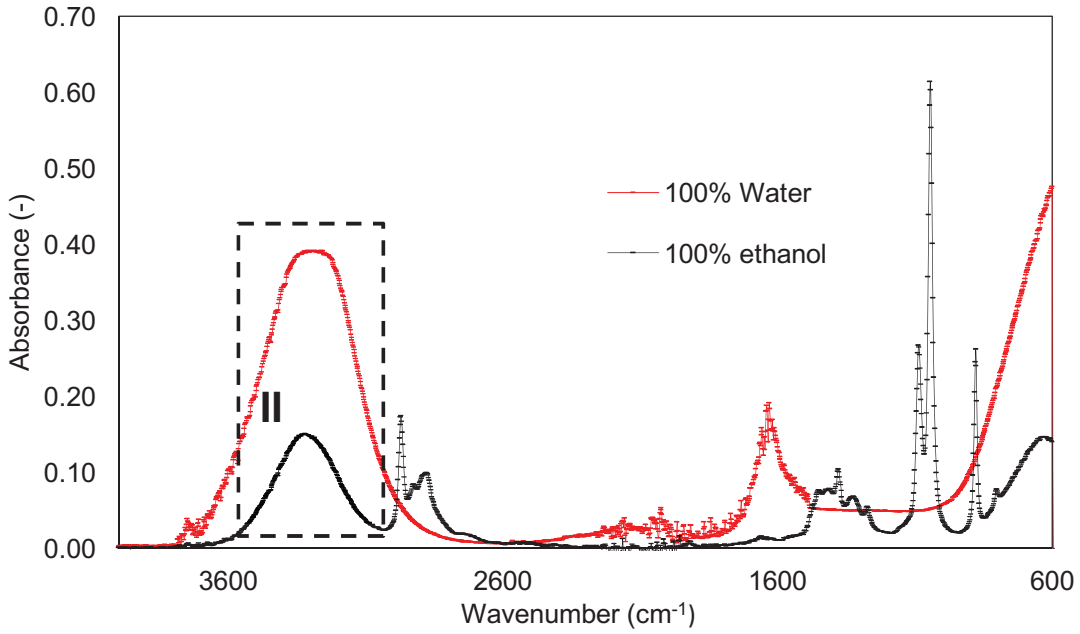

Figure 6.20. FTIR spectra of water and ethanol.

Therefore, when the hydroxyl groups wavenumber is of interest, the strong water absorption in the aqueous samples could have influenced the results obtained and in turn, relatively led into misinterpretation of the data.

Despite the limitation of this method, and consequently the poor results in the analysis of unmodified lignin samples, the findings do however suggest that dehydration of sample could be conducted or the precipitated lignin used for analysis in future to reduce the intense IR absorption of water (Trenerry and Rochfort, 2010). Therefore, the spectra of unmodified lignin based on the spectra subtraction method could not be comparable with the spectra of modified lignin.

6.3.2.2 Comparison of Modified Lignin at Different Lignin Concentration

Figure 6.21 provides the schematic diagram of sample analysed via FTIR for esterification study.

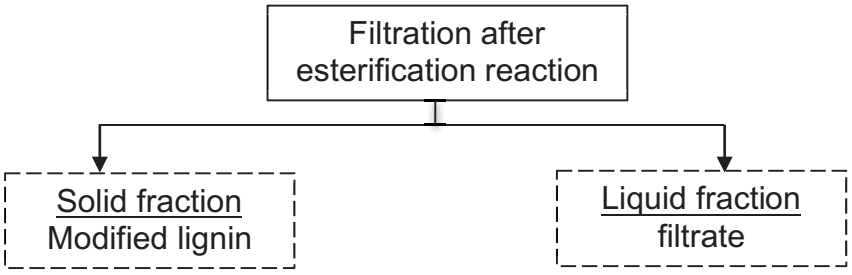

*Additional sample analysed for comparison study (1) dodecanoyl chloride (2) blank solution contains ethanol-water mixture (50% by volume), pyridine, dodecanoyl chloride and 2% of ice-cold hydrochloric acid.

Figure 6.21. Schematic diagram of sample analysed via FTIR for esterification study.

The FTIR spectra of the resulting modified lignin at 5 and 1 mg/mL lignin concentration were compared in Figure 6.22. The wavenumbers at 3400, 2938, 2850, 1800, 1760, 1740, and 1700 cm^{-1} of FTIR spectra could be used as physiological fingerprints to assess the efficacy of esterification process.

The presence of 3400 cm^{-1} (region I) was noted with broad intensity at 5 mg/mL (0.04) rather than 1 mg/mL (0.03), and the wavenumber of 3400cm^{-1} was attributed to O-H stretching of aromatic and aliphatic hydroxyl groups (Alriols *et al.*, 2010; Boeriu *et al.*, 2014; Pandey, 1999). The peak of 3400 cm^{-1} at 1 mg/mL become more flattened. As hypothesised, the findings showed that more material or lignin concentration in the soluble lignin extract, the more source of O-H bonds in the esterified lignin.

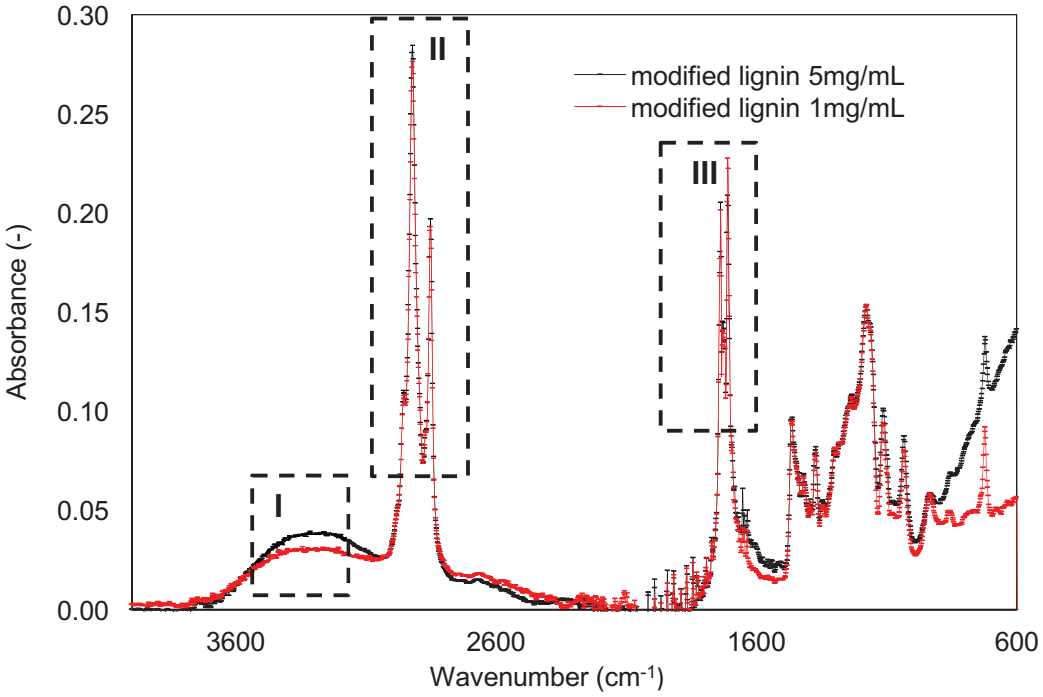

Figure 6.22. FTIR spectra of modified lignin at different ethanol concentration.

When comparison was made to modified lignin prepared to 1 mg/mL, the region II and III in Figure 6.22 of modified lignin from 5 mg/mL showed no difference in intensity of the peaks around 2938, 2850, 1760 and 1740 cm^{-1}. Strong absorptions at 2938 and 2850 cm^{-1} of modified lignin (region II) at both lignin concentrations arise from long chain alkyl groups (aliphatic carbon) which are present in fatty acid chloride, dodecanoyl chloride (Gordobil *et al.*,

concentration, in turn the spectra produced were similar with the spectra of water and overlap with other modes of interest as have been shown previously in Figure 6.20.

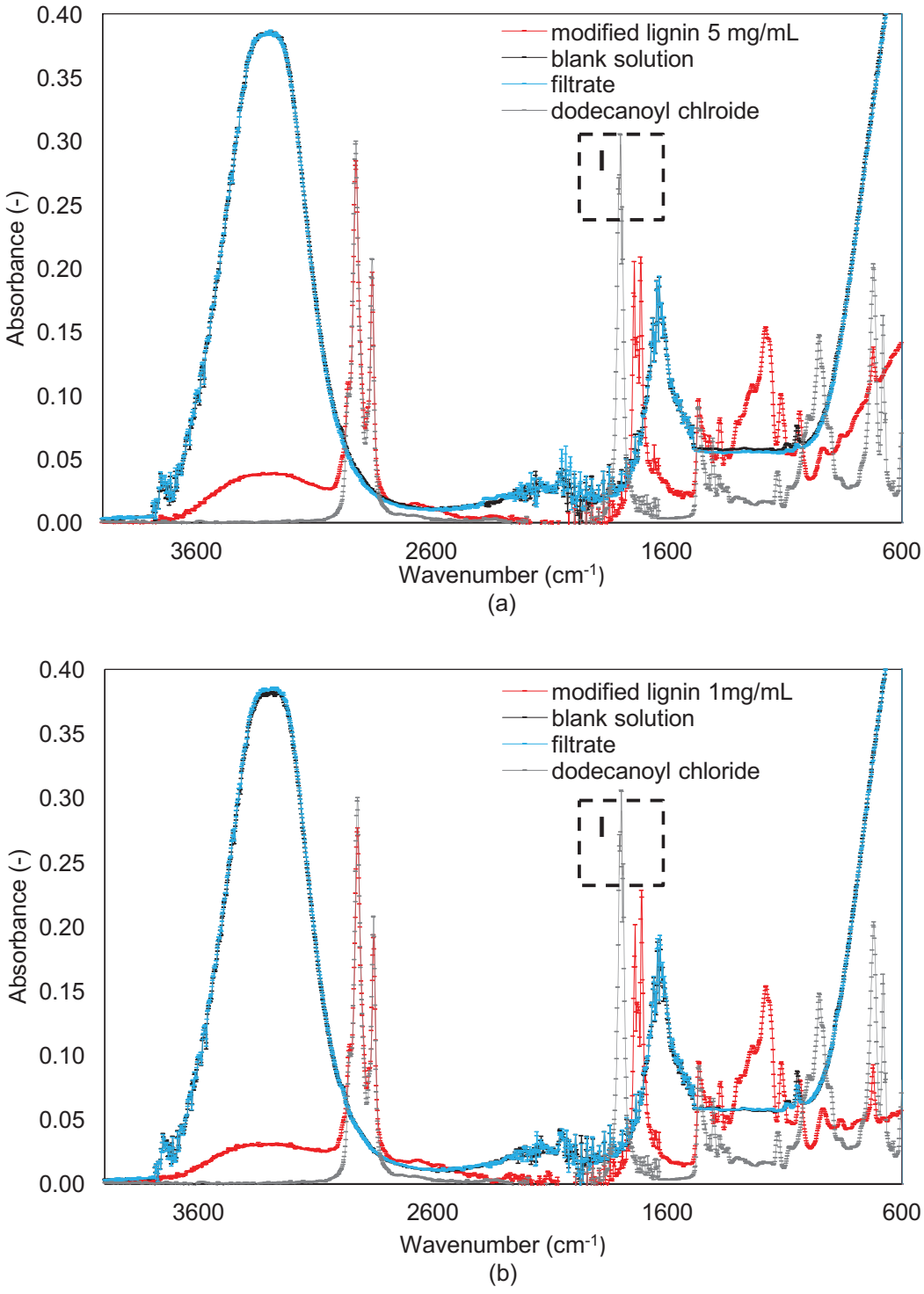

Figure 6.23. FTIR spectra of modified lignin, blank solution, filtrate and dodecanoyl chloride at (a) 5 and (b) 1 mg/mL lignin concentration.

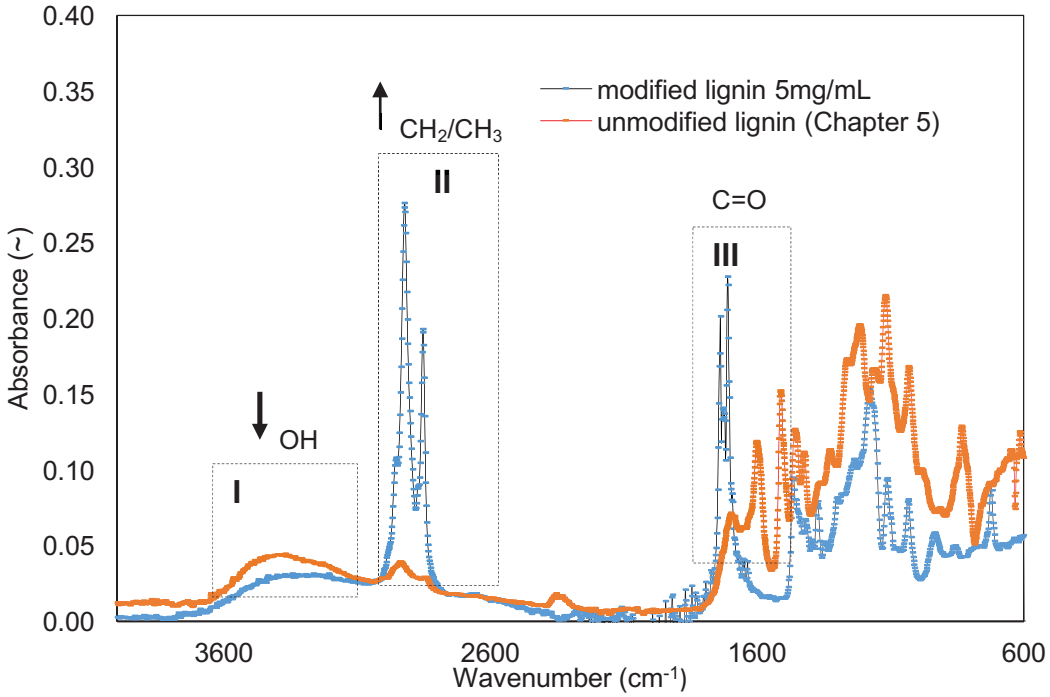

Figure 6.24. FTIR spectra of unmodified lignin and modified lignin.

Here, the esterification was assessed by FTIR which also focused on the absorbance data for quantitative analysis (Gallignani *et al.*, 2014; Khanmohammadi *et al.*, 2009). The esterification can be clearly examined by the incremental decline of the hydroxyl group at wavenumber at 3400 cm^{-1}, the incremental increase of aliphatic CH stretching from the ester groups at 2938 and 2850 cm^{-1}, and the incremental appearance of ester bonds at 1760 and 1740 cm^{-1} (phenolic and aliphatic, respectively) with a degree of added C_{12} fatty acid chloride (Koivu *et al.*, 2016; Pawar *et al.*, 2016). The dotted line in Figure 6.24 showed the specific fingerprints I, II, and III (hydroxyl group, CH stretching and ester bonds, respectively) that could be further focused for the efficacy of lignin esterification.

Overall, modified lignin showed that a decrease in the intensity of the OH stretching band in aromatic and aliphatic hydroxyl groups at 3400 cm^{-1}

CHAPTER 7: CONCLUSIONS AND RECOMMENDATIONS FOR FUTURE WORK

7.1 Conclusions

The development of economically feasible second-generation bioethanol offers promising source of energy to reduce the world's dependence on fossil fuels throughout diverse efficient separation technologies. The emerging of biorefinery concept for second-generation bioethanol produces a multitude of different valuable building blocks, namely hemicellulose, cellulose and lignin from lignocellulosic biomass. In this study, the biomass fractionation was carried out via SCW mediated hydrolysis, in which the study focused on the developing novel approaches to support enhanced added value applications of lignin.

The impact of SCW mediated hydrolysis of two different lignin extraction processing routes, DE and SE were assessed with regards to physical and chemical properties of lignin macromolecules. An assessment on percentage of delignification from DE was 81.5% whereas the SE yielded 58.0%. Although the SE showed lower efficacy of delignification than DE, the lignin macromolecules of SE exhibited higher purity of lignin and lignin derived from dried supernatant than DE. The percentage of lignin recovery was not significantly different for both lignin extraction processing routes. The FTIR analysis demonstrated that the lignin obtained by different processing routes had different chemical compositions. Overall, even though SE exerted negative impact specifically on percentage of delignification, the SE process

REFERENCES

Abbas, K. A., Mohamed, A., Abdulamir, A. S., and Abas, H. A. (2008). A review on supercritical fluid extraction as new analytical method. *American Journal of Biochemistry and Biotechnology*, *4*(4), 345–353.

Abdel-Ghani, N. T., El-Chaghaby, G. A., and Helal, F. S. (2014). Individual and competitive adsorption of phenol and nickel onto multiwalled carbon nanotubes. *Journal of Advanced Research*, *6*(3), 405–415.

Abdelaziz, O. Y., Brink, D. P., Prothmann, J., Ravi, K., Sun, M., García-Hidalgo, J., … Gorwa-Grauslund, M. F. (2016). Biological valorisation of low molecular weight lignin. *Biotechnology Advances*, *34*(8), 1318–1346.

Abdelaziz, O. Y., and Hulteberg, C. P. (2017). Physicochemical characterisation of technical lignins for their potential valorisation. *Waste and Biomass Valorization*, *8*(3), 859–869.

Abdul Khalil, H. P. S., Bhat, A. H., and Ireana Yusra, A. F. (2012). Green composites from sustainable cellulose nanofibrils: A review. *Carbohydrate Polymers*, *87*(2), 963–979.

Abidi, N., Hequet, E., Cabrales, L., Gannaway, J., Wilkins, T., and Wells, L. W. (2008). Evaluating cell wall structure and composition of developing cotton fibers using Fourier transform infrared spectroscopy and thermogravimetric analysis. *Journal of Applied Polymer Science*, *107*(1), 476–486.

Abiven, S., Heim, A., and Schmidt, M. W. I. (2011). Lignin content and chemical characteristics in maize and wheat vary between plant organs and growth stages: consequences for assessing lignin dynamics in soil. *Plant Soil*, *343*(1–2), 369–378.

Achyuthan, K. E., Achyuthan, A. M., Adams, P. D., Dirk, S. M., Harper, J. C., Simmons, B. A., and Singh, A. K. (2010). Supramolecular self-assembled chaos: Polyphenolic lignin's barrier to cost-effective lignocellulosic biofuels. *Molecules*, *15*(12), 8641–8688.

Agarwal, U. P., and Atalla, R. H. (2010). Vibrational Spectroscopy. In J. Heitner, Cyril, R. Dimmer, Donald, A. Schmidt (Ed.), *Lignin and Lignans Advances in Chemistry* (pp. 104–129). Boca Raton, United States of America: CRC Press.

Agbor, V. B., Cicek, N., Sparling, R., Berlin, A., and Levin, D. B. (2011). Biomass pretreatment: Fundamentals toward application. *Biotechnology Advances*, *29*(6), 675–685.

Alberts, B., Johnson, A., Lewis, J., Raff, M., Roberts, K., and Peter Walter. (1989). Cells in Their Social Context. In *Molecular Biology of The Cell* (Fourth, Vol. 53, p. 160). New York, USA: Garland Science.

Aleš, H., Michal, J., Lenka, D., Alexandra, S., and Igor, Š. (2015). Thermal properties and size distribution of lignins precipitated with sulphuric acid. *Wood Research*, *60*(3), 375–384.

Allen, E., Paul Smith, and Henshaw, J. (2001). *A review of particle agglomeration*. Dorset, United Kingdom.

Alriols, M. G., García, A., Llano-ponte, R., and Labidi, J. (2010). Combined organosolv and ultrafiltration lignocellulosic biorefinery process. *Chemical Engineering Journal*, *157*(1), 113–120.

APPENDICES

Appendix A

Table A1. Analysis of variance of SE and DE.

ANOVA

		Sum of Squares	df	Mean Square	F	Sig.
Purity of lignin derived supernatant	Between Groups	138.817	1	138.817	107.581	.000
	Within Groups	5.161	4	1.290		
	Total	143.978	5			
Purity of precipitated lignin	Between Groups	14.045	1	14.045	264.508	.000
	Within Groups	.212	4	.053		
	Total	14.258	5			
Percentage of delignification	Between Groups	827.905	1	827.905	3741.662	.000
	Within Groups	.885	4	.221		
	Total	828.790	5			
Percentage of lignin recovery	Between Groups	1.540	1	1.540	.956	.383
	Within Groups	6.442	4	1.610		
	Total	7.982	5			
Percentage of biomass solubilisation	Between Groups	142.984	1	142.984	229.669	.000
	Within Groups	2.490	4	.623		
	Total	145.474	5			

LIST OF PUBLICATIONS

M.H. Hamzah, S. Bowra, M.J.H Simmons and P.W. Cox (2016). Proceedings from the 24th European Conference and Exhibition: *The Impact of Process Parameters on the Purity and Chemical Properties of Lignin Extracted from Miscanthus x giganteus* using a Modified Organosolv Method. Amsterdam, The Netherlands.

M.H. Hamzah, S. Bowra, P.W. Cox and M.J.H. Simmons (2016). Proceedings from the 4th CIGR Agricultural Engineering Conference: *The Effect of Ethanol Concentration upon Formation of Organosolv Lignin Aggregates from Miscanthus x giganteus.* Aarhus, Denmark.

CHAPTER 1: INTRODUCTION

1.1 Background

Lignin is the second most abundant natural polymer on earth after cellulose and is found in all terrestrial plants and some aquatic species. The biosphere is estimated to contain 3×10^{11} tonnes of lignin with an annual biosynthetic rate of 2×10^{10} tonnes (Argyropoulos and Menachem, 1997; Hu *et al.*, 2011). Currently, lignin is recovered in large quantities as a by-product from pulping industry (Gan *et al.*, 2014). Lignin is produced by a chemical pulping process which results in a black liquor, leaving cellulose fibres for pulp production. However, the black liquor is predominantly dewatered and burned to supplement the heat requirement of the pulping operation (Mahmood *et al.*, 2016) and only 1 to 2% of the total amount of lignin produced is used in bio-based material applications (Gordobil *et al.*, 2016).

There are two basic pulping processing 1) the sulphite process which uses a mixture of an aqueous sulphur dioxide and a base such as calcium, sodium, magnesium or ammonium bisulphide and 2) the Kraft process which is based on cooking with a sodium hydroxide and sodium sulphide (Hamaguchi *et al.*, 2012; Laurichesse and Avérous, 2014; Tarabanko and Petukhov, 2003). Lignin derived from the Kraft or the sulphite process are recovered from black liquor by acidification. Lignosulphonates contains sulfonic acid groups that makes lignin water soluble. Lignosulphonates exhibit a high molecular weight with a broad distribution of polydispersity index (around 6-8) and are the most utilised lignins with applications including

CHAPTER 2: LITERATURE REVIEW

2.1 Introduction

The literature review describes the refining of biomass (biorefining) to produce diverse marketable bio-based products and bioenergy. More importantly, the use of lignocellulosic biomass focusing on *Miscanthus x giganteus (MxG)* is explored. The various lignin extraction methods published in the available literature are discussed. Finally, methods of lignin depolymerisation and modification to alter the chemical structure of lignin and to improve lignin reactivity, therefore, the range of biochemicals produced are also discussed.

2.2 Bio-based Economy and Integrated Biorefinery

Energy and material needs play an essential role in the world's future. Currently, about 80% of the world's energy markets rely on crude oil, coal and natural gas which is expected to last for around another 60 and 120 years at the current rate of consumption (Balat and Ayar, 2005; Potumarthi *et al.*, 2014). Global energy requirements, depletion of fossil fuel reserves, high cost of fossil fuels and greenhouse effects caused by fossil fuel usage have caused workers all over the world to seek another alternative and sustainable energy sources (Duku *et al.*, 2011).

First generation biofuels were produced from sugar or starch rich food crops such as sugarcane, corn and wheat. Of major environmental and ethical

and straw contain mainly xylan (Agbor *et al*., 2011). Figure 2.6 shows the main constituents of hemicelluloses.

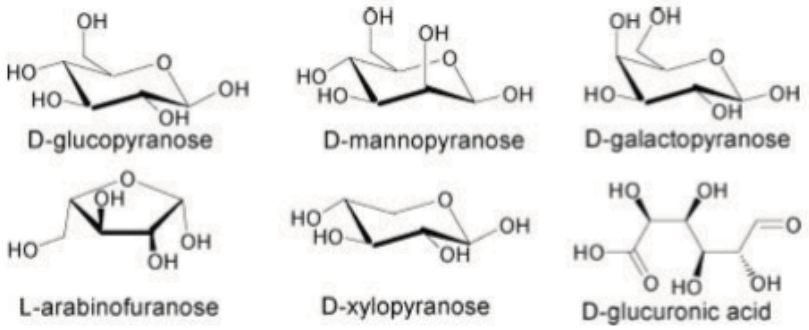

Figure 2.6. Main constituents of hemicellulose. (Source: Adapted from Mohammad, 2008).

Hemicelluloses are easily hydrolysed due to their lower molecular weight compared to cellulose and their branched structure with short lateral chain (Li *et al.*, 2010; Saha, 2003). The degree of polymerisation of hemicelluloses is between 80 to 200 sugar units and average molecular weight of < 30,000 (Anwar *et al.*, 2014; Mohammad, 2008). Substantial amount of hemicelluloses and lignin need to be removed from cellulose fibres, rendering the cellulose more accessible for enzymatic hydrolysis process (Agbor *et al*., 2011). Nevertheless, process conditions including temperature, reaction time, moisture content and pH must be carefully chosen to prevent formation of undesirable products such as fulfural and hydroxymethylfulfural that have been shown to hinder the fermentation process (Agbor *et al.*, 2011; Jönsson and Martín, 2016).

Hemicelluloses provide a renewable material supply for wide variety of industrial applications, for example, xyloglucans from hemicellulose have been used for pharmaceutical applications such as antibiotics and a treatment

for ulcers (Pauly *et al.*, 2013). Hemicellulose sugars, pentose (xylose and arabinose) and hexose (glucose, galactose and mannose) also have been utilised for conversion of lignocellulosic materials to fuel ethanol and other value added fermentation products including 5-hydroxymethylfurfural (HMF), furfural, levulinic acid, and xylitol (Canilha *et al.*, 2003; Saha, 2003). Moreover, hemicelluloses act as wet strength additives in papermaking, viscosity modifiers in food packaging film as well as tablet binders (Peng *et al.*, 2012).

2.4.3 Lignin

Lignin is built up from three different phenyl propane monomers, which form complex macromolecules, which then form an amorphous, three-dimensional polymer. The three phenyl propane monomers, namely *p*-coumaryl, coniferyl and sinapyl alcohol differ in the substitution at the 3 and 5 positions (Mansouri and Salvadó, 2006) as shown in Figure 2.7. Lignin is formed via two types of linkages; condensed linkages (e.g. 5-5 and β-1 linkages) and ether linkages (e.g. α-O-4 and β-O-4 linkages) (Abiven *et al.*, 2011; Zobel and Buijtenen, 1989). Figure 2.8 shows the structure of major bonds in lignin.

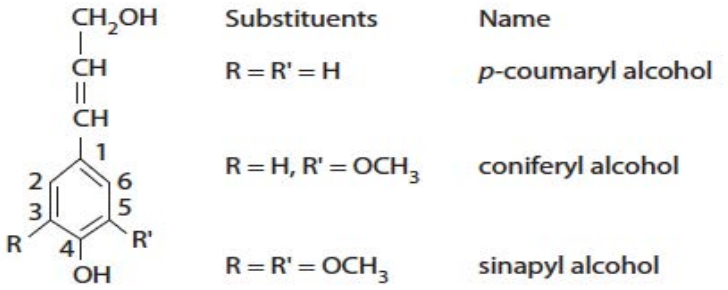

Figure 2.7. Lignin monomeric building blocks. (Source: Adapted from Lapierre, 2010).

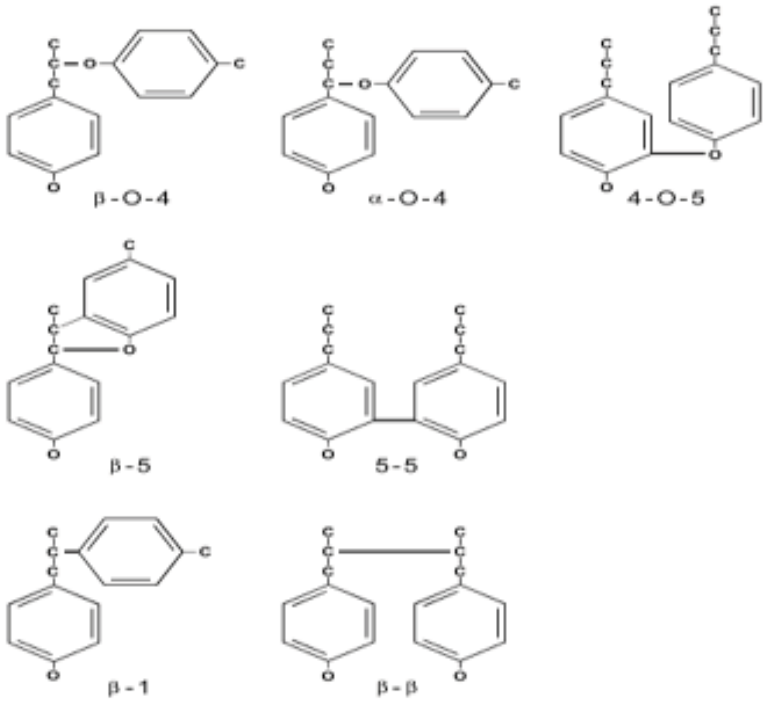

Figure 2.8. Structure of the major bonds in lignin. (Source: Adapted from Kogel-Knobner, 2002).

The starting points for the formation of guaiacyl and syringl structures of lignin are derived from coniferyl and sinapyl alcohol as outlined in Figure 2.9.

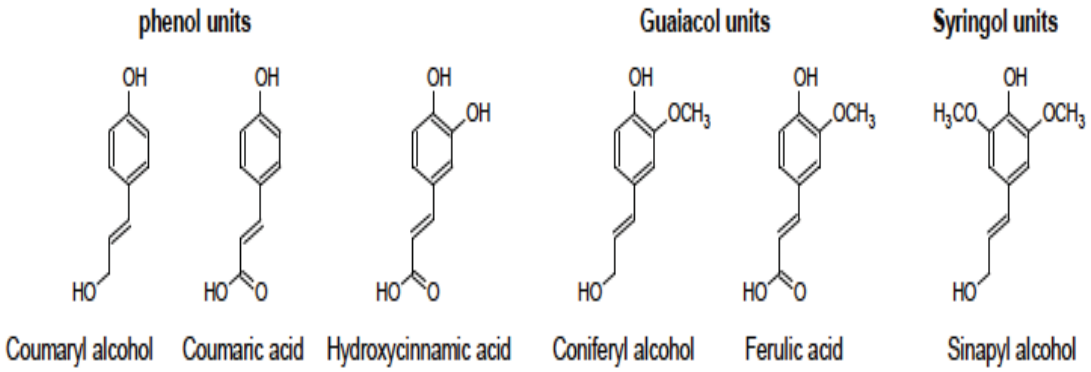

Figure 2.9. Types of phenyl propanoids units found in lignin. (Source: Adapted from Holladay *et al.*, 2007).

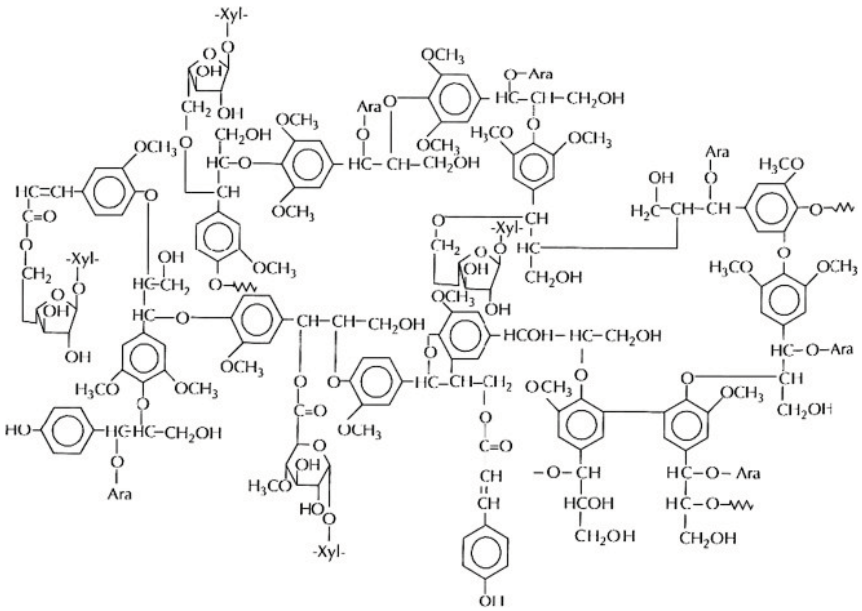

Figure 2.10. A structural model of wheat straw lignin. (Source: Adapted from Ghaffar and Fan, 2014).

Lignin plays various roles in plants, alongside the main natural components of cellulose and hemicellulose. Lignin gives stiffness and structural stability of a plant cell wall by cementing and fixating lignin with other polysaccharides in the plant cell wall (Alberts *et al.*, 1989). The presence of lignin makes the plant fibres more rigid and stiff, providing mechanical support for the stem and branches enabling healthy plant growth (Henriksson, 2009). Besides, lignin also works as glue that binds the individual plant cells and the other carbohydrate polymers in the complex secondary wall (Achyuthan *et al.*, 2010). Lignin makes the cell wall in intercellular regions of xylem by providing the hydrophobic capillary surface needed for nutrient transport (Leisola *et al.*, 2012; Myburg *et al.*, 2013). Moreover, lignin serves an essential function in plant defense. The lignified cell wall serves as a barrier against microorganisms by preventing the

from 2 to 44 tonnes/ha dry matter; yields range from 27 to 44 tonnes/ha in Europe and the USA Midwest, and from 10 to 11 tonnes/ha in Canada (Heaton *et al.*, 2008; Pyter *et al.*, 2007; Scurlock, 1999; Xi and Jezowski, 2004).

Figure 2.11. *Miscanthus* sp. energy crop. (Source: Adapted and modified from Falter *et al.*, 2015).

Miscanthus spp. originated in Japan and first cultivated in Europe in the 1930s (Brosse *et al.*, 2012). Seasonal changes and with its bioclimatic location may have affected the relative composition of biomass including *MxG* (Savy and Piccolo, 2014). Other factors that affect the biomass yield and composition of *Miscanthus* sp. are genotypes, soil types, nutrients used as well as crop age (Brosse *et al.*, 2012).

When comparisons are made with other genotypes, *MxG* has a strong range of potential benefits including the possibly unique and exclusive trait for

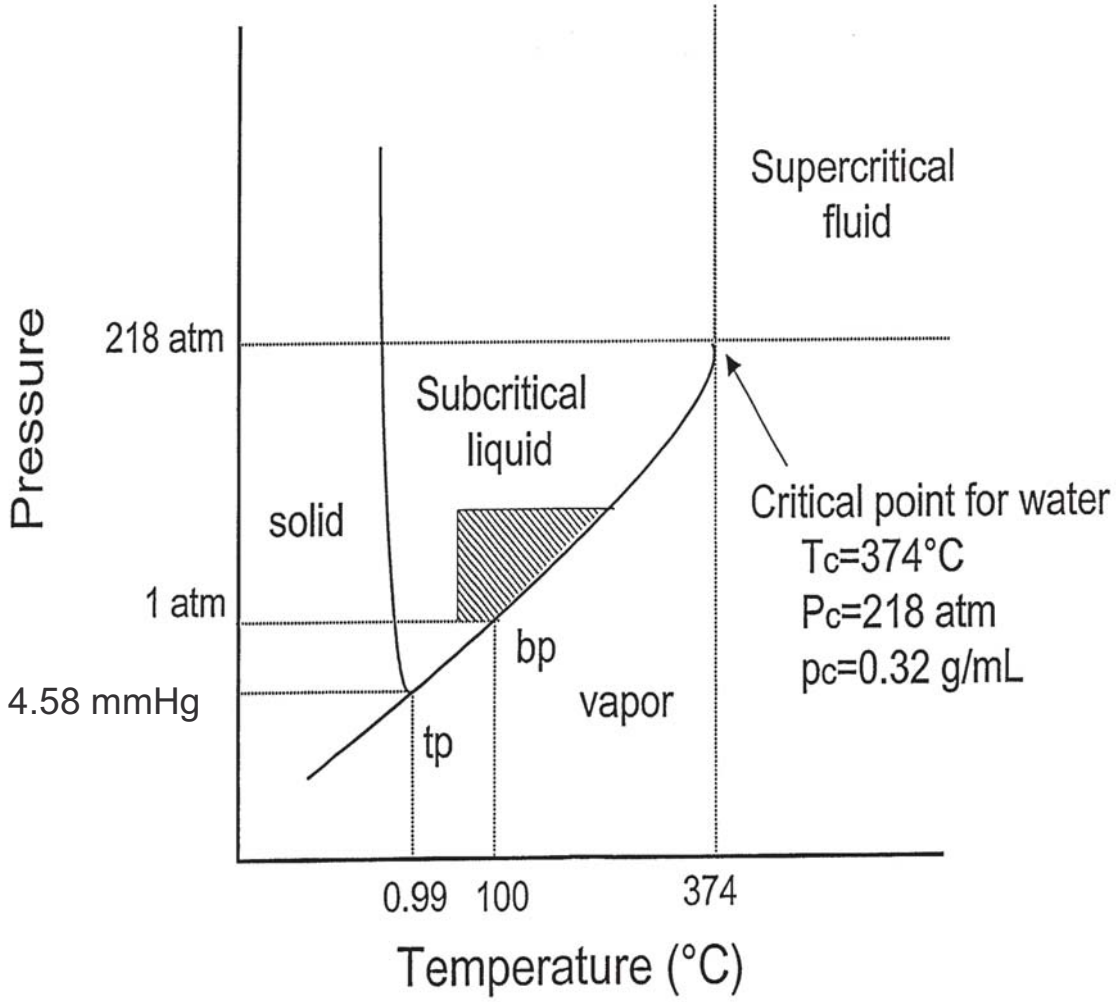

Figure 2.14. Phase diagram of water as a function of temperature and pressure. (Source: Adapted from King and Grabiel, 2007).

The SCW has several unique properties compared to water at ambient conditions especially for its dielectric strength and ionic product that causes dramatic changes in physical properties (Rogalinski *et al.*, 2008). Dramatic rise of temperature in SCW causes a decrease in permittivity, an increase in the diffusion rate and a decrease in the viscosity and surface tension (Asl and Khajenoori, 2013). As a result, more polar target materials with high solubility in water at ambient conditions are extracted most effectively at lower temperatures, while moderately polar and non-polar materials need a less polar medium influenced by elevated temperature (Asl and Khajenoori, 2013;

pulping agent, the pulping medium will become highly acidic and alkaline for sodium sulphite. The main reaction scheme for lignosulphonate formation during acid sulphite pulping is illustrated in Fig. 2.16.

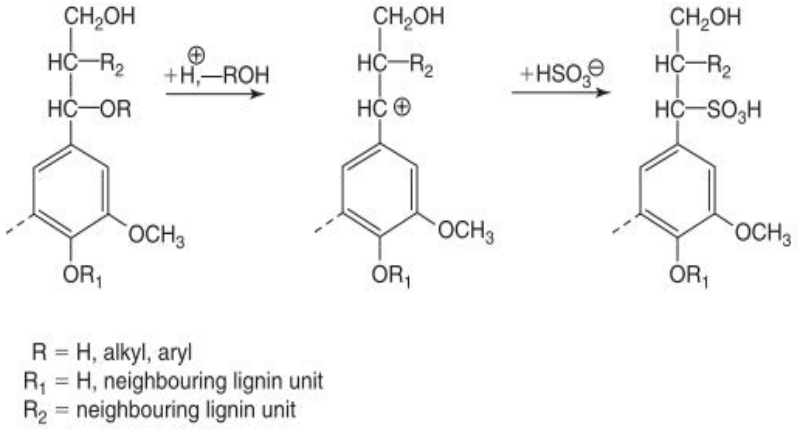

Figure 2.16. Main reaction scheme for lignosulphonate formation during acid sulphite pulping. (Source: Adapted from Lora, 2008).

Lignosulphonate has good water solubility at all values of pH and has been used by industry in a wide variety of applications. Lignosulphonate has been used as a binder or glue in pellets or compressed materials (Tumuluru *et al.*, 2011) and also used to reduce dust particles and stabilise the road surfaces (Edvardsson, 2010). This binding ability makes lignosulfphonate an essential component of materials such as ceramics, animal pellets, coal briquettes and others (Lora, 2008). In addition, lignosulphonate also acts as a dispersant especially in concrete mixes. Lignosulphonate attaches to the particle surface, keeps the particle from being attracted to the other particles and reduces the amount of water needed for cement or concrete mixes (Yang *et al.*, 2008).

ester substituent by nucleophilic substitution (Cachet *et al.*, 2014; Wang *et al.*, 2017) and thus, reduce the intermolecular interactions of hydrogen bonding, providing a plasticisation phenomena and mobility of the chains (Lisperguer *et al.*, 2009). Figure 2.17 showed the esterification mechanism of kraft lignin modified using acid chlorides that produces kraft lignin with more reactive aliphatic hydroxyl units.

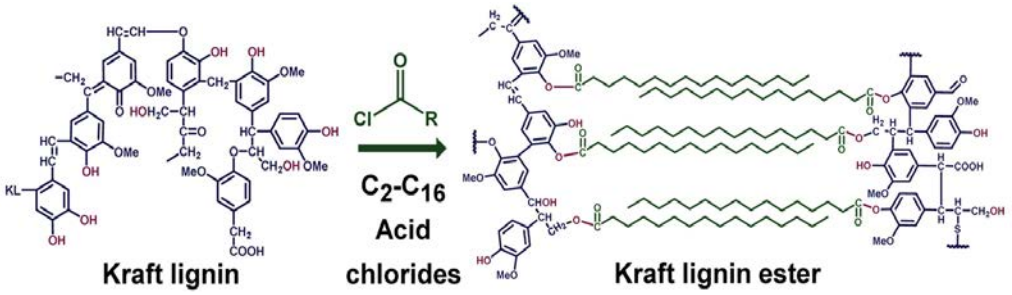

(a)

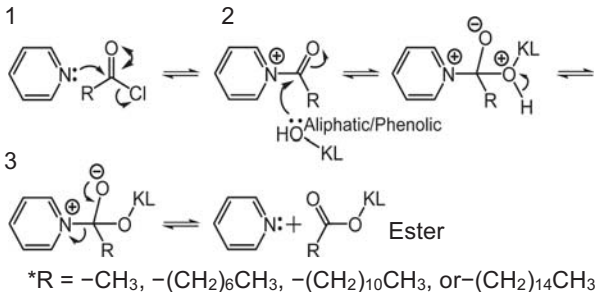

1.Addition of the nucleophile.
2.Elimination of the leaving group, forming the tetrahedral intermediate.
3.Loss of a proton.

(b)

Figure 2.17. (a) Esterification of kraft lignin using acid chlorides (b) Mechanism of pyridine catalysed klason lignin esterification with C_2–C_{16} fatty acid chlorides (Source: Adapted and modified from Koivu *et al.*, 2016).

2.9.2.1 Esterification

Esterification is one of the simplest ways to modify the hydroxyl groups within lignin and depends on the reaction parameters and reactants used

2.9.2.4 Urethanisation

The first urethane was discovered as early as 1849 by Wurtz. Works conducted by Dr. Otto Bayer at IG Farbenindustrie, Germany in 1937 synthesised the first polyurethane using the urethanisation process involving terminal hydroxyl groups in reaction with addition of di-isocyanates or polyisocyanates, forming polyurethane groups in the polymer backbone as shown in Figure 2.22 (Ionescu, 2005; Upton and Kasko, 2015).

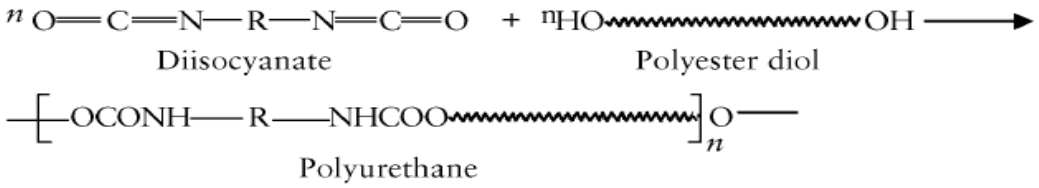

Figure 2.22. Reaction involving hydroxyl groups with isocyanate groups, active RNC=O sites to form a urethane. (Source: Ionescu, 2005).

Lignin is utilised either directly without further chemical modification or after chemical modification with different polyols to produce polyurethane; the latter approach is the most practical method for industrial applications (Laurichesse and Avérous, 2014). A study by Ciobanu *et al.* (2004) of lignin-polyurethane films reported various properties in a series of blends prepared by solvent casting technique obtained in dimethyl formamide solutions from a polyurethane elastomer and different proportions of flax/soda pulping lignin. A major finding was observed in that adding up to 5% lignin contributed to the polyurethane elastomer strength and biodegradability, simultaneously with lower decomposition temperature and elasticity. Hatakeyama *et al.* (2005) studied the mechanical properties of polyurethane-based biocomposites derived from lignin and molasses that could be applied in the field of housing

CHAPTER 3: MATERIALS AND METHOD

3.1 Introduction

This chapter describes the general materials and methods used throughout the work for characterisation and quantification analysis.

3.2 Feedstock and Reagents

Miscanthus x giganteus (*MxG*), a lignocellulosic biomass, was grown and harvested in Aberystwyth, Wales, United Kingdom and provided by the Institute of Biological, Environmental and Rural Sciences (IBERS, UK) and Phytatec (UK) Ltd. The biomass was stored dry and in the dark.

Absolute ethanol (Fisher Scientific, UK), nitrogen (compressed oxygen free nitrogen, BOC, UK) and carbon dioxide (vapour withdrawal, BOC, UK) used had ≥ 99.8% purity. 72% sulphuric acid (Fluka-Sigma Aldrich, UK), pyridine (Sigma-Aldrich, UK), dodecanoyl chloride (Sigma-Aldrich, UK), hydrochloric acid (VWR, UK), and HPLC grade water, HiPerSolv CHROMANOR® (VWR Chemicals, France) were used as reagents.

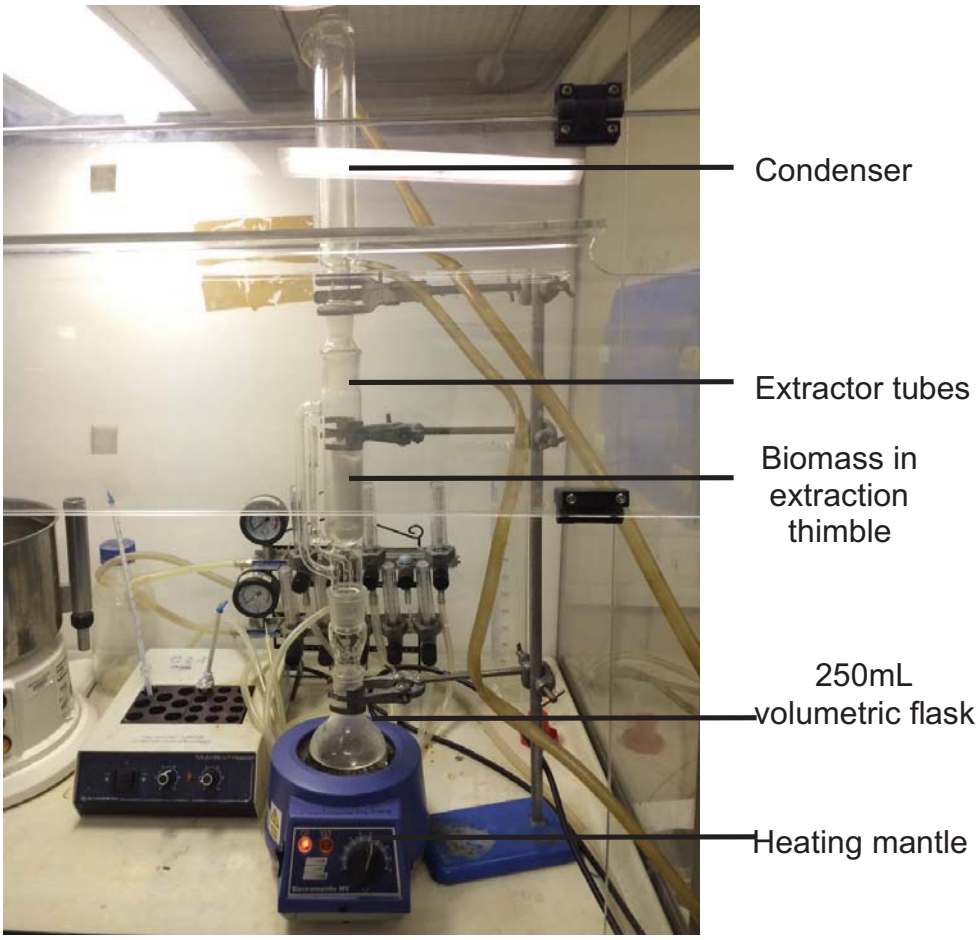

Figure 3.1. Soxhlet apparatus experimental set-up.

The thimble containing the Miscanthus biomass was placed into a Soxhlet apparatus. 200 mL of HPLC grade water added to the receiving flask before it was coupled to the Soxhlet apparatus. The water was refluxed through the biomass for 16 hours, before replacing with 200 mL ethanol. The ethanol was again refluxed for another 16 hours. At the end of ethanol extraction step, the thimble was removed from the Soxhlet apparatus and the residual biomass was filtered through a Pyrex sintered disc funnel porosity 2 using a vacuum filtration unit (VP100 High Savant Vacuum Pump). The biomass was washed three times with 100 mL of fresh ethanol and then dried

species present in the sample (Manley, 2014). Thus, it is very challenging to interpret the overlapping peaks.

In summary, FTIR spectra contain a large amount of information including chemical bonds and compositional; thus, chemometric techniques analysis, such as multivariate analysis, are promising methods for further details of spectra analysis (Xu *et al.*, 2013).

3.4.2 Principal Component Analysis (PCA) on FTIR data

PCA is an essential mathematical tool to verify the correlations that exists within multivariable data. Analysis of FTIR spectra datasets by PCA determines the differences between spectra in terms of chemical structure and composition of the samples (Chen *et al.*, 1998; Labbé *et al.*, 2006). PCA transforms a one-dimensional dataset to multi-dimensional dataset that is dependent on the projection of principal components. The principle of PCA is denoted with a matrix of data with N rows (observations) or Y and K columns (variables) or X in a multidimensional variable space as shown in Figure 3.2. Y can be analytical samples and X can be spectral origin or chromatographic origin.

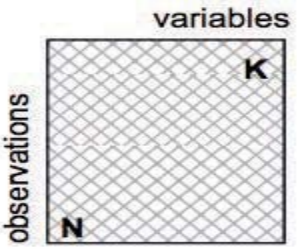

Figure 3.2. Notation used in PCA. (Source: Adapted from Eriksson *et al.*, 2006).

Each observation is represented by a point in the variable space. The whole dataset then constitutes a swarm of points in the variable space. PCA finds a line or planes in K dimensional variable space that approximates the data using the principle of least squares and statistically minimising the variance (Eriksson *et al.*, 2006). Figure 3.3 shows the derivation of a PCA model. The line is the direction of the first principal component (PC1) and points in the direction of the maximum variation.

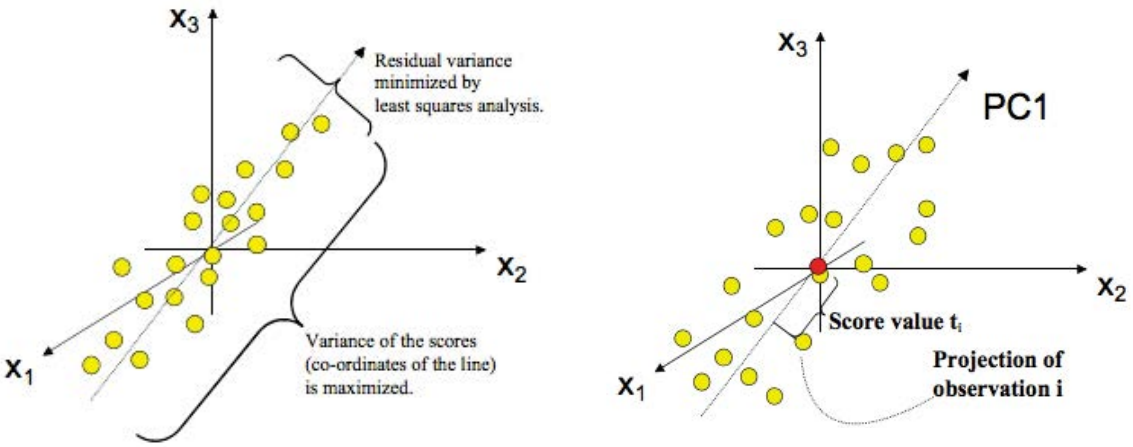

Figure 3.3. Derivation of a PC1 model. (Source: Adapted from Eriksson *et al.*, 2006).

The first principal component may not be enough to explain the data variation. By projecting the samples onto the new coordinate system, there may still unexplained variance. If the projection process is extended orthogonal to the first PC in the remaining part of the space, the second principal component (PC2) is created as shown in Figure 3.4. The process can be continued to find more PCs.

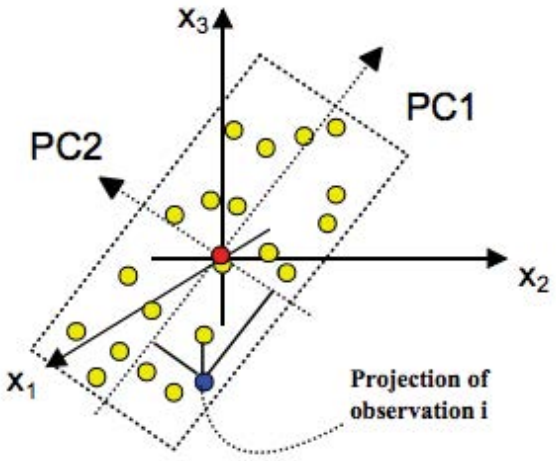

Figure 3.4. Second Principal Component (PC2). (Source: Adapted from Eriksson *et al.*, 2006).

The percentage of explained variance decreases with increasing of principal components, and could describe the variability between spectra (Grootveld, 2012). The explained variance gives the results based on calibrated and validated variance. The calibrated variance measures the model fit whereas the validated variance measures the new variance data or predicting the difference or error associated between projected and measurement data (Esbensen *et al.*, 2002).

A two-dimensional plot of the projected objects by using PC1 and PC2 create a new coordinate system and a map of objects in the principal components plot a so-called a score plot. In the case of spectra analysis, score is described by the degree of correlation for each spectra of each principal component whereas each principal component is associated with loadings that contribute by wavenumbers (Cordella, 2012; Kline *et al.*, 2010).

The score plot reveals the sample patterns, groupings, similarities and differences amongst the distribution of samples. For instance, in the

determination of lignin content in grass, hard and soft woods following analysis of biomass dissolved in ionic liquids, the cluster of grass, hard and soft wood could be observed in Figure 3.5. Thereby, spectra that cluster together on the scores plot reveal any similarity of chemical composition and structure between spectra. Thus, if the spectra from samples showed similar characteristics, these spectra were chosen for analysis.

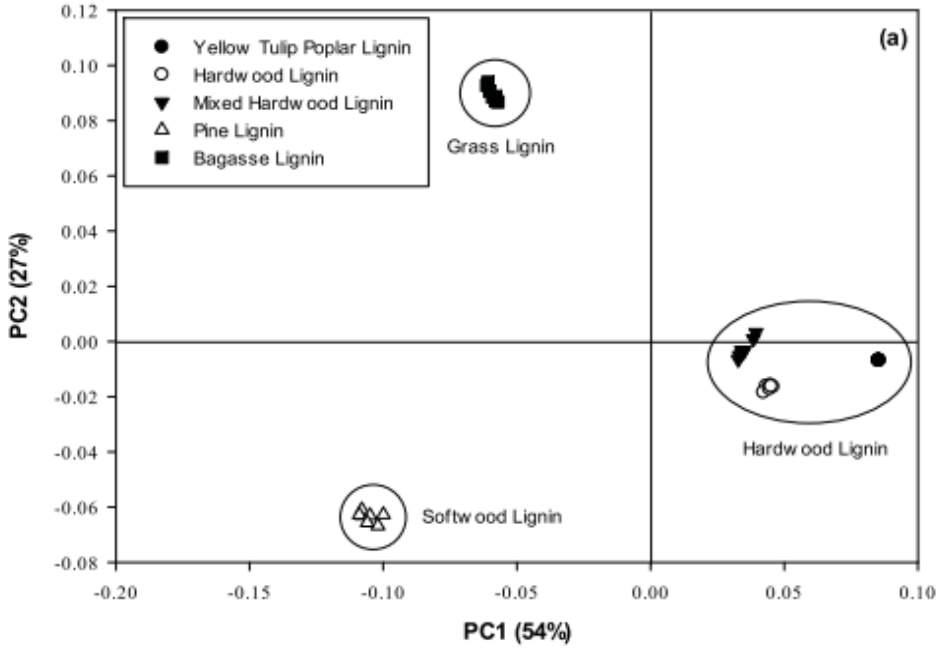

Figure 3.5. Score plot as a function of PC1 and PC2. (Source: Adapted from Kline *et al.*, 2010).

Loading plot is used to find correlation patterns among variables and the more significant variables (Lupoi *et al.*, 2013). For example, in the work to evaluate the influence of formulation and process variables on mechanical properties of oral mucoadhesive films using multivariate analysis, further analysis on data of films without a nonwoven textile were studied (Landová *et al.*, 2014). In the loading plot shown in Figure 3.6, the variables that are close to each other to the left loadings plot (dotted line of circle) and far from the center circle, very close to the 100% explained variance, which means,

therefore, they correlate positively (Cordella, 2012). Here, the analysis of the loadings plot emphasises the PC1 that captures maximum variability in the data.

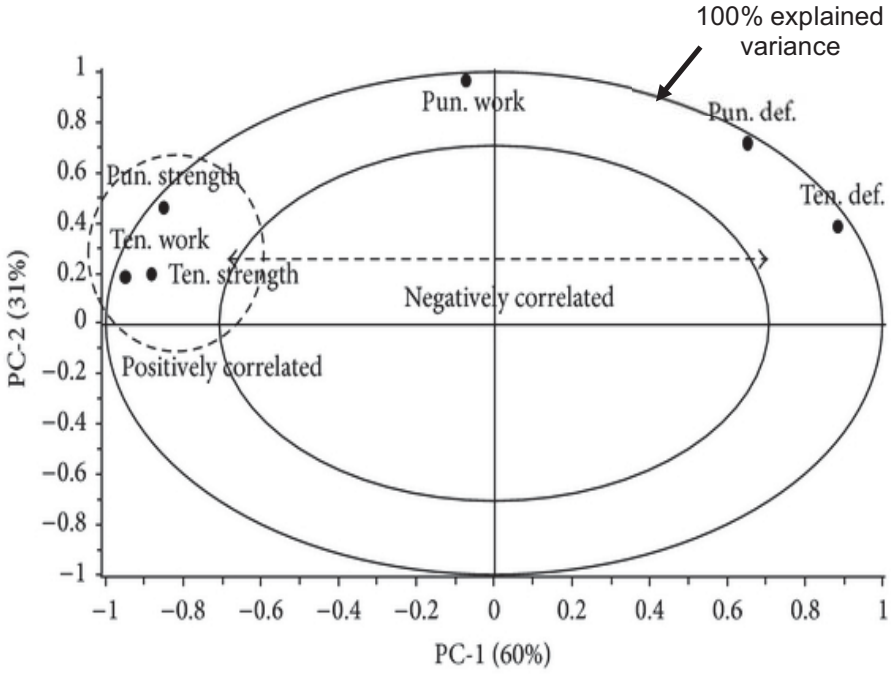

Figure 3.6. Loading plot for PC1 and PC2 for data of films without a nonwoven textile (Source: Adapted and modified from Landová *et al.*, 2014).

In general, the similarities or differences among sample and variables could not be detected easily in terms of the raw data. In practice, there is often a need to slightly modify the shape of the data to better suit an analysis, such modification is called preprocessing or pretreatment. There are various pretreatments including baseline correction, scatter correction, derivatives, normalisation or spectroscopic transformations (Luthria *et al.*, 2013).

Here, the spectra data collected was subjected to two types of pretreatment including smoothing and normalisation prior to PCA analysis. A smoothing function is to reduce noise and improve spectral resolution (Stuart, 2004). Normalisation of FTIR data transforms and maps the data into a

CHAPTER 4: AN EVALUATION OF IMPACT OF DIRECT AND SEQUENTIAL EXTRACTION PROCESSES ON THE PURITY AND CHEMICAL PROPERTIES OF LIGNIN FROM *MISCANTHUS X GIGANTEUS*

4.1 Introduction

In the biorefinery approach, lignin and carbohydrates which are the biomass recalcitrant components need to be removed, so that the cellulose fibres become more accessible and amenable for bioethanol production via enzymatic and microbial hydrolysis (Pu *et al.*, 2013). In such a context of the biorefinery approach, this work is carried out by sequential processing, thus enabling recovery of multiple naturally occurring biopolymers namely hemicellulose, cellulose and lignin which then become the feedstock for either direct application or subsequent downstream transformation.

In this chapter, sub-critical water (SCW) is applied at pressures up to 50 bar over a temperature range from 120°C to 200°C, depending on the targeted components to recover. Several studies have demonstrated that temperature has a pronounced influence on conversion rate of lignocellulosic biomass in SCW hydrolysis. The extraction temperature used is commonly within the range of 130°C to 240°C, conversion also depends on other factors such as particle size and solid to liquid ratio (Borrega *et al.*, 2011). From another point of view, Yedro *et al.* (2014) proposed that the SCW fractionation can be performed at mild conditions (<100°C) to remove the water-soluble

extraction (**DE**), *MxG* was subjected to a single treatment step which is similar to third treatment in SE by the SCW with associated modifiers.

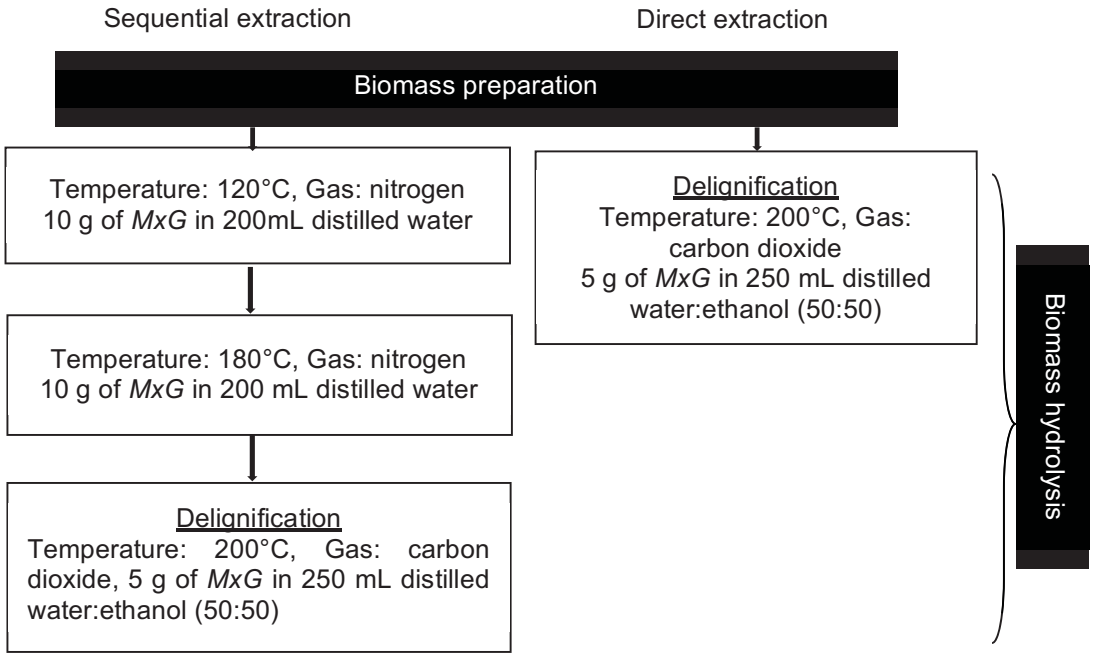

Figure 4.1. Flow chart of SE and DE.

4.2.2 Biomass Preparation

Materials used in this work are described in section 3.2. Prior to hydrolysis, the Miscanthus biomass was mixed in distilled water, then warmed to 50°C to soften the grass. The mixture was then soaked for 20 minutes to rehydrate the grass. The mixture was milled for three minutes in a domestic blender to reduce the particle size of material. The grinding conditions of temperature, soaking time, grinding time and solid:liquid ratio were previously optimised to yield an average particle size of 500 μm (Roque, 2013).

The Miscanthus biomass slurry was placed inside the reactor directly after sample preparation for SE at 120°C. Then, the sequentially processed

after cooling in a desiccator for calculation of biomass solubilisation. The percentage of biomass solubilisation was calculated using Eq 4.1.

$$\%\ \text{of biomass solubilisation} = \frac{\text{A}}{\text{B}}\ \text{x}\ 100\% \quad (4.1)$$

Where A is the weight of dried solution, g; B is the initial weight of biomass, g.

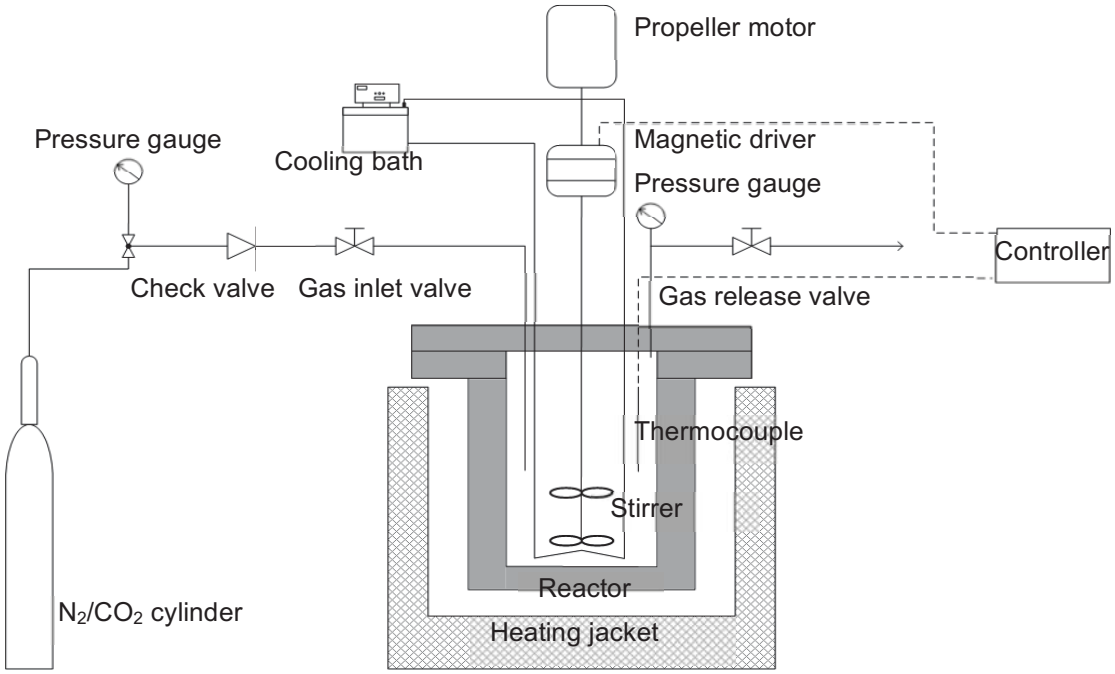

Figure 4.2. Schematic diagram of experimental set-up of Miscanthus biomass hydrolysis for DE and SE.

4.2.4 Lignin Precipitation

The filtrate from vacuum filtration was placed in a freezer at -20°C for 2 hours, after which the ethanol concentration was adjusted to 25% by adding distilled water. Lignin was recovered using a Beckman, model J2-21 centrifuge with a JA-10 rotor at 4°C and at 10,000 revolutions per minute (RPM), 17700 relative centrifugal force (RCF) for 10 minutes. The remaining supernatant was dried at 65°C for further Klason lignin assay and FTIR

MxG fibre after delignification for *MxG* which had been subjected to sequential sub-critical water mediated hydrolysis (SE). A second cluster on the right hand side, consists of the spectra for *MxG* fibre before and after delignification for DE. Thereby, Figure 4.9 shows the spectra of DE and SE were distinguishable from each other.

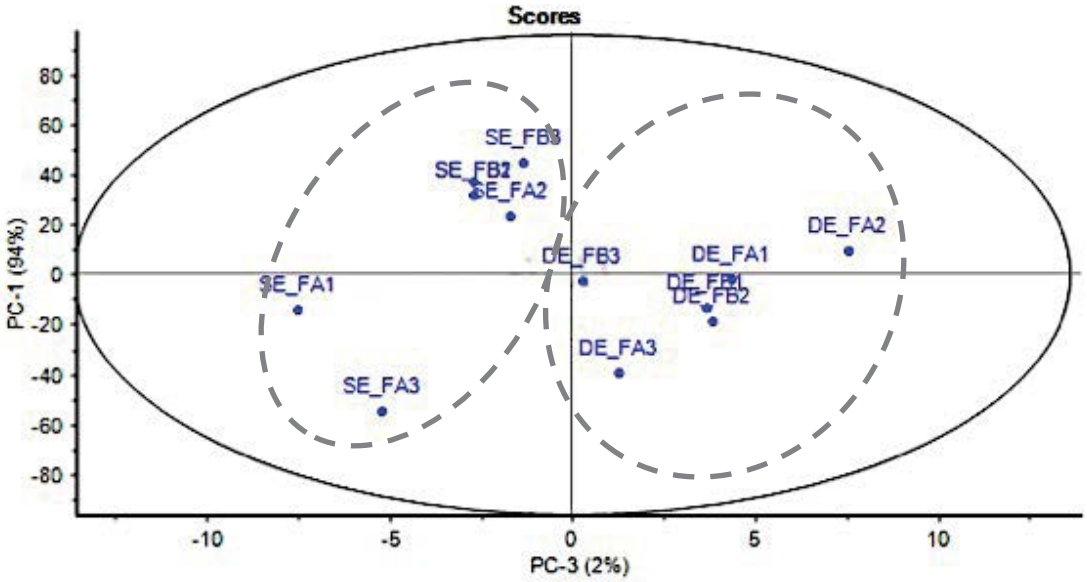

Legend:
SE_FA: Sequential extraction- *MxG* fibre after delignification
SE_FB: Sequential extraction- *MxG* fibre before delignification
DE_FA: Direct extraction- *MxG* fibre after delignification
DE_FB: Direct extraction- *MxG* fibre before delignification
**1,2,3- Repetition of spectra

Figure 4.9. PCA scores plot for solid fraction.

When comparison is made between samples among SE itself, (SE_FB1 and SE_FB2) and (SE_FA1 and SE_FA3) correlations were in the same quadrant. For DE, (DE_FB1 and DE_FB2) and (DE_FA1 and DE_FA3) correlations were in the same quadrant too. The closer the spectra are in the same quadrant; the spectra possess similar chemical composition. Thus, only a spectra was chosen from spectra that have similar chemical composition to be analysed for FTIR analysis.

Based on the correlation loadings plot in Figure 4.10, it is possible to acquire information related the chemical aspects involved in the DE and SE process. All wavenumbers related to lignocellulosic biomass as identified by FTIR (4000 to 600 cm^{-1}) have an extreme position on the top of the correlation loadings plot except for a wavenumber of 780 cm^{-1}.

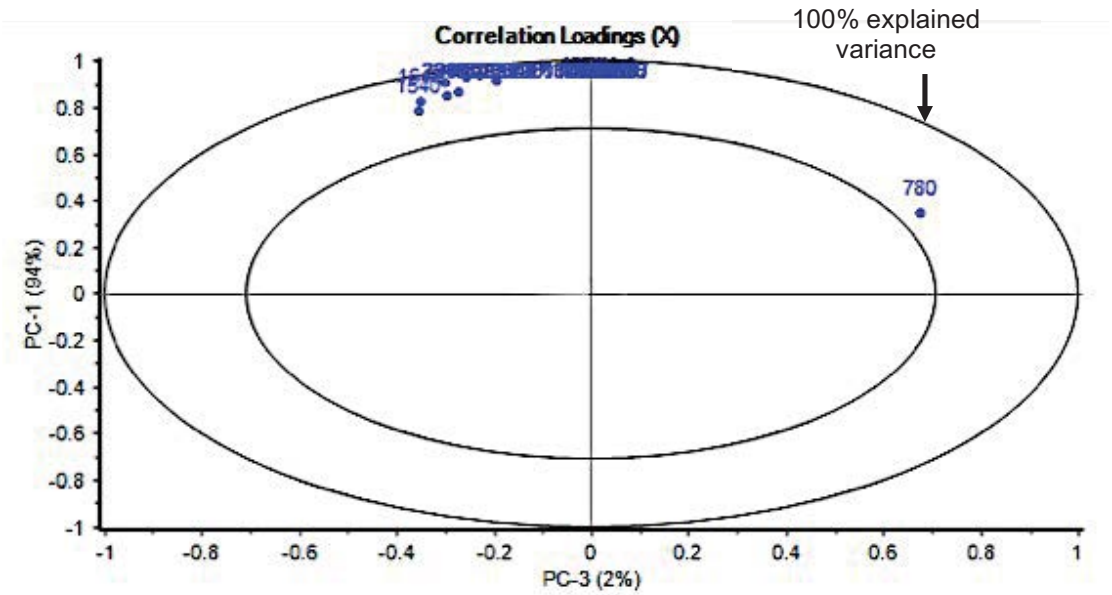

Figure 4.10. PCA correlation loadings plot for solid fraction.

The wavenumbers at the top of the plot are close to each other, and far from the centre of circle, very close to the 100% explained variance circle; they correlate positively. Wavenumber of 780 cm^{-1} which refers to 1,2-disubstitution (ortho) C-H aromatic ring (aryl) groups (Coates, 2000) had influenced the result of PCA score plot. In spite of fact that, even though the loadings plot could not explain clearly what PC1 and PC3 describes, the score plot can differentiate the samples according to different extraction methods and to answer simple questions such as if the spectra represent significant differences.

scores illustrated that the spectra possess similar chemical composition.

Table 4.2. Scores table for similar chemical composition.

Spectra category	Spectra of similar chemical composition
SE_L	SE_L2 and SE_L3
SE_S	SE_S1 and SE_S2
DE_L	DE_L1 and DE_L2
DE_S	DE_S1, DE_S2 and DE_S3

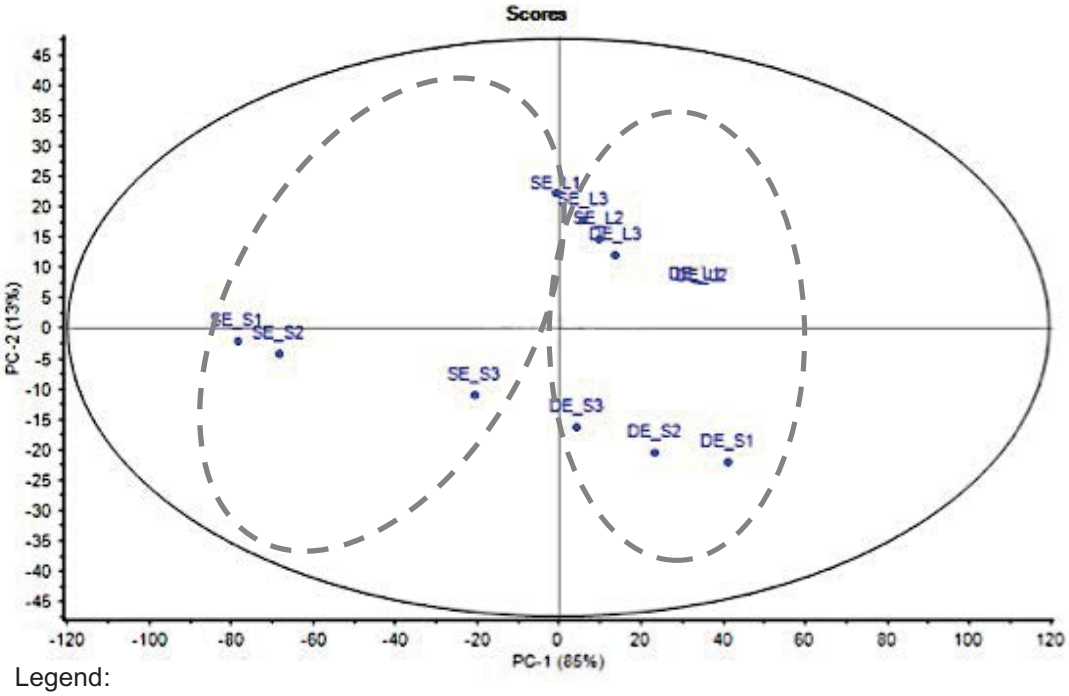

Legend:
SE_L: Sequential extraction- Precipitated lignin
SE_S: Sequential extraction- Dried supernatant
DE_L: Direct extraction- Precipitated lignin
DE_S: Direct extraction- Dried supernatant
**1,2,3-repetition of spectra

Figure 4.12. PCA scores plot for liquid fraction.

PCA correlation loadings are shown in Figure 4.13. Two wavenumbers, 2340 and 780 cm^{-1} are separated from the other wavenumbers corresponding to lignocellulosic biomass of FTIR analysis (4000 to 600 cm^{-1}) which affected the data variability of PCA. The wavenumbers of 2340 and 780 cm^{-1} are negatively correlated negatively as they are near to the centre and far from

the circle at 100% explained variance.

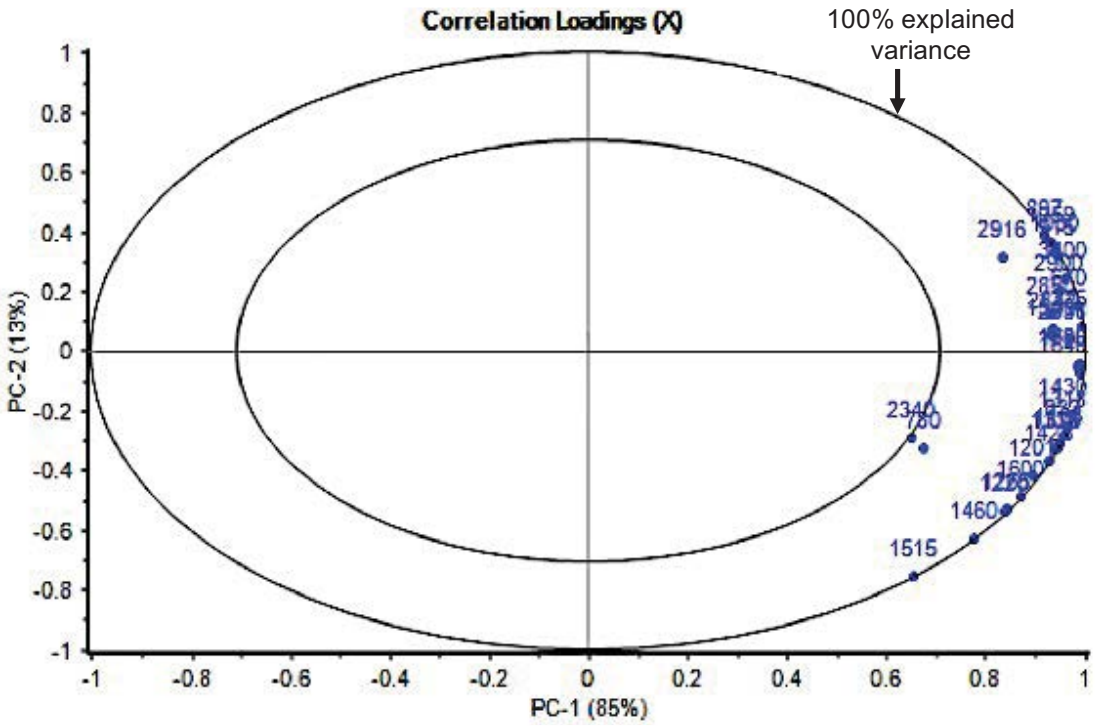

Figure 4.13. PCA correlation loadings plot for liquid fraction.

4.3.5.3 Spectra of Precipitated Lignin

Spectra of precipitated lignin, analysed by FTIR, for both DE and SE are shown in Figure 4.14. In general, spectra of precipitated lignin for SE presents stronger and broader intensity spectra than DE. The typical peaks at wavenumbers of lignin were found: 3400, 1705, 1600, 1650, 1515, 1460, 1425, 1326, 1265, 1220, 1033, 1118, 915 and 833 cm^{-1}. The details of wavenumbers and interpretations are outlined in Table 4.3.

CHAPTER 5: AN ASSESSMENT OF ETHANOL CONCENTRATION EFFECT UPON FORMATION OF ORGANOSOLV LIGNIN AGGREGATES FROM *MISCANTHUS X GIGANTEUS*

5.1 Introduction

Lignin isolated via different extraction methods can vary widely in terms of chemical composition and molecular structure. The differences also affect the physical properties such as solubility and molecular weight (Bruijnincx *et al.*, 2016). Therefore, in the context of the growing interest in developing value added uses for lignin, this chapter examines the characterisation of lignin extracted via a SCW method; with particular emphasis on the formation of lignin aggregates.

There is insufficient information available to describe the association behaviour of lignin macromolecules in solution as this depends on the solvent conditions and lignin structure (Ratnaweera *et al.*, 2015). But an understanding of the formation and assembly of lignin aggregates in solution are relevant and significant, as the heterogeneity and complex lignin structure become the greatest bottleneck in lignin utilisation for bio-based materials (Baker and Rials, 2013; Vishtal and Kraslawski, 2011).

Numerous studies on lignin aggregates have been conducted in conjunction with different methods and sources of lignin such as aggregation and assembly of alkali lignin in iodine (Deng *et al.*, 2011), the impact of lignin source on its self assembly in dimethyl sulfoxide solution (Ratnaweera *et al.*, 2015) and the aggregation of acetylated lignins in *N,N*-dimetylacetamide

respectively. Figure 5.4 of PCA scores plot for precipitated lignin and dried supernatant elucidated that there were two definite clusters observed and were distinguishable within each other. At the top are the spectra for the precipitated lignin at different ethanol concentrations. A second cluster at the bottom, consists of spectra for the dried supernatant.

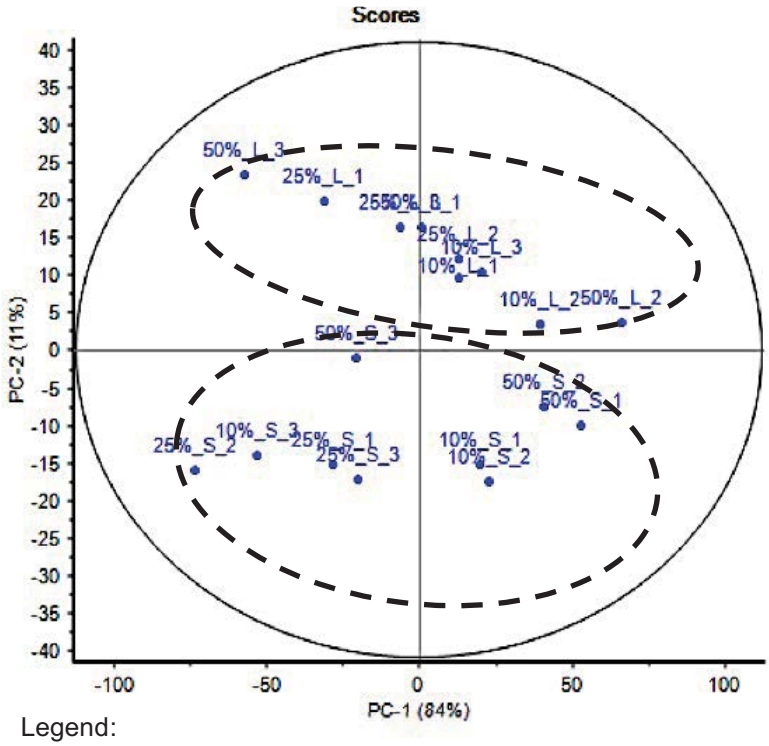

Legend:
10%_L: Precipitated lignin of 10% ethanol concentration
25%_L: Precipitated lignin of 25% ethanol concentration
50%_L: Precipitated lignin of 50% ethanol concentration
10%_S: Dried supernatant of 10% ethanol concentration
25%_S: Dried supernatant of 25% ethanol concentration
50%_S: Dried supernatant of 50% ethanol concentration
**1,2,3- repetition of spectra

Figure 5.4. PCA scores plot at different ethanol concentration.

When comparison was made between similar type of spectra within samples, scores of precipitated lignin (10%_L_1 and 10%_L3, 25%_L_1 and 25%_L_3, 50%_L_1 and 50%_L_2) and scores of dried supernatant (10%_S_1 and 10%_S_2, 25%_S_1 and 25%_S_3, 50%_S_1 and 50%_S_2) were close within each other, indicating that the samples within similar type of spectra possess similar composition. Thus, only a spectra was chosen from

spectra that have similar chemical composition to be analysed for FTIR analysis.

PCA correlation loadings are shown in Figure 5.5. Two wavenumbers, 2340 and 780 cm^{-1} were far apart compared with other wavenumbers which had influence the result of PCA score plot. The wavenumbers of 2340 and 780 cm^{-1} were correlated negatively as both wavenumber near to the center and far from the center of 100% explained variance.

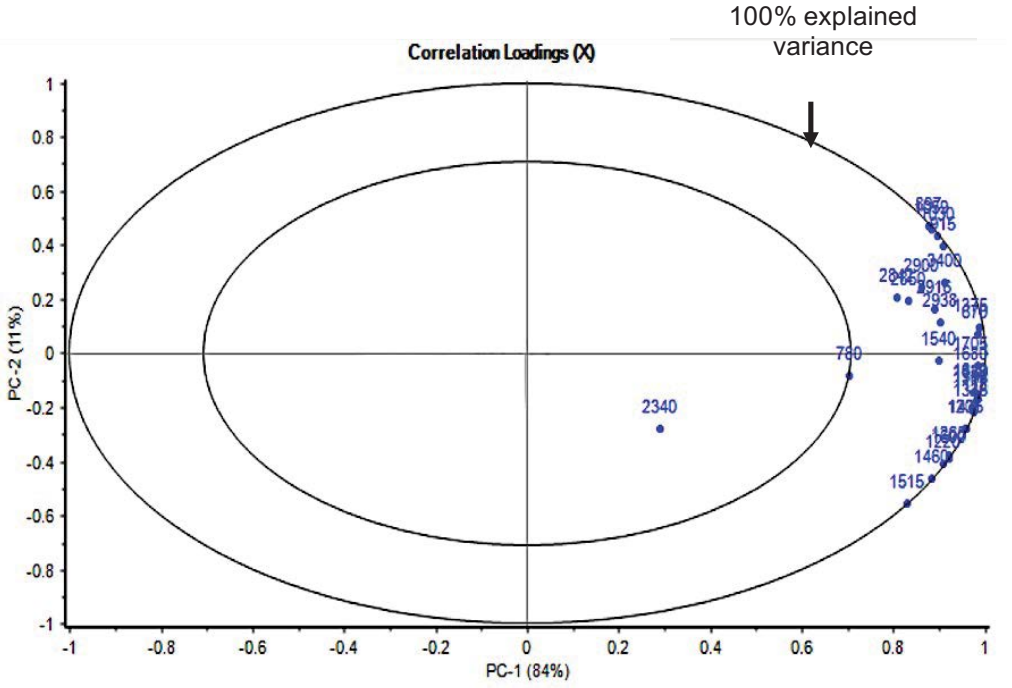

Figure 5.5. PCA correlation loadings plot at different ethanol concentration.

5.3.3.2 Spectra of Precipitated Lignin

The FTIR spectra of precipitated lignin at different ethanol concentration were shown in Figure 5.6. The indicative wavenumbers apportioned to lignin are found: 1705 to 1720, 1680, 1640, 1515, 1460, 1425, 1326, 1265, 1220, 1118, 1030, 915 and 833 cm^{-1}. The details of

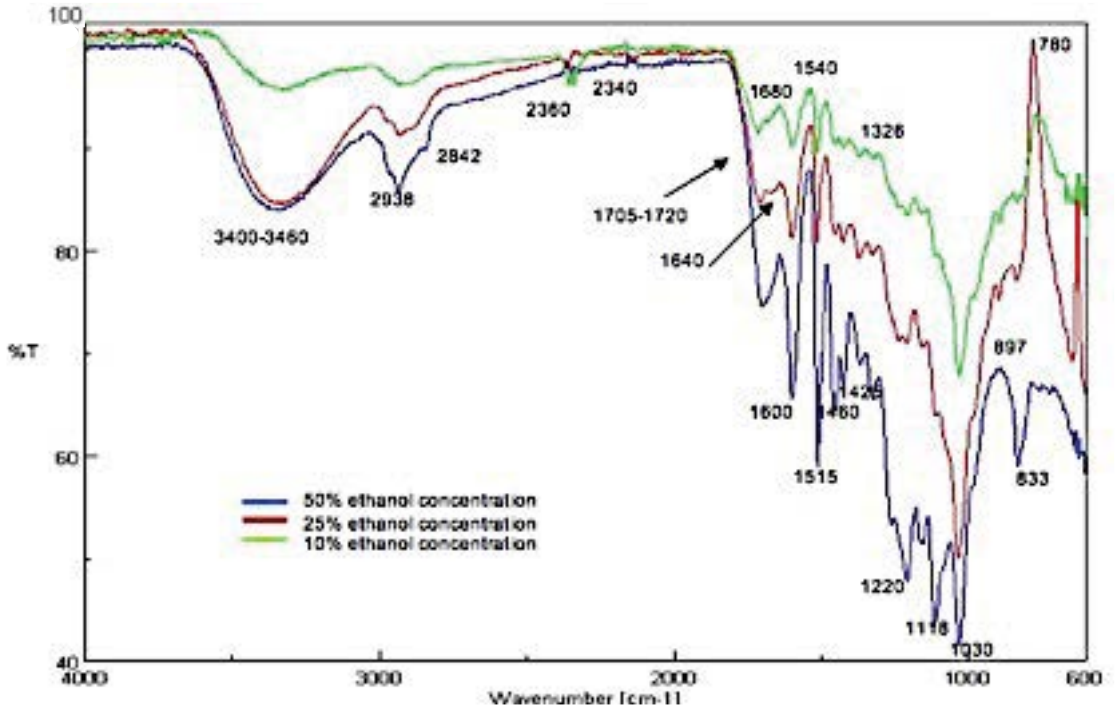

Figure 5.7. FTIR spectra for dried supernatant from different ethanol concentrations.

A new distinct peak of 1540 cm^{-1}, related to an aromatic ring stretching in lignin, was found in both spectra for the precipitated lignin and the dried supernatant (Radotić *et al.*, 2012). In summary, from the spectra in Figure 5.7, it is apparent that wavenumbers of 897 and 1705 to 1720 cm^{-1} related to the contamination of cellulose and hemicellulose were in high intensity and broader peak at 50% ethanol concentration than 25 and 10% ethanol concentration, thus less purity of lignin derived from supernatant was obtained.

monomers, lignin had random polymer globule structure with non-linearly and random cross-linked with other constituents, and the structure of lignin is not as the other two main components of lignocellulosic biomass, cellulose and hemicellulose which has a more linear shape structure (Chen, 2014). A schematic representation of lignin globule structure is illustrated in Figure 5.17.

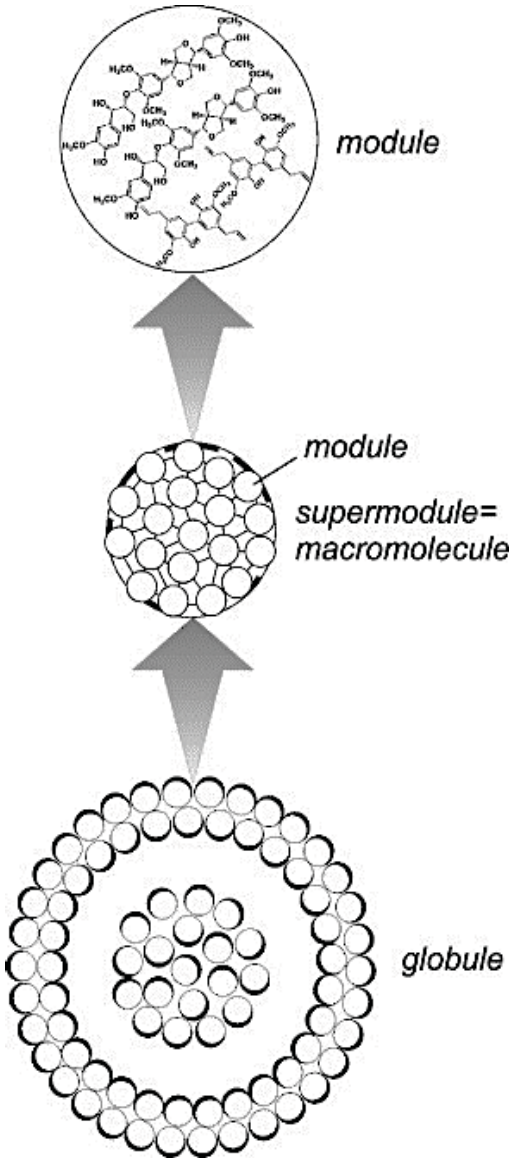

Figure 5.17. Schematic representation of lignin globule structure. (Source: Adapted from Micic *et al.*, 2004; Radotić *et al.*, 2005).

range of the instruments (Malvern, 2014). Nevertheless, the Mastersizer 2000 gave volume-weighted distribution, which within the relative volume contribution is proportional to size of particles (Malvern, 2012).

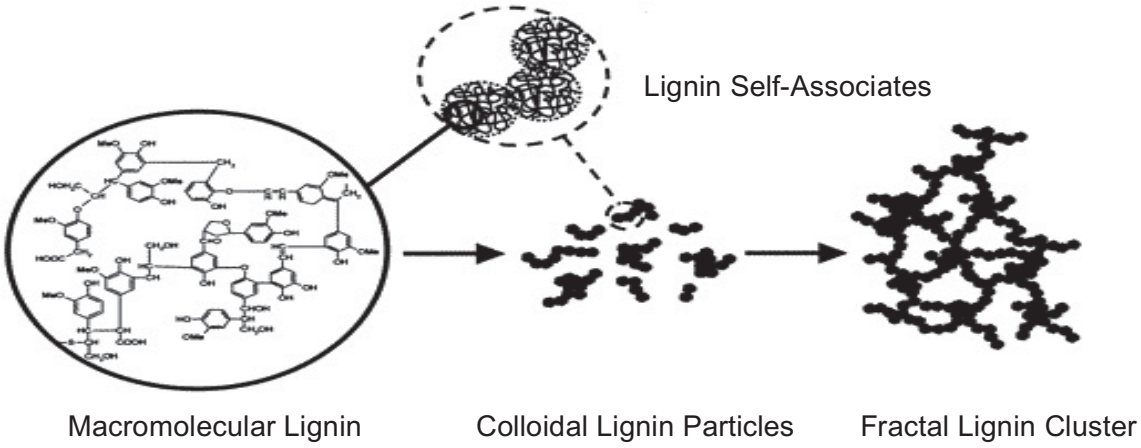

Figure 5.18. A schematic representation of the modes of aggregation in lignin solution system (Source: Adapted and modified from Norgren *et al.*, 2002).

All in all, the two sets of data obtained by Zetasizer Nano ZS and Mastersizer 2000 had common similarities on explaining the behaviour of lignin macromolecules of precipitated lignin and supernatant as well as lignin aggregates in ethanol-water solution. The surface weighted mean diameter by Mastersizer 2000 was reported in terms of the $D_{3,2}$ values. The $D_{3,2}$ refers to the diameter of a sphere of equivalent volume to surface area ratio of the particles in the sample. The value of surface weighted mean was indicative of phenomenon of particle aggregation (McClements, 2015). Decreasing aggregate sizes were found very effective on decreasing the aggregate stability and weighted mean diameter (An *et al.*, 2013; Yonter, 2015). Thus, it suggested that the surface weighted mean obtained is the size of lignin macromolecules in precipitated lignin, supernatant and soluble lignin extract.

5.3.6 Preliminary Study of Particle Size Analysis of Soluble Lignin Extract

5.3.6.1 Zetasizer

Table 5.3 summarised the average particle size of lignin at different ethanol concentrations of soluble lignin extract. Overall, a descending trend was observed for reduction of ethanol concentration from 50% to 10%.

Table 5.3. Average particle size of soluble lignin extract at different ethanol concentrations by Zetasizer.

Ethanol concentration (%)	Particle size (nm)
10	441.5 ± 17.2
25	1077.0 ± 43.4
50	1768.2 ± 45.2

Irrespective of particle size distribution at different ethanol concentration, which are shown in Figure 5.23, 50% ethanol concentration of soluble lignin extract had a monomodal distribution whereas 25% and 10% showed a bimodal and multimodal distribution, respectively.

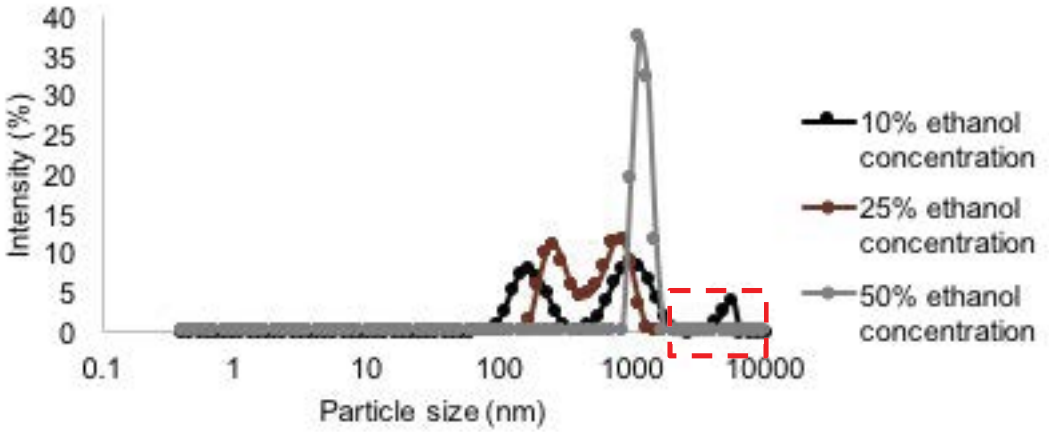

Figure 5.23. Particle size distribution at 50%, 25% and 10% ethanol concentration of soluble lignin extract by Zetasizer.

CHAPTER 6: THE INFLUENCE OF CHEMICAL PROPERTIES OF ORGANOSOLV LIGNIN AGGREGATES AT DIFFERENT LIGNIN CONCENTRATION ON THE EFFICACY OF LIGNIN ESTERIFICATION

6.1 Introduction

The solvent concentration had an influence on the lignin purity and recovery as well the other physical, chemical and structural properties of precipitated lignin, supernatant and soluble lignin fraction. The relationship between the solvent concentration and the resultant lignin macromolecules' is complex, therefore the investigation presented in the previous preliminary study is imperative and could facilitate improved understanding of structural complexity of lignin for lignin obtained via the sub-critical water extraction.

The complex behaviour of lignin aggregates may result also from the interaction of the solute with a solvent containing two components with different concentrations (Da Silva *et al.*, 2002; Maitra and Bagchi, 2008). Associations of the lignin molecule under different conditions vary: the rearrangement of the hydrogen bonds of hydroxyl group play major role and the availability of the hydroxyl group in soluble lignin extract could influence the physicochemical properties of lignin aggregates in modifying and converting lignin into useful renewable materials (Bevilaqua *et al.*, 2006; Buhvestov *et al.*, 1998).

The aim of this chapter was using extracts obtained from sequential extraction that had high purity of lignin and abundance of hydroxyl groups (Chapter 4) in the study of the effect of wider range of ethanol concentration

size analysis was obtained using the Zetasizer Nano ZS and Mastersizer, following methods described in section 3.5.2 and 3.5.3, respectively.

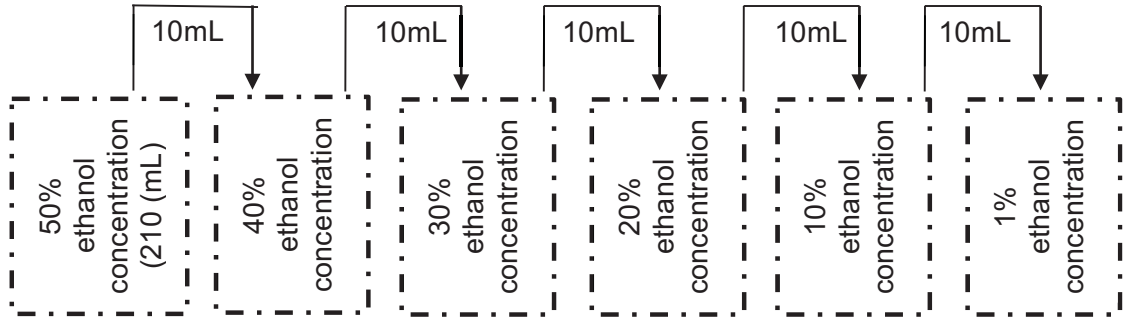

Figure 6.1. Scheme of dilution of soluble lignin extract.

6.2.1.2 LM Analysis

Images of the soluble lignin extract at different ethanol concentrations were captured following method mentioned in section 3.5.5.

6.2.1.3 ImageJ Analysis

Subsequently, 15 recorded images from LM analysis of three different microscope slides were analysed via ImageJ freeware (1.50v) according to method explained in section 3.5.6.

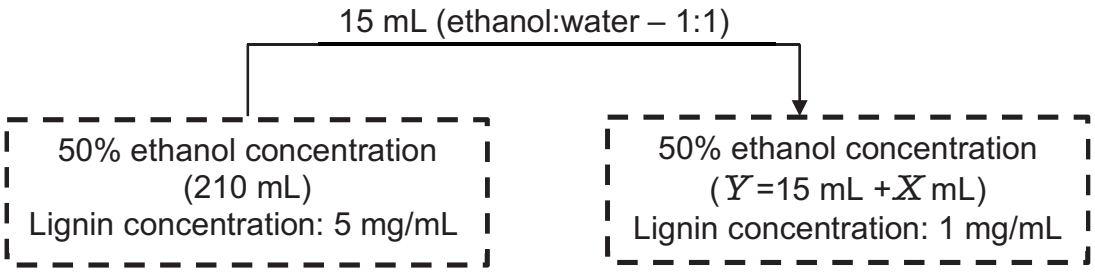

Where Y mL is the volume of soluble lignin extract at 50% ethanol concentration for 1 mg/mL (V_2); and X mL is the amount of ethanol-water mixture (1:1) need to be added to the soluble lignin extract.

Figure 6.2. Scheme of dilution of soluble lignin extract of 5 and 1 mg/mL.

6.2.2.2 Lignin Esterification

Lignin-fatty acid derivatives were synthesised using a method described by (Gordobil *et al.*, 2016) with modification, which the soluble lignin extract was used directly for analysis. Lignin esterification was performed for 5 and 1 mg/mL of soluble lignin extract to enable comparison of the chemical properties of esterified lignin at both these concentrations. 15 mL of soluble lignin extract was placed into a 250 mL beaker and stirred with a magnetic stirrer. Pyridine (2.75 mL) (Sigma-Aldrich, United Kingdom) was used as catalyst and dodecanoyl chloride (0.9 mL) (Sigma-Aldrich, United Kingdom) was added into the soluble lignin extract. The reaction was carried out at 20°C for two hours, after which the solution was decanted directly into 650 mL of 2% ice-cold hydrochloric acid (VWR, United Kingdom) and stirred for five minutes, resulting formation of a brownish ester layer at the top of a yellowish solution, mainly consisting of the excess acid, alcohol and water which separated under the ester layer. The ester layer was separated via a Buchner funnel with filter paper (Fisher Scientific, Qualitative, 150mm), and washed

with excess distilled water and ethanol (1:1) to remove unreacted fatty acids. Then, the esterified lignin was further directly analysed for its chemical structure characterisation via FTIR. The esterification reaction is shown in Figure 6.3.

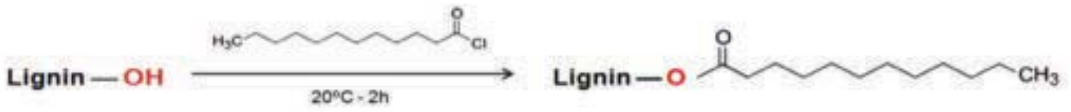

Figure 6.3. Reaction of scheme of lignin-fatty acid derivatives. (Source: Adapted from Gordobil *et al.*, 2016).

6.2.2.3 FTIR Analysis

FTIR analysis was performed on the unmodified and modified lignin samples at different lignin concentration without any pre-treatment for the samples containing 5 and 1 mg/mL lignin concentration. The IR spectra measurements were taken via a Nicolet 380 FTIR-Thermo Electron Corporation over a spectral range from 4000 to 600 cm^{-1} with resolution of 4 cm^{-1} and accumulation of 32 scans. The experiments were done in triplicate for each sample. Area-normalised and smoothed spectra in the regions of 4000 to 600 cm^{-1} were subjected to PCA using Unscrambler^{TM} software (Version 10.3, CAMO). For comparison study, FTIR analysis also was carried out on water, ethanol, water-ethanol (50% by volume), filtrate, blank solution prior esterification (mixture of ethanol:water (1:1), pyridine (2.75 mL), dodecanoyl chloride (0.9 mL), 2% ice cold hydrochloric acid (650 mL)) and dodecanoyl chloride.

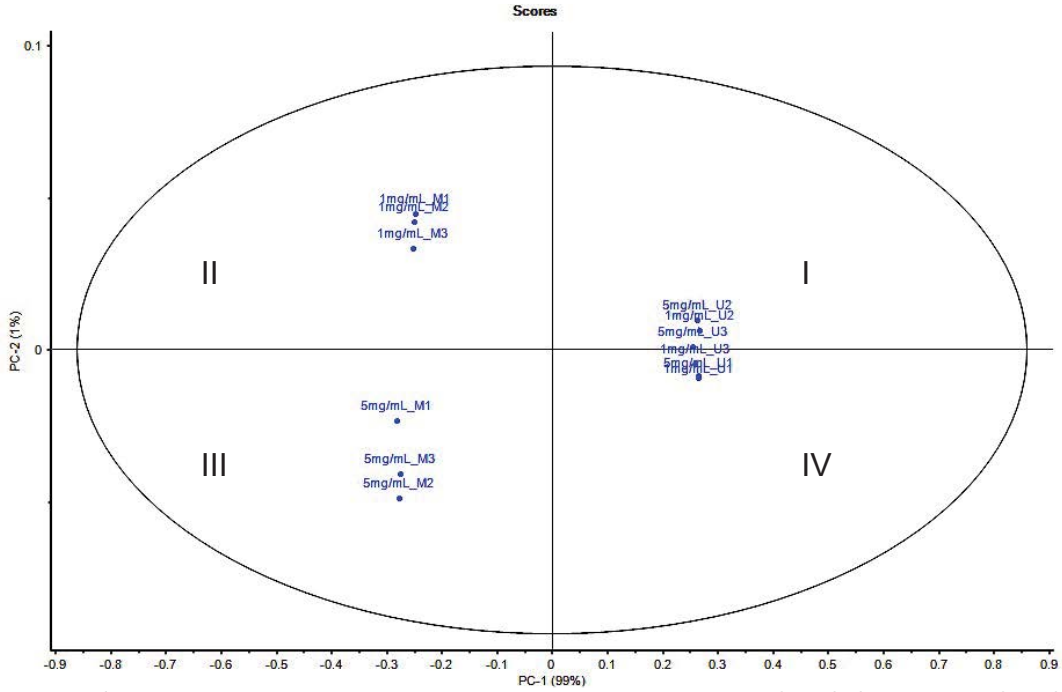

Xmg/mL_AB whereby X is the lignin concentration, A is modified (M) or unmodified (U) lignin and B is repetition of spectra.

Figure 6.16. PCA scores plot of unmodified and modified lignin at different lignin concentration.

Table 6.2. Scores table for similar chemical composition of unmodified and modified lignin at different lignin concentration.

Lignin concentration (mg/mL)	Type of lignin	Spectra of similar chemical composition
5	Unmodified	5mg/mL_U2, 5mg/mL_U3
	Modified	5mg/mL_M2, 5mg/mL_M3
1	Unmodified	1mg/mL_U3,1mg/mL_U1
	Modified	1mg/mL_M1, 1mg/mL_M2

The scores plot of PC2 against PC1 shown in Figure 6.16 illustrates the groupings, however the interpretation of the correlation loadings plot was not straightforward and complicated. The correlation loadings plot in Figure 6.17 showed the specific wavenumbers that influenced the scores plot.

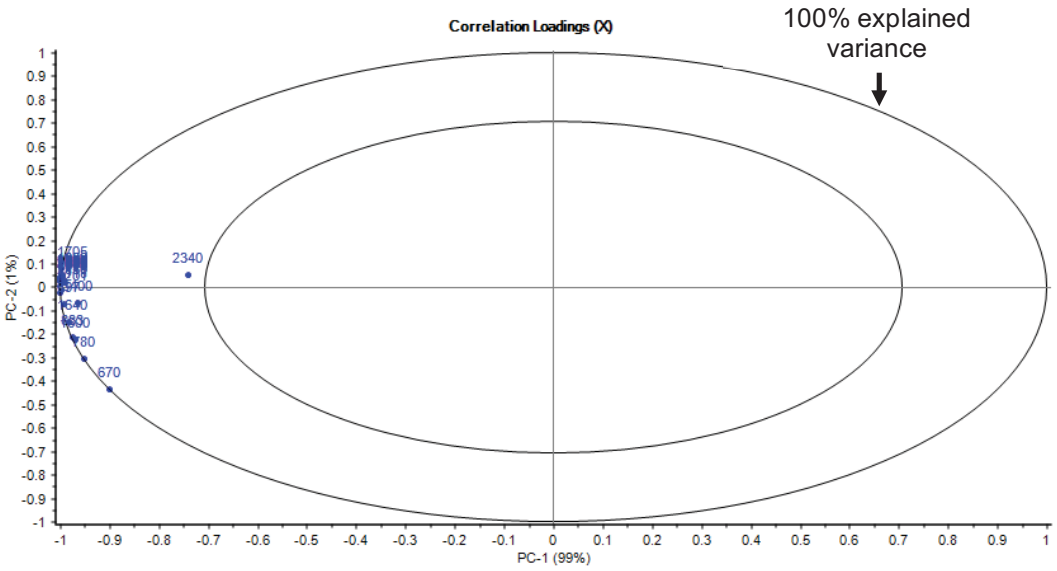

Figure 6.17. PCA correlation loadings plot of unmodified and modified lignin at different lignin concentration.

All wavenumbers related to lignocellulosic biomass identified by FTIR in the range from 4000 to 600 cm^{-1} were correlated positively as the wavenumbers very close to 100% explained variance except for wavenumber of 2340 cm^{-1}. The wavenumber of 2340 cm^{-1} contributed the most variability that affect the position of the samples. The wavenumber at 2340 cm^{-1} referred to OH stretch from strong H-bonded-COOH (Davis *et al.*, 1999). The location of wavenumbers either in positive or negative loadings in quadrant is not clearly explained. Even though the loadings plot could not have explained clearly what PC2 and PC1 describe, the scores plot can differentiate the spectra of samples according to different lignin concentration.

A representative FTIR spectra of unmodified soluble lignin extract at 5 and 1 mg/mL lignin concentration after spectra subtraction can be seen in Figure 6.19.

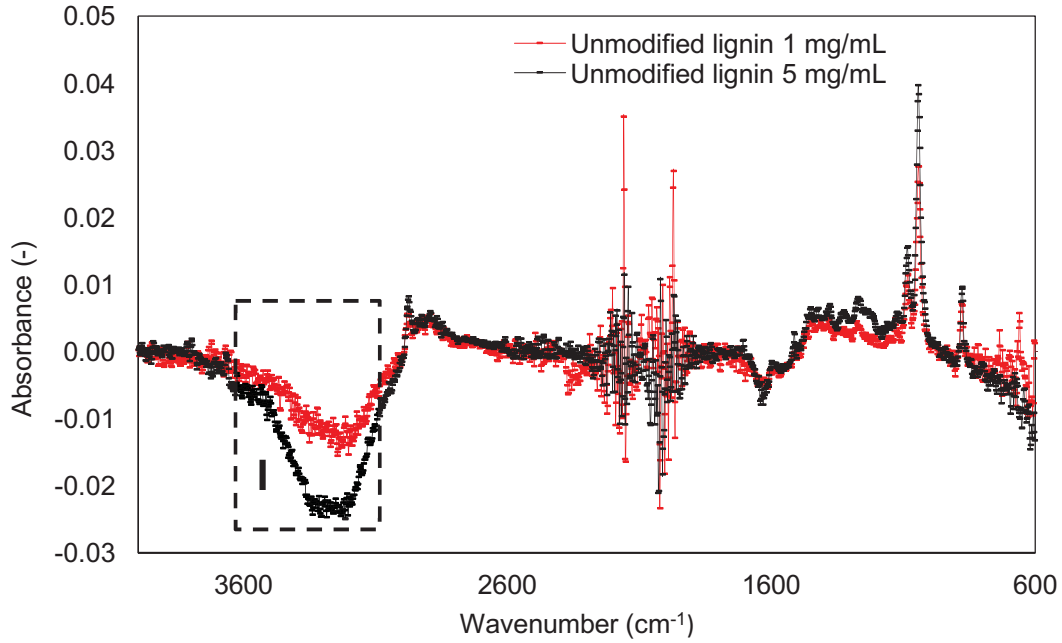

Figure 6.19. FTIR spectra of unmodified lignin at 5 and 1 mg/mL lignin concentration.

Even though the spectra subtraction method is quite useful for most applications using IR accessories, an attempt to remove the water spectra from FTIR spectra will be complicated in most cases (Nishikida *et al.*, 1995). A representative of specific fingerprint around 3400 cm^{-1} attributed to O-H stretching vibrations in aromatic and aliphatic hydroxyl groups can be seen in Figure 6.19 (labeled as I). Initially, as anticipated, the absorbance of unmodified lignin at 5 mg/mL was stronger than 1 mg/mL; indicating the high availability hydroxyl groups of intramolecular and intermolecular hydrogen bonding formed and existed between lignin and dual solvent in the soluble

lignin extract (Wang *et al.*, 2016). The source of O-H bonds could be originated from water, ethanol and lignin.

However, a more careful analysis revealed that the negative value of absorbance especially in the region I (Figure 6.19) corresponds to the stretch of O-H bonds in water molecules causes dominant absorbance in the wavenumber of 3400 cm^{-1} (Zaiqun, 2007). The finding appears to be well supported by Barth (2007) which the strong absorbance of water in the IR spectra region overlaps with sample modes of interest. Figure 6.20 has proved that the peak at 3400 cm^{-1} of water (labeled as II) had strong absorption (0.39) rather than ethanol (0.15).

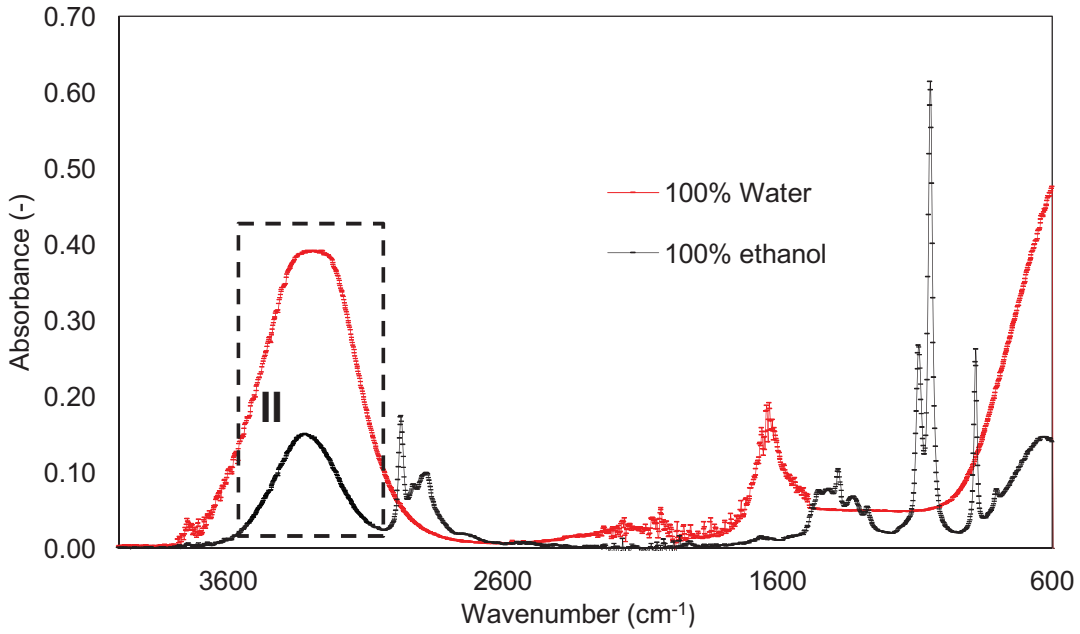

Figure 6.20. FTIR spectra of water and ethanol.

Therefore, when the hydroxyl groups wavenumber is of interest, the strong water absorption in the aqueous samples could have influenced the results obtained and in turn, relatively led into misinterpretation of the data.

Despite the limitation of this method, and consequently the poor results in the analysis of unmodified lignin samples, the findings do however suggest that dehydration of sample could be conducted or the precipitated lignin used for analysis in future to reduce the intense IR absorption of water (Trenerry and Rochfort, 2010). Therefore, the spectra of unmodified lignin based on the spectra subtraction method could not be comparable with the spectra of modified lignin.

6.3.2.2 Comparison of Modified Lignin at Different Lignin Concentration

Figure 6.21 provides the schematic diagram of sample analysed via FTIR for esterification study.

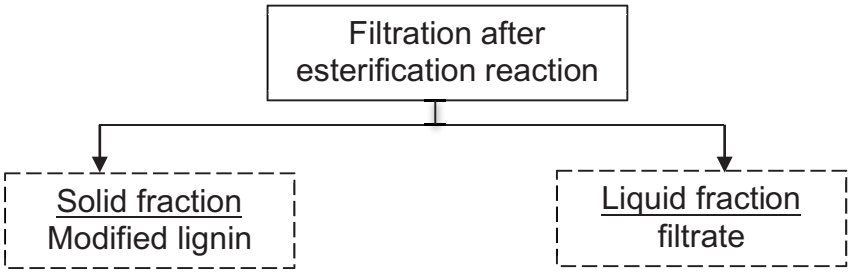

*Additional sample analysed for comparison study (1) dodecanoyl chloride (2) blank solution contains ethanol-water mixture (50% by volume), pyridine, dodecanoyl chloride and 2% of ice-cold hydrochloric acid.

Figure 6.21. Schematic diagram of sample analysed via FTIR for esterification study.

The FTIR spectra of the resulting modified lignin at 5 and 1 mg/mL lignin concentration were compared in Figure 6.22. The wavenumbers at 3400, 2938, 2850, 1800, 1760, 1740, and 1700 cm^{-1} of FTIR spectra could be used as physiological fingerprints to assess the efficacy of esterification process.

The presence of 3400 cm^{-1} (region I) was noted with broad intensity at 5 mg/mL (0.04) rather than 1 mg/mL (0.03), and the wavenumber of 3400cm^{-1} was attributed to O-H stretching of aromatic and aliphatic hydroxyl groups (Alriols *et al.*, 2010; Boeriu *et al.*, 2014; Pandey, 1999). The peak of 3400 cm^{-1} at 1 mg/mL become more flattened. As hypothesised, the findings showed that more material or lignin concentration in the soluble lignin extract, the more source of O-H bonds in the esterified lignin.

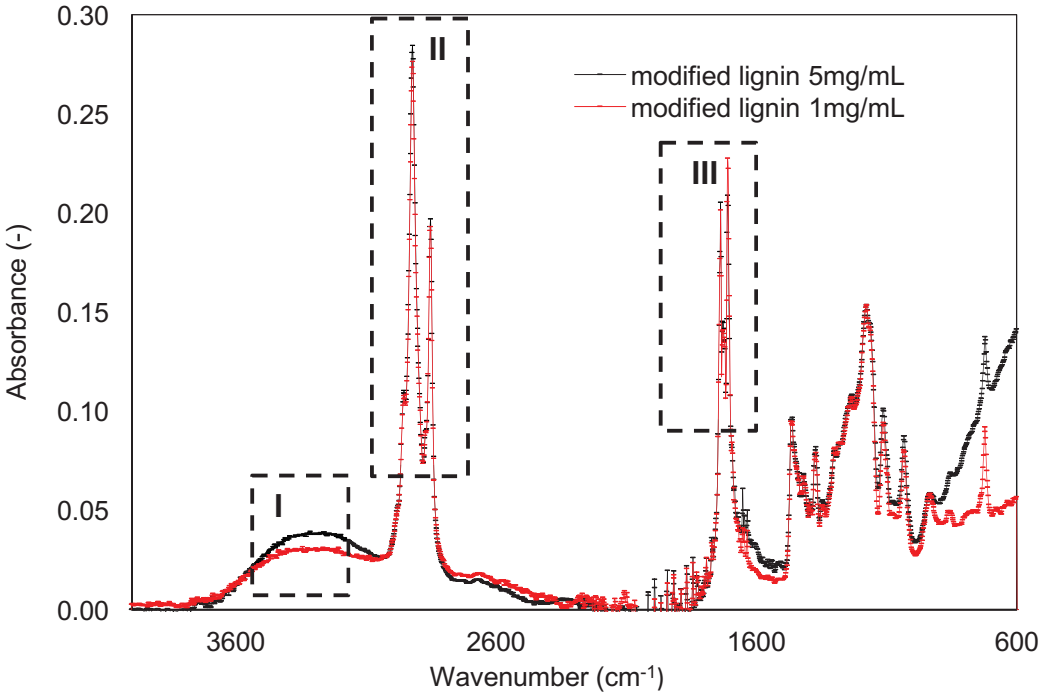

Figure 6.22. FTIR spectra of modified lignin at different ethanol concentration.

When comparison was made to modified lignin prepared to 1 mg/mL, the region II and III in Figure 6.22 of modified lignin from 5 mg/mL showed no difference in intensity of the peaks around 2938, 2850, 1760 and 1740 cm^{-1}. Strong absorptions at 2938 and 2850 cm^{-1} of modified lignin (region II) at both lignin concentrations arise from long chain alkyl groups (aliphatic carbon) which are present in fatty acid chloride, dodecanoyl chloride (Gordobil *et al.*,

concentration, in turn the spectra produced were similar with the spectra of water and overlap with other modes of interest as have been shown previously in Figure 6.20.

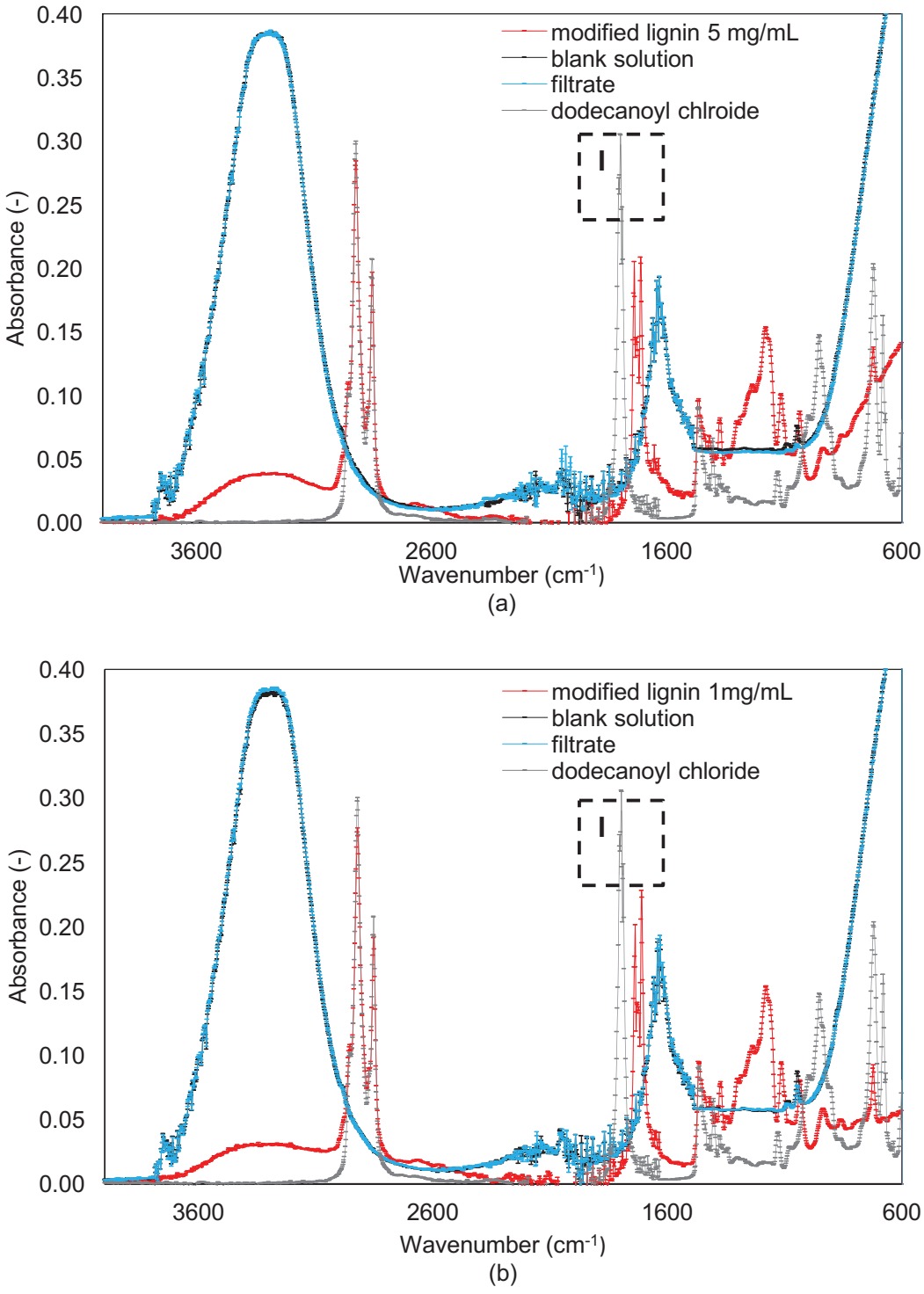

Figure 6.23. FTIR spectra of modified lignin, blank solution, filtrate and dodecanoyl chloride at (a) 5 and (b) 1 mg/mL lignin concentration.

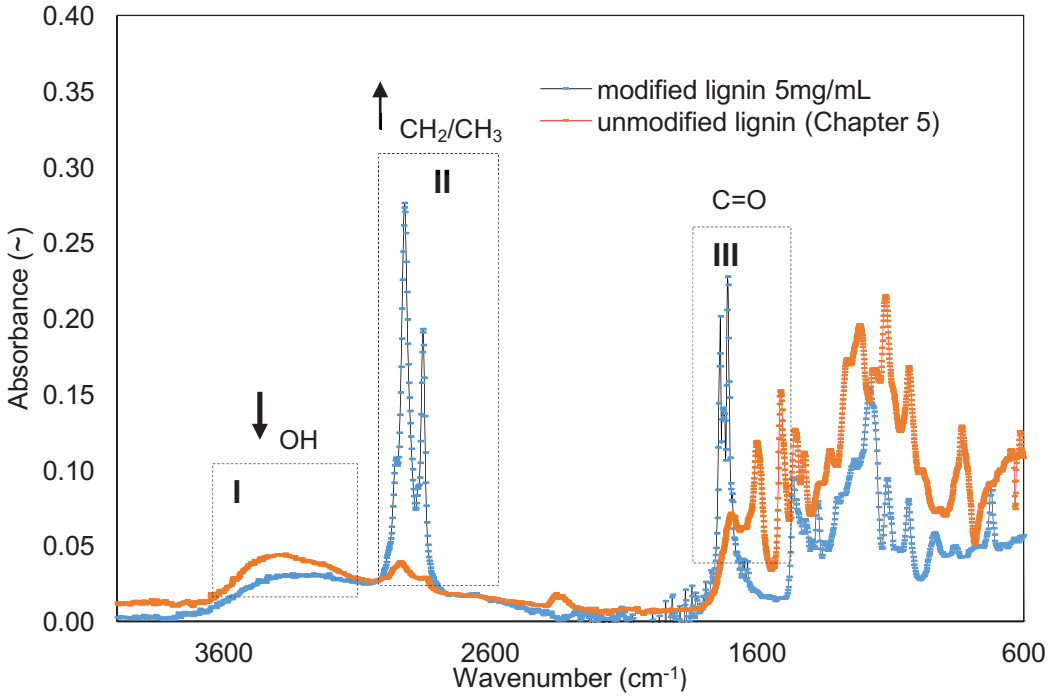

Figure 6.24. FTIR spectra of unmodified lignin and modified lignin.

Here, the esterification was assessed by FTIR which also focused on the absorbance data for quantitative analysis (Gallignani *et al.*, 2014; Khanmohammadi *et al.*, 2009). The esterification can be clearly examined by the incremental decline of the hydroxyl group at wavenumber at 3400 cm^{-1}, the incremental increase of aliphatic CH stretching from the ester groups at 2938 and 2850 cm^{-1}, and the incremental appearance of ester bonds at 1760 and 1740 cm^{-1} (phenolic and aliphatic, respectively) with a degree of added C_{12} fatty acid chloride (Koivu *et al.*, 2016; Pawar *et al.*, 2016). The dotted line in Figure 6.24 showed the specific fingerprints I, II, and III (hydroxyl group, CH stretching and ester bonds, respectively) that could be further focused for the efficacy of lignin esterification.

Overall, modified lignin showed that a decrease in the intensity of the OH stretching band in aromatic and aliphatic hydroxyl groups at 3400 cm^{-1}

CHAPTER 7: CONCLUSIONS AND RECOMMENDATIONS FOR FUTURE WORK

7.1 Conclusions

The development of economically feasible second-generation bioethanol offers promising source of energy to reduce the world's dependence on fossil fuels throughout diverse efficient separation technologies. The emerging of biorefinery concept for second-generation bioethanol produces a multitude of different valuable building blocks, namely hemicellulose, cellulose and lignin from lignocellulosic biomass. In this study, the biomass fractionation was carried out via SCW mediated hydrolysis, in which the study focused on the developing novel approaches to support enhanced added value applications of lignin.

The impact of SCW mediated hydrolysis of two different lignin extraction processing routes, DE and SE were assessed with regards to physical and chemical properties of lignin macromolecules. An assessment on percentage of delignification from DE was 81.5% whereas the SE yielded 58.0%. Although the SE showed lower efficacy of delignification than DE, the lignin macromolecules of SE exhibited higher purity of lignin and lignin derived from dried supernatant than DE. The percentage of lignin recovery was not significantly different for both lignin extraction processing routes. The FTIR analysis demonstrated that the lignin obtained by different processing routes had different chemical compositions. Overall, even though SE exerted negative impact specifically on percentage of delignification, the SE process

REFERENCES

Abbas, K. A., Mohamed, A., Abdulamir, A. S., and Abas, H. A. (2008). A review on supercritical fluid extraction as new analytical method. *American Journal of Biochemistry and Biotechnology*, *4*(4), 345–353.

Abdel-Ghani, N. T., El-Chaghaby, G. A., and Helal, F. S. (2014). Individual and competitive adsorption of phenol and nickel onto multiwalled carbon nanotubes. *Journal of Advanced Research*, *6*(3), 405–415.

Abdelaziz, O. Y., Brink, D. P., Prothmann, J., Ravi, K., Sun, M., García-Hidalgo, J., … Gorwa-Grauslund, M. F. (2016). Biological valorisation of low molecular weight lignin. *Biotechnology Advances*, *34*(8), 1318–1346.

Abdelaziz, O. Y., and Hulteberg, C. P. (2017). Physicochemical characterisation of technical lignins for their potential valorisation. *Waste and Biomass Valorization*, *8*(3), 859–869.

Abdul Khalil, H. P. S., Bhat, A. H., and Ireana Yusra, A. F. (2012). Green composites from sustainable cellulose nanofibrils: A review. *Carbohydrate Polymers*, *87*(2), 963–979.

Abidi, N., Hequet, E., Cabrales, L., Gannaway, J., Wilkins, T., and Wells, L. W. (2008). Evaluating cell wall structure and composition of developing cotton fibers using Fourier transform infrared spectroscopy and thermogravimetric analysis. *Journal of Applied Polymer Science*, *107*(1), 476–486.

Abiven, S., Heim, A., and Schmidt, M. W. I. (2011). Lignin content and chemical characteristics in maize and wheat vary between plant organs and growth stages: consequences for assessing lignin dynamics in soil. *Plant Soil*, *343*(1–2), 369–378.

Achyuthan, K. E., Achyuthan, A. M., Adams, P. D., Dirk, S. M., Harper, J. C., Simmons, B. A., and Singh, A. K. (2010). Supramolecular self-assembled chaos: Polyphenolic lignin's barrier to cost-effective lignocellulosic biofuels. *Molecules*, *15*(12), 8641–8688.

Agarwal, U. P., and Atalla, R. H. (2010). Vibrational Spectroscopy. In J. Heitner, Cyril, R. Dimmer, Donald, A. Schmidt (Ed.), *Lignin and Lignans Advances in Chemistry* (pp. 104–129). Boca Raton, United States of America: CRC Press.

Agbor, V. B., Cicek, N., Sparling, R., Berlin, A., and Levin, D. B. (2011). Biomass pretreatment: Fundamentals toward application. *Biotechnology Advances*, *29*(6), 675–685.

Alberts, B., Johnson, A., Lewis, J., Raff, M., Roberts, K., and Peter Walter. (1989). Cells in Their Social Context. In *Molecular Biology of The Cell* (Fourth, Vol. 53, p. 160). New York, USA: Garland Science.

Aleš, H., Michal, J., Lenka, D., Alexandra, S., and Igor, Š. (2015). Thermal properties and size distribution of lignins precipitated with sulphuric acid. *Wood Research*, *60*(3), 375–384.

Allen, E., Paul Smith, and Henshaw, J. (2001). *A review of particle agglomeration*. Dorset, United Kingdom.

Alriols, M. G., García, A., Llano-ponte, R., and Labidi, J. (2010). Combined organosolv and ultrafiltration lignocellulosic biorefinery process. *Chemical Engineering Journal*, *157*(1), 113–120.

APPENDICES

Appendix A

Table A1. Analysis of variance of SE and DE.

ANOVA

		Sum of Squares	df	Mean Square	F	Sig.
Purity of lignin derived supernatant	Between Groups	138.817	1	138.817	107.581	.000
	Within Groups	5.161	4	1.290		
	Total	143.978	5			
Purity of precipitated lignin	Between Groups	14.045	1	14.045	264.508	.000
	Within Groups	.212	4	.053		
	Total	14.258	5			
Percentage of delignification	Between Groups	827.905	1	827.905	3741.662	.000
	Within Groups	.885	4	.221		
	Total	828.790	5			
Percentage of lignin recovery	Between Groups	1.540	1	1.540	.956	.383
	Within Groups	6.442	4	1.610		
	Total	7.982	5			
Percentage of biomass solubilisation	Between Groups	142.984	1	142.984	229.669	.000
	Within Groups	2.490	4	.623		
	Total	145.474	5			

LIST OF PUBLICATIONS

M.H. Hamzah, S. Bowra, M.J.H Simmons and P.W. Cox (2016). Proceedings from the 24th European Conference and Exhibition: *The Impact of Process Parameters on the Purity and Chemical Properties of Lignin Extracted from Miscanthus x giganteus* using a Modified Organosolv Method. Amsterdam, The Netherlands.

M.H. Hamzah, S. Bowra, P.W. Cox and M.J.H. Simmons (2016). Proceedings from the 4th CIGR Agricultural Engineering Conference: *The Effect of Ethanol Concentration upon Formation of Organosolv Lignin Aggregates from Miscanthus x giganteus.* Aarhus, Denmark.